CRANFIELD UNIVERSITY

Andrew J. Claydon

# Resonant Acoustic Mixing of Polymer Bonded Explosives

Cranfield Defence and Security

PhD
Academic Year: 2019 - 2020

Supervisors: Dr Philip P. Gill, Dr Guillaume Kister, Miss Sally Gaulter, and Dr Nathan Flood

August 2020, Revised January 2021

CRANFIELD UNIVERSITY

Cranfield Defence and Security

PhD
Academic Year: 2019 - 2020

Andrew J. Claydon

# Resonant Acoustic Mixing of Polymer Bonded Explosives

Supervisors: Dr Philip P. Gill, Dr Guillaume Kister, Miss Sally Gaulter, and Dr Nathan Flood

August 2020, Revised January 2021

# Abstract

Current Polymer Bonded Explosive (PBX) formulation is limited by a compromise - optimised final properties against processability. While solid loading (explosive content) would ideally be maximised and plasticiser content would ideally be minimised, this would make the formulation too viscous to cast into its casing and require long and arduous mixing processes using conventional techniques. However, with Resonant Acoustic Mixing (RAM), PBX formulation does not have to be constrained. Instead of traditional mixing blades, mixing is achieved by the use of a vibrating platform to impart acoustic pressure waves (vibrations) into the mixture, agitating it. The added ability to mix in the end use casing (mixing 'in-situ') also renders casting obsolete in many scenarios. In order to maximise the benefits of RAM with regards to next generation formulation-optimised PBX manufacture ('PBneXt'), the underlying mechanisms of how the technique works, how efficiency (time and energy required for homogeneity) can be determined and maximised, and how final material properties may change between casting and 'in-situ' processing methods, must be better understood. The research aim of the PhD is therefore to assess how mixing efficiency of RAM can be measured and optimised to maximise its benefits, with a focus on how aspects of machine control and mixing vessel design can be altered to improve the mixing mechanisms on which the technique relies. Areas investigated experimentally include the effects of acceleration and mixer intensity (linked to power draw) setting, mixer model and unit, vessel material (with regards to surface free energy and thermal properties), and vessel surface finish (with regards to roughness). It is found that by modifying these variables, the time and energy required for mixing can be substantially reduced. A comparison between material properties of composites mixed 'in-situ' and 'mixed and cast' is also undertaken. The findings are then reconciled with wider literature observations and recommendations are made as how to best implement RAM for 'PBneXt' manufacture, ultimately allowing for explosive compositions with improved performance, mechanical, safety, and ageing properties.



**Keywords:** Resonant Acoustic Mixing, Polymer Bonded eXplosive, PBneXt, Efficiency

## Acknowledgements

I would like to first thank my sponsors, MBDA Systems and Cranfield University, without the financial support of whom the research wouldn't have been possible. A special thanks must also go to Falcon Project Ltd., who went above and beyond in providing material support and technical expertise during the most difficult times of the work, BAE Systems Land UK for providing equipment and ingredients when needed, and Chemring Nobel Norway for supplying the explosives required for live mixing.

My greatest thanks go to my supervisory team, Dr Philip Gill for his advice and help in steering the project, Dr Guillaume Kister for his extensive materials science knowledge, and Sally Gaulter for sharing her expertise in mixing and formulation. I would also like to thank Dr Nathan Flood for his guidance in the early stages of the project. A special thanks must also go to Jim Clements and Dr Chris Stennett for providing the necessary facilities for live explosives work.

My thanks also go to Karl Norris and the workshop team for their engineering expertise in the manufacture of custom components, and the laboratory technicians for helping to keep the experimental work running smoothly.

Finally, I'd like to thank my family and friends (and cat!) for their moral support over the past four years.

# Contents

# List of Figures

**Paper 4 - Vessel Material**



**Paper 5 - Surface Finish**



**Paper 6 - Mixing 'In-situ'**



**Overall Perspective, Conclusions, and Future Work**



**Appendices**

# List of Tables

**Paper 5 - Surface Finish**



**Paper 6 - Mixing 'In-situ'**



**Overall Perspective, Conclusions, and Future Work**



**Appendices**

# Acronyms

| | |
|---|---|
| 3D | Three dimensional |
| ABS | Acrylonitrile butadiene styrene |
| AO | Anti oxidant |
| B | Bulk motion |
| CAM | Continuous acoustic mixing |
| CNC | Computer numerical control |
| CT | Computerised tomography |
| DEHA | Di(2-ethylhexyl) adipate |
| FDM | Fused deposition modelling |
| FL | Flat-line stage |
| G | Acceleration due to Earth's gravity |
| HDI | Hexamethylene diisocyanate |
| HMX | 1,3,5,7-tetranitro-1,3,5,7-tetrazoctane |
| HTPB | Hydroxyl-terminated polybutadiene |
| IPDI | Isophorone diisocyanate |
| LabRAM | Laboratory Resonant acoustic mixer |
| M | Mixing stage |
| NATO | North Atlantic Treaty Organisation |
| PBneXt | Next generation PBX |
| PBX | Polymer Bonded eXplosive |
| PE | Polyethylene |
| PEEK | Polyether ether ketone |
| PERME | Propellants, Explosives, and Rocket Motor Establishment |
| PET | Polyethylene terephthalate |
| PHFP | Poly(hexafluoropropylene) |
| PMMA | Poly(methyl methacrylate) |
| PP | Polypropylene |
| PS | Polystyrene |
| PTFE | Polytetrafluoroethylene |
| PVC | Polyvinyl chloride |
| RAM | Resonant acoustic mixer / Resonant acoustic mixing |
| RBM | Rigid body mass |
| RDX | 1,3,5-trinitro-1,3,5-triazinane |
| SA | Surface area |
| SFE | Surface free energy |
| SFT | Surface tension |
| Ti | Titanium |
| TNT | 2,4,6-trinitrotoluene |
| TPB | Triphenylbismuth |
| UK | United Kingdom |
| USA | United States of America |
| V | Volume |

# Introduction

In a simple definition, mixing can be described as a process in which non-uniformity within a mixture is reduced,[1] and may take place between solids (granular materials), liquids, and gasses. In this work, powder-liquid mixing is of interest, particularly with regards to the production of homogeneous viscous suspensions. Such high viscosity mixing is a necessity across a range of industries, such as in the manufacture of cosmetics and food products.[1] This work, however, is focused on the manufacture of energetic materials, particularly Polymer Bonded eXplosives (PBXs). PBXs typically contain explosive crystals (such as RDX[a] or HMX[b]) dispersed throughout and bound by an elastomeric rubber binder. In 'castable' formulations, the elastomer is typically the product of a hydroxyl terminated polybutadiene (HTPB) binder pre-polymer, which is cured (crosslinked) with a multifunctional isocyanate once cast into a mould.[2] During manufacture, the explosive powder, viscous binder and curative must be mixed together. Other ingredients may also be included in the formulation depending on the desired properties, such as plasticiser (to improve processability), aluminium (to improve blast effect), additives such as wetting and bonding agents (improved material strength), antioxidants (improved shelf life), and curing catalysts (faster polymerisation).[2] Homogeneity is required in order for the properties of the cured composite to be uniform across the entire volume of an explosive charge, optimising its properties.[3]

To mix the ingredients into the form of a homogeneous suspension, a high shear mixer is conventionally used.[3] Such mixers employ intrusive mixing blades which agitate the mixture by folding or kneading, and break down agglomerates.[1] While effective and well characterised, high shear mixing has drawbacks. Shear is localised to the immediate area around the mixing blades, leading to long mix times (up to several hours[3]) and the requirement to frequently pause the mixer while unmixed material on the vessel wall and mixing blades is scraped down. A large amount of

[a] 1,3,5-trinitro-1,3,5-triazinane
[b] 1,3,5,7-tetranitro-1,3,5,7-tetrazoctane

waste is also produced (∼12.5 % on industrial scale[4]) since the blades and mixing vessel must be cleaned after use. This is labour intensive and hazardous process for workers,[5] and has to be disposed of by open burning.

Resonant Acoustic Mixing (RAM) is a novel mixing technique that has gained considerable attention[6] and investment[7] as an alternative to traditional high shear mixing for energetic materials. The mixer operates by using a vibrating platform (∼60 Hz, ≤100 G acceleration) to impart low frequency, high intensity acoustic waves into an affixed mixing vessel, agitating the contents.[8, 9] RAM is reported to have many advantages over conventional high shear mixing. Since shear is not localised, mixing time is drastically reduced (tens of minutes as opposed to hours[5]), and the absence of mixing blades removes the need for pausing to scrape them down. The technique also brings the possibility for 'in-situ' mixing, whereby the final receptacle of the PBX doubles as the mixing vessel,[10] removing the need for casting. This is particularly significant since the requirement for cleaning and associated waste would be reduced drastically,[4] significantly reducing costs, hazard for workers, and the environmental impact of open burning explosive waste. Mixing 'in-situ' could also allow novel high viscosity PBXs, which could not otherwise be feasibly pour cast or extruded into moulds, to be manufactured. It is claimed that RAM can operate with viscosities well in excess of 10,000,000 cP.[8] Put in context, the measured end-of-mix viscosity for a typical castable formulation (a PBXN-109[11] analogue, 64 % w/w RDX and 20 % w/w aluminium in binder, plasticiser, and additives) is 100,000 cP at 60 ℃.[12] In current castable formulations, particle size is typically quite coarse (usually ranging from the tens to the hundreds of microns in diameter[13]). However, it is not unusual for a minority proportion (∼30 %) of micronised particles to be added to improve packing density, with the filler typically comprising 87 % w/w of the formulation.[14] Plasticiser is also typically added in similar quantities to the binder to minimise viscosity. Using mixed 'in-situ' RAM, plasticiser content could be reduced and solids loading increased (with increasingly smaller particle size fractions) at the expense of increased viscosity. The benefits of reduced particle size on the micron-scale are well documented and are as follows:

1. Improved mechanical strength[15–23] - where larger surface area to volume ratio improves adhesion to the binder, reducing the likelihood of debonding.

2. Improved hazard properties[24–26] - where smaller particles have fewer internal defects that can compromise safety as hotspot[27] initiation sites when exposed to incidental stimuli.

3. Better performance - with the additional inclusion of increasing smaller particle size fractions (bi-modal, tri-modal, and beyond), the packing density can be maximised.

The benefits of reduced or eliminated plasticiser content are:

1. Improved mechanical strength[28] - greater binder to plasticiser ratio increases the number of crosslinks in the composite.

2. Improved ageing properties - eliminated plasticiser will prevent the material properties changing over time due to plasticiser migration, leading to longer shelf-life.

The high solids loading expected from the addition of increasing smaller particle size fractions (tri-modal and tetra-modal) has the potential to closely approximate the loadings of hot pressed PBXs (>94 % w/w[29]), which are typically reserved only for applications in which performance is of greatest importance. This is because the pressing procedure is hazardous, solvent intensive, and the end material has poor mechanical properties[29] in comparison to cast PBX. Mixed 'in-situ' therefore has the potential to create PBXs that have similar performance to pressed PBX and similar mechanical properties to cast PBX, without the need for a pressing procedure. Using RAM to create such novel formulations 'in-situ' is an ultimate aim of industry, where next generation PBXs (termed 'PBneXt' by BAE Systems) could be designed for improved safety, better performance, and longer shelf-life, as well as producing reduced waste during manufacture.

Of the research and development performed on RAM of PBX to date, most studies have focused on proof of concept in terms of its novel capabilities. As a consequence, the factors that underpin the effectiveness of the technique are still poorly understood. In other words, the major focus has jumped straight to asking what can RAM do, without first asking how RAM can be optimised to do it. Of particular interest in this work is gaining a better understanding the factors that affect mixing efficiency, here defined as the time and energy required for homogeneity, and product outcome.

## Objectives

Jointly funded by Cranfield University and MBDA Missile Systems, this work aims to further the understanding of the factors that affect the efficiency and product outcome of RAM when applied to loaded polymer suspensions, and relate the findings to the impact they may have on PBX manufacture. This is summarised below.

**Core research question:**

How can RAM be optimised to maximise its benefits?

**Key objectives:**

Objective 1: To determine the current state of understanding with regards to the factors affecting PBX mixing efficiency with RAM, and identify the research gaps.

Objective 2: To develop a robust methodology to assess RAM efficiency by determination of the end of mix time and the energy supplied up until that point.

Objective 3: To further the understanding of the effects mixing variables regarding the machine (acceleration, intensity, calibration) and mixing vessel (material, roughness) have on RAM efficiency.

Objective 4: To investigate how product outcome may vary when a formulation is mixed 'in-situ' as opposed to 'mixed and cast'.

Objective 5: To discuss the expected impacts of the findings with regards to 'PBneXt' implementation.

## Thesis structure

The thesis is presented as six linked, self-contained papers, supplemented with an overall discussion and conclusion chapter. Additional data from incomplete work is also given in appendices. A brief description of the content of each work is given below. Figure I-1 gives a visual indication of the kind of variables under consideration in each case, superimposed on a simplified graphic of LabRAM mixer.

## Paper 1 - A Review of Resonant Acoustic Mixing Efficiency for Polymer Bonded Explosives

**Overview:** Since RAM itself is a recently developed technology, many aspects of the technique are poorly understood. Although some studies address the way mixing parameters affect the movement of the material and process efficiency, complementary and conflictual results have not previously been reconciled. Therefore, a thorough literature review on the effects of differing mixing parameters is undertaken. This chapter addresses Objective 1.

**Outcomes:** The three major documented movement modes for mixing viscous suspensions are identified as 'quiescent', where there is no bulk motion, 'churning' (also referred to as 'bulk mixing'), where there is bulk rolling and smearing, and 'decoupled' where there is bouncing or levitation.[30] 'Churning' is believed to be the most effective,[30, 31] and is reported to be reliant on a velocity gradient across the vessel contents, whereby material in contact with the wall couples to it, ideally in a 'no-slip' condition. Conversely, the bulk of the material is acted upon by the acoustic pressure waves (vibrations), which accelerate the material vertically.[32, 33] It is this velocity gradient that is responsible for inducing medium shear across the entire volume of the vessel, compelling the mixing process. It is deduced that the establishment of churning and its effectiveness relies on the degree of movement in the material, and the extent to which there is 'no-slip' at the wall. The degree of movement in the material is found to depend on the inertial forces acting upon it and its compliance (ease of deformation), while the degree of wall slip is found (or hypothesised) to depend on interfacial drag at the wall, chemical adhesion, and tack. A summary of the conditions determined to be of importance are given in Table I-1.

It is found that the variables that are reported (or hypothesised) to determine the conditions given in Table I-1 broadly concern: 1) the machine, 2) the mixing vessel, and 3) the formulation. Table I-2 summarises these. Since the formulation of 'PBneXt' will be optimised for final properties, machine and vessel variables are of greatest relevance for optimising mixing. Machine and vessel variables identified as being omitted or under-reported (anecdotal or unsubstantiated claims) in the literature (coloured red) are further studied in this thesis. The expected effects of these factors are here briefly explained; acceleration setting and 'intensity' setting (linked to machine power draw) are expected to affect acceleration, as may mixer model and mixer unit depending on calibration or variation between machines. Wall material, specifically with regards to surface free energy is expected to affect work

Table I-1: The salient factors affecting the efficiency of churning.

| | Reduces wall-slip | Increases movement |
|---|---|---|
| Physical | | Higher acceleration<br>Higher density<br>-Greater inertial forces |
| | Higher viscosity formulation<br>-Greater interfacial drag<br>-Greater tackiness | Lower viscosity formulation<br>-Greater compliance |
| | Smaller diameter vessel<br>Optimised roughness average<br>-Greater interfacial drag | Larger diameter vessel<br>-Greater compliance |
| | | Vacuum application<br>-Greater inertial forces<br>-Greater compliance |
| Chemical | Lower surface tension<br>Higher surface free energy<br>-Greater spreadability | Lower surface tension<br>-Greater compliance |
| Other | | Mixer calibration<br>-Greater inertial forces |

of adhesion, while surface finish is expected to affect the surface roughness thus interfacial drag. Figure I-2 shows the variables under investigation in context of the how they are believed to change the efficiency of mixing. The figure is based on the findings of the literature review, the experimental outcomes of this thesis, and the author's conjecture. A more detailed explanation of the figure is given in the 'Overall Discussion' chapter of the thesis.

Table I-2: Machine variables, vessel variables, and formulation variables for Resonant Acoustic Mixing.

| Machine variables | Vessel variables | Formulation variables |
|---|---|---|
| Acceleration setting | Vacuum setting | Binder content |
| Intensity setting | Wall material | Plasticiser content |
| Mixer model | Wall surface finish | Additives |
| Mixer unit | Diameter | Solids loading |
| | Insulation | Particle shape |
| | Active heating | Filler type |
| | Active cooling | |

A method to determine the point of mixing completion for loaded suspensions is also identified, from a study in which RAM was applied to concrete mixing.[34]

The method is non-intrusive, relying on the interpretation of either acceleration or machine 'intensity' (related to machine power draw) data. It is based on the assumption that once the material is homogeneous, the rheology will stop changing, thus the power required to move the material will become constant. This can be interpreted from a graphical plot of mixer intensity against time, where different stages of mixing correspond to different features on the profile. A method to determine the energy supplied to the mixture as derived by the manufacturer is also identified.[35, 36] The method is based on the calculation of mechanical work being done by the mixer at any given point, and suggested to be applied over the duration of a mixing cycle to determine the cumulative energy supplied to the mixture. It is noted that the effectiveness of the method has not been independently verified, and the use of alternative methods based on thermal and electrical monitoring could also be explored.

### Paper 2 - A Method to Determine the Process Efficiency of Resonant Acoustic Mixing

**Overview:** Using an inert PBX simulant based on glass microbeads as an idealised filler, the aforementioned method to assess mixing evolution by the interpretation of mixer 'intensity' data is assessed. Three techniques to determine the energy supplied to the mixture are used to assess the cumulative mixing energy. These methods are based on mechanical, electrical, and thermal data monitoring. The mechanical method as originally presented by the manufacturer[35, 36] has previously been employed,[34, 37] while an electrical method and thermal method have been developed by the author from literature data and methodology presented by the manufacturer[38] and academia.[39] This chapter addresses Objective 2.

**Outcomes:** This chapter gave a positive result, with the interpretation of intensity profiles successfully being used to determine the stages of mixing evolution with respect to time. It is also found that beyond the end of mix point (where the rheology, thus intensity readout, was expected to become constant), further rheological changes occur due to the strong temperature dependence of viscosity for the polymer bonded system; as the system continues to heat up after the end of mix the viscosity continues to fall. Easily distinguishable features are apparent in the profiles, which directly relate to the rheological changes during mixing and after mixing completion. These features are suggested to be of use when comparing the time required for mixing under different conditions. The three different methods used to

determine the energy supplied are found to give the same trend at the same order of magnitude, although there are some discrepancies in the absolute values.

### Paper 3 - The Effect of Machine Variables on the Efficiency of Resonant Acoustic Mixing for Polymer Bonded Explosives

**Overview:** This chapter is concerned with machine variables as listed in Table I-2. The effects of changing acceleration (45 G, 50 G, 55 G), mixer intensity (67 % and 75 %), mixer model (500 g scale LabRAM and 1 kg scale LabRAM II), and mixer unit (three different LabRAM units) on mixing efficiency are explored using the aforementioned glass microbead formulation. The easily distinguishable features of the intensity profiles (as previously mentioned) are used to determine and compare the times required for the end of mix point and onset of further rheological changes in each case. The mechanical, electrical, and thermal methods are used to determine the energy supplied. This chapter partially addresses Objective 3.
**Outcomes:** This chapter gave a positive result, with higher acceleration and higher intensity setting requiring reduced time, and unexpectedly, reduced energy to mix (thus greater efficiency), by each metric considered. Mixing at constant intensity as opposed to constant acceleration was found to have no intrinsic drawbacks. Interestingly, changing mixer model to a LabRAM II was found to increase the time required for mixing by approximately 50 %, despite the acceleration setting, vessel variables, and formulation variables remaining constant. This was attributed to better acceleration control meaning brief but frequent fluctuations to higher acceleration (observed when mixing with a LabRAM) were not present. Additionally, significant variation was found between LabRAM units, with mixing on one of the LabRAM units taking approximately a third of the time required by another. This was attributed to potential variations in manufacture and calibration.

### Paper 4 - The Effect of Vessel Material on the Efficiency of Resonant Acoustic Mixing for Polymer Bonded Explosives

**Overview:** This chapter is concerned with vessel variables, specifically vessel wall material. The effects of vessel materials with low, medium, and high surface free energies (poly(tetrafluoroethylene) (PTFE), poly(methyl methacrylate) (PMMA), and titanium) on mixing efficiency are explored, again using the aforementioned glass microbead formulation and methodology. This chapter partially addresses Objective 3.

**Outcomes:** This chapter gave a positive result, with the higher surface free energy PMMA vessel requiring reduced time and energy to mix (thus greater efficiency) than the PTFE vessel by each metric considered. This was attributed to a higher work of adhesion to surface tension ratio (lower contact angle) between the binder and vessel wall reducing the amount of wall slip. Titanium, which was expected to have the highest surface free energy (from its metal oxide surface) was in fact found to have a surface free energy similar to that of PMMA, likely because of surface contamination. Despite having a similar mixing time to PMMA, the rate at which further rheological changes occurred were shifted to a significantly longer duration than expected. This was due to the conductive thermal properties of titanium in comparison to the polymeric PMMA and PTFE, where a heatsink effect was believed to reduce the rate of temperature increase, reducing the rate of viscosity reduction.

### Paper 5 - The Effect of Vessel Surface Finish on the Efficiency of Resonant Acoustic Mixing for Polymer Bonded Explosives

**Overview:** This chapter is concerned with vessel variables, specifically vessel wall surface finish. The effects of changing surface finish (smooth, rough, and ribbed) on mixing efficiency are explored, again using the aforementioned glass microbead formulation. This chapter partially addresses Objective 3.

**Outcomes:** This chapter gave a null result, with no significant difference being found between the vessels, despite it being expected that the roughened vessel would provide better coupling thus faster mixing. Additionally, the clear mixing stages as seen in the intensity profiles in the previous experiments were not apparent. This was attributed to the lack of vacuum application somewhat inhibiting vigorous (thus high mixer intensity) churning (bulk motion), by reducing the inertial forces. Vacuum could not be applied due to the porosity of the vessels, which were 3D printed with acrylonitrile butadiene styrene (ABS) plastic. It is recommended the experiment be repeated using machined vessels, and cautioned that 3D printed vessels (at least in the form considered) are unsuitable for mixing under vacuum.

### Paper 6 - The Effect of Mixing 'In-situ' on the Tensile Properties of Resonant Acoustic Mixed Polymer Bonded Explosives

**Overview:** The degree to which product outcome (based on tensile properties) is reproducible between 'mixed and cast' and 'in-situ' mixed is investigated with an inert (ammonium sulphate) formulation. An ad hoc method to manufacture

small samples of PBX 'in-situ' is developed for this purpose. This chapter partially addresses Objective 4.

**Outcomes:** This chapter gave a null result, with no statistically relevant differences in elongation at break or elastic modulus being observed between each processing method. However, it should be noted that any differences (which were expected to be subtle) may have been masked by solid settling, which occurred during curing to a similar extent across all the samples manufactured. Interestingly, also observed was a layering effect whereby elongation at break increased and elastic modulus decreased further down each sample, the causes of which are unclear. It is recommended this experiment be repeated with a higher solids loaded formulation, and an industry use casting process.

### Overall Perspective, Conclusions, and Future Work

**Overview:** The findings of the literature review and experimental chapters are summarised and discussed in a broader context. The main conclusions of the work are then linked back to their industrial consequences for PBX manufacture, and a short guide of how to optimise the efficiency of PBX mixing with RAM is provided. Recommendations for future work are also given. This chapter addresses Objectives 3, 4, and 5.

### Appendices

**Overview:** Additional data is presented for partially completed experiments that aimed to investigate the mixing behaviour when different filler shapes (spherical glass beads and angular crushed glass) and filler types (live explosives - RDX) are used. Mixer intensity profiles for these experiments are presented and briefly commented on in Appendix 1 and Appendix 2 respectively. Appendix 3 presents and describes the mixer intensity profile that was observed during the catastrophic failure of a mixing vessel. Appendix 4 reports on preliminary compatibility testing between Araldite 2011 epoxy resin (used in Paper 6 - Mixing 'In-situ') and RDX.

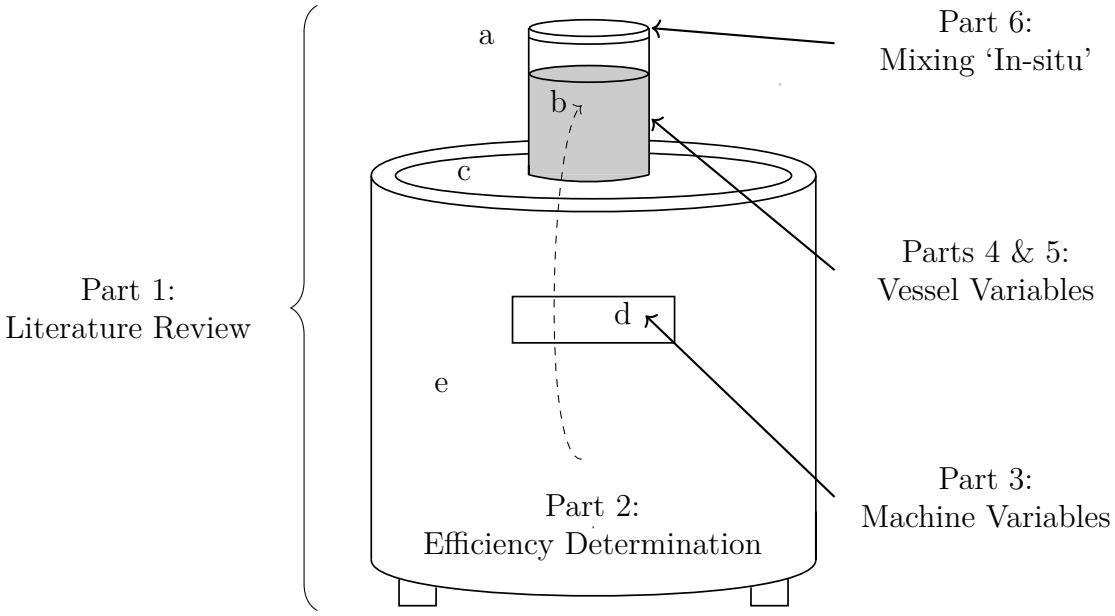


Figure I-1: Simplified graphic of a LabRAM, showing: a - mixing vessel, b - mixture, c - vibrating platform, d - control panel, e - resonator housing.

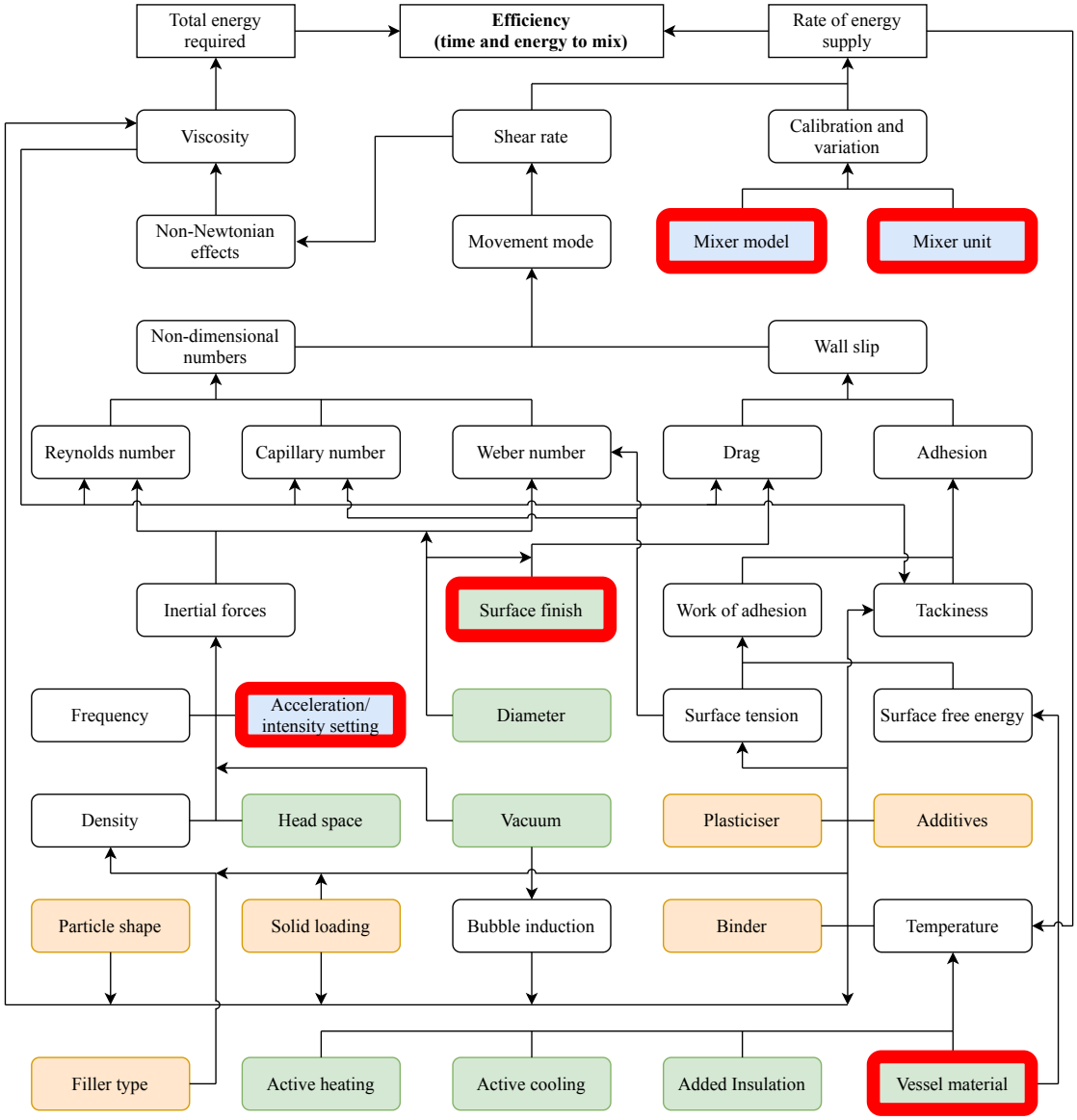


Figure I-2: Chart linking the factors believed to affect mixing efficiency, and their interdependence. Highlighted red are the factors investigated in this thesis. Coloured cells indicate: blue - machine variables, green - vessel variables, orange - formulation variables.

## References

[1] D.B. Todd. Mixing of highly viscous fluids, polymers, and pastes. In *Handbook of Industrial Mixing: Science and Practice*. John Wiley & Sons, Inc., 2004.

[2] M.A. Daniel. Polyurethane Binder Systems for Polymer Bonded Explosives. Australian Defence Science and Technology Organisation, December 2006. DSTO-GD-0492.

[3] A.C. Hordijk and A.E.D.M. van der Heijden. Mixing. In *Energetic Materials; Particle Processing and Characterization*. Wiley-VCH Verlag GmbH, 2005.

[4] R.J. Davey, J.M. Wilgeroth, and A.O. Burn. Processing Studies of Energetic Materials using Resonant Acoustic Mixing Technology. BAE Systems Land UK, Glascoed, Monmouthshire, UK, 2019.

[5] A. Nelson and M. Miller. Resonant Acoustic Mixing of High- Energy Composite Materials. SERDP & ESTCP Symposium, Washington D.C., USA, 2018.

[6] M. Andrews, C. Collet, A. Wolff, and C. Hollands. ResonantAcosutic Mixing Processing and Safety. Munitions Safety Information Analysis Center, May 2019.

[7] BAE Systems Land UK. New mixing technology achieves more explosive power. `https://www.baesystems.com/en/article/new-mixing-technology-achieves-more-explosive-power`. Accessed 14-07-2020.

[8] Inc. Resodyn Acoustic Mixers. Resonant Acoustic Mixing (Technical White Paper). ResoDyn Corp, Butte, MT, USA, 2009.

[9] Inc. Resodyn Acoustic Mixers. LabRAM Resonant Acoustic Mixer Manual. ResoDyn Corp, Butte, MT, USA, February 2012.

[10] M.D. McPherson. Propellant and explosives production method by use of resonant acoustic mix process. Patent WO 2009/091430 A1, July 2010.

[11] Department of Defense (US). Explosive, Plastic Bonded, Cast PBXN-109. MIL-E-82886(OS).

[12] R.M. Dexter, B.M. Hamshere, and I.J. Lochert. Evaluation of an Alternative Grade of CXM-7 for Use in PBXN-109, The Explosive Fill for the Penguin ASM Warhead. Australian Defence Science and Technology Organisation, August 2002. DSTO-TN-0441.

[13] NATO. Explosives, Specification for RDX (Hexogene). STANAG-4022.

[14] U. Teipel, A.C. Hordijk, U. Förter Barth, D.M. Hoffman, C. Hübner, V. Valtsifer, and K.E. Newman. Rheology. In *Energetic Materials; Particle Processing and Characterization*. Wiley-VCH Verlag GmbH, 2005.

[15] A.N. Gent. Detachment of an Elastic Matrix from a Rigid Spherical Inclusion. Institute of Polymer Science, University of Akron, Akron, Ohio, USA, 1980.

[16] D.W. Nicholson. On the detachment of a rigid inclusion from an elastic matrix. *J. Adhesion*, 10:255–260, 1979.

[17] J. E. Field, S. J. P. Palmer, P. H. Pope, R. Sundararajan, and G. M. Swallowe. Mechanical properties of PBXs and their behaviour during drop-weight impact. Proc. 8th Symp. (Int.) on Detonation, (ed. J.M. Short), White Oak, MD: Naval Surface Weapons Center, 1985.

[18] S.J.P. Palmer, J.E. Field, and J.M. Huntley. Deformation, strengths and strains to failure of polymer bonded explosives. *Proc. R. Soc. Lond. A*, 440:399–419, 1993.

[19] W.G. Proud, S.J.P. Palmer, J.E. Field, G. Kennedy, and A. Lewis. AFM studies of PBX systems. *Thermochimica Acta*, 384:245–251, 2002.

[20] C.R. Siviour, M.J. Gifford, S.M. Walley, W.G. Proud, and J.E. Field. Particle size effects on the mechanical properties of a polymer bonded explosive. *J. Mater. Sci.*, 39:1255–1258, 2004.

[21] D.M. Williamson, S.J.P. Palmer, and W.G. Proud. Fracture Studies of PBX Simulant Materials. Shock Compression of Condensed Matter, July 2006.

[22] C.R. Siviour, P.R. Laity, W.G. Proud, J.E. Field, D. Porter, P.D. Church, P. Gould, and W. Huntingdon-Thresher. High strain rate properties of a polymer bonded sugar: their dependence on applied and internal constraints. Proceedings of the Royal Society, 464, 1229-1255, January 2008.

[23] J.E. Balzer, C.R. Siviour, S.M. Walley, W.G. Proud, and J.E. Field. Behaviour of ammonium perchlorate based propellants and a polymer-bonded explosive under impact loading. Proceedings of the Royal Society A, 460, March 2004.

[24] H. Moulard, J.W. Kury, and A. Delclos. The Effect of RDX Particle Size on the Shock Sensitivity of Cast PBX Formulations. 8th Symposium (International) on Detonation, Albuquerque, New Mexico, USA., 1986.

[25] H. Moulard. Particular Aspect of the Explosive Particle Size Effect on Shock Sensitivity of Cast PBX Formulations. 9th Symposium (International) on Detonation, Portland, Oregon, USA., 1989.

[26] A.C. van der Steen, H.J. Verbeek, and J.J. Meulenbrugge. Influence of RDX Crystal Shape on the Shock Sensitivity of PBXs. 9th Symposium (International) on Detonation, Portland, Oregon, USA., 1989.

[27] F.P. Bowden and A.D. Yoffe. *Fast Reactions in Solids*. Butterworths Scientific Publications, 1958.

[28] J.L. Jordan, D. Montaigne, P. Gould, C. Neel, G. Sunny, and C. Molek. High Strain Rate and Shock Properties of Hydroxyl-Terminated Polybutadiene (HTPB) with Varying Amounts of Plasticizer. *J. Dyn. Behav. Mater.*, 2:91–100, 2016.

[29] J.P. Agrawal. *High Energy Materials - Propellants, Explosives and Pyrotechnics*. WILEY-VCH Verlag GmbH & Co. KGaA, Weinheim, 2010. pp. 108, 163-166, 173-174, 268.

[30] P.A. Lucon and J. Whaley. Liquids and Pastes. Resodyn Technical Interchange, Butte, Montana, USA, 2016.

[31] E.L. McCloy, P. Wilkinson, and P.P. Gill. Resonant Acoustic Mixing: Pushing The Boundaries. Master's thesis, Cranfield University, 2016.

[32] P.A. Lucon, G. Sperry, and J. Whaley. RAM Mixing of Liquids and Pastes. Resodyn Technical Interchange, Butte, Montana, USA, 2016.

[33] P.A. Lucon. Mixing with Vacuum Assist. Resodyn Technical Interchange, Butte, Montana, USA, 2016.

[34] A. Vandenberg and K. Wille. Evaluation of resonance acoustic mixing technology using ultra high performance concrete. *Constr. Build. Mater.*, 164:716–730, 2018.

[35] J.T. Miller, A. Luebbering, S. Coguill, and P. Lucon. Mix Power. Resodyn Forum: Industrial Outcomes in ResonantAcoustic Mixing, Butte, Montana, 2013.

[36] P.A. Lucon. RAM Power Considerations. Resodyn Technical Interchange, Butte, Montana, USA, 2016.

[37] J.G. Osorio and F.J. Muzzio. Evaluation of resonant acoustic mixing performance. *Powder Technol.*, 278:46–56, 2015.

[38] J. Whaley. Private Communication, Resodyn Acoustic Mixers, April 2020.

[39] J. Hilden, M. Sullivan, M. Polizzi, J. Wade, J. Greer, and M. Keeney. Power consumption during oscillatory mixing of pharmaceutical powders. *Powder Technol.*, 338:44–54, 2018.

# Paper 1 - A Review of Resonant Acoustic Mixing Efficiency for Polymer Bonded Explosives

Andrew J. Claydon, Guillaume Kister, Sally Gaulter, and Philip P. Gill

**Abstract:** Resonant Acoustic Mixing (RAM) is a promising alternative for the mixing of Polymer Bonded Explosives (PBXs) in comparison to conventional high shear techniques. Here, an overview of conventional PBX manufacture is given, followed by a review of RAM with regards to the operation of the technique, the potential to create novel PBX formulations, and the factors that are known to affect mixing efficiency. The major benefit of RAM is found to be the ability to mix formulations 'in-situ', allowing for the production of novel high viscosity of PBX formulations without the need for casting, and the production of little to no waste. Viscous mixing with RAM is found to rely on a churning motion, whereby shear is generated from bulk rolling and smearing brought about by a velocity gradient across the vessel contents. The bulk of the material is acted upon by acoustic pressure waves (vibrations), while there is ideally 'no-slip' at the vessel wall. Greater efficiency (reduced time and energy required for mixing) is determined to be achieved when there is greater bulk movement and the 'no-slip' condition is better fulfilled. It is reported these conditions can be affected by aspects of the machine (e.g. acceleration setting, intensity setting), the vessel (e.g. diameter, vacuum application), and the formulation (e.g. solids loading, plasticiser content). However, the effects of many variables are found to be under-reported or omitted from the literature.

**Keywords:** Resonant Acoustic Mixing, Polymer Bonded eXplosive, PBneXt, Efficiency

## Introduction

Mixing can be described as a process in which non-uniformity within a mixture is reduced, and is a necessity in many different industries such as energetics, food, and pharmaceuticals.[1] Mixing is often required between solids (i.e. powders), liquids, and gases in various combinations depending on the nature of the starting materials and the desired outcome of the mixing process, and the method of mixing is chosen accordingly. For viscous suspension mixing a large amount shear is required, and can be achieved with a high shear mixer that uses intrusive blades to stretch, knead, or smear the material.[1, 2] The manufacture of Polymer Bonded eXplosives (PBXs) is one such instance where high shear mixers are employed, whereby explosive crystals are mixed into a viscous polymer binder.[2] The resultant mixture can then be cast-cured to form a rubbery explosive composite. Resonant Acoustic Mixing[3, 4] (RAM) is a novel approach to mixing that has recently gained considerable attention[5] as an alternative to conventional techniques for PBX mixing. Simply put, the technique relies on acoustic pressure waves (vibrations) to agitate the material, in a non-intrusive mixing process. RAM is expected to bring benefits such as considerably reduced mixing times[6, 7] and the possibility for mixing 'in-situ' (or 'in-case'), whereby the end use container doubles as the mixing vessel, omitting the need for casting.[6–8] This is expected to allow for the formulation of next generation high viscosity PBXs with improved properties and reduced waste.[9]

### Aims of this review

The aim of this work is to initially provide a background of explosives and mixing as subject matters, identify what should be expected of next generation PBX formulations, and determine how RAM could be used in their implementation. The review then goes on to assess the extent of current knowledge with regards to how mixing behaviour can be characterised and the factors that affect mixing efficiency.

## Energetic materials

Encompassing the broad terms of explosives, propellants and pyrotechnics, energetic materials have various uses in a diverse selection of military and civil applications. These substances hold large amounts of chemical potential energy, which can be

rapidly released during a chemical reaction. Explosives are energetic materials that can rapidly combust in a chemical explosion, which can be defined as an fast (microsecond scale) chemical reaction which suddenly releases gas and heat. Deflagration can be defined as a combustion reaction whereby a self sustaining flame front propagates through a material by heat transfer at subsonic[a] speed. Conversely, detonation can be defined as a rapid combustion reaction constituting an explosion in which initiation is propagated through the material by way of a supersonic[b] shock wave, rather than by heat transfer from a flame front. Secondary explosives, commonly known as high explosives, detonate given suitable conditions, and primarily assume the role of the main charge (and booster charge if required) in explosive devices. An important class of high explosives are nitroamines (or nitramines), with the two most prevalent being RDX[c] and HMX[d]. HMX is used in applications where high detonation pressure is required, whereas RDX is used in most other applications due to its lower cost, wider availability, and lower sensitivity.

### Polymer Bonded Explosives

Polymer Bonded eXplosives (PBXs) are rubbery composite materials that consist of high explosive crystals dispersed in a polymeric binder. Many PBXs are 'cast-cured', beginning as viscous suspensions before being cast into their casing to undergo a curing reaction to form a solid material. The ubiquitous filler ingredients for general use are typically RDX or HMX as previously described, though depending on application, a reactive metal such as aluminium powder may also be incorporated to improve blast effect.[10] End-use binders are typically a cross-linked elastomeric polyurethane, resultant of the product of a hydroxyl-terminated pre-polymer cured with an isocyanate. The purpose of the binder is to hold the crystals together while preventing direct contact between them. This prevents hotspot formation and potential initiation[11] from frictional heating or shear between crystals under accidental stimuli.[12] The elastomeric nature of the binder also acts as a cushion under shock and impact, preventing cracks that would otherwise form with a brittle binder such as TNT.[e] Such cracks within energetic composites are susceptible to adiabatic compression under accidental stimuli and can act as hotspot[11] initiation sites, potentially leading to unintended explosions. Brittleness is therefore an undesirable

[a] Subsonic relative to the speed of sound in the medium
[b] Supersonic relative to the speed of sound in the medium
[c] 1,3,5-trinitro-1,3,5-triazinane
[d] 1,3,5,7-tetranitro-1,3,5,7-tetrazoctane
[e] 2,4,6-trinitrotoluene

characteristic, and should ideally be avoided.

Of the binder pre-polymers available, hydroxy-terminated polybutadiene (HTPB) pre-polymer is the most prevalent,[13] and is available in several grades such as continuously processed commercial grade R-45HTLO, and higher quality batch processed R-45M (military). The latter is however not normally required since the cheaper R-45HTLO typically complies with PBX specification requirements.[13, 14] With regards to curative, isophorone diisocyanate (IPDI) is commonly used, as is di(2-ethylhexyl) adipate[f] (DEHA) as a plasticiser. Plasticiser is usually included to make the PBX easier to process (mix and cast). Other binders, curatives, and plasticisers can alternatively be employed in some instances, such as hydroxy-terminated polyethers and multifunctional isocyanates such as hexamethylene diisocyanate (HDI) biuret. HTPE is particularly required in instances where incorporation of energetic plasticisers (which improve explosive output) such as N-butylnitratoethylnitramine (butyl-NENA) is required, due to their miscibility.[13]

Additives that can be incorporated include bonding agents such as Dantocol DHE,[g] which adsorbs onto the nitramine filler and cures into the binder,[15] improving the interfacial strength. Processing aids such as lecithin are also used to promote interfacial interactions by reducing the surface tension of the binder, allowing it to better wet the filler surface. Furthermore, curing catalysts such as triphenylbismuth (TPB) and antioxidants such as AO 2246[h] can be included to decrease curing time and increase shelf-life respectively.[13]

As part of the manufacturing process, the ingredients must first be mixed together to disperse each component evenly, so the performance, mechanical, hazard, thermal, and ageing properties are the same over the whole volume of the product.[2] Optimisation of mechanical properties is particularly important since they can affect the failure modes of the material under deformation and subsequent hazard response.[16] For the same reason, the crystals must be fully wetted and incorporated into the binder as to prevent weak points such as voids and defects within the matrix.

[f] Commonly referred to as dioctyl adipate or DOA
[g] N,N-di(2-hydroxyethyl) dimethyl hydantoin
[h] 2.2-methylenebis-(4-methyl-6-tertiary-butylphenol)

## Mixing overview

Different mixing techniques are suitable for different applications, and relevant mixers are chosen accordingly. For example, powder mixing often employs tumbling motions, such as in rotating drum mixers.[17] Since such mixers are inherently gentle and have low shear, they are generally unsuitable for incorporating liquids and solids. Videos of drum mixers in operation are available online.[18] Detailed reviews of power mixing have been given by Muzzio *et al*,[19] and Sastry *et al*.[17]

### Low shear

For mixing low viscosity suspensions ($<$ 10,000 cP),[1] agitating blades are required. Axial flow impellers are often used, where relative to the plane of rotation the blade has an angle of $<90°$. The impeller shaft is typically mounted off centre, and may be at an angle ($\sim$15°) relative to vertical. This creates a flow pattern parallel to the drive shaft,[20] that imparts gentle shear throughout the mixture (dispersed shear). One such design for very low viscosity mixing is the propeller blade mixer,[21] which has a shallow blade angle as low as 10°.[22] Pitched blade turbines, which have a steeper blade angle of 45°, achieve flow both parallel (axial flow) and perpendicular (radial flow) to the impeller shaft. This provides a good compromise of flow (thus gentle shear) throughout the volume of the vessel, and slightly higher shear in the vicinity of the blades (localised shear). This makes it more versatile than propeller mixers, being suitable for slightly higher viscosities.[21]

However, the above mixers are unsuitable for mixing highly loaded viscous suspensions such as those found in PBX manufacture. This is because they rely on turbulent flow, which is only possible when inertial forces (deforming the material) are large in comparison to viscous forces (resisting deformation). Additionally, the low viscosity materials for which they were designed are required to be drawn into the blades, and as such, there is typically a large clearance between the impellers and vessel wall. This leads to large unmixed areas when bulk flow is impeded by high viscosity. Without effectively circulating the material, such impellers can even create an isolated void in the vicinity of the blades, into which no material at all is drawn.[1, 20] Photographs of impeller mixers are available online.[21] More detailed reviews of techniques for low shear applications have been given by Atiemo-Obeng *et al*,[23] Hemrajani and Tatterson,[22] and Dahlstrom *et al*.[20]

### High shear

A number of methods can be employed for mixing highly loaded powder-liquid compositions (> 10,000 cP),[1] where contrary to circulating the material, stretching, kneading, or smearing actions are used to agitate and deform it. The key difference to low viscosity mixing is that high viscosity mixing is laminar; that is to say there is no turbulent flow. A range of mixers are suited to this role, and employ metal blades that move in order to maximise shear. Such mixers typically have a smaller clearance between blades and the mixing vessel wall, a larger power to volume ratio, and slower blade speeds in comparison to low shear impeller mixers.[1, 20] One such mixer is the helical blade mixer, which consists of a rotating helical or double helical ribbon that may be either conical or cylindrical. The shape of the blade acts as a screw, rapidly conveying material and shearing it in doing so. Photographs are available online.[21] However, the two most common high shear mixers for PBX manufacture are vertically oriented 'change-can' mixers such as the planetary mixer, and horizontally oriented double-arm kneading mixers such as the z-blade mixer. These mixers respectively consist of orbiting blades that also rotate on their own axes, or two specially designed 'z' or 'sigma' (ς) shaped blades which rotate in close proximity at different speeds to knead the material.[24, 25] Photographs of high shear mixers can be found online.[24]

Although readily available and well characterised, high shear batch mixing of this type has several drawbacks. Pinch points between the blades can comminute filler particles, leading to a change in particle size distribution.[2] This may alter the characteristics of the product such as end of mix viscosity[26] mechanical response,[27] and energetic properties,[2] though such changes are usually accounted for in industrial manufacture. In addition, the areas of maximum shear occur only in proximity of the blades themselves, localising mixing to only small volumes of material at any one time. This can lead to the requirement for long mixing durations, whereby the process must also be repeatedly paused for both the blades and vessel wall to be manually scraped down. The incremental addition of ingredients is also required.[2, 7] For example, coarse filler is typically mixed into the binder before fine filler addition to minimise peak viscosity. Traditional mixing also produces a significant amount of waste (∼12.5 % of the total formulation on industrial scale,[7]) since the mixing container and blades must be cleaned after use. This has environmental and cost implications, as well as being labour intensive and hazardous for workers.[6] Furthermore, scale-up from laboratory-use mixers to industrial manufacturing can require

special consideration, for reasons such as design limitations on agitator speed[20] and decreasing blade surface area to mix volume ratio as size is increased.

### Continuous mixing

Production rate can be increased with the use of continuous mixing, whereby feedstock is constantly supplied and mixed material constantly produced. Twin screw extrusion is one such technique for continuous mixing of high viscosity materials, and consists (in its most common form[20]) of co-rotating intermeshed screws which act to convey the material along the length of the barrel (screw housing) through groups of kneading paddles under high shear.[20] While high throughputs can be achieved with continuous mixing in general, the input flow rate of ingredients must be sufficiently accurate such that fluctuations in product output are within the permitted limits for reproducibility and quality control.[17] More detailed reviews of traditional techniques for a high-shear applications have been given by Dahlstrom *et al*,[20] Todd,[1] and in the context of energetic materials, Hordijk and Heijden.[2]

### Casting

Once mixed, the pre-cured PBX must be cast into its intended receptacle. Since this process involves the transfer of the material, the viscosity must be low enough such that the process is possible. For this reason, casting is typically carried out at elevated temperatures (∼60 ℃), where the strong inverse proportionality of viscosity to temperature improves the castability without altering the contents of the formulation. It has been reported that the viscosity of a binder/plasticiser (85/15 % w/w) mixture was reduced by over an order of magnitude by increasing the temperature from 21 ℃ to 60 ℃.[28] Furthermore, casting is often carried out under vacuum,[12] to help 'pull' the material into the case, and should be undertaken in a timely manner due to the progression of the curing reaction (polymerisation) incrementally increasing the viscosity.

Changes to the formulation can also be made to reduce viscosity, with plasticisers (low molecular weight polymers) typically included in PBX formulations for this purpose.[13] In the same study in which temperature was increased as referenced above,[28] reducing the binder/plasticiser ratio (to 70/30 % w/w) was reported to further reduce viscosity by a factor of two. Additionally, a relatively low (in comparison to pressed PBX) solids loading (∼87 % w/w) is typically used,[12] and particle size is typically kept quite coarse (usually ranging from the tens to the hundreds

of microns in diameter[29]), since the greater surface area to volume ratio of smaller fillers increases the viscosity. In summary, casting is a laborious but conventionally unavoidable procedure, which imposes limits on the viscosity of the formulation.

## Resonant Acoustic Mixing

Resonant Acoustic Mixing (RAM) is a novel mixing technique which basically consists of a spring mounted platform that vibrates vertically at mechanical resonance. Attached to the vibrating platform is an enclosed mixing vessel, through which energy is imparted on the mixture in the form of longitudinal acoustic pressure waves (vibrations). This provides medium shear over the whole volume of the vessel. A brief comparison of RAM compared to other batch mixing techniques is given in Table 1-1.

Table 1-1: Comparison of batch mixing techniques.[1–3, 17, 19–25]

| Mixer | Operation | Shear | Viscosity (cP) |
|---|---|---|---|
| Tumble | Horizontally oriented rotating drum | Extremely low, dispersed | Powders |
| Propeller | Axial flow impeller 10° blade angle | Very low, dispersed | 5,000 |
| Pitched blade turbine | Axial flow impeller 45° blade angle | Low, dispersed | 25,000 |
| Helical blade | Vertically oriented rotating helix | Medium, localised | 150,000 |
| Planetary | Vertically oriented orbiting blades | High, localised | 2,000,000 |
| Z-blade | Horizontally oriented rotating ‘z’ blades | Very High, localised | 10,000,000 |
| Resonant acoustic | Vertically oscillating platform | Medium, dispersed | 100,000,000 |

### Benefits of RAM

PBX mixing has been found to take significantly less time in comparison to conventional mixing, with mix times of tens of minutes as opposed to hours being reported.[6, 7] This is attributed to the shear being distributed over the entire mixing volume instead of being localised to the vicinity of mixing blades.[3, 4] The absence of mixing blades also means the mixer does not have to be paused to scrape them

down, further streamlining the process and reducing the hazard exposed to workers. Despite the reduced mixing times, product outcome in terms of mixture quality (thus mechanical and energetic properties) has been found to match[7, 30, 31] or even exceed[31–33] that seen with conventional high shear techniques, suggesting more thorough mixing is occurring.

Though RAM is being developed up to industrial scale batch production for PBX casting with the 420 kg capacity RAM 55 (55 US gallon / 208 litre mixing vessel), a major advantage is the possibility for 'in-situ' mixing. This concept is also referred to as 'mixed in-case', and refers to scenarios in which the warhead or bomb case doubles as the mixing vessel of the PBX, removing the need for casting and the associated complexities.[6–8] Waste could be virtually eliminated since there would be no requirement for cleaning, significantly reducing costs and time. This would also have a positive environmental impact since waste is typically disposed of by open burning. The technique may also allow for the production of highly viscous novel formulations. While conventional z-blade mixers can operate with viscosities up to 10,000,000 cP,[24, 25] the actual viscosity of the formulation used must be restrained to levels required to enable casting. For context, the measured end-of-mix viscosity for a typical castable formulation[14] is approximately 100,000 cP at a typical elevated processing temperature of 60 ℃.[34] Conversely, it is claimed that RAM can mix materials with viscosities on the order 100,000,000 cP,[3] and when mixing 'in-situ', could be used with formulations of such viscosities. This ability opens up an opportunity for improved next generation PBXs (termed 'PBneXt' by BAE Systems) to be developed.

A major theme of 'PBneXt' formulations is expected to be the addition of increasingly smaller particle size filler, from the current standards (tens to the hundreds of microns in diameter[29]) down to the micronised and sub-micronised range. Since suspension viscosity increases as solids loading increases this has not previously been practical. Such additions are expected to push the limits of solids loading, from the current castable bi-modal standard[28] (∼78% v/v, or ∼87 % w/w) towards the theoretical maxima of tri-modal (∼95% v/v, spherical approximation) or even tetra-modal (∼98% v/v, spherical approximation) distributions.[35] In terms of filler content by weight, such loadings would closely approximate those of pressed PBXs (>94 % w/w[12]), which consist of explosive crystals coated by solvent deposition with binders such as Estane or Viton that are then compacted under high temperature. For example PBX-9501 (95 % w/w HMX, 2.5 % w/w Estane, and 2.5 % w/w nitroplasticiser) has been pressed under 20,000 psi pressure at a temperature of 90

℃.[36, 37] Such formulations are typically reserved for scenarios where performance is paramount, due to the hazardous processes involved, use of solvents, and the poor mechanical properties[12] in comparison to castable formulations. Suitably loaded formulations manufactured using 'in-situ' RAM may therefore be able to provide pressed explosive performance without the need for solvent binder deposition and a laborious pressing procedure, while bringing the benefits of castable formulation mechanical properties. In essence there is the potential to create a new 'mixed-in-case-able' category of PBXs, alongside the current 'castable' and 'pressable' PBX classifications, which combine the benefits of both while removing the drawbacks.

Compared to current castable formulations, 'PBneXt' is expected to bring benefits such as better performance (more explosive component), improved mechanical properties[27, 38–42] (since affinity to the binder increases with larger particle surface area, thus smaller size), and improved hazard response (since smaller particle size has been correlated to fewer internal defects which can act as hotspot[11] initiation sites[43–48]). Another step that may be taken is the reduction or elimination of plasticiser, which is typically added to lower the viscosity of the formulation to aid the casting process.[12, 13] Without plasticiser being included, better ageing characteristics may be expected since plasticiser migration[12] (which leads to embrittlement and cracking) would no longer occur. Simply put, current castable PBX formulations are a compromise between processability on one hand, and performance, mechanical, and ageing properties on the other. Using 'in-situ' RAM, processability essentially becomes irrelevant.

It may also be found that mixed 'in-situ' PBX has superior properties to 'mixed and cast' PBX, without making changes to the formulation. Possible differences may arise from variation in particle packing arrangement, where it is reported that anisometric particles in suspension align their longitudinal axis with flow direction.[49] The pouring process as found when casting may therefore result in poorer packing (thus lower density) compared with a PBX mixed in-situ, especially since the vibration of the RAM process may settle particles closer together in the same way powder bulk density increases after subjected to vibration.[17] Increased packing density may alter the mechanical properties of the composite as shown in Equation 1-1.[50i]

$$E = E_0 \left(1 - \frac{\phi}{\phi_{max}}\right)^{-[\eta]\phi_{max}} \qquad \text{(Equation 1-1)}$$

[i] The analogous relation for suspension viscosity (Equation 1-10) is discussed later in this review.

where $E$ is the elastic modulus ( MPa), $E_0$ is the elastic modulus of the continuous phase ( MPa), $\phi$ is the volume fraction of the solid (dimensionless), $[\eta]$ is a parameter that describes the distortion of the strain field due to particle shape (dimensionless), and $\phi_{max}$ is the maximum possible volume fraction for the particle shape and size distribution under consideration (dimensionless). By increasing the volume fraction, $\phi$, closer to $\phi_{max}$, it can be seen that the elastic modulus of the composite will increase. Additionally the casting process has the potential to fold air bubbles back into the material after degassing, whereas the process is eliminated with 'in-situ' mixing. Removal of entrapped gas is important since voids within the material can compromise the mechanical, hazard, and performance properties. This should be investigated as future work.

### Drawbacks of RAM

The aforementioned factors make RAM attractive for future explosives formulation and manufacture. However, RAM is not without drawbacks. For example, while RAM is wholly suitable for *distributive* mixing (increasing spatial uniformity of the components[1]), a concern within industry[51] is that the comparatively low shear imparted on the mixture (in comparison to conventional high shear techniques) may be insufficient for adequate *dispersive* mixing (the break-down of agglomerates[1]). This can be explained with the terms of *intensity of segregation* (the uniformity of the dispersed phase concentration), and *scale of segregation* (the size of the packets of the dispersed phase that can be distinguished from the continuous phase). Using these terms, RAM may therefore provide a sufficient reduction in *intensity of segregation* to provide adequate homogeneity, without providing a sufficient reduction in the *scale of segregation* to provide adequate homogeneity. A pre-processing stage in which agglomerates are broken down may therefore be required in some cases to prepare powders for RAM.[52] More gentle mixing is also believed to be responsible for little observed particle damage, even when mixing dry materials.[53] Although it could be argued this has the advantage of increased safety, conventionally mixed formulations (where particle damage is accounted for) may have different properties to when RAM is used. Additionally, while the ability to add all the materials in a single step (so-called 'one-shot' mixing) without regard for peak viscosity issues simplifies and hastens the overall processing procedure, a multi-step ingredient addition when RAM processing may still be required in cases where there is a hazard posed (i.e. unintended ignition) by dry contact between oxidising and reducing agents (e.g.

ammonium perchlorate oxidiser and aluminium powder reactive metal).[2]

Furthermore, the technology is currently limited by scale in comparison to conventional mixing (208 litre maximum as opposed to 1000+ litre for conventional), and is generally less well characterised. In particular, relatively little research has been undertaken on how to characterise mixing and optimise efficiency, with much of the work that has been carried out known to have been conducted by industry or governments. Such documents are therefore rarely peer reviewed and are often withheld from the public domain, though some academic studies[33, 54–59] are available.

### Continuous RAM

The drawback that RAM batch mixing and mixing 'in-situ' are limited in scale in comparison to conventional techniques has been addressed with the development of continuous mixing adapters, whereby formulation ingredients are continuously loaded into the top of a processing chamber stack mounted to the vibrating platform. Mixed material then leaves the stack via the base and is conveyed into the receptacle to be filled. It is claimed that continuous RAM ('CAM') can achieve material output rates orders of magnitude higher than those possible with batch mixing, and has the benefits of disconnecting the amount waste produced from production volume, since no matter how much material is produced, the same coverage of waste is left in the chamber stack at the end ($\sim$5 kg reported[6] for the CAM modified RAM 5). 'Cleaning in Place' procedures, whereby cleaning solutions are put through the chamber stack and agitated, have also proven very effective at removing residual material whilst producing minimal amounts of aqueous waste.[6] However, a concern within industry is that continuous munition filling without entraining voids into the material may be difficult, and errors associated with controlling the rate of ingredient addition may also adversely affect product quality.[60] In comparison to mixed 'in-situ', where solids loading has been controlled to $\pm$0.3% w/w (3 standard deviations) across the volume of a fill, continuous mixing output has been demonstrated to control solids loading to $\pm$1.5% w/w (3 standard deviations).[6]

### Implementing 'PBneXt'

It is clear that the three possible RAM operation modes (batch mixed, mixed 'in-situ', and continuous mixed) each have advantages and disadvantages, and as such suit different applications. From an industrial standpoint, the 'PBneXt' formula-

tion developed and RAM operating mode used for any particular requirement will be designed as to provide the most benefit and best value for money to the customer.[60] This will obviously have to be undertaken within the practical limitations of each method in mind. For example, if the customer requirement was for a high performance shaped charge or a high stress application (involving large accelerations/decelerations), the lower product quality achieved with CAM may preclude the technique, thus an 'in-situ' approach may be better applicable. However, if a large volume fill is required, an 'in-situ' approach may be impractical (for example if the casing mass is large), thus a batch mixing process may be used instead. Regardless, the formulation used would have to be designed such that it has a processability compatible with the mixing technique, potentially limiting viscosity to a degree.[60] Table 1-2 gives a summary of the advantages and disadvantages of each operating mode, as compared to conventional high shear mixing techniques. Factors addressed are whether there is a requirement for transferring the material (casting or conveying) into the receptacle, the relative time requirement for mixing a given amount of material, the relative product quality (homogeneity across the charge volume), and the relative amount of waste produced.

In order to fully implement RAM for 'PBneXt' manufacture, an understanding of the factors that influence the effectiveness of the technique must first be acquired. By better understanding the mixing mechanisms that underpin the technique, the mixing parameters can be optimised as to maximise efficiency, which for the purposes of this work refers to the time and energy required for mixing completion. This will ultimately unlock the full potential of RAM to revolutionise PBX mixing.

### Further application of RAM

While this review is focused mainly on PBX mixing (high viscosity explosive suspensions), it should be noted that RAM has also found applications in energetics mixing beyond this.[j] Much of what is discussed will be equally applicable to composite propellants, which differ from PBXs only in the sense that their intended use is deflagration (as opposed to detonation), and as such are mainly filled with oxidiser (e.g. ammonium perchlorate) as opposed to nitramine explosives, although a smaller proportion of the latter is often included. Composite propellants will also contain a slightly different selection of additives, such as burn rate modifiers and bonding agents that are applicable to the fillers used.

[j] And indeed other industries such as pharmaceuticals.[58, 59, 61–63]

Mixing of pyrotechnics and energetic moulding powders have also been investigated with RAM, in applications such as nanothermites[64, 65] and pressable propellant[66] and explosive[67] compositions. RAM has even been trialled with primary explosives.[68] In these cases, mixing or coating of powders is required (with or without solvent), and as such will rely on different mixing mechanisms to those applicable to high viscosity PBX and composite propellant suspensions. Though beyond the scope of this work, the mixing mechanisms relevant to powder and low viscosity mixing are briefly discussed later in the review. It should however be cautioned that mixing energetic powders that are sensitive to stimuli need special consideration in comparison to inert materials. For example, while the review goes on to state that powders mix more quickly at higher acceleration setting, acceleration sufficiently high that significant fictional heating occurs may need to be avoided. Other applications of RAM, such as its use in cocrystallisation of energetic materials[53, 69, 70] are not reviewed.

Table 1-2: Comparison of the three RAM configurations as compared to conventional high shear mixing. Green - beneficial, yellow - potential issue, red - drawback.

| | 'In-situ' RAM | Batch conventional | Batch RAM | Continuous conventional | Continuous RAM |
|---|---|---|---|---|---|
| Material transfer | No | Yes | Yes | Yes | Yes |
| Time requirement | Medium | High | Medium | Low | Low |
| Quality control | High | High | High | Medium | Medium |
| Applicable fill volume | <208 L | >1000 L | 208 L | Unlimited | Unlimited |
| Waste produced | Low | High | Medium | Medium | Low |
| Best suited applications | High stress applications (Optimised fill) | Current uses where applicable | High stress applications (Transferable fill) | Current uses where applicable | General use applications (Transferable fill) |
| Best suited munitions | -Missiles<br>-Artillery shells | | -Missiles<br>-Artillery shells | | -Free fall bombs<br>-Torpedoes |

## RAM Overview

The principles which underpin RAM have been discussed in detail elsewhere[3, 4, 71] and will not be exhaustively repeated here. However, it is useful to give a short introduction to the hardware and basic operation in order to understand the factors which affect the mixing process, and contextualise the observations reported in the literature.

### Basic principle

The apparatus consists of a vertically oscillating spring mounted platform to which an enclosed mixing vessel is affixed. For illustrative purposes, the behaviour of the system can be simplified to a one dimensional under-damped sinusoidally driven harmonic oscillator, as given in Equation 1-2.[3, 72]

$$m\frac{d^2}{dt^2}x(t) + c\frac{d}{dt}x(t) + kx(t) = Fsin(\omega_d t) \qquad \text{(Equation 1-2)}$$

where $m$ is the mass of the system ( kg) (i.e. the vibrating plate, mixing vessel and contents), $x(t)$ is the displacement of the plate as a function of time ( m), $c$ is the damping coefficient ( $kg\,s^{-1}$), $k$ is the spring constant ( $N\,m^{-1}$), $F$ is the peak driving force ( N), $\omega_d$ is the angular frequency of the driving force ( rad $s^{-1}$), and $t$ is time ( s).

Each term of Equation 1-2 respectively represents the inertial force, the damping forces (including 'mixing forces',[3] since energy is dissipated in the mixing process, and those from losses due to non-idealities such as internal friction, air resistance, and noise[57]), the spring force, and the driving force. When operating at resonance, the spring force and the inertial force are equal and opposite over one oscillation period, so the first and third terms cancel out. Therefore the mechanical force driving the system is equal to the 'mixing forces' and the force required to overcome other losses to maintain inertia and charge the springs.

When mixing, the exact value of the angular frequency ($\omega_d$) for the subject payload and damping is found and monitored automatically by the inbuilt software. However, since the heaviest aspect of the system is the vibrating plate, with the additional attached mass being incidental in comparison, the mechanical resonant frequency of the system is similar to that of vibrating plate alone, which remains at approximately 60 Hz. The vibrations occur at low amplitude, up to a maximum of

1.4 cm at the highest achievable acceleration of 100 G. This is the same across all mixer sizes.

A choice of two basic user defined parameters are available to control a mixing cycle. These are desired acceleration (given as multiples of acceleration due to gravity, 'G', equal to 9.81 $m\,s^{-2}$) between 0-100 G (and by extension, desired peak inertial force) or desired mixer 'intensity' between 0-100 % (and by extension, desired peak driving force).[k] Percentage in this case is actually that of current supplied to the driver motor up to 5 A in the case of the bench-top scale LabRAM, though this increases for larger models.[l] This parameter is seldom considered in absolute units, instead being left as a percentage. By setting a desired acceleration, the intensity is modified to maintain that acceleration, or vice versa. It would follow that both higher acceleration setting or higher intensity setting would lead to a higher acceleration being achieved, but it is unclear if one 'drive mode' has any implicit benefits over the other.

The imparted acceleration is important since it directly affects the amount of energy which is imparted on the vessel contents.[4] It can therefore be inferred that the damping coefficient $c$ in Equation 1-2 is dependent on the acceleration (amongst other factors). This was shown experimentally by Hilden *et al*[57] where power consumption increased with acceleration when the mixing vessel was unloaded (thus non-ideal contributions to damping increased), with additional energy expenditure when loaded (thus mixing contribution to damping increased). Complementary observations have been made in the literature, where higher acceleration setting[58, 59, 63] (or higher intensity setting that leads to higher acceleration being achieved[33]) and longer mix durations[54, 58, 59, 63] have been reported to improve mix quality, since increasing either parameter imparts more energy on the mixture. Imparted energy has been correlated to the degree of homogeneity when considering both RAM[62] and conventional mixing.[73]

### Energy to mix completion

In conventional mixing, the cumulative energy supplied to a mixture can be determined by the integration (with respect to time) of the power supplied over the duration of a mixing cycle. The power to the mixture is often derived from measurements of the impeller shaft torque.[73] Similarly, it would follow that analogous

[k] Intensity as stated here is often referred to as 'power' or 'power intensity' in the manufacturer's documents.

[l] The maximum power outputs for all the RAM models are given later in this review (Table 1-3).

methods would be applicable to RAM.

When the RAM mixing vessel is not filled, it behaves as a rigid body mass, thus any energy dissipation during operation is wholly due to non-idealities. Therefore, by comparison of the machine's behaviour between when the vessel is filled and unfilled, the power being supplied to the vessel contents at any given time can be discerned from that of other losses. The manufacturer[74, 75] has presented an empirical relation to determine the power transferred into the mixture at any given point from interpretation of intensity and acceleration readouts. The relation is applicable to the bench-top scale LabRAM model, and is given in Equation 1-3. Similar relations are under development for the larger RAM models.[75]

$$P_{mix} = 0.707\mathscr{F}\frac{\Delta I}{100}\frac{a}{2\pi f} \qquad \text{(Equation 1-3)}$$

where $P_{mix}$ is the power going into the mixture ( W) at any given time, $\mathscr{F}$ is an empirically derived LabRAM root mean square force constant (70±4 N),[58] $\Delta I$ is the difference in displayed intensity between when the mixing vessel is and is not filled (%), $a$ is the peak acceleration ( $m\,s^{-2}$) with a 'peak' to root mean square correction factor of 0.707,[58, 75] and $f$ is the normal frequency of the vibration ( Hz). Values for $P_{mix}$ as found at each point throughout a mixing cycle could by extension be used to find the energy required for mix completion by the summation given in Equation 1-4.

$$E_{EOM} = \sum_{t_0}^{t_{EOM}} P_{mix}(t)\Delta t \qquad \text{(Equation 1-4)}$$

where $E_{EOM}$ is the total energy required for mixing ( J), $P_{mix}(t)$ is the instantaneous power going into the mixture ( W), $\Delta t$ is the time increment over which the instantaneous $P_{mix}$ value applies ( s), $t_0$ is the start of mix time ( s), and $t_{EOM}$ is the end of mix time ( s).

Equation 1-3 seems to depend on the assumption that 70±4 N is the maximum force that can be supplied, where the fraction of the force delivered at any given time is proportional to the difference in mixer intensity when loaded to unloaded. This term is then multiplied by the second bracketed term, which equates to the root mean square velocity of the vibration. The resulting units are $N\,m\,s^{-1}$, equivalent to units of power ( W). Hilden *et al*[57] used a different approach in which the electrical power drawn by the mixer (in this case a 1 kg scale LabRAM II) was evaluated both when loaded with mix media and as a rigid body mass. The difference in the two was then taken to be $P_{mix}$ at any given time. Since power was taken to be the product

of current and voltage supplied to the mixer, the method did not account for the non-idealities associated with the machine such as power factor.[76] Nevertheless, the recorded power closely corresponded to the rate of the thermal energy uptake of the vessel contents when applied to powder mixing.

Thermal energy uptake was determined by Hilden *et al*[57] using Equation 1-5.

$$E_{EOM} = [(C_p m)_{mixture} + (C_p m)_{vessel}](T_{EOM} - T_{amb})_{mixture} \quad \text{(Equation 1-5)}$$

where $E_{EOM}$ is the total energy required for mixing ( J), $C_p$ is specific heat capacity ( J g $^{-1}$ K $^{-1}$), $m$ is mass ( g), $T_{EOM}$ is the temperature reached at the end of mix (℃), and $T_{amb}$ is the ambient temperature (℃). While likely providing a decent estimate of energy uptake over the short mixing times (∼5 minutes) considered and small temperature increases (∼ 5 ℃) observed with powder mixing, such a method may be less applicable to PBXs where mix times extend into the tens of minutes and temperatures can reach 80 - 90 ℃.[53] This is because much more thermal dissipation would be expected with longer mixing times and greater temperature increases. Thermal dissipation beyond the mixing vessel is not accounted for in Equation 1-5, though it may be possible that an empirical correction factor could be added to do so. This possibility should be explored in future work. A comparison of all the aforementioned methods should also be undertaken to determine their veracity.

### Mixing evolution

Since the nature of the material being mixed evolves from separate powder and liquid phases into one homogeneous phase over a mixing cycle, so too do aspects of the mixing process. As the material becomes more homogeneous its rheology changes, which affects parameters such as Reynolds number,[77] movement mode,[3] damping coefficient,[4] and by extension the variable parameters which balance Equation 1-2. This is why parameters such as resonant frequency,[4] intensity for desired acceleration, or acceleration for desired intensity[33] can vary as the mixing cycle progresses.

Mixing progression has been broken down by Lucon *et al*[78] into three stages - 'wetting', 'incorporation' and 'mixing'. The wetting stage first introduces the solids and liquids, and results in the spreading of the liquids across the solid surfaces. It is reported that when mixing at constant acceleration large swings in power consumption (thus mixer intensity) are apparent in this stage,[78] likely due to the homogeneity, thus damping coefficient (see Equation 1-2), rapidly changing. During the incorporation stage the solid and liquid phases become cohesive, and as such

resist movement. As a result, low energy is imparted in this stage,[78] until mixing progresses to a point at which the mixture becomes more fluidised. During the mixing stage, a 'mixing regime' becomes apparent, and is characterised by a 'movement mode' - a description of *how* the material is moving, such as churning or bouncing. Movement modes are described in more detail in the next section.

The evolution of the mixing process when considering the mixing of a liquid component (water) into a dry powder (cement and sand) was also examined by Vandenberg and Wille.[33] When considering a mixing cycle at constant intensity, it was found that five characteristic stages of mixing (defined by the force dissipation mechanisms believed to be occurring in the mixture[79, 80]) corresponded with five discrete sections of the acceleration response profile. The concrete mixing acceleration profile (average of three) is reproduced in Figure 1-1. The mixing stages and corresponding dissipation origin forces are; a- 'dry granular' mixture (friction), b- 'wet granular' mixture (friction/cohesion), c- 'hard paste' (cohesion), d- 'soft granular fluid suspension' (cohesion/viscous), e- 'fluid suspension' (viscous).

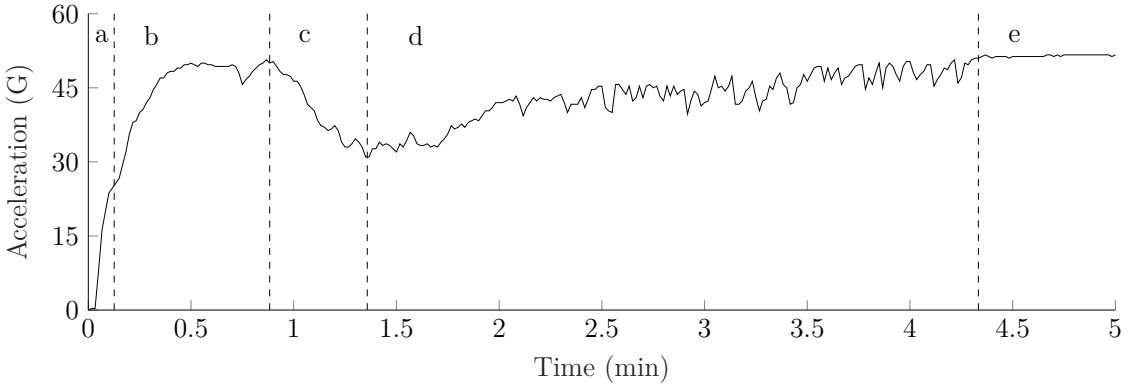


Figure 1-1: The average acceleration profile for concrete mixing (concrete mix 91 % w/w, water 9 % w/w) at 50 % intensity reproduced from Vandenberg and Wille.[33] Vacuum was not applied.

The initial dry granular state was dominated by frictional forces, and resulted in a rapid increase in acceleration. The next stage was a wet granular state where frictional and cohesive forces dominated, and the acceleration continued to increase before levelling off as the powder became saturated. This was followed by a hard paste state where cohesive forces dominated, and corresponded to a significant drop in acceleration. A soft granular fluid suspension state which was dominated by cohesive and viscous forces followed, where acceleration slowly built up again. The final stage consisted of a fluid suspension state where viscous forces dominated, and produced a levelled acceleration curve where the rheology of the material became

constant as mixing completed. The authors[33] did not elaborate on why the changes (general increases/decreases) in acceleration with different mixing stages occurred in the way they did, though this may be possible by correlating the five stages described ('a'-'e' of Figure 1-1) with the three stages ('wetting', 'incorporation' and 'mixing') as considered by Lucon *et al.*[78] However, this is difficult since in this case, the mixer was controlled at constant intensity setting, rather than constant acceleration setting. It would be expected that had the experiment that underpins Figure 1-1 been carried out at a constant acceleration and the intensity been measured, an 'inverse' profile would be seen. This is because when the power to the mixture is high when mixing at constant acceleration, the mixer intensity increases to prevent reduction in acceleration, whereas when mixing at constant intensity, the achieved acceleration will fall to prevent reduction in intensity. With this in mind, it would appear that stage 'a' of Figure 1-1 would roughly correspond to the wetting stage as described by Lucon *et al*,[78] stages 'b' and 'c' of Figure 1-1 would roughly correspond to the incorporation stage as described by Lucon *et al*,[78] and stages 'd' and 'e' of Figure 1-1 would roughly correspond to the mixing stage as described by Lucon *et al.*[78] Overall, these findings suggest that mixing progression with RAM can be effectively monitored by interpretation of acceleration or intensity readouts. Similar methods are indeed used with conventional mixing, where since torque is related to viscosity, the point of constant torque can be considered the point of constant viscosity.[73] A possible drawback to the use of this method (or indeed directly measuring viscosity) to determine the end of mix point is that it would likely only determine that the *intensity of segregation* has reached its minimum, without necessarily determining if the *scale of segregation* is sufficiently reduced. That is to say, agglomerates may still be present despite the bulk rheological properties appearing constant.

### Movement modes

While the evolving rheology of loaded suspensions was examined by Vandenberg and Wille,[33] other authors[4, 55, 57, 78, 81] have more closely investigated *how* the mixing occurs under certain conditions, by characterising the movement modes of the material. The salient movement modes for solids (powders), low viscosity liquids/suspensions, and high viscosity liquids/suspensions, as described by the manufacturer[3, 78, 81, 82] are set out below. It should be noted that the accelerations stated are to give a rough indication only, since the actual values will depend on the viscosity used in any particular case.

For dry powders, mixing phenomena is attributed to inter-particle collisions and collisions with the vessel base and lid, which are said to lead to harmonic vibrations which further enhance dispersion.[3] Whaley and Lucon[82] identified several characteristic movement modes that were apparent depending on the operating conditions (namely acceleration setting), and materials properties (namely granular powders, e.g. caster sugar, or cohesive powders, e.g. talc). At very low accelerations ($\leq$5 G for caster sugar, $\leq$10 G for talc), there is no movement and 'quiescent' conditions are apparent. With increasing acceleration, granular mixtures can display 'oscillon' conditions, whereby there is some movement at the surface in a 'wave' effect. At similar accelerations ($\sim$10 G for caster sugar, $\sim$20 G for talc), both granular and cohesive powders can display 'bouncing', whereby there is particle movement but no bulk mixing. With further acceleration increases ($\sim$30 G for caster sugar, $\sim$60 G for talc), a 'fluidised' state occurs, and bulk motion is apparent - a requirement for mixing. However, the most effective movement for mixing is considered to be 'chaotic mixing', typically occurring at high acceleration settings ($\sim$80+ G for caster sugar, $\sim$100 G for talc), where collisions also occur between the powder and vessel lid. With this mode there is vigorous bulk movement uniformly distributed throughout the entire volume of the vessel. Hilden *et al*[57] found that the confinement of the powder can affect the effectiveness of mixing, where more tightly packed powders were found to consume less power, as they more closely approximate a rigid body mass. It should therefore be expected that at least a small amount of head space is required, to allow the powder to become fluidised. Similar observations have been reported for concrete mixing, where increasing fill level was found to increase the time required for mixing.[33]

For low viscosities (<100,000 cP), such as with liquids and low solids loaded suspensions, a similar set of movement modes are possible.[81] As with powders, 'quiescent' conditions are observed at low accelerations ($\leq$4 G, water) and the material does not move. Surface waves can be seen at similar accelerations (>5 G, water) and are described as an 'oscillon' movement, analogous to that seen with granular powders. At higher acceleration, 'chaotic' movements are apparent, whereby splashing occurs. Similar modes are seen for slightly higher viscosities, though the onset accelerations are higher (e.g. for Dow 200 silicone oil, 'quiescent' $\sim$30 G, 'oscillon' $\sim$50 G, 'chaotic' $\sim$80 G).

For highly loaded suspensions and pastes (>100,000 cP) such as PBXs, several movement modes are again possible depending on the configuration of the system. 'Quiescent' conditions typically occur when operating at low accelerations (<40 G,

epoxy) below the threshold for mixing, thus no movement occurs.[81] 'Churning' is characterised by movement of the bulk of the material and typically occurs at higher accelerations (∼50+ G, epoxy). It has been widely suggested that the churning motion is the most desirable for mixing solid-liquid suspensions, where the characteristic bulk rolling and smearing motion with accompanying temperature increase has been attributed to shear generation,[78] analogous to that found in traditional mixing techniques.[55] High intensity churning is often referred to as 'bulk mixing' in Resodyn documents.[78, 81, 83] 'Decoupled' motion can also occur at similarly high accelerations (∼80+ G, 76 % w/w loaded polymer) to bulk mixing if the material is shear thickening, and is characterised by the material decoupling from the vessel interior and coalescing into one or more spheres which bounce or levitate. Since this movement mode is not efficient for mixing, Lucon and Whaley[81] recommend care should be taken to avoid the transition between the two mixing modes, suggesting this be achieved by lowering the acceleration setting if it becomes apparent.

### Linking mixing evolution to mixing mode

In the initial state immediately before the mixer is switched on, the PBX ingredients will be fully separated into layers of the order in which they were loaded. It would therefore follow the movement mode in each layer will pertain to the physical phase (powder, liquid etc.) of the layer at the point of mixer start. The introduction of solid components into the liquid components (wetting) has been attributed to Faraday instabilities. These non-linear waves on the surfaces of liquids occur under high amplitude periodic driving forces, and are reported by the manufacturer to manifest as 'fingers' or 'spikes' above the liquid surface, or 'cavities' below it. Videos of the phenomenon are available online.[72, 84] It is said that the presence of these instabilities at the boundary between materials of different densities (i.e. layers of material) is responsible for the rapid wetting observed. This would appear to have been validated computationally[85] for two viscous liquid layers (HTPB resins) by Nance,[86] whereby the associated vortices and eddy currents were modelled. The presence of particles was however omitted, and it was cautioned that the underlying physics requires further investigation to be better understood.

It is not explicitly documented what underlying phenomena may be responsible for the incorporation process, where the rheology of the material rapidly changes. From the videos available online[84] it would seem as though the movement mode associated with it is a combination of decoupled movement, whereby lumps of ma-

terial levitate or bounce around the interior of the vessel, followed by attempts at churning as the material becomes more fluidised and better able to couple to the vessel wall. Once sufficiently fluidised, it would appear churning then takes over as the dominant movement mode.

### Churning mechanism

The desired churning movement relies on a velocity gradient across the material, whereby material in contact with the vessel wall couples to it, ideally in a 'no-slip' condition. Conversely, the bulk of the material is acted upon by acoustic pressure waves (vibrations) from the oscillations of the plate, which cause it to accelerate in the direction of propagation. Consequently, bulk rolling occurs throughout the medium, which compels the mixing process.[78, 81, 83] For the velocity gradient to exist, at least some minimum degree of viscosity is required since consecutive 'layers' of the material must 'adhere' to one another. This is in essence the same principle that underpins conventional high shear mixing; material in contact with the blades moves along with them, creating the velocity gradient required for shear generation.

### Wall slip

Wall slip in filled polymer systems can occur in two different forms: true slip and apparent slip.[87–89] With true slip, there is a loss of adhesion between the polymer and the wall, resulting in the slippage of the material layer in immediate contact with it on the molecular level. With apparent slip there is a polymer-rich, low viscosity layer immediately adjacent to the wall on the order of the particle radius. This phenomenon arises because of wall depletion, whereby the dispersed phase is displaced away from the wall due to the particles being unable to penetrate it,[90–93] locally diminishing the volume fraction of the solid.[m] This has the effect of lubricating the bulk flow, resulting in a much steeper velocity gradient at the wall in comparison to that across the bulk of the material, giving the appearance (and effect) of slip. Observations of wall slip when using RAM and methods of mitigation are revisited later in this review.

[m] Other mechanisms for wall depletion have also been proposed and are reviewed elsewhere[87, 88]

## Effect of Reynolds number

Coguill and Martineau[77] found that the vibrational Reynolds number (which describes the ratio of inertial to viscous forces) is an important parameter with regards to RAM effectiveness, and can be affected by the viscosity of the mixing media, applied acceleration, and vessel diameter. This is intuitive since it would be expected that with larger inertial forces or lesser viscous forces (thus a greater compliance), there would be greater movement within the bulk of the material, thus a greater velocity gradient between the vessel wall (where there is ideally no-slip) and the vessel centre. By considering six different vessel diameters between 9.7 mm and 82.6 mm filled to a constant height (30 mm), an empirical relationship for the onset of effective mixing (churning) with increasing acceleration from quiescent conditions was observed, and is given in Equation 1-6.

$$\frac{Re_v}{D} > 87(10^3 D)^{-0.9} \qquad \text{(Equation 1-6)}$$

where $Re_v$ is vibrational Reynolds number (dimensionless), and $D$ is vessel diameter ( m). The relation as given in the original text has here been augmented with a conversion factor ($10^3$), so all variable parameters can be considered in SI units. It should however be noted that the relation is not dimensionally consistent without the empirically derived coefficient (87) also having units of its own. By inspection, the units should take the non-standard form of $\mathrm{m}^{-0.1}$.

By substituting an expression for vibrational Reynolds number into Equation 1-6, an expression for efficient mixing in the form of Equation 1-7 is apparent.

$$\frac{a\rho(10^3 D)^{0.9}}{87(2\pi)f\eta} > 1 \qquad \text{(Equation 1-7)}$$

where $a$ is the applied peak acceleration ( $\mathrm{m\,s^{-2}}$), $\rho$ is density ( $\mathrm{kg\,m^{-3}}$), $D$ is vessel diameter ( m), $f$ is vibrational frequency ( Hz), and $\eta$ is absolute viscosity ( Pa s). Although caution must be taken in extrapolating an expression based on the findings of a single study to the general case, a relationship of this form could explain several observations in the literature. Authors have reported experiments in which below an acceleration threshold[55] or below a minimum vessel diameter,[77, 94] efficient mixing is not observed. Qualitatively, McCloy *et al*[55] attributed the lack of mixing below a threshold acceleration to be analogous to the solid-like behaviour of a Bingham

plastic or Bingham pseudoplastic material below its yield stress. Highly loaded suspensions often display Bingham pseudoplastic behaviour.[35] Equation 1-7 would also suggest that depending upon the values of aforementioned parameters for any given case, a maximum mixable viscosity should be apparent. Using typical values of 100 G acceleration, 1000 kg m$^{-3}$ density, 74 mm vessel diameter and 60 Hz frequency, Equation 1-7 would suggest a maximum mixable viscosity of approximately 1400 Pa s (1,400,000 cP). This number is somewhat at odds with the manufacturer's claims[3] and anecdotal evidence that viscosities of the order 100,000,000 cP are not beyond limitations, though it must again be cautioned that the value was extrapolated from a single study.

The effect of vessel diameter can be qualitatively rationalised by considering the wall contact surface area to volume (SA/V) ratio, where the wall surface area scales linearly with diameter, while the volume of material scales quadratically with the diameter. Therefore with very small diameter vessels, the viscous drag at the wall is large compared to the forces induced by the acceleration on the mass of the material, impeding bulk flow. In essence, a larger diameter can be considered to make the material easier to move (more compliant). Lucon[78] describes this in the context of fill height to diameter (H/D) ratio, where a higher H/D ratio would result in a higher SA/V ratio, thus large amounts of drag making it more difficult to agitate the material. While this would certainly be the case if the higher H/D ratio was resultant of a smaller diameter, it does not account for a higher H/D ratio brought about by a greater fill height. For example, doubling the fill height would double the H/D ratio, though the SA/V ratio would be the same, since both the surface area and volume would double. It would therefore appear the assertion that H/D ratio is consequential for this reason is not strictly true, since only changes in diameter affect the SA/V ratio, regardless of fill height. Indeed, Equation 1-6 and Equation 1-7 make no reference to the fill height when determining the conditions under which mixing is apparent. That said, it would be expected that the fill height needs to be such that churning is physically able to take place. Equation 1-6 and Equation 1-7 also have further limitations. While they suggest that increasingly larger diameters are beneficial, it has been reported that (unspecified) very large diameters may result in poor coupling as the vessel contact area (thus viscous drag at the wall) becomes very small in comparison to the bulk volume.[78] It should also be noted that the equations do not account for the effects of vacuum application, where evacuation of the head space is believed to reduce resistance to bulk flow (in effect increasing net inertial forces), nor does it reference the effects of surface tension (which may

also effect compliance), or wall-slip (which will affect the velocity gradient). These factors are further discussed later in this review.

### Other non-dimensional numbers

Since the above discussion on Reynolds number only concerns the inertial to viscous forces, an interesting thought may be how similar dimensionless numbers in fluid mechanics could relate deforming inertial forces to stabilising surface tension forces when mixing. Analogous to Reynolds number, Weber number[95] describes the ratio of inertial to surface tension forces. Following the same logic as Coguill and Martineau,[77] a vibrational form is apparent in Equation 1-8.

$$We_v = \frac{(\delta\omega)^2 \rho D}{\sigma} = \left(\frac{a}{2\pi f}\right)^2 \frac{\rho D}{\sigma} \qquad \text{(Equation 1-8)}$$

where $We_v$ is vibrational Weber number (dimensionless), $\delta$ is the vibrational amplitude ( m), $\omega$ is the vibrational angular frequency ($rad\,\mathrm{s}^{-1}$), $u = \delta\omega$ is peak flow speed ( $\mathrm{m\ s^{-1}}$), $\rho$ is density ( $\mathrm{kg\,m^{-3}}$), $D$ is vessel diameter ( m), $\sigma$ is surface tension ( $\mathrm{N\,m^{-1}}$), $a$ is the applied acceleration ( $\mathrm{m\,s^{-2}}$), and $f$ is vibrational ordinary frequency ( Hz). It is apparent that lower acceleration, lower density, lower diameter, higher frequency, and higher surface tension (thus in any of these cases a lower Weber number) would be undesirable for churning.

Regarding the relative importance of viscous forces and surface tension forces, it is surmised that the viscous forces (Reynolds number) would be of greatest influence on how much the material moves. That is to say, large changes in movement mode would only be expected when changing the viscosity, while changes in surface tension would have a more nuanced effect. Another dimensionless number, the capillary number (Ca), represents the relative importance of viscous forces and surface tension forces,[96] and can be used to support this argument. Following the logic[77] for vibrational Reynolds number and vibrational Weber number, its vibrational form is given in Equation 1-9.

$$Ca_v = \frac{\delta\omega\eta}{\sigma} = \frac{a}{2\pi f}\frac{\eta}{\sigma} \qquad \text{(Equation 1-9)}$$

where $Ca_v$ is vibrational capillary number (dimensionless), $\delta$ is the vibrational amplitude ( m), $\omega$ is the vibrational angular frequency ($rad\,\mathrm{s}^{-1}$), $u = \delta\omega$ is peak flow speed ( $\mathrm{m\ s^{-1}}$), $\eta$ is absolute viscosity ( Pa s), $\sigma$ is surface tension ( $\mathrm{N\,m^{-1}}$), $a$ is the applied acceleration ( $\mathrm{m\,s^{-2}}$), and $f$ is vibrational ordinary frequency ( Hz).

Equation 1-9 shows the surface tension would have to be far larger than that seen for polymers (typically tens of $\mathrm{mJ\,m^{-2}}$) to be of any consequence in making the material more compliant. Using typical values of 50 G acceleration, 62 Hz frequency, 60 Pa s viscosity, and $30\,\mathrm{mN\,m^{-1}}$ surface tension, $Ca_v = 2518$, suggesting viscous forces dominate surface tension forces. That is not to say, however, that changing the surface tension will not have an effect on mixing. This is because the surface tension is also a factor that likely affects the work of adhesion at the vessel wall, thus the no-slip wall coupling condition. This is discussed in more detail later in this review.

## Effect of formulation

Qualitatively, it would be expected that materials with higher viscosity would dissipate more mechanical energy into heat, increasing the amount of inputted energy required to complete the mixing process. Yew *et al*[54] found that premixing the binder and plasticiser components into a single phase aids mixing, since the viscosity of the liquid phase is reduced. Viscosity can be further reduced by increasing temperature,[97, 98] with processing temperatures typically around 60 °C used to aid conventional mixing. However, it is important that runaway temperature increases from frictional heating in the mixing process are avoided, particularly when inputted energy is large when mixing high viscosity materials.[78]

Viscosity of the mixture can also be varied by modifying particle shape, where more rounded particles exhibit lower viscosities than anisometric particles. This is summarised in the empirical Krieger-Dougherty relation,[99] as given in Equation 1-10. The equation is analogous to that discussed for filled composites as described in Equation 1-1.[50]

$$\eta = \eta_0 \left(1 - \frac{\phi}{\phi_{max}}\right)^{-[\eta]\phi_{max}} \qquad \text{(Equation 1-10)}$$

where $\eta$ is the apparent viscosity ( Pa s), $\eta_0$ is the (Newtonian) viscosity of the continuous phase ( Pa s), $\phi$ is the volume fraction (dimensionless), $[\eta]$ is the intrinsic viscosity (a dimensionless property dependant on filler particle shape), and $\phi_{max}$ is the maximum volume fraction (dimensionless). The intrinsic viscosity describes the distortion of the flow field by the suspended particles, and for rigid spherical fillers is equal to 2.5.[100, 101] When particle shape is anisometric, the value increases

(e.g. ground gypsum - 3.25, quartz grains - 5.80, glass micro-rods - 9.25).[102] $\phi_{max}$ corresponds to the maximum volume that can be occupied by filler in relation to the total volume considered, where more spherical particles increase packing efficiency.[103–106] With increasing anisometry, the intrinsic viscosity increases while the maximum packing fraction decreases, resulting in the exponent term of Equation 1-10 ($-[\eta]\phi_{max}$) approximating negative two[50, 104, 107, 108] over a range of particle shapes.[102] However, the viscosity is still dependant on $\phi/\phi_{max}$, thus fillers with a higher degree of anisometry (resulting in reduced $\phi_{max}$) have the consequence of higher suspension viscosities. In the context of energetic crystals, Hudson *et al*[109] found suspension viscosity can be reduced by more than a third by replacing angular RDX for a more rounded reprocessed filler grade. Similar viscosity reductions have been reported by other researchers.[34, 106, 110] Multiple authors have produced more comprehensive literature reviews on the topic of suspension rheology, such as Shenoy,[35] Barnes,[111] Goodwin and Hughes,[50] Nielsen and Landel,[112] and in the context of energetic materials, Teipel.[28]

Viscosity can also be modified with the addition of processing aids. These are surface active additives which lower the binder's surface tension to aid wetting and dispersion by allowing the polymer to spread over the filler surface with greater ease.[13, 113] Lecithins are a commonly used processing aid in PBXs, and are naturally occurring products (found in substances such as egg yolk and soya beans) which typically consist of phosphatidylcholines (PCs), a kind of glycerophospholipid. PCs are amphiphilic, containing both a choline head group bonded to glycerophosphoric acid (polar), and long chain fatty acids (non-polar).[114] Since nitramines (polar) are known to have poor affinity to polyurethane binders (non-polar),[115, 116] the inclusion of lecithin is beneficial since the polar head group is able to adsorb onto nitramines and the fatty acids are able to interact with the binder.[113] Furthermore, a 2.75 fold reduction in viscosity in an 85 % w/w loaded PBX was reported by Sinha[117] after lecithin was included at 0.3 % concentration. Viscosity reduction is believed to arise from the fatty acid chains, whereby overlap of the chains is prohibited by an entropic barrier.[113] This barrier then acts as a 'lubricant' between RDX particles, since their close approach is thermodynamically unfavourable. The molecular structures of lecithin and RDX are shown in Figure 1-2. It could be expected that lower surface tension may make the material more compliant (easier to move), encouraging bulk flow (discussed above). However, to the author's knowledge, no studies have investigated the effect of surface tension on mixing efficiency.

From the information presented so far, it may be expected that mixing will

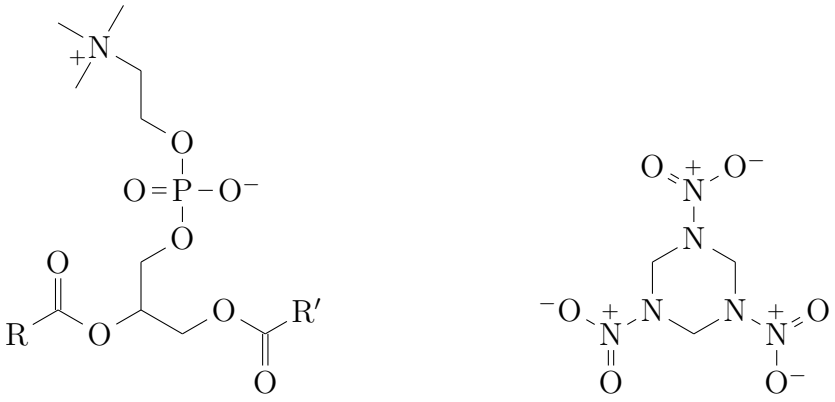

(a) Lecithin (b) RDX

Figure 1-2: The skeletal formulae of L-α-phosphatidylcholine (where R and R' are fatty acid residues), the main component of lecithins, and RDX, a nitramine explosive.

be aided by modifying formulations to contain more rounded explosive particles and processing aids such as lecithin, since the viscosity of the formulation would be lowered. However, work by Patil and Gill[56] on idealised systems (containing millimetre sized glass beads at high volume fraction) found that higher viscosities can actually aid mixing with RAM. By considering four binder viscosities between 1.78 Pa s and 58.12 Pa s (1780 cP and 58120 cP), it was found that substantially lower accelerations were required to initiate mixing with the higher viscosity binders. This was attributed to improved energy transfer between the vessel wall and contents, based on the assumption that higher viscosity binders are more difficult to decouple from the vessel wall. This would be intuitive since higher viscosity would be expected to lead to greater viscous drag at the wall, thus reduced true wall slip. It is therefore possible there is a trade-off between the effects of low and high viscosities, with lower viscosity formulations resulting in greater movement within the material, and higher viscosity formulations reducing wall slip. Another effect not previously reported on is the tackiness (contact adhesiveness) of the formulation, where tackiness (or 'stickiness') is a rheological property related to viscosity.[118] As well as increased viscous drag, increased viscosity may therefore also be expected to 'stick' better to the wall, further reducing the risk of true wall slip. Another property that would influence adhesion to the wall (thus true wall slip) is the chemical work of adhesion, which is discussed later in this review.

Patil and Gill[56] also found that higher loaded formulations resulted in higher intensity mixing, which was attributed to better kinetic energy transfer between

particles as they are closer together. Layering of ingredients has also been noted to be of consequence. The addition of the liquid component above the filler component has been found to be beneficial since it hastened integration, possibly due to gravitational assistance,[54] though this has been contradicted in other work.[81]

To the author's knowledge, no studies have considered the effect of overall formulation density, though the effects of increasing solid loading[55, 56] and differing the true densities of the filler[56] have been investigated. In the latter of these studies, Patil and Gill[56] considered an idealised system where 1 mm diameter spheres of three densities between 1.325 g cm$^{-3}$ and 7.995 g cm$^{-3}$ were compared under vacuum at very low volume fraction. It was found that higher density spheres required higher intensity (more power) to maintain the set acceleration. This was attributed to the higher density beads requiring a greater momentum (thus greater kinetic energy) than those with lower density, thus expending more energy as they move a greater distance through the binder. Higher density fillers with intensified movement were thus postulated to have an enhancing effect on mixing.

Since the changes in filler density in this study occurred at such low volume fraction 0.14 % v/v, it is unlikely the observations reported were due to increases in the overall density of the formulation as a whole, since the increase in total formulation density would have only been around 1 %, or even less as a percentage of the total mass of the system. It is unclear what differences may be apparent should a filler density comparison be carried out at much higher volume fractions typical of PBXs, where other factors such as overall formulation mass, density and viscosity would be considerably different. Beyond minimum mixing requirements, the above parameters will also affect the magnitude of the damping coefficient, thus efficiency across a mixing cycle.

## Effect of vessel construction

Besides internal diameter (as discussed above), other aspects of vessel design are also known to affect mixing, such as the observation that vessels with a curved base rather than sharp corners assist mixing by more quickly eradicating unmixed areas.[54] Work by Beckel[67] suggests that the substance out of which the mixing vessel is manufactured is also of consequence, where the use of PTFE (poly(tetrafluoroethylene), Teflon$^{TM}$) resulted in (true) wall slip, thus ineffective coupling, between the mixture and the vessel wall. This was attributed to the low surface free energy of PTFE

(approximately[119] 20 mJ m$^{-2}$) leading to the vessel contents gliding along the internal surface. This explanation would agree with the findings of Piau *et al*[89] who examined polybutadiene flows in stainless steel and PTFE coated extrusion dies. Significant (true) slip was observed in the latter case, with it commented that the low surface energy of the PTFE die wall was responsible. Such a scenario would be expected to substantially reduce the velocity gradient across the material that is required for RAM shear generation. This was believed to be the cause of reduced mixing efficiency and separation of the vessel contents, which led to void formation when recombination occurred after the mixing cycle.[67] Other researchers have reported no such problems when mixing in vessels manufactured from stainless steel, aluminium and titanium,[54, 120] where clean metal oxide[n] surfaces have higher surface free energies typically hundreds of mJ m$^{-2}$.[121] Perplexingly, other routinely used vessel materials such as polystyrene,[67, 94, 122] acrylic (poly(methyl methacrylate)),[94] and polycarbonate,[55, 77] which have surface free energies in the range[119] 30-50 mJ m$^{-2}$, have not been reported to cause similar issues to PTFE, despite their surface free energy values being only slightly greater. However, none of the aforementioned works comment on other potentially consequential factors such as vessel cleanliness, which can alter the apparent surface free energy,[121] and surface finish, which can affect liquid spreading.[123, 124]

The reason for low surface free energy resulting in (true) slip would be attributed to a low chemical work of adhesion in comparison to the cohesive forces (surface tension) in the binder. That is to say the binder must prefer to adhere to the wall rather than move along with the bulk of the material. Work of adhesion is defined as the energy required to separate a liquid from a solid surface, and can be found using Equation 1-11.[125–127]

$$W_A = 2(\sqrt{\sigma^d_{SFT}\sigma^d_{SFE}} + \sqrt{\sigma^p_{SFT}\sigma^p_{SFE}}) \qquad \text{(Equation 1-11)}$$

where $W_A$ is the work of adhesion ( mJ m $^{-2}$), $\sigma_{SFT}$ is the surface tension of the liquid ( mJ m $^{-2}$), $\sigma_{SFE}$ is the surface free energy of the solid ( mJ m $^{-2}$), and the remaining terms are the dispersive force and polar force components thereof ( mJ m $^{-2}$). It would therefore be expected that a higher surface free energy would result in higher work of adhesion to surface tension ratio (presuming no changes are made to the surface tension of the formulation), thus better coupling. However, as previously

[n] Stainless steel, aluminium and titanium undergo passivation in air, thus have a thin coating of chromium(III) oxide, aluminium(III) oxide, and titanium(IV) oxide respectively

mentioned, the degree of adhesion will also depend on the formulation's tackiness, a rheological property that determines contact adhesion, that may also reduce (true) wall slip.

Apparent slip at the interface may be influenced by the vessel surface roughness, where textured surfaces are often employed as a mitigation technique in shear rheometry of suspensions.[87] The asperities of such surfaces are believed to break through the lubricating binder-rich layer, allowing the shearing surface (which would be the vessel wall in the case of RAM) to directly interact with the bulk of the material.[88] Methods previously employed to texture shearing surfaces have included sand blasting,[128–133] machining,[134, 135] embedding or attaching particles,[136–140] and attaching sandpaper.[141–145] Some surfaces are also manufactured with cross-hatched grooves or serrations.[146, 147] Aral and Kalyon[137] quantitatively studied the effect of surface roughness on apparent slip mitigation by determining the roughness average ($R_a$) value, the arithmetic mean deviation of the profile from the centreline over an assessed length.[148] It was found that wall slip decreased with decreasing particle diameter ($R$) to roughness average ($R_a$) ratio ($R/R_a$) until fully inhibited at $R/R_a \cong 1$. It would therefore follow that surface roughness is optimal when it approximates the particle size, with other studies[147] in agreement. It is unclear to what extent surface roughness may have affected mixing in the aforementioned RAM studies, and to the author's knowledge, no studies have investigated the effects of varying vessel surface roughness on mixing behaviour.

Other factors to be noted when considering vessel construction materials include thermal conductivity (for efficient heat application or dissipation), electrical conductivity (static build up can occur to a greater extent in some materials than others and should be mitigated by grounding[149]), points of friction (unintended explosions have occurred when mixing nanothermites, believed to be caused by friction due to poor vessel design), density (lighter mixing vessels are preferred since the equipment is limited by payload mass), mechanical strength (some materials have been found to lack adequate mechanical strength to maintain their integrity under applied vacuum[67, 78] and hydrodynamic forces[78]), machinability (to aid in manufacturing), and cost.

## Effect of vacuum

Another variable which can be considered over a mixing cycle is vacuum application, where, several studies have previously applied reduced pressure to RAM cycles to observe the effect on mixing. Yew *et al*[54] found that partial vacuum substantially reduced the time required for homogeneity to be achieved, attributing the observation to lower air pressure in the sealed mixing vessel reducing resistance against bulk flow. A similar explanation has been given by Lucon,[83] though in this case, the induction of bubbles in the material due to partial vacuum application was also reported to have the effect of making the material more compliant (easier to move). With greater compliance, it would be expected there would be greater movement within the material, thus a larger velocity gradient and greater shear. When subjected to acoustic pressure waves, it is also known that air bubbles can influence the flow of surrounding liquid, in a mixing enhancement process known as acoustic microstreaming.[150] This phenomenon is referred to as 'bubble pumping' in the RAM patent.[71] It has however been forewarned by Yew *et al*[54] and others[83] that premature application of vacuum can cause unmixed material to be evacuated from the mixing vessel. The incremental reduction of pressure and a low acceleration initial stage in the mixing sequence have subsequently been found to mitigate this complication.[151] In all, the aforementioned studies suggests the presence of gas bubbles brought about by partial vacuum application is beneficial to mixing.

With this in mind, it would follow that premature degassing of the mixture is not beneficial. McCloy *et al*[55] found that vacuum application over extended periods of time had the effect of impeding the mixing process after initially aiding the process, attributed to the gradual loss of air bubbles by evacuation. Similarly, Lucon[83] states that the removal of air bubbles with hard vacuum will lessen the compliance of the material (i.e. make it more difficult to move), resulting in the reduction of the velocity gradient required for shear generation. Hard vacuum for degassing purposes should therefore be reserved for the final stages of a mixing sequence, where evacuation of air is specifically required to prevent the inclusion of voids within the cured material. Such voids would otherwise compromise mechanical integrity and act as hotspot[11] initiation sites under adiabatic compression when exposed to incidental stimuli. Indeed, conventional mixing and casting includes a distinct degassing stage in mixing sequences for this purpose.[2]

Further studies considering the effect of vacuum on idealised systems contain-

ing glass beads were undertaken by Patil and Gill.[56] In nearly all cases considered across differing acceleration, binder viscosity, filler density, particle size, and volume fraction, vacuum application was required to some degree to initiate mixing, with stronger vacuum having the most pronounced effect. These observations were attributed to the application of vacuum inducing the formation of air bubbles around the filler particles, with the effect of aiding the movement of the solids through the binder. When the binder was degassed before the mixer was started, no signs of mixing were apparent at any acceleration. It should however be noted that the idealised systems considered are not wholly representative of real systems, where the fillers used typically have dimensions several orders of magnitude smaller than the majority of the spheres considered throughout Patil and Gill,[56] are irregular in shape, have different chemical interaction considerations, and are mixed on much larger scales. Indeed, vacuum application is not a prerequisite for mixing real systems, with researchers[33] reporting mixing completion without application of vacuum. In reality, the effects of vacuum on mixing efficiency likely stem from a contribution of bubble induction improving material compliance (i.e. make it easier to move), acoustic microstreaming, and lower pressure in the head space encouraging bulk flow (essentially increasing net inertial forces). Overall, it is apparent that while not imperative for mixing to occur, vacuum application brings the benefits of reduced mixing time and improved product outcome.

## Effect of mixer model

There are several RAM models available depending on scale, and are summarised in Table 1-3. Most of the models are also offered in a 'hazard' version, modified specifically for energetic material processing. These 'H' models feature remote operation, numerous grounding routes, and a purged casing. All but the two largest models (which are driven by eccentric masses) are driven electromagnetically by a voice coil (linear motor), though regardless of the size or configuration of the mixer used, the principle of operation (a platform vibrating vertically at 60 Hz up to 100 G acceleration) is the same. It would therefore be expected that when using the same size mixing vessel, the mixing behaviour of a formulation would be the same across all capacity mixers and all units of the same mixer model, provided a constant acceleration was used. However, it may be expected that larger mixing vessels on larger mixer models will present differences, due to the aforementioned

differences in surface area to volume ratio as vessel diameter is increased. It is unknown what variations may be present between different units of the same mixer model, though the components used (driver motors, accelerometers, springs etc.) may have variation associated with them. Calibration may also differ between machines, and could be tested by comparing the achieved mixer intensity as a function of acceleration (perhaps using rigid body masses of known weights) across several units of a particular RAM model.

Table 1-3: Comparison of Resonant Acoustic Mixer models.†Denotes a discontinued model.

| | Bench scale | | | Pilot/production scale | | |
|---|---|---|---|---|---|---|
| | LabRAM† | LabRAM I | LabRAM II | OmniRAM | RAM 5 | RAM 55 |
| Capacity (kg) | 0.5 | 0.5 | 1 | 5 | 36 | 420 |
| Power (W) | 37 | 410 | 640 | 4100 | 23200 | 244000 |
| 'H'? (Y/N) | N | N | Y | Y | Y | Y |

## The important factors

In all, it would appear that the way to maximise efficiency with regards to PBX mixing is to ensure the establishment of a churning movement mode, and maximise the velocity gradient by 1) increasing the amount of movement in the material, and 2) reducing wall slip. The former can likely be brought about by making the material more compliant (easier to move) and increasing inertial forces, while the latter can likely be brought about by better coupling the mixture to the vessel by increasing drag and adhesion. This is summarised in Table 1-4. The PBX formulator can ultimately achieve this through the optimisation of machine variables, vessel variables, and formulation variables, as summarised in Table 1-5. However, since 'PBneXt' formulation will be based on the optimisation of final material properties, optimisation of the mixing process will likely concern only the selection of machine and vessel variables.

Table 1-4: The salient factors affecting the efficiency of churning.

| | Reduces wall-slip | Increases movement |
|---|---|---|
| Physical | | Higher acceleration<br>Higher density<br>-Greater inertial forces |
| | Higher viscosity formulation<br>-Greater interfacial drag<br>-Greater tackiness | Lower viscosity formulation<br>-Greater compliance |
| | Smaller diameter vessel<br>Optimised roughness average<br>-Greater interfacial drag | Larger diameter vessel<br>-Greater compliance |
| | | Vacuum application<br>-Greater inertial forces<br>-Greater compliance |
| Chemical | Lower surface tension<br>Higher surface free energy<br>-Greater spreadability | Lower surface tension<br>-Greater compliance |
| Other | | Mixer calibration<br>-Greater inertial forces |

Table 1-5: Machine variables, vessel variables, and formulation variables for Resonant Acoustic Mixing.

| Machine variables | Vessel variables | Formulation variables |
|---|---|---|
| Acceleration setting | Vacuum setting | Binder content |
| Intensity setting | Wall material | Plasticiser content |
| Mixer model | Wall surface finish | Additives |
| Mixer unit | Diameter | Solids loading |
| | Insulation | Particle shape |
| | Active heating | Filler type |
| | Active cooling | |

### Literature gaps

This review has highlighted several gaps in the understanding of how user-defined parameters can affect the mixing process. Of the machine variables listed in Table 1-5, the effect of acceleration is well documented to increase the rate of energy supply, but the effect it has on time to mixing completion has not been quantitatively reported. While this has been undertaken for the effect of intensity setting by Vandenberg and Wille[33] for concrete mixing (a ∼30 % reduction in mixing time between 60 % and 80 % mixer intensity apparent from their data), similar analysis

has not been undertaken for polymer bound suspensions. Additionally, no study has directly compared the differences in the observed profile between controlled acceleration and controlled intensity (drive mode), or determined whether one is inherently a better choice than the other. Possible differences between mixer models and units (variation and calibration) have also not been previously reported. With regards to vessel variables, no studies have investigated the effect of wall surface finish (where rougher surfaces may reduce wall slip), and there has been only one anecdotal report[67] of the effects of wall material surface properties (where low surface free energy, thus lower work of adhesion, when mixing in PTFE was believed to result in wall slip). These factors should be examined more closely in controlled experiments.

## Conclusions

The aim of this work was to initially provide a background of explosives and mixing as subject matters, identify what should be expected of next generation PBX formulations, and determine how RAM could be of use in their implementation. The major drawback of conventional PBX formulation, mixing, and casting is found to be that formulations must compromise processability (low enough viscosity to mix and cast), against performance, mechanical, and ageing properties. Using 'in-situ' RAM, there is the potential for processability to become irrelevant, given that casting would no longer be required. This will allow next generation PBX to push the limits of solids loading and reduce plasticiser content, optimising performance, mechanical, and ageing properties.

The second aim was to assess the extent of current knowledge with regards to how mixing behaviour can be characterised and the factors that affect mixing efficiency. It is found that much work is yet to be done to fully understand the mechanisms behind mixing operation and the factors that affect efficiency. Churning is identified as the most effective movement mode for mixing of viscous suspensions to occur, and is found to be of greatest benefit when wall slip is minimised and movement is maximised. It is found that this can be achieved by optimising parameters relating to: 1) the machine, 2) the vessel, and 3) the formulation. To date, no studies have systematically investigated how such parameters can be selected in order to maximise the efficiency (reduce the time and energy requirement) of mixing. Beyond PBX mixing, it would appear the greatest advantage of RAM is the ability to mix

'universally'. That is to say mixing of powders and liquids in any combination is possible under suitable operating conditions, removing the need for a range of specialist mixers.

## References

[1] D.B. Todd. Mixing of highly viscous fluids, polymers, and pastes. In *Handbook of Industrial Mixing: Science and Practice*. John Wiley & Sons, Inc., 2004.

[2] A.C. Hordijk and A.E.D.M. van der Heijden. Mixing. In *Energetic Materials; Particle Processing and Characterization*. Wiley-VCH Verlag GmbH, 2005.

[3] Inc. Resodyn Acoustic Mixers. Resonant Acoustic Mixing (Technical White Paper). ResoDyn Corp, Butte, MT, USA, 2009.

[4] Inc. Resodyn Acoustic Mixers. LabRAM Resonant Acoustic Mixer Manual. ResoDyn Corp, Butte, MT, USA, February 2012.

[5] M. Andrews, C. Collet, A. Wolff, and C. Hollands. ResonantAcosutic Mixing Processing and Safety. Munitions Safety Information Analysis Center, May 2019.

[6] A. Nelson and M. Miller. Resonant Acoustic Mixing of High- Energy Composite Materials. SERDP & ESTCP Symposium, Washington D.C., USA, 2018.

[7] R.J. Davey, J.M. Wilgeroth, and A.O. Burn. Processing Studies of Energetic Materials using Resonant Acoustic Mixing Technology. BAE Systems Land UK, Glascoed, Monmouthshire, UK, 2019.

[8] M.D. McPherson. Propellant and explosives production method by use of resonant acoustic mix process. Patent WO 2009/091430 A1, July 2010.

[9] A. Burn. Private Communication, BAE Systems Glascoed, 2018.

[10] P.P. Vadhe, R.B. Pawar, R.K. Sinha, S.N. Asthana, and A. Subhananda Rao. Cast Aluminized Explosives (Review). *Combust. Explos. Shock Waves*, 44:461–477, 2008.

[11] F.P. Bowden and A.D. Yoffe. *Fast Reactions in Solids*. Butterworths Scientific Publications, 1958.

[12] J.P. Agrawal. *High Energy Materials - Propellants, Explosives and Pyrotechnics*. WILEY-VCH Verlag GmbH & Co. KGaA, Weinheim, 2010. pp. 108, 163-166, 173-174, 268.

[13] M.A. Daniel. Polyurethane Binder Systems for Polymer Bonded Explosives. Australian Defence Science and Technology Organisation, December 2006. DSTO-GD-0492.

[14] Department of Defense (US). Explosive, Plastic Bonded, Cast PBXN-109. MIL-E-82886(OS).

[15] C.A. Williams. *Investigation into the interaction of Dantocol in polymer bonded explosives and bonding agent development*. PhD thesis, Flinders University, 2015.

[16] A.M. Mellor, D.A. Wiegand, and K.B. Isom. Hot spot histories in energetic materials. *Combust. Flame*, 101:26–35, 1995.

[17] K.V.S. Sastry, H. Cooper, R. Hogg, T.L.P Jespen, F. Knoll, B.Parekh, R.K. Rajamani, T. Sorenson, I. Wechsler, C. McCleary, and D.B. Todd. Solid-solid operations and equipment. In *Perrys Chemical Engineers' Handbook, Seventh Edition*. McGraw-Hill Pub., 1997.

[18] J.R. Boone - Rotary Drum Blender. `https://www.jrboone.com/rotary-drum-mixers`. Accessed 29-05-2020.

[19] F.J. Muzzio, A. Alexander, C. Goodridge, E. Shen, and T. Shinbrot. Solids mixing. In *Handbook of Industrial Mixing: Science and Practice*. John Wiley & Sons, Inc., 2004.

[20] D.A. Dahlstrom, R.C. Bennett, R.G. Emmet, P. Harriott, T. Laros, W. Leung, S.A. Miller, B. Morey, J.Y. Oldshue, G. Priday, C.E. Silverblatt, J.S. Slottee, and J.C. Smith. Liquid-solid operations and equipment. In *Perrys Chemical Engineers' Handbook, Seventh Edition*. McGraw-Hill Pub., 1997.

[21] Euromixers - Impeller Types. `https://www.euromixers.co.uk/impeller-types/`. Accessed 29-05-2020.

[22] R.R. Hemrajani and G.B. Tatterson. Mechanically stirred vessels. In *Handbook of Industrial Mixing: Science and Practice*. John Wiley & Sons, Inc., 2004.

[23] V.A. Atiemo-Obeng, W.R. Penney, and P. Armenante. Solidliquid mixing. In *Handbook of Industrial Mixing: Science and Practice*. John Wiley & Sons, Inc., 2004.

[24] Charles Ross & Son Company. High Viscosity Mixer Designs and Applications. `https://www.mixers.com/whitepapers/hvm_designs_whitepaper.pdf`. Accessed 14-07-2020.

[25] Charles Ross & Son Company. How to choose the right mixer for high-viscosity mixing applications. `https://www.mixers.com/whitepapers/high%20viscosity%20mixing.pdf`. Accessed 14-07-2020.

[26] R.J. Farris. Prediction of the Viscosity of Multimodal Suspensions from Unimodal Viscosity Data. *J. Rheol*, 12:281–301, 1968.

[27] C.R. Siviour, M.J. Gifford, S.M. Walley, W.G. Proud, and J.E. Field. Particle size effects on the mechanical properties of a polymer bonded explosive. *J. Mater. Sci.*, 39:1255–1258, 2004.

[28] U. Teipel, A.C. Hordijk, U. Förter Barth, D.M. Hoffman, C. Hübner, V. Valtsifer, and K.E. Newman. Rheology. In *Energetic Materials; Particle Processing and Characterization*. Wiley-VCH Verlag GmbH, 2005.

[29] NATO. Explosives, Specification for RDX (Hexogene). STANAG-4022.

[30] M. Zebregs, A.E.H.J. Mayer, and A.E.D.M. van der Heijden. Comparison of Propellant Processing by Cast-Cure and Resonant Acoustic Mixing. *Propellants Explos. Pyrotech.*, 45:87–91, 2020.

[31] A. Nelson and T. Cross. Processing Benefits of Resonance Acoustic Mixing on High Performance Propellants and Explosives. The 37th Meeting of the Technical Cooperation Program Subcommittee on Non-Atomic Military Research and Development WPN Group, Edinburgh, Australia., 2012.

[32] N. Rumeau, D. Threlfall, and A. Wilmet. Resonant Acoustic Mixing Processing and Formulation Challenges for Cost Effective Manufacturing. Roxel France, Saint-Médard-en-Jalles (33167), 2009.

[33] A. Vandenberg and K. Wille. Evaluation of resonance acoustic mixing technology using ultra high performance concrete. *Constr. Build. Mater.*, 164:716–730, 2018.

[34] R.M. Dexter, B.M. Hamshere, and I.J. Lochert. Evaluation of an Alternative Grade of CXM-7 for Use in PBXN-109, The Explosive Fill for the Penguin ASM Warhead. Australian Defence Science and Technology Organisation, August 2002. DSTO-TN-0441.

[35] A.V Shenoy. *Rheology of Filled Polymer Systems.* Springer-Science+Business Media, B.V., 1999.

[36] C.B. Skidmore, D.S. Phillips, and N.B. Crane. Microscopical Examination of Plastic-Bonded Explosives. Los Alamos National Laboratory, July 1997. LA-UR-97-2807.

[37] B. Olinger. Compacting Plastic-Bonded Explosive Molding Powders to Dense Solids. Los Alamos National Laboratory, August 2005. LA-14173.

[38] J. E. Field, S. J. P. Palmer, P. H. Pope, R. Sundararajan, and G. M. Swallowe. Mechanical properties of PBXs and their behaviour during drop-weight impact. Proc. 8th Symp. (Int.) on Detonation, (ed. J.M. Short), White Oak, MD: Naval Surface Weapons Center, 1985.

[39] S.J.P. Palmer, J.E. Field, and J.M. Huntley. Deformation, strengths and strains to failure of polymer bonded explosives. *Proc. R. Soc. Lond. A*, 440:399–419, 1993.

[40] W.G. Proud, S.J.P. Palmer, J.E. Field, G. Kennedy, and A. Lewis. AFM studies of PBX systems. *Thermochimica Acta*, 384:245–251, 2002.

[41] D.M. Williamson, S.J.P. Palmer, and W.G. Proud. Fracture Studies of PBX Simulant Materials. Shock Compression of Condensed Matter, July 2006.

[42] C.R. Siviour, P.R. Laity, W.G. Proud, J.E. Field, D. Porter, P.D. Church, P. Gould, and W. Huntingdon-Thresher. High strain rate properties of a polymer bonded sugar: their dependence on applied and internal constraints. Proceedings of the Royal Society, 464, 1229-1255, January 2008.

[43] R.J. Hudson, P. Zioupos, and P.P. Gill. Investigating the Mechanical Properties of RDX Crystals Using Nano-Indentation. *Propellants Explos. Pyrotech.*, 37:191–197, 2012.

[44] R.M. Doherty and D.S. Watt. Relationship Between RDX Properties and Sensitivity. *Propellants Explos. Pyrotech.*, 33:4–13, 2008.

[45] H. Moulard, J.W. Kury, and A. Delclos. The Effect of RDX Particle Size on the Shock Sensitivity of Cast PBX Formulations. 8th Symposium (International) on Detonation, Albuquerque, New Mexico, USA., 1986.

[46] H. Moulard. Particular Aspect of the Explosive Particle Size Effect on Shock Sensitivity of Cast PBX Formulations. 9th Symposium (International) on Detonation, Portland, Oregon, USA., 1989.

[47] L. Borne. Influence of Intragranular Cavities of RDX Particle Batches on the Sensitivity of Cast Wax Bonded Explosives. 10th Symposium (International) on Detonation, Boston, Massachusetts, USA., 1993.

[48] F. Baillou, J.M. Dartyge, C. Spyckerelle, and J. Mala. Influence of Crystal Defects on Sensitivity of Explosives. 10th Symposium (International) on Detonation, Boston, Massachusetts, USA., 1993.

[49] F. Ramsteiner and R Theysohn. On the tensile behaviour of filled composites. *Composites*, 15:121–128, 1984.

[50] J.W. Goodwin and R.W. Hughes. *Rheology for Chemists; An Introduction, Second Edition.* RSC Publishing, 2008.

[51] D. Fossey. Private Communication, Falcon Project Ltd., June 2020.

[52] D. Fossey. Private Communication, Falcon Project Ltd., January 2018.

[53] K.S. Hope, H.J. Lloyd, D. Ward, A.A.L. Michalchuk, and C.R. Pulham. Resonant Acoustic Mixing Its applications to energetic materials. New Trends in Research of Energetic Materials (NTREM), Pardubice, Czech Republic., 2015.

[54] T.G. Yew, P.P. Gill, and P. Wilkinson. Process Parameters for Resonant Acoustic Mixers (RAM). Master's thesis, Cranfield University, 2015.

[55] E.L. McCloy, P. Wilkinson, and P.P. Gill. Resonant Acoustic Mixing: Pushing The Boundaries. Master's thesis, Cranfield University, 2016.

[56] A.N. Patil and P.P. Gill. Resonant Acoustic Mixing  The Future of Propellant Manufacturing. Master's thesis, Cranfield University, 2018.

[57] J. Hilden, M. Sullivan, M. Polizzi, J. Wade, J. Greer, and M. Keeney. Power consumption during oscillatory mixing of pharmaceutical powders. *Powder Technol.*, 338:44–54, 2018.

[58] J.G. Osorio and F.J. Muzzio. Evaluation of resonant acoustic mixing performance. *Powder Technol.*, 278:46–56, 2015.

[59] J.G. Osorio, E. Hernández, R.J. Romañach, and F.J. Muzzio. Characterization of resonant acoustic mixing using near-infrared chemical imaging. *Powder Technol.*, 297:349–356, 2016.

[60] A. Burn. Private Communication, BAE Systems Glascoed, 2020.

[61] Inc. Resodyn Acoustic Mixers. RAM Drives Innovation at Catalent Pharmaceutical. `https://resodynmixers.com/2019/05/29/ram-drives-innovation-at-catalent-pharmaceutical/`. Accessed 29-11-2020.

[62] J.G. Osorio, K. Sowrirajan, and F.J. Muzzio. Effect of resonant acoustic mixing on pharmaceutical powder blends. *Adv. Powder Technol.*, 27:1141–1148, 2016.

[63] R. Tanaka, N Takahashi, Y Nakamura, Y. Hattori, K. Ashizawac, and M. Otsuka. Verification of the mixing processes of the active pharmaceutical ingredient, excipient and lubricant in a pharmaceutical formulation using a resonant acoustic mixing technology. *RSC Adv.*, 6:87049–87057, 2016.

[64] R.R. Nellums, B.C. Terry, B.C. Tappan, S.F. Son, and L.J. Groven. Effect of Solids Loading on Resonant Mixed Al-Bi2O3 Nanothermite Powders. *Propellants Explos. Pyrotech.*, 38:605–610, 2013.

[65] D.G. Kelly, P. Beland, P. Brousseau, and C.F Petre. Formation of Additive-Containing Nanothermites and Modifications to their Friction Sensitivity. *J. Energetic Mater*, 35:331–345, 2017.

[66] P.J. Wilkinson. *Evaluation of Novel Propellants Manufactured from Commercially Available Thermoplastic Elastomers (TPE) using Resonant Acoustic Mixing.* PhD thesis, Cranfield University, 2020.

[67] E.R. Beckel, K.E. Lee, J.C. Marin, and A.H. Shah. Processing of Explosives at ARDEC Using the LabRAM. U.S. Army Armament Research, Development and Engineering Center, September 2016.

[68] M. Puszynski, R. Cook, D. Perkins, G. Cheng, and N. Mehta. Using RAM Technology to Mix Primary Explosive Based Composites for Additive Manufacturing. 43rd International Pyrotechnic Society Seminar, Denver, CO, USA, July 2018.

[69] S.R. Anderson, D.J. am Ende, J.S. Salan, and P. Samuels. Preparation of an Energetic-Energetic Cocrystal using Resonant Acoustic Mixing. *Propellants Explos. Pyrotech.*, 39:637–640, 2014.

[70] S.R. Anderson, P. Dubé, M. Krawiec, J.S. Salan, D.J. Am Ende, and P. Samuels. Promising CL-20-Based Energetic Material by Cocrystallization. *Propellants Explos. Pyrotech.*, 41:783–788, 2016.

[71] H. Howe, J. Warriner, A. Cook, S. Coguill, and L. Farrar. Apparatus and Method for Resonant Vibratory Mixing. Patent US 7188993 B1, March 2007.

[72] Inc. Resodyn Acoustic Mixers. How RAM Mixes. `https://resodynmixers.com/how-ram-mixes/#faraday`. Accessed 16-07-2020.

[73] R.A. Layton, W.R. Murray, and J.L. Garbini. The Control of Power for Efficient Batch Mixing. *Propellants Explos. Pyrotech.*, 22:269–278, 1997.

[74] J.T. Miller, A. Luebbering, S. Coguill, and P. Lucon. Mix Power. Resodyn Forum: Industrial Outcomes in ResonantAcoustic Mixing, Butte, Montana, 2013.

[75] P.A. Lucon. RAM Power Considerations. Resodyn Technical Interchange, Butte, Montana, USA, 2016.

[76] J. Whaley. Private Communication, Resodyn Acoustic Mixers, April 2020.

[77] S.L. Coguill and Z.R. Martineau. Vessel Geometry and Fluid Properties Influencing Mix Behavior of Resonant Acoustic Mixing. 38th International Pyrotechnics Seminar, Denver, CO, USA., 2012.

[78] P.A. Lucon, G. Sperry, and J. Whaley. RAM Mixing of Liquids and Pastes. Resodyn Technical Interchange, Butte, Montana, USA, 2016.

[79] B. Cazacliu and J. Legrand. Characterization of the Granular-to-Fluid State Process During Mixing by Power Evolution in a Planetary Concrete Mixer. *Chem. Eng. Sci.*, 63:4617–4630, 2008.

[80] B. Cazacliu and N. Roquet. Concrete mixing kinetics by means of power measurement. *Cem. Concr. Res.*, 39:182–194, 2009.

[81] P.A. Lucon and J. Whaley. Liquids and Pastes. Resodyn Technical Interchange, Butte, Montana, USA, 2016.

[82] J. Whaley and P. Lucon. Processing of Solids. Resodyn Technical Interchange, Butte, Montana, USA, 2016.

[83] P.A. Lucon. Mixing with Vacuum Assist. Resodyn Technical Interchange, Butte, Montana, USA, 2016.

[84] Inc. Resodyn Acoustic Mixers. How RAM Mixes. `https://resodynmixers.com/applications/viscous/`. Accessed 16-07-2020.

[85] D. Nance. Simulating the Resonant Acoustic Mixer. Air Force Research Laboratory, Elgin, FL, USA, 2013. AFRL-RW-EG-TR-2013-079.

[86] D. Nance. An examination of the resonant acoustic mixer's flow field. Air Force Research Laboratory, Elgin, FL, USA, 2013. AFRL-RW-EG-TR-2013-108.

[87] H.A. Barnes. A review of the slip (wall depletion) of polymer solutions, emulsions and particle suspensions in viscometers: its cause, character, and cure. *J. Non-Newton Fluid*, 56:221–251, 1995.

[88] M. Cloitre and R.T. Bonnecaze. A review on wall slip in high solid dispersions. *Rheol Acta*, 56:283305, 2017.

[89] J-M. Piau, N. Kissi, and A. Mezghani. Slip flow of polybutadiene through fluorinated dies. *J. Non-Newton Fluid*, 59:11–30, 1995.

[90] U. Yilmazer and D.M. Kelyon. Slip effects in capillary and parallel disk torsional flows of highly filled suspensions. *J. Rheol.*, 33:11971212, 1989.

[91] D.M. Kalyon. Apparent slip and viscoplasticity of concentrated suspensions. *J. Rheol.*, 49:621640, 2005.

[92] P. Ballesta, G. Petekidis, L. Isa, W.C.K. Poon, and R. Besseling. Slip and flow of hard-sphere colloidal glasses. *Phys. Rev. Lett.*, 101:258201, 2008.

[93] P. Ballesta, G. Petekidis, L. Isa, W.C.K. Poon, and R. Besseling. Wall slip and flow of concentrated hard-sphere colloidal suspensions. *J. Rheo.*, 56:10051037, 2012.

[94] J.T. Miller, D.A. Bode, and S.L. Coguill. ResonantAcoustic Mixing; Design and Process Considerations Concerning Vessel/Case Geometry and Mix versus Cure Time When Preparing Composite Solid Propellant. JANNAF 36th Propellant and Explosives Development and Characterization Joint Subcommittee Meeting, December 2010.

[95] F.M. White. *Fluid Mechanics, Seventh Edition.* McGraw-Hill, 2011. pp. 314.

[96] B.E. Rapp. *Microfluidics: Modelling, Mechanics and Mathematics.* Elsevier Inc., 2017.

[97] R.M. Muthiah, R. Manjari, V.N. Krishnamurthy, and B.R. Gupta. Effect of temperature on the rheological behavior of hydroxyl terminated polybutadiene propellant slurry. *Polym. Eng. Sci.*, 31:61–66, 1991.

[98] B.M. Bandgar, K.C. Sharma, T. Mukundan, and V.N. Krishnamurthy. Rheokinetic Modeling of HTPBTDI and HTPBDOATDI Systems. *J. Appl. Polym. Sci.*, 89:1331–1335, 2003.

[99] I.M. Krieger and T.J. Dougherty. A Mechanism for Non-Newtonian Flow in Suspensions of Rigid Spheres. *T. Soc. Rheol.*, 3:137–152, 1959.

[100] A. Einstein. Eine neue Bestimmung der Moleküldimensionen (German). *Ann. Phys.*, 19:289–306, 1906.

[101] A. Einstein. Bemerkung zu meiner Arbeit: "Eine Beziehung zwischen dem elastischen Verhalten...". *Ann. Phys.*, 34:591–592, 1911.

[102] H.A. Barnes, J.F. Hutton, and K. Walters. *An Introduction to Rheology*. Elsevier Science Publishers, Amsterdam, 1989.

[103] G.R. Riley and G.R. Mann. Effects of Particle Shape on Angles of Repose and Bulk Densities of a granular solid. *Mater. Res. Bull.*, 7:163–170, 1972.

[104] T. Kitano, T. Kataoka, and T. Shirota. An empirical equation of the relative viscosity of polymer melts filled with various inorganic fillers. *Rheol Acta*, 20:207–209, 1981.

[105] S. Mueller, E.W. Llewellin, and H.M. Mader. The effect of particle shape on suspension viscosity and implications for magmatic flows. *Geophys. Res. Lett.*, 38, 2011. L13316.

[106] D. Sharabi, T. Kaully, C-A. Yael, C. Nadiv, D.Shaham, and T. Tenanbaum. Particle rounding technology (PRT) for highly energetic PBX. 39th International Annual Conference of ICT, Karlsruhe, Germany., June 2008.

[107] S.H. Maron and P.E. Pierce. Application of Ree-Eyring generalized flow theory to suspensions of spherical particles. *J. Colloid Sci.*, 11:80–95, 1956.

[108] D. Quemada. Rheology of concentrated disperse systems and minimum energy dissipation principle. *Rheol Acta*, 16:82–94, 1977.

[109] R.J. Hudson, M. Moniruzzaman, and P.P. Gill. Investigation of Crystal Morphology and Shock Sensitivity of Cyclotrimethylenetrinitramine Suspension by Rheology. *Propellants Explos. Pyrotech.*, 40:233–237, 2015.

[110] I.J. Lochert, R.M. Dexter, and B.M. Hamshere. Evaluation of Australian RDX in PBXN-109. Australian Defence Science and Technology Organisation, August 2002. DSTO-TN-0440.

[111] H.A. Barnes. A Review of the Rheology of Viscoelastic Systems. Rheology Reviews, The British Society of Rheology, 2003.

[112] L.E. Nielsen and R.F. Landel. *Mechanical Properties of Polymers and Composites*. Marcel Dekker, Inc., 1994.

[113] A.E.D.M. van der Heijden, J. ter Horst, J. Kendrick, K.-J. Kim, H. Kröber, F. Simon, and U. Teipel. Crystallization. In *Energetic Materials; Particle Processing and Characterization*. Wiley-VCH Verlag GmbH, 2005.

[114] D. Myers. *Surfactant Science and Technology, Third Edition*. John Wiley & Sons, Inc., 2005.

[115] J.M. Bellerby and Ch. Kiriratnikom. Explosive-Binder Adhesion and Dewetting in Nitramine-filled Energetic Materials. *Propellants Explos. Pyrotech.*, 14:82–85, 1989.

[116] J.S. Gharia, R.K. Sinha, V.V. Tadas, V. Prakash, and V.K. Phadke. Studies on Physico-Mechanical and Explosive Characteristics of RDXHMX-Based Castable Plastic-Bonded Explosives. *Def. Sci. J.*, 48:125–130, 1998.

[117] R.K. Sinha. *Studies on Castable Plastic Bonded High Explosives (PBXs).* PhD thesis, High Energy Materials Research Laboratory, Sutarwadi, Pune (India), 2004.

[118] D.W. Aubrey. Tack. In *Handbook of Adhesion, Second Edition.* John Wiley & Sons, Ltd., 2005.

[119] M. Lewin, A. Mey-Marom, and R. Frank. Surface free energies of polymeric materials, additives and minerals. *Polym. Adv. Technol.*, 16:429–441, 2005.

[120] D. Jubb. Private Communication, Falcon Project Ltd., July 2017.

[121] J.E. Castle. The Composition of Metal Surfaces After Atmospheric Exposure: An Historical Perspective. *J. Adhes.*, 84:368–388, 2008.

[122] M.D. McPherson. Process and Formulation Development of Castable Energetic Formulations using the LabRAM and RAM5 Mixer. 38th International Pyrotechnics Seminar, Denver, CO, USA., June 2012.

[123] R.N. Wenzel. Resistance of Solid Surfaces to Wetting by Water. *Ind. Eng. Chem.*, 28:988–994, 1936.

[124] A.B.D. Cassie and S. Baxter. Wettability of Porous Surfaces. *Trans. Faraday Soc.*, 40:546–551, 1944.

[125] D.K. Owens and R.C. Wendt. Estimation of the surface free energy of polymers. *J. App. Polym. Sci.*, 13:1741–1747, 1969.

[126] D. H. Kaelble. Dispersion-Polar Surface Tension Properties of Organic Solids. *J. Adhesion*, 2:66–81, 1970.

[127] W. Rabel. Einige Aspekte der Benetzungstheorie und ihre Anwendung auf die Untersuchung und Veränderung der Oberflächeneigenschaften von Polymeren. *Farbe und Lack*, 77:997–1005, 1971.

[128] R. Buscall, J.I. McGowan, and A.J. Morton-Jones. The rheology of concentrated dispersions of weakly attracting colloidal particles with and without wall slip. *J. Rheol.*, 37:621641, 1993.

[129] T.G. Mason, J. Bibette, and D.A. Weitz. Yielding and flow of monodisperse emulsions. *J. Colloid Interface Sci.*, 79:439448, 1996.

[130] S.P. Meeker, R.T. Bonnecaze, and M. Cloitre. Slip and flow of soft particle pastes. *Phys. Rev. Lett.*, 92:198302, 2004.

[131] S.P. Meeker, R.T. Bonnecaze, and M. Cloitre. Slip and flow in pastes of soft particles: direct observation and rheology. *J. Rheol.*, 48:12951320, 2004.

[132] T. Gibaud, C. Barentin, and S. Manneville. Influence of boundary conditions on yielding in a soft glassy material. *Phys. Rev. Lett.*, 101:258302, 2008.

[133] P. Lettinga and S. Manneville. Competition between shear banding and wall slip in wormlike micelles. *Phys. Rev. Lett.*, 103:248302, 2009.

[134] A. Magnin and J.M. Piau. Cone-and-plate rheometry of yield stress fluids. Study of an aqueous gel. *J. Non-Newton Fluid*, 36:85108, 1990.

[135] S.A. Gulmus and U. Yilmazer. Effect of volume fraction and particle size on wall slip in flow of concentrated suspensions. *J. Appl. Polym. Sci.*, 98:439448, 2005.

[136] D.M. Kalyon, P. Yaras, B. Aral, and U. Yilmazer. Rheological behavior of a concentrated suspension: a solid rocket fuel stimulant. *J. Rheol.*, 37:3563, 1993.

[137] B.K. Aral and D.M. Kalyon. Effects of temperature and surface roughness on time-dependent development of wall slip in steady torsional flow of concentrated suspensions. *J. Rheol.*, 38:957972, 1994.

[138] S.V. Kao, L.E. Nielsen, and C.T. Hill. Rheology of concentrated suspensions of spheres I. Effect of the liquid-solid interface. *J. Colloid Interface Sci.*, 53:358366, 1975.

[139] S. Marze, D. Langevin, and A. Saint-Jalmes. Aqueous foam slip and shear regimes determined by rheometry and multiple light scattering. *J. Rheol.*, 52:10911111, 2008.

[140] R. Besseling, L. Isa, E.R. Weeks, and W.C.K. Poon. Quantitative imaging of colloidal flows. *Adv. Colloid Interf. Sci.*, 146:1–17, 2009.

[141] S.A. Khan, C.A. Schnepper, and R.C. Armstrong. Foam rheology: III. Measurement of shear flow properties. *J. Rheol.*, 32:6992, 1988.

[142] P. Coussot, Q.D. Nguyen, H.T. Huynh, and D. Bonn. Avalanche behavior in yield stress fluids. *Phys. Rev. Lett.*, 88:175501, 2002.

[143] J.M. Piau. Carbopol gels: elastoviscoplastic and slippery glasses made of individual swollen sponges: meso- and macroscopic properties, constitutive equations and scaling laws. *J. Non-Newton Fluid*, 144:1–29, 2007.

[144] T. Divoux, D. Tamarii, C. Barentin, S. Teitel, and S. Manneville. Yielding dynamics of a HerschelBulkley fluid: a critical-like fluidization behaviour. *Soft Matter*, 8:41514164, 2012.

[145] F. Ahonguio, L. Jossic, and A. Magnin. Influence of slip on the flow of a yield stress fluid around a flat plate. *AIChE J.*, 62:1356–1363, 2016.

[146] C. Nickerson and J. Kornfield. A novel "cleat" geometry for suppressing wall slip. *J. Rheol.*, 49:865874, 2005.

[147] V. Mansard, L. Bocquet, and A. Colin. Boundary conditions for soft glassy flows: slippage and surface fluidization. *Soft Matter*, 10:69846989, 2014.

[148] J.T. Black and R.A. Kohser. *Materials and Processes in Manufacturing, Tenth Edition*. John Wiley & Sons, Inc., 2008.

[149] P.A. Lucon, S.L. Coguill, and Z.R. Martineau. Electrostatic Generation and Methods to Mitigate Electrostatic Discharge while using the ResonantAcoustic Mixer. 38th International Pyrotechnics Seminar, Denver, CO, USA., June 2012.

[150] R. Manasseh. Acoustic bubbles, acoustic streaming, and cavitation microstreaming. In *Handbook of Ultrasonics and Sonochemistry*. Springer Singapore, 2016.

[151] D. Jubb. Private Communication, Falcon Project Ltd., January 2018.

# Paper 2 - A Method to Determine the Process Efficiency of Resonant Acoustic Mixing

Andrew J. Claydon, Guillaume Kister, Sally Gaulter, and Philip P. Gill

**Abstract:** An investigation into how the efficiency (time and energy required for homogeneity) of Resonant Acoustic Mixing (RAM) can be determined is undertaken, using an idealised Polymer Bonded eXplosive (PBX) simulant based on glass microbeads (28.3 micron D50, 62% v/v in HTPB and plasticiser). Mixing evolution is monitored using machine output data, whereby the mixer 'intensity' (related to power draw) is plotted against time. Different stages of the intensity profile were found to correspond to discrete stages of mixing. Though it was expected the mixer 'intensity' would become constant after mixing completion, further changes in the profile were observed due to continuing frictional heating (thus viscosity reduction) beyond homogeneity being achieved. Three techniques, based on mechanical, electrical, and thermal power monitoring respectively are used to find the energy supplied to the mixture, and gave values of the same magnitude. The relative accuracies of each method should be investigated over a range of different mixing conditions as part of future work. Reasonably good agreement in time to mix completion is found between repeat measurements, with a standard deviation of ±11 % in the average time to completion, and ±3 % in the average time to a profile 'flat-line' feature (coinciding with maximum temperature), as taken over three measurements.

**Keywords:** Resonant Acoustic Mixing, Polymer Bonded eXplosive, LabRAM, Efficiency, End of mix, Energy

## Introduction

High shear mixing of loaded suspensions is required in industries such as food, cosmetics, and energetic materials, where the requirement to mix high viscosity pastes precludes the use of turbulent mixing techniques such as those involving impeller blades. Typically, the mixing action employed will instead involve laminar flow, and rely on shearing, kneading, or pulling actions to disperse and distribute the solid component.[1] In the case of Polymer Bonded eXplosive (PBX) manufacture, it is necessary to distribute crystalline high explosive filler particles throughout a liquid rubber prepolymer, and other ingredients such as plasticiser, and curative.[2] This is necessary to optimise properties such as mechanical strength once the suspension has been cast into a warhead or bomb case, and cured into a rubbery explosive composite. During PBX manufacture, the high shear mixing method typically used is planetary or z-blade mixing, which respectively consist of orbiting blades that move in close contact as to maximise shear, or horizontally rotating 'z' or 'ς' (sigma) shaped blades that knead the material.[1, 3–5] However, conventional high shear mixing of this type has drawbacks such as long mix times (up to several hours[2]) and the production of a large amount of waste (∼12.5 % on industrial scale[6]) since the mixing vessel and blades must be cleaned after use.

Resonant Acoustic Mixing (RAM) is a novel alternative to high shear mixing, which instead consists of a vertically vibrating spring-mounted platform to which a mixing vessel is attached. The vibrations occur at low amplitude (up to 1.4 cm) at the mechanical resonance of the system (approximately 60 Hz), and conveys energy to the mixture through longitudinal acoustic pressure waves (vibrations). This results in uniform medium shear mixing over the entire volume of the mixing vessel, as opposed to high shear mixing localised to the vicinity of mixing blades.[7, 8] Advantages of RAM over conventional techniques include shorter mixing times,[7, 8] reduced cleaning requirement and associated waste, and the ability to mix 'in-situ',[9] whereby the intended casing of the cured product is also used as the mixing vessel. This potentially allows for the manufacture of high viscosity novel PBX formulations that would otherwise be difficult to cast, and remove the requirement for cleaning. However, the technique is still poorly characterised in comparison to conventional methods.

A literature review by the author[10] found that in order for the full potential of RAM to be realised, a better understanding of the factors determining mixing

efficiency (time and energy required for homogeneity) must first be sought. The aim of this work is to develop a method to determine the efficiency of RAM applied to a loaded polymer suspension, and relate the findings to PBX manufacture. The use of the methodology developed can then be used in subsequent work to compare mixing efficiency under different operating conditions.

## Basic principles

The operation of RAM has been previously reviewed by the author[10] and will not be repeated here, though it is useful to understand the basic principles. One of two parameters can be defined by the user to control a mixing cycle - set peak acceleration of the vibrating plate up to 100 G, or set driver 'intensity' up to 100 %. Intensity in this case refers to applied current to the driver motor up to 5 A,[a] and by extension, peak driving force. Intensity is commonly referred to as 'power' or 'power intensity' by the manufacturer. The relation between acceleration and driving force is given in Equation 2-1.[7]

$$m\frac{d^2}{dt^2}x(t) + c\frac{d}{dt}x(t) + kx(t) = Fsin(\omega_d t) \qquad \text{(Equation 2-1)}$$

where $m$ is the mass of the system ( kg), $x(t)$ is the displacement of the plate as a function of time ( m), $c$ is the damping coefficient ( $kg\,s^{-1}$), $k$ is the spring constant ( $N\,m^{-1}$), $F$ is the peak driving force ( N), $\omega_d$ is the driving force angular frequency ( $s^{-1}$), and $t$ is time ( s). The inertial force (product of mass and acceleration), damping forces (losses from mixing and non-ideal losses), and stored forces constitute the first three terms, while the driving force constitutes the final term. Inertial and stored forces cancel out over each oscillation period since the system is held in resonance by the control software.

As mixing progresses and the rheology of the material changes, so too does the energy required for mixing, and thus the damping coefficient, $c$. Therefore the variables which balance Equation 2-1 must also vary over a mixing cycle. This means that for a set acceleration or set intensity, there will be a corresponding achieved intensity or acceleration, depending on the 'mixing forces' present in any particular instance. During mixing, several movement modes of the material are possible.[8, 11–14] After the incorporation of the solid component into the liquid component, the most important of these is churning,[13] whereby the vessel contents couple to the vessel wall, ideally with a no-slip condition at the interface. Since the bulk of the material

[a] In the case of the LabRAM (original model)

is being acted on by acoustic pressure waves (vibrations) from the oscillation of the plate, a velocity gradient facilitated by the viscosity of the material (which allows adjacent layers of material to 'adhere' to each other) extends perpendicularly across the material,[12, 14, 15] providing the shear required for mixing. High intensity churning is referred to as bulk motion by the manufacturer.[12, 14] When the mixing vessel is not filled, the system acts as a rigid body mass (RBM). In this case, any damping is purely consequential of non-ideal losses in the system, such as air resistance, friction, and noise. Once filled, additional losses are attributed to energy being absorbed during mixing. When using conventional high shear techniques, the energy consumed for mixing can be derived by integrating the power supplied to the mixture, where power can be found at any given time by measuring impeller shaft torque.[16] It would be expected that analogous methods could be employed with RAM. Here three methods to determine energy supplied to the mixture are considered.

### Mechanical method

Using Newtonian mechanics, the manufacturer has developed Equation 2-2 to determine power (and by extension, energy) consumption. The method is valid for the LabRAM (original) mixer model,[17, 18] and has been previously applied in academic studies.[19, 20]

$$E_{EOM} = \sum_{t_0}^{t_{EOM}} P_{mix}(t)\Delta t \qquad \text{where} \qquad P_{mix} = \left(\mathscr{F}\frac{\Delta I}{100}\right)\left(0.707\frac{a}{2\pi f}\right) \tag{Equation 2-2}$$

where $E_{EOM}$ is the total energy consumption ( J), $P_{mix}(t)$ is the power to the mixture for any given time ( W), $\Delta t$ is the time increment where $P_{mix}$ is valid ( s), $t_0$ and $t_{EOM}$ are the start and end times respectively ( s), $\mathscr{F}$ is an empirically derived LabRAM constant (70±4 N), $\Delta I$ is the difference in intensity between the mixing vessel when filled and unfilled (%), $a$ is peak acceleration ( m s$^{-2}$) with a statistical correction factor to root mean square acceleration (0.707),[19] and $f$ is the normal frequency of vibration ( s$^{-1}$).

### Electrical method

In the case of the original model LabRAM, information supplied by the manufacturer suggests the maximum power able to be supplied by the motor is 37 W.[21] Since the

intensity readout displays the current supplied up to 100 % current (which will provide the maximum power), the author suggests that by comparing the mixer intensity when the vessel filled to when the vessel is unfilled, the energy supplied to the mixture can be derived. This is shown in Equation 2-3.

$$E_{EOM} = \sum_{t_0}^{t_{EOM}} P_{mix}(t)\Delta t \qquad \text{where} \qquad P_{mix} = \frac{\Delta I}{100} P_{max} \qquad \text{(Equation 2-3)}$$

where $E_{EOM}$ is the total energy consumption ( J), $P_{mix}(t)$ is the power to the mixture for any given time ( W), $\Delta t$ is the time increment where $P_{mix}$ is valid ( s), $t_0$ and $t_{EOM}$ are the start and end times respectively ( s), $\Delta I$ is the difference in intensity between the mixing vessel when loaded and unloaded (%), and $P_{max}$ is the maximum power able to be supplied (37 W).

It should be noted that Hilden *et al*[11] used a different approach in which the electrical power drawn by the mixer (in their case a 1 kg scale LabRAM II) when filled and unfilled was evaluated by determining the product of current and voltage. However, direct measurement of voltage was not possible in this work.

### Thermal method

Here the author builds upon a method by Hilden *et al*[11] that considers the temperature changes observed as the mixing progresses. Since all energy transferred into the vessel does work on the vessel contents (i.e. rearranges the vessel contents into a homogeneous suspension), the energy applied will ultimately manifest itself as heat. In an ideal closed system mixing vessel with no thermal losses, simply recording the temperature increase from ambient at the point of mix completion could be used to calculate the increase in thermal energy (which would be equivalent to the energy supplied by the mixer), by use of Equation 2-4.

$$E_{EOM} = (C_p m)_{mixture}(T_{EOM} - T_{amb})_{mixture} \qquad \text{(Equation 2-4)}$$

where $E_{EOM}$ is the total energy required for mixing ( J), $C_p$ is specific heat capacity ( J $g^{-1}$ $K^{-1}$), $m$ is mass ( g), $T_{EOM}$ is the temperature reached at the end of mix (°C), and $T_{amb}$ is the ambient temperature (°C). Obviously, real mixing vessels are not ideal closed systems, and will lose (or potentially gain if using an externally heated vessel) heat to the surroundings over the course of a mixing cycle. Hilden *et al*[11] considered powder mixing on short time-scales up to approximately five minutes,

where energy input was taken to be equal to the thermal energy increase of the mixture plus thermal energy dissipated into the enclosing mixing vessel, as shown in Equation 2-5.

$$E_{EOM} = [(C_p m)_{mixture} + (C_p m)_{vessel}](T_{EOM} - T_{amb})_{mixture} \quad \text{(Equation 2-5)}$$

where the terms are the same as previously. In this case, the temperature increase of the mixing vessel (a plastic bottle) was taken to be equal to that of the mixture, and heat dissipated beyond the mixing vessel exterior was considered insignificant. The recorded temperature increases were small, up to only 5 ℃. PBX mixing is expected to require longer mixing durations than dry powder mixing (on the order tens of minutes as opposed to minutes) since the powder has to be incorporated into a viscous binder. With longer mixing times, larger temperature increases are therefore also expected, with viscous polymer mixtures previously reaching temperatures of 80 - 90 ℃.[22] A far more significant degree of heat dissipation beyond the mixing vessel must therefore be accounted for. In this work, an additional term is proposed by the author to compensate for dissipative losses by estimating the cooling behaviour of the system. The temperature of the mixing vessel is also considered separately to that of the mixture.

A body will lose heat to the surroundings at a rate dependent on its temperature and that of the surroundings, according to Newton's Law of Cooling, as given in Equation 2-6.

$$T(t) = T_{amb} + (T_0 - T_{amb})e^{-kt} \quad \text{(Equation 2-6)}$$

where $T(t)$ is temperature as a function of time (℃), $T_{amb}$ is the ambient temperature (℃), $T_0$ is the initial temperature (℃), $k$ is the cooling constant ($min^{-1}$), and $t$ is time (min). The cooling constant, $k$, describes the rate of cooling (where the instantaneous rate of temperature change is equal to $-k(T_0 - T_{amb})$) and can be found empirically by observing the rate of temperature drop when the material is not mixing.[b] Therefore by also recording the temperature of the material and ambient temperature incrementally over a mixing cycle, the temperature, and thus energy lost over each incremental time increase can be found. By summation of these increments, the total energy lost over the mixing cycle can be found, thus the

[b] It should be noted that $k$ is not an intrinsic property of the material, rather a system specific parameter that will change depending on aspects such as the fill level, thermal properties of the mixture and mixing vessel, added insulation, and vacuum application.

total energy required for mixing can be found. This is summarised in Equation 2-9 with reference to Equation 2-7 and Equation 2-8.

$$(E_{EOM})_{retained} = [(C_p m)(T_{EOM} - T_{amb})]_{mixture} + [(C_p m)(T_{EOM} - T_{amb})]_{vessel} \quad \text{(Equation 2-7)}$$

$$(E_{EOM})_{dissipated} = [C_p m \sum_{t_0}^{t_{EOM}} k(T_t - T_{amb})\Delta t]_{mixture} \quad \text{(Equation 2-8)}$$

$$E_{EOM} = (E_{EOM})_{retained} + (E_{EOM})_{dissipated} \quad \text{(Equation 2-9)}$$

where $E_{EOM}$ is the total energy required for mixing ( J), $C_p$ is specific heat capacity ( J $g^{-1}$ $K^{-1}$), $m$ is mass ( g), $T_{EOM}$ is the temperature at the end of mix (℃), $T_{amb}$ is the ambient temperature (℃), $k$ is the cooling constant ($min^{-1}$), $T_t$ is the temperature at an arbitrary time t (℃), and $\Delta t$ is the time increment over which $T_t$ is valid (i.e. until the next temperature measurement is taken) (min). The caveat to this method is that it will not be valid when using externally heated or cooled vessels.

### Mixing progression

Vandenberg and Wille[20] examined the acceleration profile of mixes performed at constant intensity on liquid-solid suspensions (concrete mix), and found that distinct sections of the profile corresponded to the changing rheology of the mixture. The concrete mixing acceleration profile (average of three) is reproduced in Figure 2-1. At the time the acceleration became constant, a fluid suspension was achieved. Since the rheology of the suspension at this point was no longer changing, it could be used to determine the end of mix point.

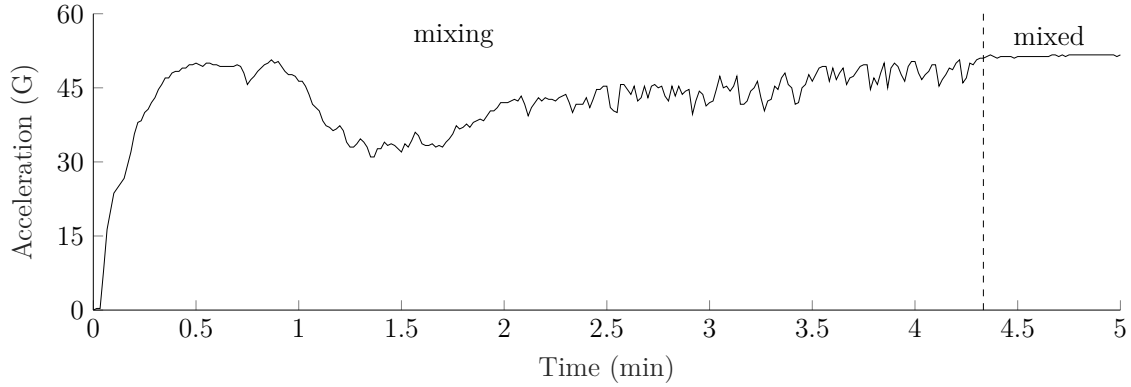


Figure 2-1: The average acceleration profile for concrete mixing (concrete mix 91 % w/w, water 9 % w/w) at 50 % intensity reproduced from Vandenberg and Wille.[20] Vacuum was not applied.

## Experiment

An idealised inert formulation based on glass microbeads (28.3 µm D50, Glass Sphere s.r.o., Czech Republic), hydroxy-terminated polybutadiene (HTPB) (type Poly bd® R-45HTLO, Cray Valley, USA) binder, and di(2-ethylhexyl) adipate (DEHA) ($\geq$ 97 %, Merck, UK) plasticiser was used, and is given in Table 2-1. Curative was not used since only the mixing behaviour is of interest, and not the properties of the final composite.

Table 2-1: The glass bead formulation used for mixing.

| | Glass | DEHA | HTPB | Curative |
|---|---|---|---|---|
| Volume (%) | 62.00 | 19.00 | 19.00 | - |
| Actual mass (%) | 81.65 | 9.30 | 9.05 | - |
| RDX equivalent mass (%) | 76.48 | 11.91 | 11.60 | - |

### Characterisation of materials

The particle size distribution of the glass beads was assessed by laser particle size analysis (Cilas 1190, dry mode) over three measurements. The density of the microbeads was measured by helium pycnometry (Micromeritics AccuPyc 1330) over five measurements. The specific heat capacity ($C_p$) of the mixture was assessed over three measurements by Differential Scanning Calorimetry (DSC, Mettler Toledo DSC 3+), using a standard sapphire disc as a reference material. Values for $C_p$ were determined between 10 ℃ and 90 ℃. The cooling behaviour of the system when

not mixing (as required for the thermal method) was taken by logging the rate of cooling between 45 ℃ and 35 ℃ once the mixer had been switched off after each mix cycle. This was interpreted using a rearranged form of Equation 2-6, as given in Equation 2-10. The cooling constant, $k$, was found by taking the gradient of the line.

$$kt = -ln[(T(t) - T_{amb})/(T_0 - T_{amb})] \quad \text{(Equation 2-10)}$$

The temperature dependence of the rheology of the mixed formulation was assessed using shear rheometry (TA Instruments HR-1) over triplicate measurements. A shear rate of 2.5 $s^{-1}$ was used with 25 mm parallel plates at a gap height of 500 µm, between 15 ℃ and 80 ℃ at 2 ℃ per minute.

### Mixing procedure

The ingredients were weighed directly into a custom made mixing vessel (48 mm diameter, 47.5 mm height) machined from poly(methyl methacrylate) (PMMA) at the start of each mixing cycle (so called 'one-shot' mixing), with the first half of the filler being followed by the plasticiser, and the second half being followed by the binder. A total fill of 65 mL of the formulation was used. A LabRAM was used for mixing, and was controlled via aftermarket devices and software supplied by Falcon Project Ltd., which allowed for temperature logging and vacuum control. A rod thermocouple was inserted into the centre of the mixture through an airtight portal in the vessel lid. The vessel lid was of custom design and PEEK[c] construction, and was held in place with a clamshell clamp. An additional wire thermocouple was attached to the exterior of the vessel with electrical tape. The temperature of the vessel as required by the thermal method was estimated as the average reading of the thermocouples. The pressure in each vessel was reduced to 550 mbar in 12 second duration increments of 25 mbar, before the start of mixing. The formulation was mixed three times at 50 G acceleration for 50 minutes. An additional mix was performed with 15 second pauses after 0.7, 4.4, 10.7, and 24.9 minutes respectively. As required for the electrical and thermal methods, the mixer intensity required to vibrate a rigid body of mass equivalent to the filled apparatus (604 g) was found for 50 G acceleration.

[c] Polyether ether ketone

## Results and discussion

### Characterisation of materials

The glass beads analysis is shown in Table 2-2 with standard deviations. The specific heat capacity of the formulation was found to range from 0.99 $J\,K^{-1}\,g^{-1}$ and 1.13 $J\,K^{-1}\,g^{-1}$ between 10 ℃ and 90 ℃. The full analysis is shown in appendices (Figure 2-A1). The average cooling constant, $k$, was found to be 0.0432±0.0006 $min^{-1}$ over the first three mixes. The rheology analysis is shown in Figure 2-2, where the dashed lines show ±1 standard deviation. The average ambient temperature was 21±2 ℃ over the four mixes performed.

Table 2-2: Density and particle size analysis of the glass beads.

| Density ( $g\,cm^{-3}$) | D10 (µm) | D50 (µm) | D90 (µm) |
|---|---|---|---|
| 2.4905±0.0002 | 12.7±2.3 | 28.3±1.7 | 45.4±1.5 |

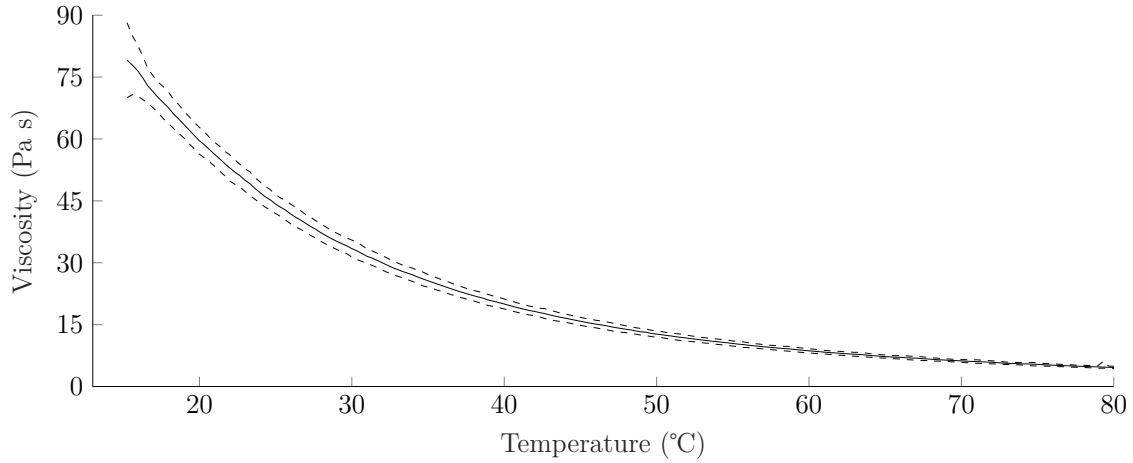


Figure 2-2: Glass bead formulation viscosity analysis after 50 minutes of mixing. Glass microbeads 62 % v/v, DEHA 19 % v/v, HTPB 19 % v/v.

### Mixing procedure

A mixer intensity profile and corresponding temperature increase (above ambient) profile is shown in Figure 2-3, where the horizontal dotted line shows the measured intensity readout (36.8 %) for an equivalent rigid body mass (RBM). Immediately after the mixer is switched on, the vessel contents are still fully segregated into layers from the loading procedure. Wetting, whereby the solids are introduced to

the liquids, then occurs rapidly in the first minute. The large intensity fluctuations are indicative of the rapidly changing rheological state as incorporation of the solids drastically changes the homogeneity of the vessel contents.[14] Between one and eight minutes, there is a fall in intensity from approximately 55 % to 45 %, with continuing intensity fluctuations of approximately 10 %, and a rapid temperature increase that slows as the mixer intensity falls. The falling intensity is indicative of a reduction in the power required to move the material as the solids and liquids become more uniformly distributed and fluidised. During this stage where homogeneity rapidly changed, the dominant movement mode seemed to rapidly switch between being decoupled from the vessel wall and attempts at churning, whereby the material would briefly couple to the wall before detaching again.

Churning was observed to be the only movement mode after eight minutes, with the emergence of a favourable wall coupling condition upon the material becoming further fluidised likely responsible. The churning became faster and more vigorous up to the 15 minute mark, probably due to the temperature increase lowering the viscosity (thus increasing the compliance) such that a larger velocity gradient across the material was made possible. With a larger velocity gradient, increased shear (thus energy expenditure) was likely responsible for mixer intensity readout (thus power consumption) building to its overall maximum of approximately 90 %. This was accompanied by a further temperature rise that steepened as mixer intensity increased, possibly due to a positive reinforcement effect.[d] The intensity curve up to this point is herein referred to as the mixing stage (M).

Between 15 and 29 minutes there is a high intensity churning stage that is characterised by high power consumption which decreases as time progresses. Such movement is referred to as 'bulk mixing' by the manufacturer, but since a movement mode (rather than a process) is being described, 'bulk motion' (B) may be a better descriptive term. It would appear the steadily increasing temperature (thus steadily decreasing viscosity) in this stage has a net effect of lowering the required mixer intensity since the material requires a decreasing power to move. The rate of temperature increase then further slows as the mixer intensity falls. Temperature reaches its maximum point at the end of this stage, where 29 minutes into the mix, there is a sharp drop in intensity after which the profile plateaus to form a flat-line.

At first glance, the flat-line stage (FL) would seemingly correspond to that seen

[d] Higher temperature → lower viscosity → greater compliance → greater velocity gradient → higher shear → higher energy expenditure → higher mixer intensity (power draw) → higher temperature

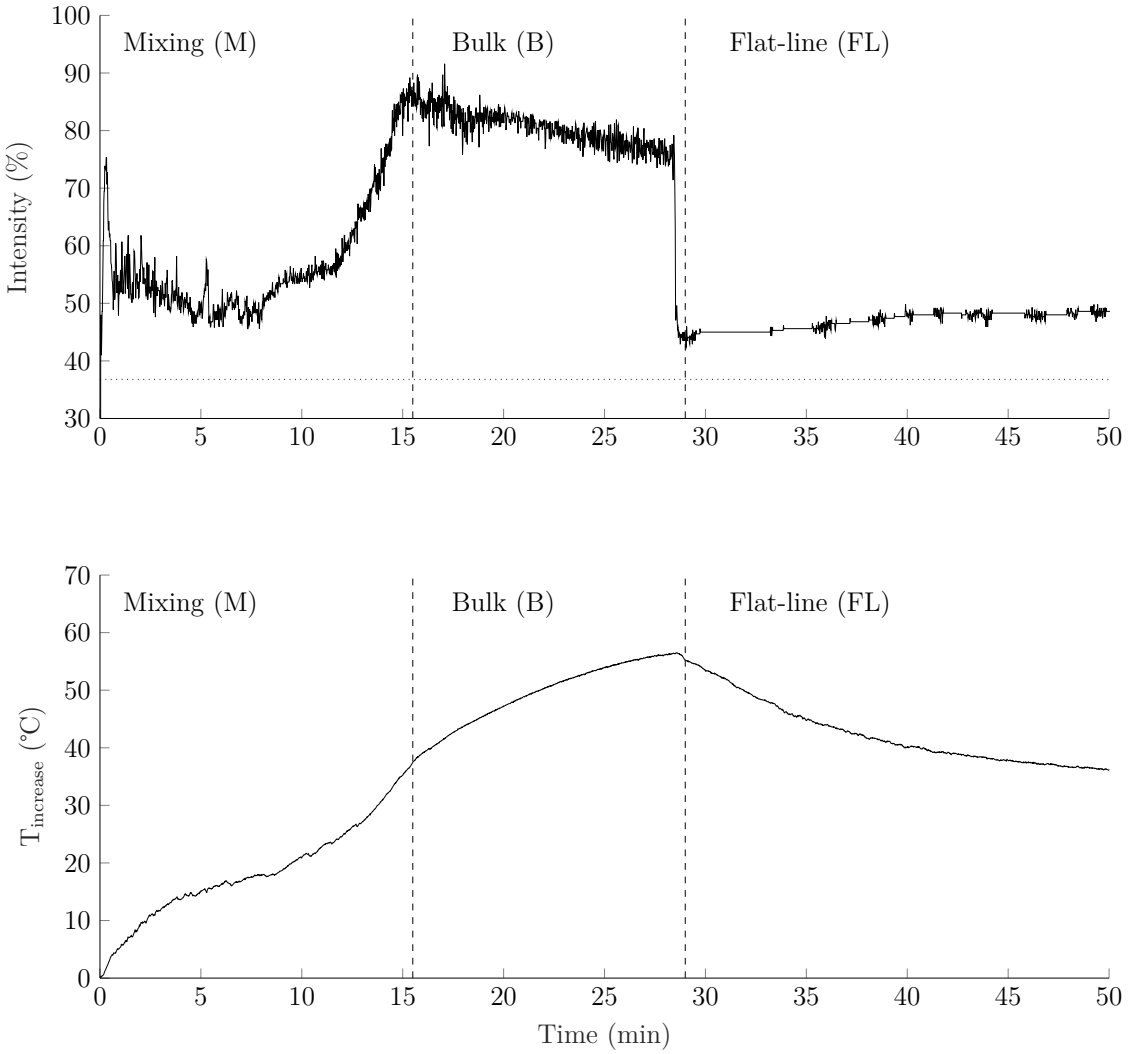


Figure 2-3: Example intensity and temperature profiles for the glass bead formulation. Glass microbeads 62 % v/v, DEHA 19 % v/v, HTPB 19 % v/v, 550 mbar pressure, 50 G acceleration.

upon mixing completion by Vandenberg and Wille[20] (see Figure 2-1), though this explanation would not account for such a large and abrupt drop in intensity (a drop of 25 % from 72 % to 47 % over approximately 2 seconds) at the flat-line onset. A more likely explanation may be a readjustment in the churning movement mode of the material. Once the temperature reaches approximately 75 ℃ (*absolute* temperature that is, noting *relative* temperature is shown on the figures), the viscosity of the material (thus viscous drag) may become so low such that significant slip abruptly occurs, resulting in a more shallow velocity gradient.

The fact that this observation is not apparent in Figure 2-1 for concrete mixing could be because of the different (much lower) viscosity ($\sim$4 Pa s) of the concrete mix in comparison to the PBX simulant used here, or a more temperature dependant

rheology when mixing polymers. That is to say that in concrete mixing (where water is the continuous phase), changes in viscosity with time will likely rely mainly on the changing degree of homogeneity, regardless of increases in temperature. Though the temperature dependence of viscosity was not studied by Vandenberg and Wille[20] for the formulation they used, other studies[23] have shown that cement viscosity falls by 5 % between 20 ℃ (room temperature) and 40 ℃ (the end of mixing temperature observed by Vandenberg and Wille[20]), whereas Figure 2-2 shows that the polymer-bound formulation used here falls by 67 % across the same range. Changes in viscosity due to both homogeneity and temperature are therefore of importance when PBX mixing, meaning the viscosity, thus intensity reading, is still significantly changing beyond the time at which homogeneity is achieved. In any case, it would appear direct comparisons in mixing behaviour between polymer suspensions and concrete mixtures are difficult to make due to their significantly different rheologies.

As for the movement mode observed during the flat-line stage, it could be seen visually that churning was still occurring, albeit at lower mixer intensity than in the bulk motion stage. Despite the decreasing temperature in this stage, energy was still being supplied to the mixture as is reflected in the positive difference between the intensity profile flat-line and the dotted line at the intensity measured for an equivalent rigid body mass (RBM). This would suggest the lower mixer intensity is corresponding to decreased movement (less vigorous churning), such that the rate of cooling exceeds the rate of heating. It would appear the system tends towards a steady equilibrium, where the effects of temperature (thus viscosity), velocity gradient, and mixer intensity become balanced.

To investigate the rheological changes occurring over time, viscosity analysis was performed on material sampled at the end of the mixing stage (bulk onset), and is shown as the solid line in Figure 2-4. The dashed lines show ± 1 standard deviation from the average of the three viscosity measurements taken after 50 minutes of mixing, as shown in Figure 2-2. Since the viscosity trace falls within the dashed lines, it can be concluded that there are few changes in homogeneity beyond the mixing stage (M). This suggests that changes in the intensity profile beyond this point are mainly dependant on rheological changes due to temperature.

Nevertheless, the profile features as described on Figure 2-3 provide excellent reference points with which intensity profiles from different mixes can be compared. The beginning of the bulk stage (end of the mixing stage) makes an excellent reference feature to take as the end of mix point, while the onset of the flat-line provides an insight into the rate of energy uptake once bulk motion is fully established. For

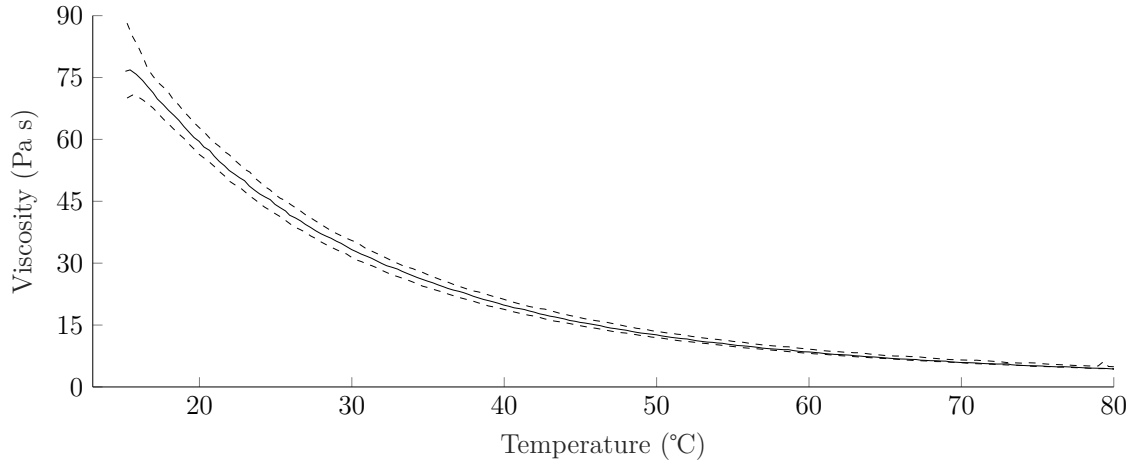


Figure 2-4: Glass bead formulation viscosity analysis after the mixing stage (bulk onset), within the standard deviations of viscosity as measured after 50 minutes of mixing. Glass microbeads 62 % v/v, DEHA 19 % v/v, HTPB 19 % v/v.

investigating the underlying factors affecting RAM efficiency using idealised systems (or when live explosives mixing is impractical), the formulation is therefore recommended for future use.

It is unclear what differences may be seen in the profiles when PBX rheology differs from that of the idealised formulation used in this work. High explosive fillers typically used in PBXs have wide particle size distributions (such as the 'Class 1' RDX[e] industry granulation standard which ranges from <75 to 850+ micron[24]), are irregular in shape, and are included at considerably higher loadings (typically 88+ % w/w). More angular particle shape is known to increase viscosity[25] and may therefore be more difficult to incorporate into the binder. As such the time and energy required for wetting and incorporation may increase, resulting in lower efficiency. Higher viscosity may also prevent the sharp drop off at the flat-line stage since the viscous drag may never fall to a low enough level upon heating for the velocity gradient to become unstable. This may result in an equilibrium being reached at a higher intensity than that seen in the flat-line stage in Figure 2-3. Alternatively, higher viscosity may preclude the build up to a high intensity bulk motion stage all together, should the material lack the compliance to allow sufficient movement for a large velocity gradient to form. In addition, it is unclear what may be seen if external heating or cooling was to be used. External heating would likely result in a shorter time and mixer energy for wetting and incorporation, and if high enough (> 75 ℃), may result in the bulk motion stage being non-existent, with the

[e] 1,3,5-trinitro-1,3,5-triazinane

profile going straight from the mixing stage to the flat-line stage. Similarly, active cooling could perhaps be used to prevent the temperature increasing to the point at which the flat-line stage occurs. This may prolong the high bulk motion stage, and result in an equilibrium being reached at higher intensity.

### Reproducibility

The triplicate dataset of the intensity profiles shown in Figure 2-5 shows there is good agreement between repeat measurements, where the slight variations in the onset points for the bulk motion and flat-line stages are likely influenced by minor differences in initial material configuration. Such differences may include filler packing density, the degree to which plasticiser and binder soaked into the filler before mixer start, and ambient laboratory conditions at the time of mixing. Table 2-3 shows the average values for the time required to reach bulk onset, and the time and energy required to reach the flat-line onset, as assessed using the mechanical, electrical, and thermal methods.

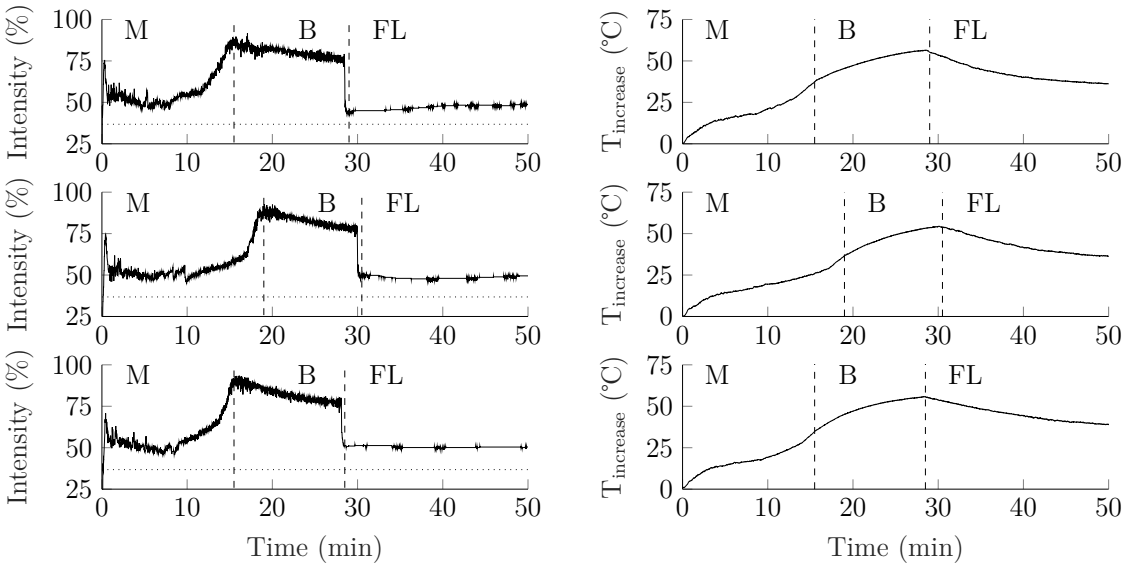


Figure 2-5: Triplicate intensity and temperature profiles. Glass microbeads 62 % v/v, DEHA 19 % v/v, HTPB 19 % v/v, 550 mbar pressure, 50 G acceleration.

Table 2-3: Mixing statistics for the three replicate mixes. Glass microbeads 62 % v/v, DEHA 19 % v/v, HTPB 19 % v/v, 550 mbar pressure, 50 G acceleration.

| | |
|---|---|
| Time of bulk onset (end of mix) (min) | 16.7±1.9 |
| Energy at bulk onset (Mechanical, kJ) | 12.1±0.7 |
| Energy at bulk onset (Electrical, kJ) | 7.3±0.4 |
| Energy at bulk onset (Thermal, kJ) | 8.0±0.3 |
| Time of flat-line (min) | 28.9±1.0 |
| Energy at flat-line (Mechanical, kJ) | 32.6±0.6 |
| Energy at flat-line (Electrical, kJ) | 19.4±0.4 |
| Energy at flat-line (Thermal, kJ) | 14.9±0.4 |

### Pausing the mix cycle

The effect of pausing the mix cycle on the intensity profile is shown in Figure 2-6. It can be seen that the time required for the intensity to recover to the pre-paused values (grey shaded areas) increases as the mixing cycle progresses, taking 0.4, 0.8 and 4.6 minutes in the first three cases respectively. The intensity did not build back up to its previous level after the pause that occurred in the bulk motion stage. A 'repaired' version of the profile is also shown, whereby the grey shaded parts of the profile are removed. This profile is in very good agreement with the profile shown for an un-paused mix, up until when mixing is resumed after pausing in the bulk stage.

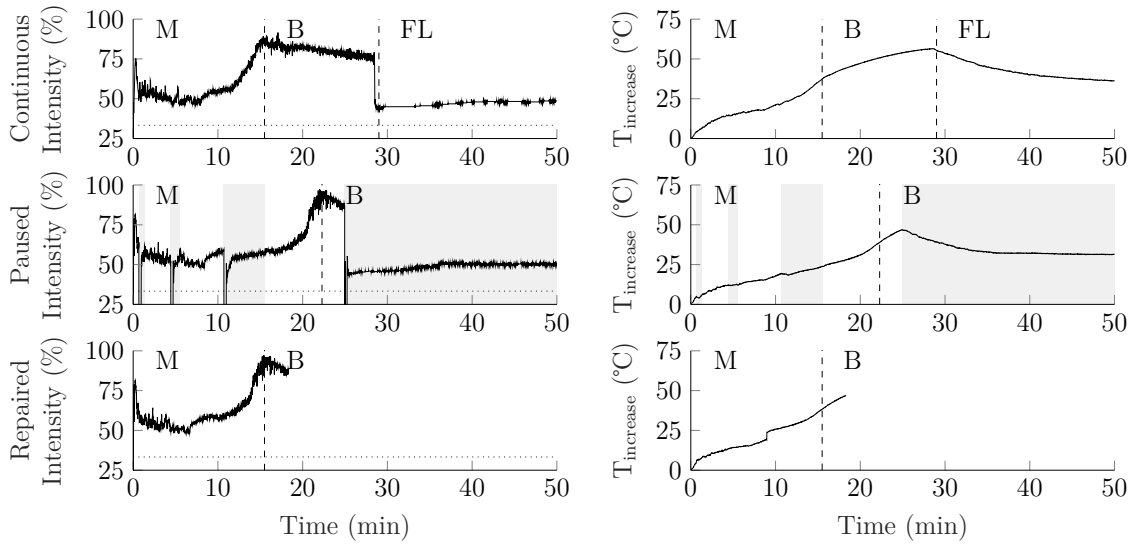


Figure 2-6: Comparison of intensity and temperature profiles when run continuously, run with pauses, and when 'repaired'. Glass microbeads 62 % v/v, DEHA 19 % v/v, HTPB 19 % v/v, 550 mbar pressure, 50 G acceleration.

The observation that bulk motion does not resume after the cycle is paused could

be explained with reference to previous observations[12] that two different wall coupling conditions (thus power consumptions) are possible for the same acceleration, despite material properties ('degree of mixedness' and temperature) being essentially the same. An effect such as this would also explain the observation that bulk motion does not resume after the temperature begins to lower (thus the viscosity begins to increase again) after the flat-line when the mixer is running continuously. Put concisely, the switch in wall coupling condition (thus the sharp intensity drop) would appear to occur naturally once the temperature reaches a certain point (∼75 ℃ absolute in this case), though it can be artificially forced to the lower intensity wall coupling condition by briefly interrupting the mixing cycle.

### Energy determination methods

The methods used to determine mix energy showed significant variation, with the mechanical method giving by far the highest values, followed by the electrical method approximately a third lower and the thermal method a quarter lower again. Figure 2-7 shows the cumulative energy uptake as found using each method. By differentiating with respect to time, the power to the mix is derived. This is shown in Figure 2-8.

With reference to Figure 2-7 and Figure 2-8, it can be seen that over the first 10 minutes of mixing, where the majority of mixing takes place, all methods are in reasonably good agreement. However, during the build up to the bulk stage, where the movement mode is high intensity churning (bulk motion), the mechanical method begins to report a significantly higher power and energy consumption than the electrical and thermal methods. At the bulk stage onset, the electrical method also begins to report higher power consumption to the thermal method. The remainder of the bulk stage most clearly shows the discrepancies between the methods, with the same trend (mechanical > electrical > thermal) continuing into the flat-line stage. The methods should be further compared over a more diverse range of mixing scenarios (e.g. different formulations, acceleration, pressure) to determine their relative accuracies.

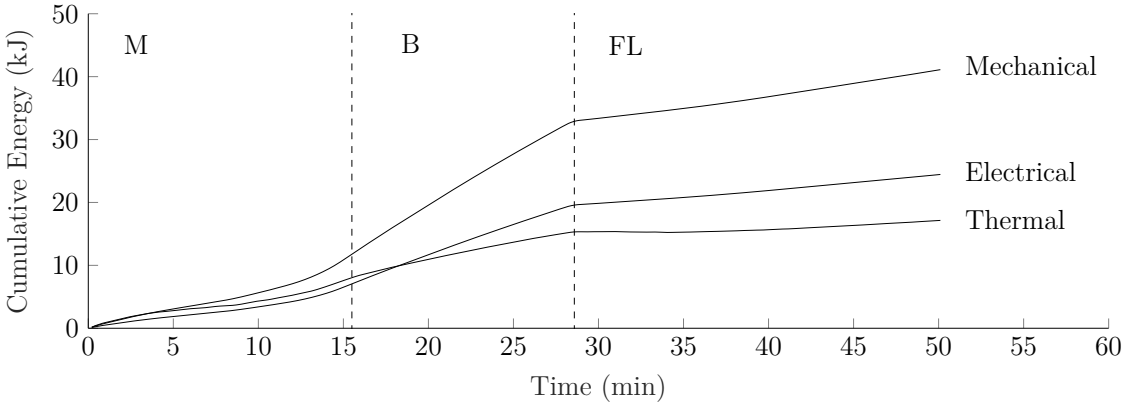


Figure 2-7: Cumulative energy consumption as measured by each method. Glass microbeads 62 % v/v, DEHA 19 % v/v, HTPB 19 % v/v, 550 mbar pressure, 50 G acceleration.

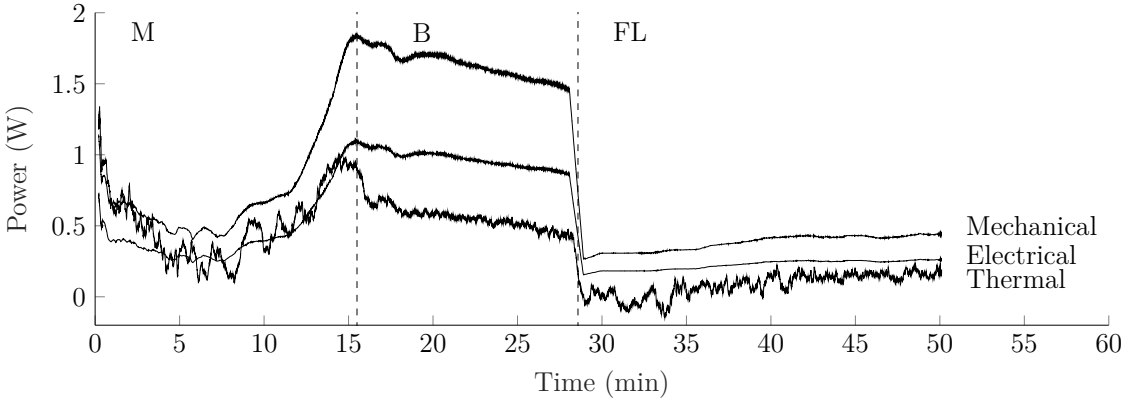


Figure 2-8: Power consumption as measured by each method. Glass microbeads 62 % v/v, DEHA 19 % v/v, HTPB 19 % v/v, 550 mbar pressure, 50 G acceleration.

## Conclusions

The aim of this work was to develop a method to determine the time and energy required for mix completion when using RAM applied to an idealised PBX stimulant. It has been demonstrated that by interpreting the machine intensity profile, the changing rheology of the vessel contents can be monitored. It was found that the shape of the intensity profile relies on rheological changes stemming from both changing homogeneity and changing temperature of the material. The sharp profile features associated with these changes provided well defined markers that allowed the mixing progression to be easily compared between repeat mixes. As such, the glass microbead formulation is recommended for use to determine mixing behaviour under various conditions in future work. Mixing behaviour has also been shown to

be repeatable, with standard deviations of ±11 % to the end of the mixing stage, and ±4 % to the onset of the flat-line over the three mixes performed. The three methods used to determine the power and energy consumption of mixing were found to give different results, but the same order of magnitude and the same trend with increasing time. A greater appraisal of each method should be undertaken after they have been applied over a more diverse range of mixing conditions than those considered in this work.

## References

[1] D.B. Todd. Mixing of highly viscous fluids, polymers, and pastes. In *Handbook of Industrial Mixing: Science and Practice*. John Wiley & Sons, Inc., 2004.

[2] A.C. Hordijk and A.E.D.M. van der Heijden. Mixing. In *Energetic Materials; Particle Processing and Characterization*. Wiley-VCH Verlag GmbH, 2005.

[3] Charles Ross & Son Company. High Viscosity Mixer Designs and Applications. `https://www.mixers.com/whitepapers/hvm_designs_whitepaper.pdf`. Accessed 14-07-2020.

[4] Charles Ross & Son Company. How to choose the right mixer for high-viscosity mixing applications. `https://www.mixers.com/whitepapers/high%20viscosity%20mixing.pdf`. Accessed 14-07-2020.

[5] D.A. Dahlstrom, R.C. Bennett, R.G. Emmet, P. Harriott, T. Laros, W. Leung, S.A. Miller, B. Morey, J.Y. Oldshue, G. Priday, C.E. Silverblatt, J.S. Slottee, and J.C. Smith. Liquid-solid operations and equipment. In *Perrys Chemical Engineers' Handbook, Seventh Edition*. McGraw-Hill Pub., 1997.

[6] R.J. Davey, J.M. Wilgeroth, and A.O. Burn. Processing Studies of Energetic Materials using Resonant Acoustic Mixing Technology. BAE Systems Land UK, Glascoed, Monmouthshire, UK, 2019.

[7] Inc. Resodyn Acoustic Mixers. Resonant Acoustic Mixing (Technical White Paper). ResoDyn Corp, Butte, MT, USA, 2009.

[8] Inc. Resodyn Acoustic Mixers. LabRAM Resonant Acoustic Mixer Manual. ResoDyn Corp, Butte, MT, USA, February 2012.

[9] M.D. McPherson. Propellant and explosives production method by use of resonant acoustic mix process. Patent WO 2009/091430 A1, July 2010.

[10] A.J. Claydon. *Resonant Acoustic Mixing of Polymer Bonded Explosives*. PhD thesis, Cranfield University, 2020. Paper 1.

[11] J. Hilden, M. Sullivan, M. Polizzi, J. Wade, J. Greer, and M. Keeney. Power consumption during oscillatory mixing of pharmaceutical powders. *Powder Technol.*, 338:44–54, 2018.

[12] P.A. Lucon and J. Whaley. Liquids and Pastes. Resodyn Technical Interchange, Butte, Montana, USA, 2016.

[13] E.L. McCloy, P. Wilkinson, and P.P. Gill. Resonant Acoustic Mixing: Pushing The Boundaries. Master's thesis, Cranfield University, 2016.

[14] P.A. Lucon, G. Sperry, and J. Whaley. RAM Mixing of Liquids and Pastes. Resodyn Technical Interchange, Butte, Montana, USA, 2016.

[15] P.A. Lucon. Mixing with Vacuum Assist. Resodyn Technical Interchange, Butte, Montana, USA, 2016.

[16] R.A. Layton, W.R. Murray, and J.L. Garbini. The Control of Power for Efficient Batch Mixing. *Propellants Explos. Pyrotech.*, 22:269–278, 1997.

[17] J.T. Miller, A. Luebbering, S. Coguill, and P. Lucon. Mix Power. Resodyn Forum: Industrial Outcomes in ResonantAcoustic Mixing, Butte, Montana, 2013.

[18] P.A. Lucon. RAM Power Considerations. Resodyn Technical Interchange, Butte, Montana, USA, 2016.

[19] J.G. Osorio and F.J. Muzzio. Evaluation of resonant acoustic mixing performance. *Powder Technol.*, 278:46–56, 2015.

[20] A. Vandenberg and K. Wille. Evaluation of resonance acoustic mixing technology using ultra high performance concrete. *Constr. Build. Mater.*, 164:716–730, 2018.

[21] J. Whaley. Private Communication, Resodyn Acoustic Mixers, April 2020.

[22] K.S. Hope, H.J. Lloyd, D. Ward, A.A.L. Michalchuk, and C.R. Pulham. Resonant Acoustic Mixing Its applications to energetic materials. New Trends in Research of Energetic Materials (NTREM), Pardubice, Czech Republic., 2015.

[23] D.K. Lee and M.S. Choi. Standard Reference Materials for Cement Paste: Part III - Analysis of the Flow Characteristics for the Developed Standard Reference Material According to Temperature Change. *Materials (Basel)*, 11:2001–2012, 2018.

[24] NATO. Explosives, Specification for RDX (Hexogene). STANAG-4022.

[25] H.A. Barnes. A Review of the Rheology of Viscoelastic Systems. Rheology Reviews, The British Society of Rheology, 2003.

# Appendices

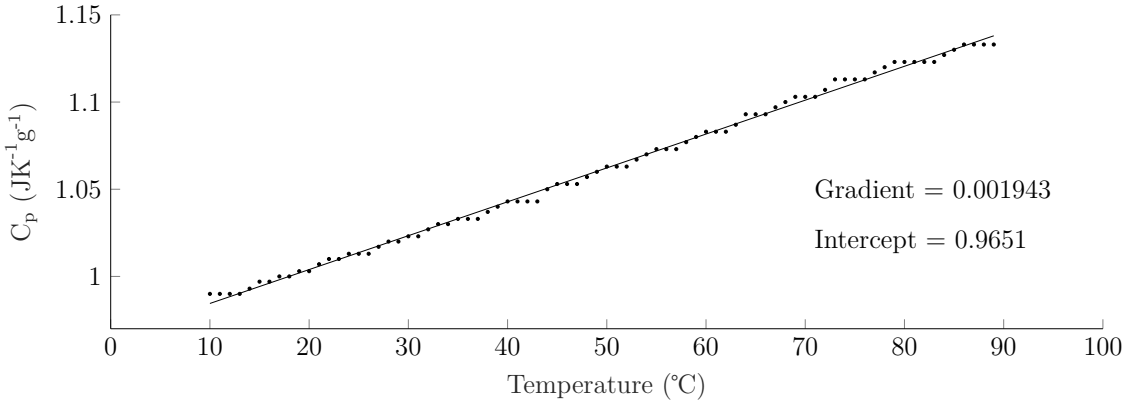


Figure 2-A1: The heat capacity analysis of the glass bead formulation. Glass microbeads 62 % v/v, DEHA 19 % v/v, HTPB 19 % v/v.

# Paper 3 - The Effect of Machine Variables on the Efficiency of Resonant Acoustic Mixing for Polymer Bonded Explosives

Andrew J. Claydon, Guillaume Kister, Sally Gaulter, and Philip P. Gill

**Abstract:** The efficiency (time and energy required for mix completion) of Resonant Acoustic Mixing (RAM) is assessed for a range of machine variables. A glass microbead based formulation (28.3 micron D50, 62% v/v in HTPB and plasticiser) was used as an inert simulant for Polymer Bonded Explosives (PBXs). Acceleration (45 G, 50 G, and 55 G) setting, mixer 'intensity' setting (67 % and 75 % mixer power), mixer size (LabRAM and LabRAM II), and mixer unit (comparison of three LabRAMs) were varied. Mixing is found to require more time and energy input at lower acceleration or lower intensity setting. Significant differences in mixing times are observed between mixing on a LabRAM (faster mix time) and mixing on a LabRAM II (slower mix time), possibly due to higher acceleration than intended being applied by the LabRAM due poorer acceleration control. Significant differences in mixing times are also observed between different LabRAM units, possibly due to acceleration calibration errors and variation between machines.

**Keywords:** Resonant Acoustic Mixing, Polymer Bonded eXplosive, Acceleration, Intensity, LabRAM, LabRAM II

## Introduction

Resonant Acoustic Mixing (RAM) has recently garnered substantial interest[1] as an alternative to conventional high shear mixers (such as a planetary or z-blade mixers[2]) for use in the manufacture of cured Polymer Bonded eXplosives (PBXs). PBXs consist of high explosive crystals dispersed in an elastomeric binder, where the binder begins as a viscous liquid prepolymer which can be cured with an isocyanate to form a solid composite material when cast into a mould. A typical pre-polymer in cast PBXs is hydroxyl-terminated polybutadiene (HTPB), which can be cured with an isocyanate to form a crosslinked polyurethane matrix. Homogeneity is important to ensure the properties of the material are consistent throughout its volume, which optimises its properties.[2] Instead of mixing blades, RAM operates by way of a vibrating spring mounted platform that vertically oscillates at mechanical resonance (approximately 60 Hz), at peak accelerations of up to 100 G. An affixed vessel is used to facilitate the mixing, whereby kinetic energy transfer to enclosed viscous suspensions (such as found in PBX manufacture) relies on a velocity gradient across the vessel contents, resulting in medium shear mixing over the entire volume of the vessel. The velocity gradient is believed to be brought about by a coupling condition between the formulation and vessel wall, where there is ideally 'no-slip' at the interface. Conversely the bulk of the material is acted on by acoustic pressure waves (vibrations) from the vibrating plate.[3–5] The resultant bulk smearing and rolling motion is referred to as churning.[6]

A literature review by the author[7] found that mixing efficiency relies on the degree to which the 'no-slip' condition is fulfilled, and the amount of movement in the material. By minimising wall slip and maximising movement in the material, the velocity gradient (thus shear) is thought to increase. It was determined that these conditions can be achieved by optimising machine variables, vessel variables, and formulation variables. The variables as reported in the literature or theorised by the author to be of consequence are summarised in Table 3-1.[7] The aim of this work is to further investigate the effects of changing machine variables on mixing efficiency. The effects of acceleration setting (45 G, 50 G, 55 G), mixer 'intensity' setting (67 % and 75 % mixer power), and mixer size (500 g payload scale LabRAM and 1 kg payload scale LabRAM II) are assessed, along with a comparison between three LabRAM units ('A', 'B', and 'C').

Table 3-1: Machine variables, vessel variables, and formulation variables for Resonant Acoustic Mixing.

| Machine variables | Vessel variables | Formulation variables |
|---|---|---|
| Acceleration setting | Vacuum setting | Binder content |
| Intensity setting | Wall material | Plasticiser content |
| Mixer model | Wall surface finish | Additives |
| Mixer unit | Diameter | Solids loading |
| | Insulation | Particle shape |
| | Active heating | Filler type |
| | Active cooling | |

### Machine variables

The two basic machine variables are acceleration (G) and mixer 'intensity' (%), where intensity refers to the amount of current being supplied to the driver motor up to 100 %. At a fixed acceleration the 'intensity' will adjust to maintain that constant acceleration throughout the different stages of mixing, depending on the power draw of the formulation at any given time. The reverse is true if a mix is undertaken at constant mixer 'intensity'. It has previously been determined that the degree of movement of the vessel contents depends on the inertial forces (where greater inertial forces deform the material more), and the compliance of the material (where greater compliance means the material is easier to deform).[7] In the context of machine variables, it follows that greater acceleration will result in greater inertial forces,[8] and can be achieved by defining a higher acceleration or intensity setting.[9] Higher acceleration has previously been found to increase the rate of energy supplied to the mixture,[3, 4] though the effect of acceleration on time to mixing completion has not been explicitly reported. Vandenberg and Wille[10] determined the effect of increasing intensity (which translated into a higher achieved acceleration) on the time required for concrete mixing, with a ∼30 % reduction in mixing time between 60 % and 80 % mixer intensity (using a LabRAM) apparent from their data. The study was not however extended to compare the differences in the observed profile with fixed acceleration, and it is unclear if one drive mode is inherently superior than the other.

Since the theory of operation is the same across all mixer models, each should exhibit the same mixing behaviour if performing the same procedure at the same acceleration setting. It is however known that scalability can be influenced by factors such as vessel diameter,[8] with which surface area (affecting interfacial drag, thus wall slip) scales linearly, whereas volume (affecting mass, thus inertia) scales

quadratically.[3] The effect of this on the effectiveness of RAM has been previously discussed by the author.[7] However, to the author's knowledge, no study to date has determined the extent to which mixing is reproducible between mixer units of the same model, or between mixers of different capacities when using the same size mixing vessel. That is to say, the extent of variation between machines due to calibration, non-idealities, and design upscaling is unknown. It is hypothesised that such differences may affect the acceleration delivered by the machines, thus the efficiency of mixing.

### Determining efficiency

The author's previous work[11] carried out on idealised inert suspensions containing glass microbeads found that by interpreting output data from the mixer, the changing rheology of the formulation (thus end of mix time) can be monitored. Mixing at constant acceleration, the profile of mixer intensity plotted against time could be broken down into easily recognisable stages.[a] It should be noted that although the shape of the profile stages observed were believed to be unique to the formulation used, they nevertheless provide excellent reference points with which mixing progression and energy uptake can be monitored. The sections were a mixing stage (M), a bulk motion stage (B), and a flat-line stage (FL). The mixing stage contained most of the rheological changes associated with increasing homogeneity, including wetting (where the solids and liquids were introduced), incorporation (where the mixture became more fluidised), and churning (where upon fluidisation the mixture coupled to the vessel wall). Upon churning taking full effect, the temperature and mixer intensity started to rapidly rise, suggesting the velocity gradient was growing in magnitude (more vigorous churning) until a peak intensity was reached, marking the end of the stage. Since the homogeneity was found to no longer change beyond this point, it was taken to be the end of mix point. However, subsequent viscosity changes as the mixture continued to vigorously churn and heat up resulted in a 'bulk motion' (high intensity churning) stage until a temperature of approximately 75 ℃ was achieved. At this temperature it was believed the viscosity had lowered to a point at which the velocity gradient became unsustainable. A minimum viscosity is indeed required for both wall coupling (which requires viscous drag), and to transmit the velocity gradient across the mixture. The loss of this viscosity was believed to have resulted in a sharp drop off in intensity as the coupling condition readjusted.

[a] Similarly, mixing at constant mixer intensity produces plots of acceleration against time.[10]

This formed a generally featureless flat-line stage where lower intensity churning occurred, and a constant mixer intensity was recorded. Here, mixer intensity, temperature (thus viscosity), and velocity gradient tended towards an equilibrium. The stages of mixing as described here have been discussed in more detail in previous work.[11] Three methods (based on mechanical, electrical, and thermal data interpretation) have also been used by the author[11] to assess the energy consumption of the mixture over a mixing cycle, and are employed here.

## Experiment

The procedure as presented previously[11] was used for mixing, whereby a custom machined poly(methyl methacrylate) (PMMA) mixing vessel (48 mm diameter, 47.5 mm height) was filled with 65 mL of an inert glass microbeads (Glass Sphere s.r.o., Czech Republic) based formulation as shown in Table 3-2. The vessel lid was manufactured out of PEEK (polyether ether ketone) and held into place with clamshell clamp. The lid included ports for vacuum application and monitoring, and a central airtight hole for a rod thermocouple to be inserted into the vessel contents. The analysis on the glass microbeads as previously reported by the author[11] is given in Table 3-3. Hydroxy-terminated polybutadiene (HTPB) (type Poly bd® R-45HTLO, Cray Valley, USA) binder, and di(2-ethylhexyl) adipate (DEHA) ($\geq$ 97 %, Merck, UK) plasticiser were used. Curative was not added. Vacuum was applied down to 550 mbar for mixing.

Table 3-2: The glass bead formulation used for mixing.

| | Glass | DEHA | HTPB | Curative |
|---|---|---|---|---|
| Volume (%) | 62.00 | 19.00 | 19.00 | - |
| Actual mass (%) | 81.65 | 9.30 | 9.05 | - |
| RDX equivalent mass (%) | 76.48 | 11.91 | 11.60 | - |

Table 3-3: Density and particle size analysis of the glass beads.

| Density ( g cm$^{-3}$) | D10 (µm) | D50 (µm) | D90 (µm) |
|---|---|---|---|
| 2.4905±0.0002 | 12.7±2.3 | 28.3±1.7 | 45.4±1.5 |

LabRAM 'A' was used in the experiment unless stated otherwise. The mixer was controlled using aftermarket equipment and software supplied by Falcon Project Ltd., which gave the option to control the mixer at constant intensity setting (default

for LabRAM units) or constant acceleration setting (default for the other RAM models). Three mixes were performed at both 45 G and 55 G acceleration, and compared to triplicate datasets for 50 G as presented previously.[11] Further mixes were carried out at constant intensities of 67 %, the average intensity achieved up until the time of flat-line in the case of the three mixes carried out at 50 G acceleration, and 75 %, an arbitrarily higher intensity.

A 604 g rigid body mass (RBM - equivalent to the total mass attached to the plate when mixing) was used to determine the base-line mixer intensity (% of maximum current) of the machines when not mixing material. The mixer intensity was recorded for integer accelerations up to 100 G for LabRAM 'A' and the RAM II. Two mixes of the formulation were then performed at 55 G acceleration using the LabRAM II. LabRAMs 'A', 'B', and 'C' were similarly characterised for their 604 g rigid body mass (RBM) intensity readouts at accelerations between 15 G and 55 G. An additional mix of the formulation was then performed at 50 G using LabRAM 'C'.

## Results and discussion

### Acceleration effect on mixing

A comparison of typical mixer intensity profiles for mixing at 45 G, 50 G, and 55 G is shown in Figure 3-1, where the horizontal dotted lines show the measured[11] mixer intensity readout for an equivalent rigid body mass (RBM). The red circles represent the point of maximum temperature for the 45 G mix. The full set of intensity profiles for 45 G and 55 G are shown in appendices (Figure 3-A1), and are all similar between repeat measurements.

Figure 3-1 shows the time required for the onset of each stage in the profile has a strong dependence on the acceleration, with higher acceleration corresponding to more rapid onset. The maximum temperature reached across all mixes was an absolute temperature of ∼75 ℃, at which point the coupling condition readjustment believed to be responsible for the flat-line onset occurred. It should be noted that temperature increase relative to ambient is shown on the figures, where the ambient temperature over the nine mixes had an average and standard deviation of 21±2 ℃. The mixes carried out at 50 G and 55 G both featured a sharp drop in intensity upon the maximum temperature (thus coupling condition readjustment) being reached,

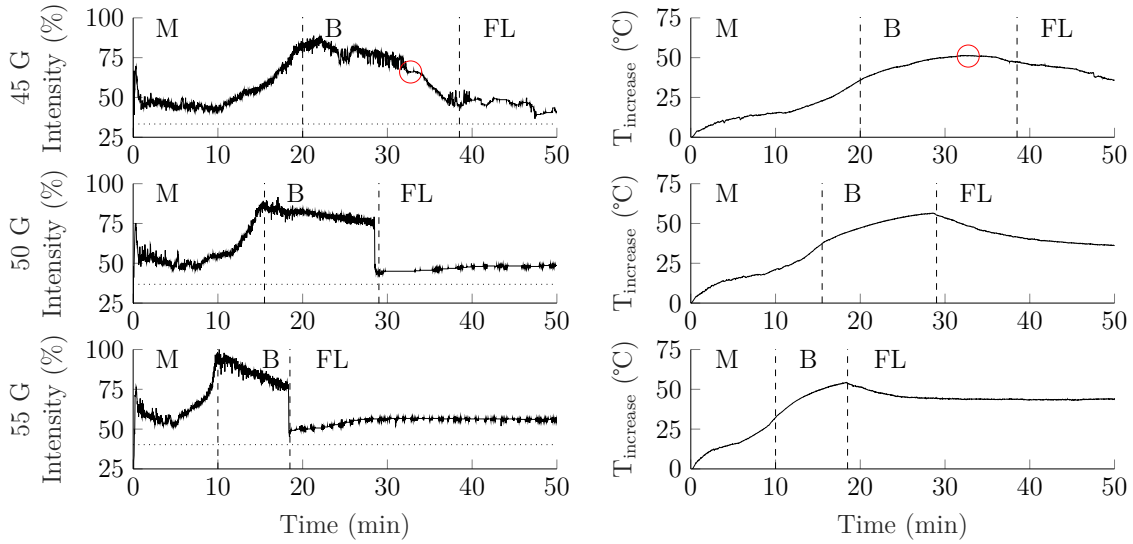


Figure 3-1: Comparison of intensity and temperature profiles at 45 G, 50 G, and 55 G acceleration. Glass microbeads 62 % v/v, DEHA 19 % v/v, HTPB 19 % v/v, 550 mbar pressure. Horizontal lines - equivalent RBM profiles, vertical lines - profile stage boundaries, red circles - maximum temperature point for 45 G profile.

marking the onset of the flat-line stage. Conversely, the mixes carried out at 45 G were slightly different in profile, lacking a sharp drop-off point at the maximum temperature point. Instead, intensity reduced over a period of several minutes before levelling off. As such, the point of maximum temperature and flat-line onset did not coincide. It is unclear why this would be apparent, though a possible explanation may be the lower acceleration imparted more gentle mixing, slowing the rate at which the wall coupling readjustment occurred.

Figure 3-2 shows the average time and energy (mechanical method as used in previous work[10, 12]) required for the end of mix point (bulk motion onset) over the three mixes performed in each case in the form of bar graphs. A full set of bar graphs for the onset of bulk motion, maximum temperature, and the flat-line are given in appendices (Figure 3-A2), with each giving the same trend as acceleration is increased. Energy as determined from the electrical and thermal methods are also given on these graphs, and in all cases give the same trend as the mechanical method with values of the same magnitude. Full data for the experiment is shown in appendices (Table 3-A1).

Figure 3-2 shows the time required for the end of mix point (bulk onset) reduced by an average of 55 % upon an increase in acceleration from 45 G to 55 G. While it would be expected that mixing time will be longer at lower accelerations (since less energy is imparted on the vessel contents at any given time), the total amount

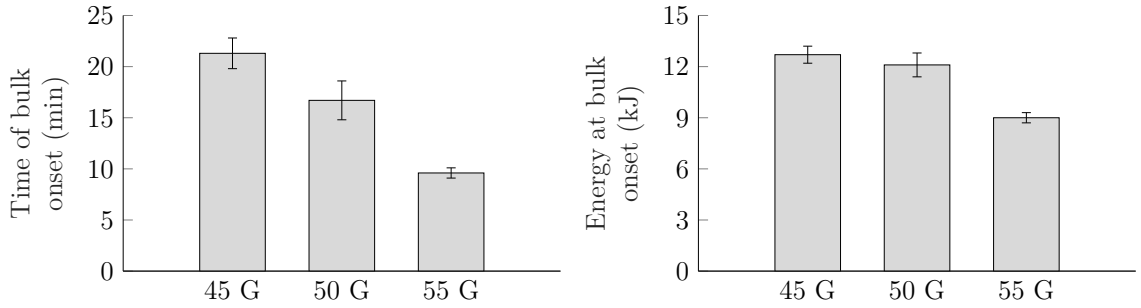


Figure 3-2: Bar graphs showing the average time (left) and energy (mechanical method, right) required for mixing completion at 45 G, 50 G, and 55 G acceleration over triplicate measurements. Glass microbeads 62 % v/v, DEHA 19 % v/v, HTPB 19 % v/v, PMMA vessel, 550 mbar pressure. Standard deviations shown.

of energy required to mix the material may be expected to remain constant, i.e. a certain amount of energy would be required to rearrange the vessel contents. However, Figure 3-2 shows that the total energy required for mixing is greater when at lower acceleration. The same trend is also observed (Figure 3-A2) for the point of maximum temperature and flat-line onset. This may be the result of two effects, with the primary effect being increased acceleration creating more intense mixing, and the secondary effect being the more intense mixing more rapidly increasing the temperature, reducing the viscosity of the formulation which then requires less energy to mix. This effect may be exacerbated by longer mix times at lower acceleration allowing more time for the vessel to lose heat to the surroundings, further limiting the rate of viscosity reduction.

### Mixing at constant intensity

The acceleration and temperature profiles of the mix performed at a constant intensity of 67 % (the average intensity observed before the flat-lines of the three mixes carried out at 50 G) is given in Figure 3-3. The red circles represent the point of maximum temperature for the 67 % mix. The full set of acceleration profiles for 75 % intensity are shown in appendices (Figure 3-A3), and are all similar between repeat measurements. Again, the maximum temperature achieved in all cases was ∼75 ℃, though temperature increase relative to ambient is shown on the figures. The ambient temperature over the four constant intensity mixes had an average and standard deviation of 27±2 ℃. The example 50 G acceleration mix shown on Figure 3-3 for comparison had an ambient temperature of 19 ℃.

It can be seen the acceleration profile as found for constant intensity (67 %) generally resembles the shape of the intensity profile found for constant acceleration

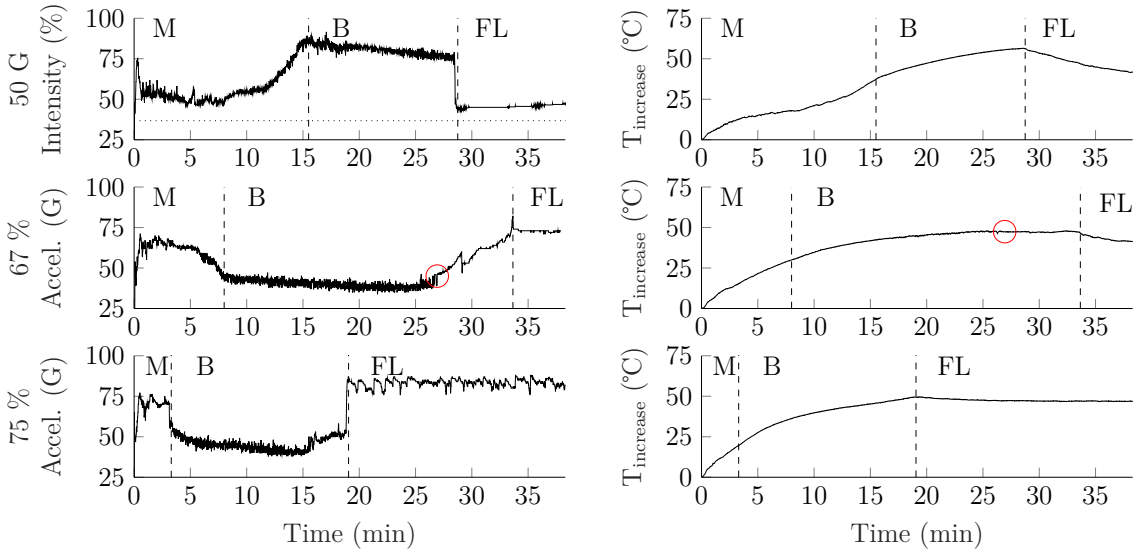


Figure 3-3: Comparison of intensity/acceleration and temperature profiles at 50 G acceleration, and 67 % and 75 % intensity. Glass microbeads 62 % v/v, DEHA 19 % v/v, HTPB 19 % v/v, 550 mbar pressure. Horizontal lines - equivalent RBM profiles, vertical lines - profile stage boundaries, red circles - maximum temperature point for 67 % profile.

(50 G) if it was to be 'inverted' along the y-axis. However, compared to the observations made at constant acceleration (50 G), the onset to bulk motion (end of mix point) occurs sooner and requires less energy. This can be seen in Figure 3-4. The reason for this is that in the initial stages, the set intensity corresponds to a higher acceleration than 50 G thus the rate of energy supply is higher, similarly to the mixes performed at 55 G. Subsequently over the bulk motion stage, the set intensity corresponds to a lower acceleration than 50 G thus the onset of the flat-line comes later, similarly to the mixes performed at 45 G. Another similarity to the 45 G mix profiles is the lack of a sharp cut-off at the flat-line, and the point of maximum temperature occurring several minutes before the flat-line. It would therefore appear that despite the *average* intensity (thus mixer power) being consistent between 50 G set acceleration and 67 % set intensity up to the flat-line point, the time required to reach bulk onset, maximum temperature, and the flat-line depends on the achieved *instantaneous* intensities or accelerations over the duration of the profile.

Three mixes were then performed at 75 %, an arbitrarily higher intensity, with an example acceleration profile also shown in Figure 3-3. Similarly to the mixes carried out at higher accelerations (50 G and 55 G), there is a sharp drop-off point at the flat-line, which coincides with the point of maximum temperature. In this case, the achieved acceleration was consistently higher throughout the mixing cycle, resulting

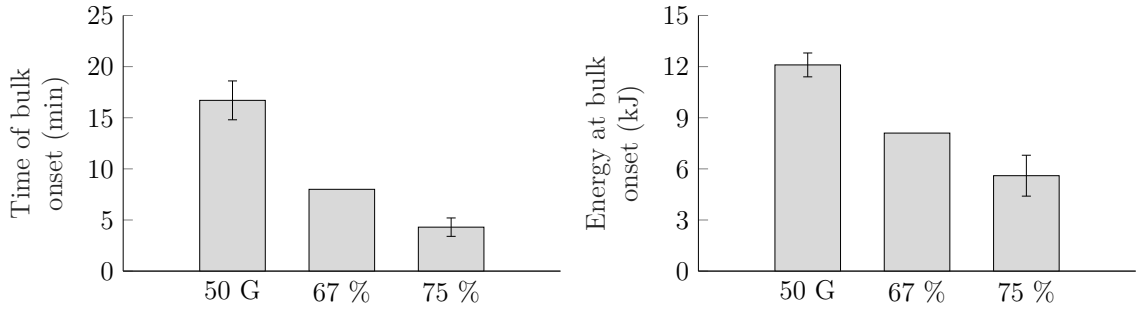


Figure 3-4: Bar graphs showing the average time (lefts) and average energy (mechanical method, right) required for mixing completion at 50 G acceleration and 67 %, and 75 % intensity over triplicate, single, and triplicate measurements respectively. Glass microbeads 62 % v/v, DEHA 19 % v/v, HTPB 19 % v/v, PMMA vessel, 550 mbar pressure. Standard deviations shown.

in the time of bulk motion onset (end of mix) occurring 3.7 minutes sooner than at 67 % (a reduction of 46 %). Less energy was also required to reach the end of mix point, likely due to the same two effects (higher intensity mixing, thus more rapid heating and viscosity reduction) as discussed above for mixing at higher acceleration. This is also shown in Figure 3-4. The time to the maximum temperature increase and flat-line were also shorter when mixing at 75 % intensity, occurring 16.4 minutes sooner than at 67 % intensity in the case of the flat-line (a reduction of 49 %). This is shown in appendices (Figure 3-A4). A data table containing the average time to bulk motion onset, maximum temperature, flat-line onset, and the energy supplied is shown in appendices (Table 3-A2). The energy as determined from the electrical and thermal methods in all cases give the same trend as the mechanical method with values of the same magnitude.

### Comparison to LabRAM II

The 604 g rigid body mass (RBM) intensity readout analysis for LabRAM 'A' and the LabRAM II is shown in Figure 3-5. For LabRAM 'A', the line of best fit is linear over the measured range, with a gradient and projected intercept of 0.6935 and 2.112 respectively. For the LabRAM II, the line of best fit is not linear, in keeping with the observations of Hilden *et al.*[13] It is instead fitted to a fourth order polynomial.

A comparison of intensity profiles between mixes carried out at 55 G acceleration on LabRAM 'A' and the LabRAM II is shown in Figure 3-6. The red circles represent the point of maximum temperature for the LabRAM II mix. Again, the maximum temperature achieved in all cases was ∼75 ℃, though temperature in-

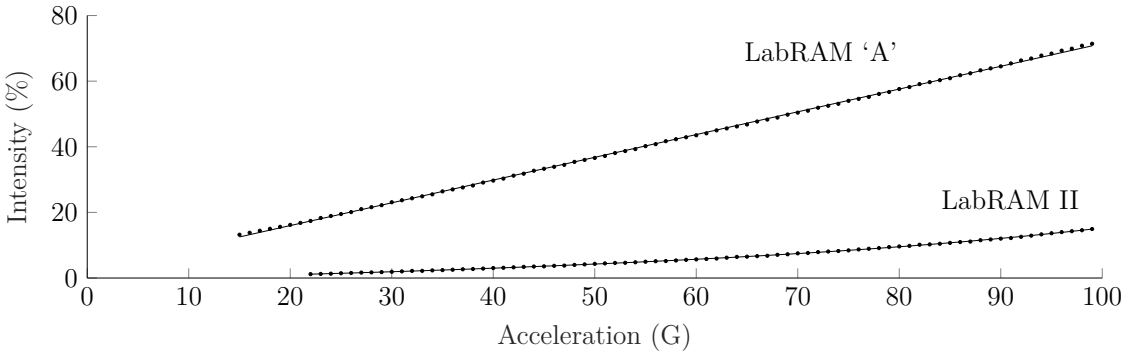


Figure 3-5: Rigid body mass (604 g) intensity analysis for LabRAM 'A' and the LabRAM II.

crease relative to ambient is shown on the figures. The ambient temperature over the triplicate LabRAM 'A' mixes and duplicate LabRAM II mixes had an average and standard deviation of 22±1 ℃. The full dataset is shown in appendices (Figure 3-A5). The required intensity to maintain the set acceleration was considerably lower for the LabRAM II, typically ranging between 7 % and 15 % as opposed to 50 % to 100 % on LabRAM 'A'. This is simply because the LabRAM II is a more powerful machine. The overall shape of the intensity profiles is similar, with each showing a high intensity bulk motion onset that is discernible from both the intensity and temperature profiles. However, the LabRAM II mix shows no distinctive flat-line onset. Furthermore, the intensity and temperature profiles are stretched out over approximately 1.5 times the time period seen for LabRAM 'A', suggesting the LabRAM II requires a longer mix time. This is shown in Table 3-4.

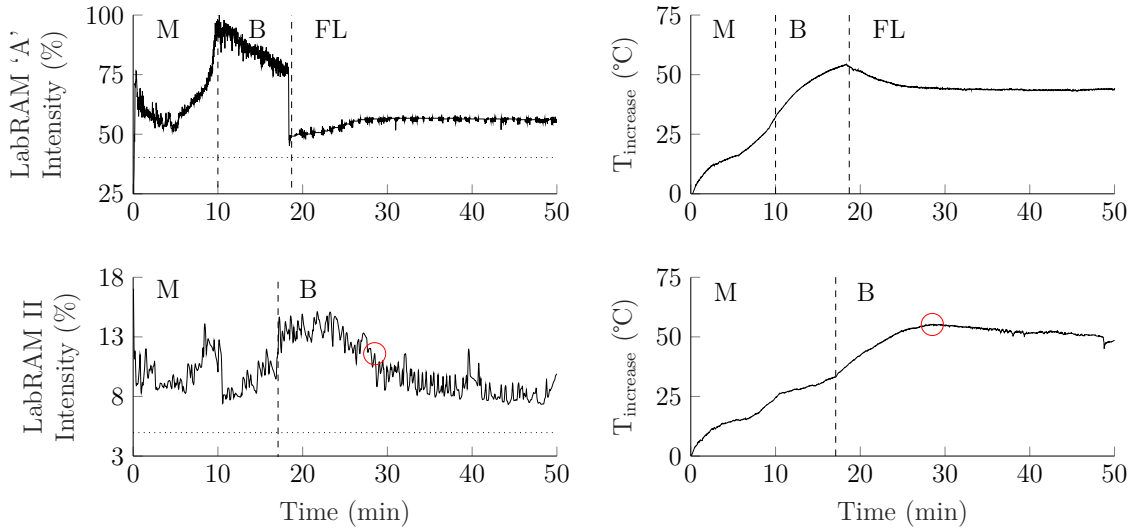


Figure 3-6: Comparison of intensity and temperature profiles at 55 G acceleration for LabRAM 'A' and a LabRAM II. Glass microbeads 62 % v/v, DEHA 19 % v/v, HTPB 19 % v/v, 550 mbar pressure. Horizontal lines - equivalent RBM profiles, vertical lines - profile stage boundaries, red circles - maximum temperature point for LabRAM II profile.

Table 3-4: Mixing statistics for the LabRAM 'A' to LabRAM II comparison over triplicate and duplicate measurements respectively. Glass microbeads 62 % v/v, DEHA 19 % v/v, HTPB 19 % v/v, 550 mbar pressure, 55 G acceleration. Standard deviations shown.

| RAM Model | LabRAM 'A' | LabRAM II |
|---|---|---|
| Time of bulk onset (end of mix) (min) | 9.5±0.7 | 15.7±1.9 |
| Time of maximum temperature (min) | 17.0±2.0 | 28.3±0.3 |
| Time of flat-line (min) | 17.0±2.0 | N/A |

This is unexpected since in both cases the acceleration set point was the same. It could however be related to the way the acceleration was controlled. Figure 3-7 shows a comparison of typical intensity profiles alongside the real-time peak acceleration recorded for LabRAM 'A' and LabRAM II mixes at (nominal) 55 G acceleration. The red circles represent the point of maximum temperature for the RAM II mix example. By comparing the recorded accelerations over the mixing cycles, it can be seen that the LabRAM II is far better at maintaining the exact acceleration set point with little or no fluctuation, thus the entirety of the mix is carried out at a single acceleration. However, acceleration can fluctuate (± 5 G) rapidly around the set point when using LabRAM 'A', especially over the periods of the highest intensity mixing. This means that aspects of the mix are briefly, but frequently, carried out at a higher acceleration than that set. This may be

responsible for more rapidly supplying energy to the material, thus shortening the mix time. Since the average acceleration was the same as the set point (55 G), it would appear that the brief periods of higher acceleration outweigh the effects of the brief periods of lower acceleration.

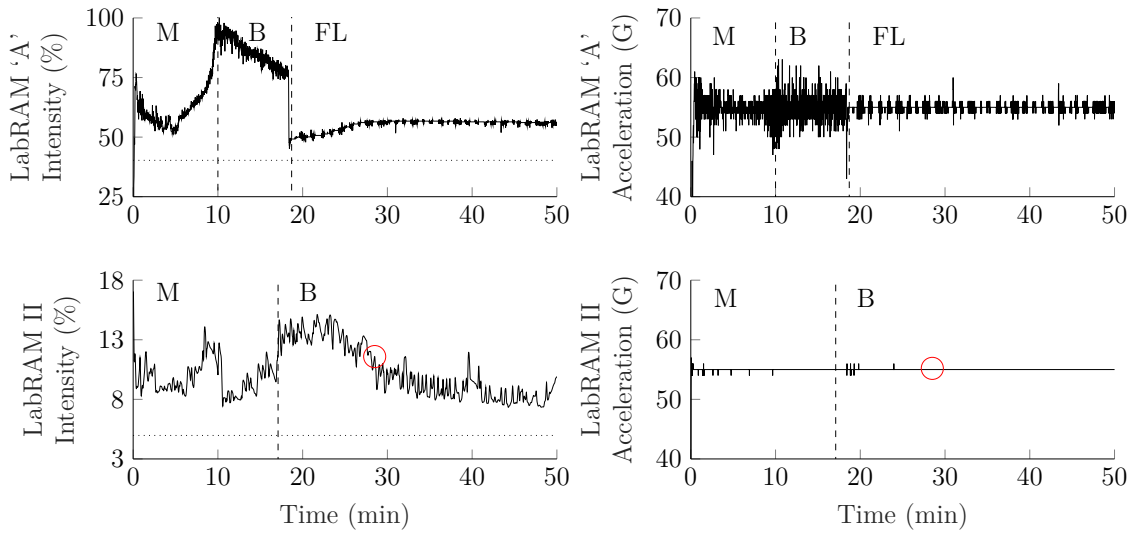


Figure 3-7: Comparison of intensity and acceleration profiles at 55 G acceleration for LabRAM 'A' and a LabRAM II. Glass microbeads 62 % v/v, DEHA 19 % v/v, HTPB 19 % v/v, 550 mbar pressure. Horizontal lines - equivalent RBM profiles, vertical lines - profile stage boundaries, red circles - maximum temperature point for LabRAM II.

It is unclear why the degree of control would differ between the LabRAM and LabRAM II models, but it may be due to a redesign in the control hardware and methodology between the two models, the after-market software that was used to control the machine in this work, or the relatively low mass of the equipment in comparison to the power of the machine. It is possible that the mixing behaviour and intensity profiles may change again between larger mixer models used for industrial scale production.

Confusingly, using literature values for the maximum power output of the LabRAM (37 W) and LabRAM II (640 W),[14] and assuming the current draw (thus % intensity) and power output are linearly related, a power-to-mix of between 29 W and 80 W is apparent for the LabRAM II, compared to between 4 W and 22 W for the LabRAM. This would suggest the power transfer to the mixing vessel is actually higher for the LabRAM II, despite the mixing progression and heating rate being slower. However, it may be the case that current draw (thus % intensity) and power output are not linearly related given the non-idealities associated with the motor,

namely its non-deal power factor.[15] Additionally, it is unclear how the values for maximum power output were derived.

### Comparison between LabRAM units

Comparisons of 604 g rigid body mass (RBM) analysis between LabRAM units showed considerable variation. Figure 3-8 shows that the intensity (thus power) required to maintain a set acceleration is higher for some machines than others. A table of the gradients and projected intercepts is shown in appendices (Table 3-A3).

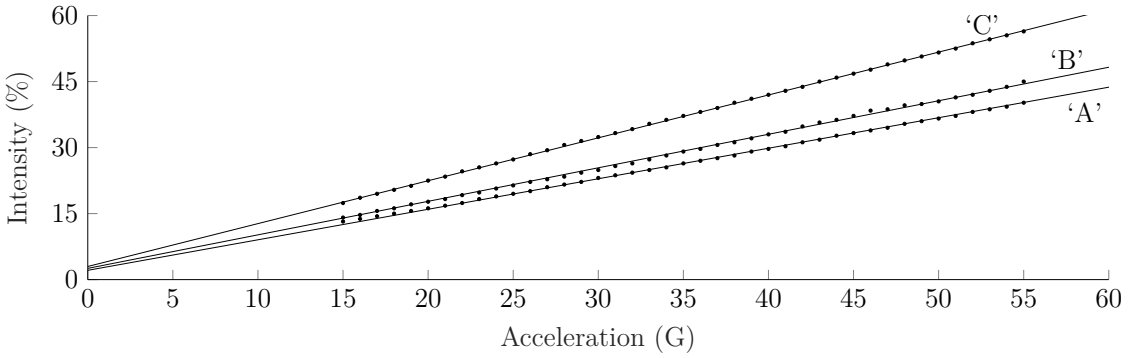


Figure 3-8: Rigid body mass (604 g) intensity analysis for LabRAM 'A', 'B' and 'C'.

The machines with the largest discrepancy (LabRAM 'A' and LabRAM 'C' in Figure 3-8) were further compared by performing the mixing procedure of the glass bead formulation as previously, with the intensity profiles shown in Figure 3-9. The maximum temperature reached for the mixes shown was an absolute temperatures of ∼75 ℃. The average ambient temperature and standard deviation for the two mixes shown was 20±2 ℃. Again note relative temperature increase is shown on the figures. It can be seen that there are considerable differences in the intensity and temperature profiles. Despite the acceleration set point being consistent, the mix performed on LabRAM 'C' was approximately twice as fast to reach the end of mix point (bulk onset) and approximately three times as fast to reach the flat-line point as the mix performed on LabRAM 'A'. LabRAM 'C' maintained a consistently higher intensity and much more rapid temperature increase. It is likely that accelerometer calibration is at least partially to blame for the discrepancies between units, although there may also be further variation in motor efficiency, plate mass, and spring constant. It is recommended proper characterisation and calibration of machines (perhaps using additional accelerometers) should be performed by researchers and industry. This will ensure mixing behaviour and product outcome are consistent across all models, units, and control methods intended to perform reproducible mixing cycles.

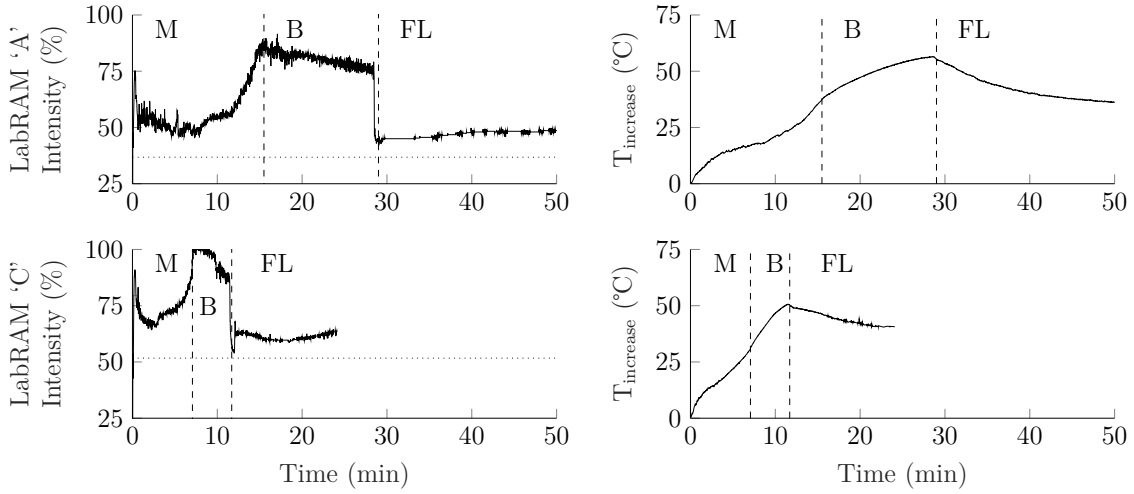


Figure 3-9: Comparison of intensity and temperature profiles at 50 G acceleration for LabRAM 'A' and LabRAM 'C'. Glass microbeads 62 % v/v, DEHA 19 % v/v, HTPB 19 % v/v, 550 mbar pressure. Horizontal lines - equivalent RBM profiles, vertical lines - profile stage boundaries.

## Conclusions

The aim of this work was to assess the effects of machine variables on mixing efficiency. Mixes performed at lower acceleration setting and lower intensity setting were found to have longer mixing times and required more energy to mix, suggesting the mixing process is less efficient in these cases. This is likely due to slower rate of energy transfer which limits temperature rise and thus viscosity reduction, which is exacerbated by greater thermal losses from the vessel over the longer mixing times. It would seem that mixing with either drive mode (constant acceleration or constant intensity) provides adequate mixing and both are viable options for machine control, though set acceleration setting may provide for easier scaling between machines. However, mixing performed in a LabRAM II was found to take nearly twice as long than LabRAM 'A', even when using the same formulation, vessel, vacuum, and acceleration setting. This is likely due to LabRAM 'A' briefly but frequently applying higher acceleration than intended due to poorer control in maintaining acceleration. Considerable variation in the mixing behaviour is apparent between different LabRAM units, and researchers are cautioned that calibration of units may be required to ensure reproducible PBX products.

## References

[1] M. Andrews, C. Collet, A. Wolff, and C. Hollands. ResonantAcosutic Mixing Processing and Safety. Munitions Safety Information Analysis Center, May 2019.

[2] A.C. Hordijk and A.E.D.M. van der Heijden. Mixing. In *Energetic Materials; Particle Processing and Characterization*. Wiley-VCH Verlag GmbH, 2005.

[3] P.A. Lucon, G. Sperry, and J. Whaley. RAM Mixing of Liquids and Pastes. Resodyn Technical Interchange, Butte, Montana, USA, 2016.

[4] P.A. Lucon and J. Whaley. Liquids and Pastes. Resodyn Technical Interchange, Butte, Montana, USA, 2016.

[5] P.A. Lucon. Mixing with Vacuum Assist. Resodyn Technical Interchange, Butte, Montana, USA, 2016.

[6] E.L. McCloy, P. Wilkinson, and P.P. Gill. Resonant Acoustic Mixing: Pushing The Boundaries. Master's thesis, Cranfield University, 2016.

[7] A.J. Claydon. *Resonant Acoustic Mixing of Polymer Bonded Explosives*. PhD thesis, Cranfield University, 2020. Paper 1.

[8] S.L. Coguill and Z.R. Martineau. Vessel Geometry and Fluid Properties Influencing Mix Behavior of Resonant Acoustic Mixing. 38th International Pyrotechnics Seminar, Denver, CO, USA., 2012.

[9] Inc. Resodyn Acoustic Mixers. LabRAM Resonant Acoustic Mixer Manual. ResoDyn Corp, Butte, MT, USA, February 2012.

[10] A. Vandenberg and K. Wille. Evaluation of resonance acoustic mixing technology using ultra high performance concrete. *Constr. Build. Mater.*, 164:716–730, 2018.

[11] A.J. Claydon. *Resonant Acoustic Mixing of Polymer Bonded Explosives*. PhD thesis, Cranfield University, 2020. Paper 2.

[12] J.G. Osorio and F.J. Muzzio. Evaluation of resonant acoustic mixing performance. *Powder Technol.*, 278:46–56, 2015.

[13] J. Hilden, M. Sullivan, M. Polizzi, J. Wade, J. Greer, and M. Keeney. Power consumption during oscillatory mixing of pharmaceutical powders. *Powder Technol.*, 338:44–54, 2018.

[14] J. Whaley. Private Communication, Resodyn Acoustic Mixers, April 2020.

[15] J. Whaley and P. Lucon. Processing of Solids. Resodyn Technical Interchange, Butte, Montana, USA, 2016.

# Appendices

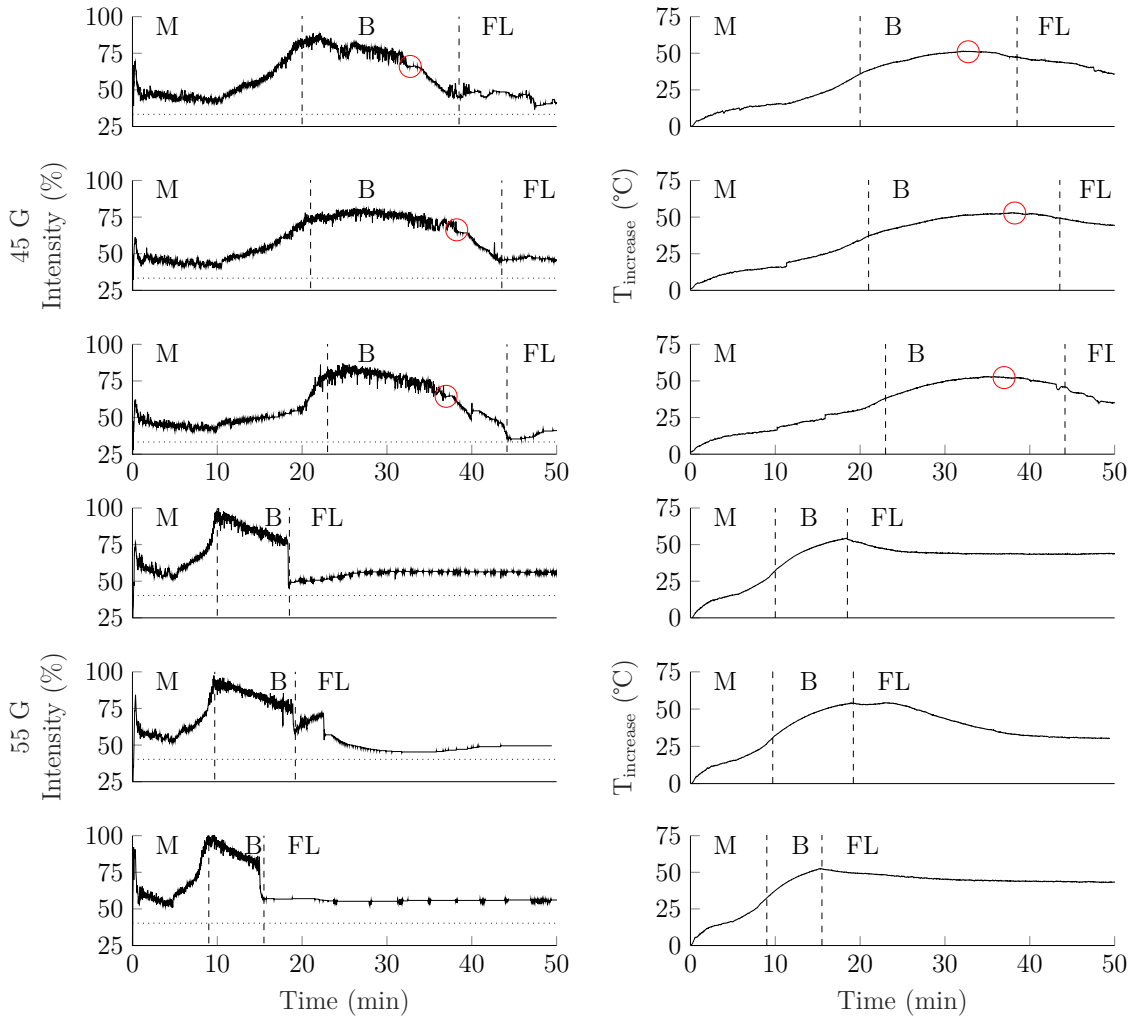


Figure 3-A1: Triplicate intensity and temperature profiles at 45 G and 55 G acceleration.* Glass microbeads 62 % v/v, DEHA 19 % v/v, HTPB 19 % v/v, 550 mbar pressure. Horizontal lines - equivalent RBM profiles, vertical lines - profile stage boundaries, red circles - maximum temperature points for 45 G profiles.

*It should be noted that the second of the 55 G mixing profiles lost vacuum application upon the intensity drop at 19 minutes due to material being ejected into the vacuum lines. The brief rise in intensity and second intensity drop after this point are believed to be an artifact of this, thus the flat-line onset was taken as the point of the initial intensity drop.

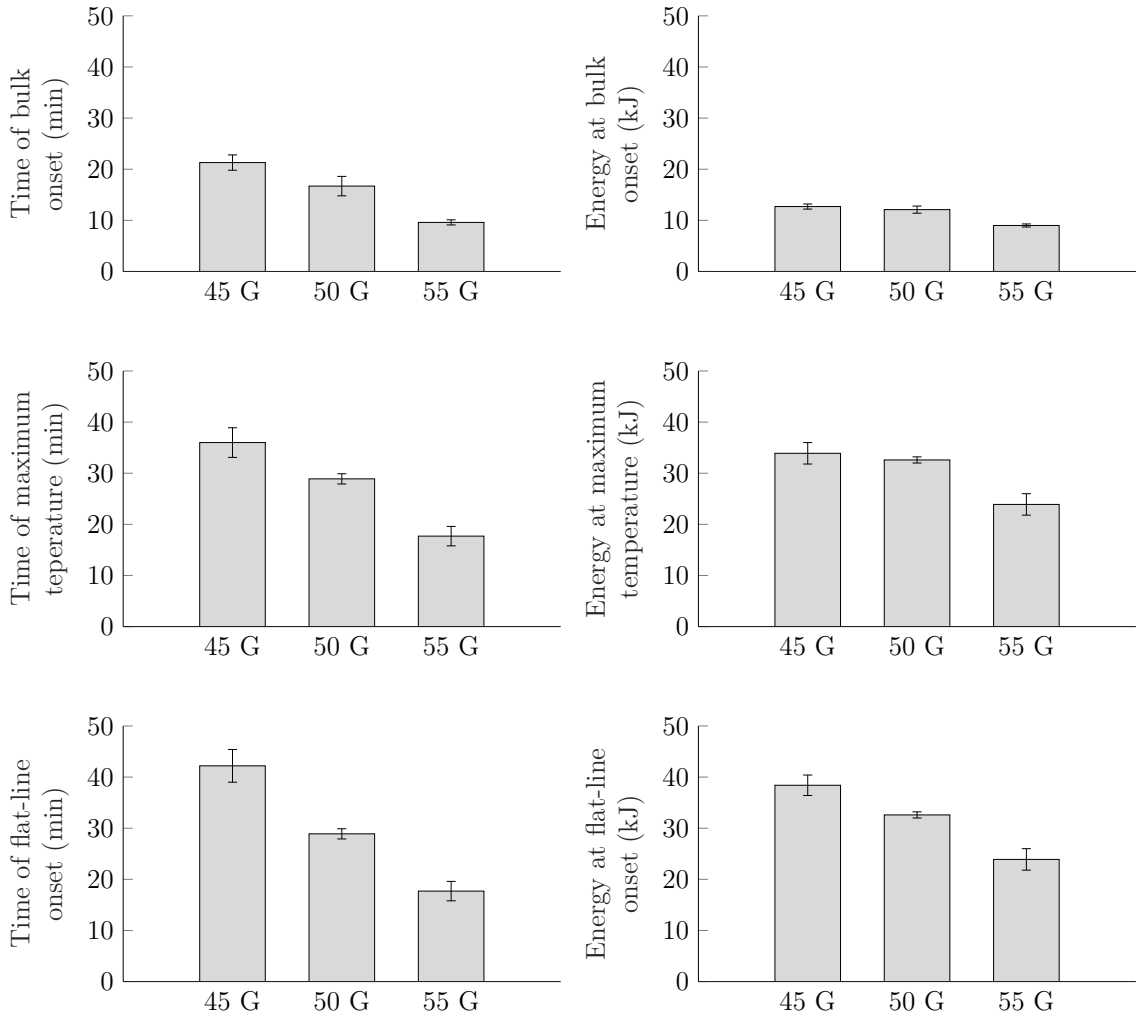


Figure 3-A2: Bar graphs showing the average time (left column) and average energy (mechanical method, right column) required for profile stages at 45 G, 50 G, and 55 G acceleration over triplicate measurements. Glass microbeads 62 % v/v, DEHA 19 % v/v, HTPB 19 % v/v, PMMA vessel, 550 mbar pressure. Standard deviations shown.

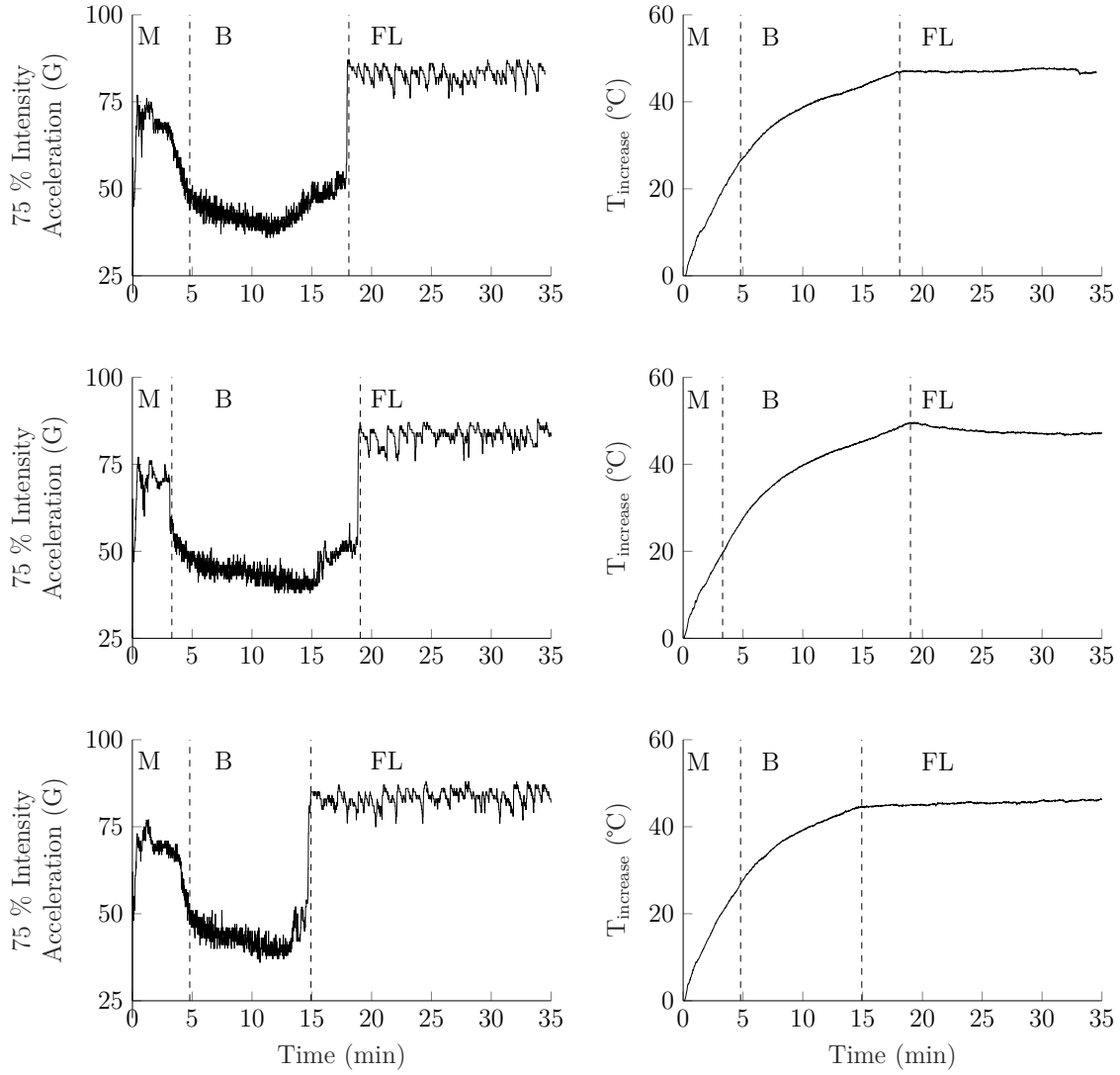


Figure 3-A3: Triplicate acceleration and temperature profiles at 75 % intensity. Glass microbeads 62 % v/v, DEHA 19 % v/v, HTPB 19 % v/v, 550 mbar pressure.

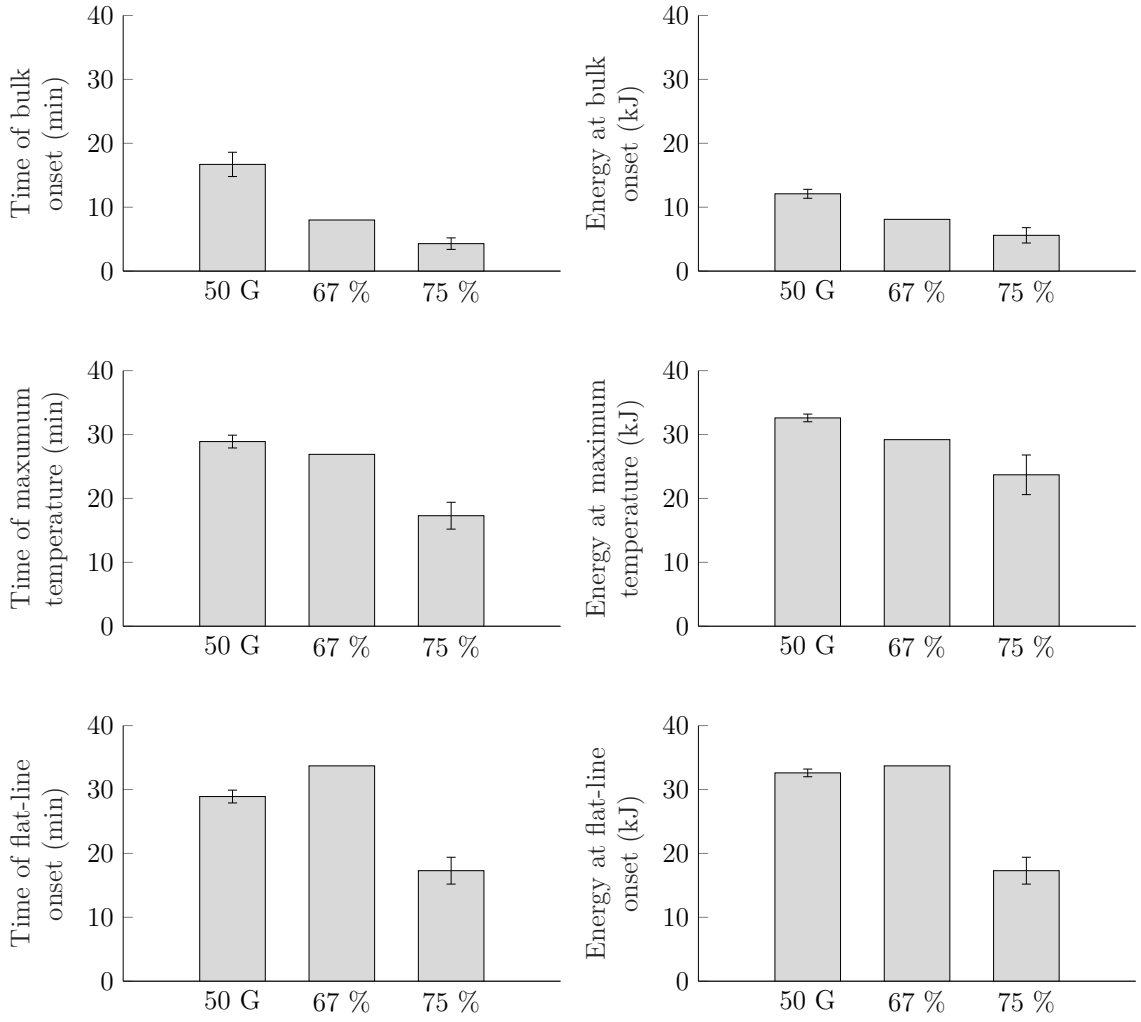


Figure 3-A4: Bar graphs showing the average time (left column) and average energy (mechanical method, right column) required for profile stages at 50 G acceleration, and 67 % and 75 % intensity over triplicate, single, and triplicate measurements respectively. Glass microbeads 62 % v/v, DEHA 19 % v/v, HTPB 19 % v/v, PMMA vessel, 550 mbar pressure. Standard deviations shown.

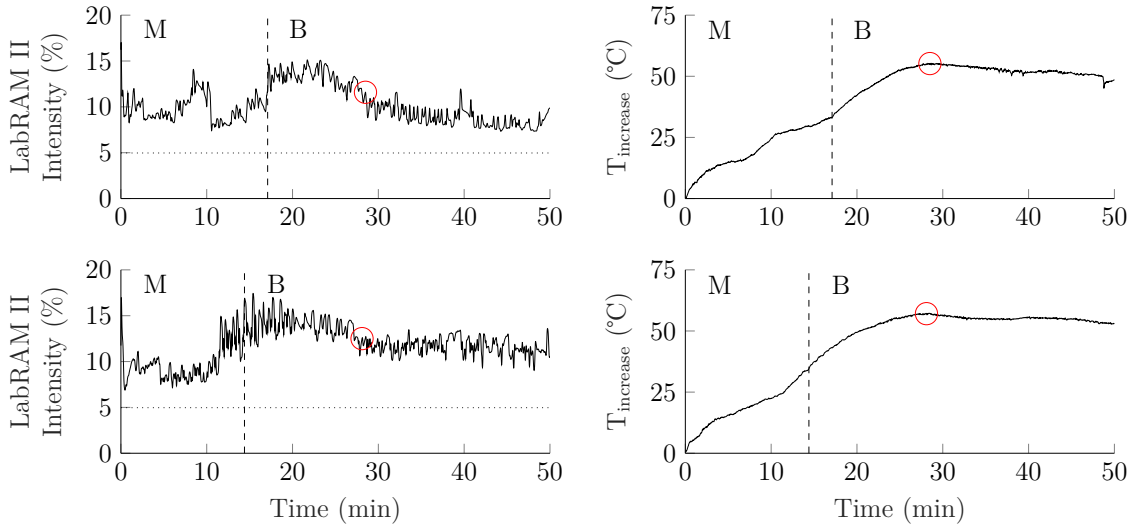


Figure 3-A5: Duplicate intensity and temperature profiles at 55 G acceleration for LabRAM II. Glass microbeads 62 % v/v, DEHA 19 % v/v, HTPB 19 % v/v, 550 mbar pressure. Horizontal lines - equivalent RBM profiles, vertical lines - profile stage boundaries, red circles - maximum temperature points for LabRAM II profiles.

Table 3-A1: Mixing statistics for the acceleration comparison over triplicate measurements. Glass microbeads 62 % v/v, DEHA 19 % v/v, HTPB 19 % v/v, 550 mbar pressure. Standard deviations shown.

| Acceleration | 45 G | 50 G | 55 G |
|---|---|---|---|
| Time of bulk onset (end of mix) (min) | 21.3±1.5 | 16.7±1.9 | 9.6±0.5 |
| Energy at bulk onset (Mechanical, kJ) | 12.7±0.5 | 12.1±0.7 | 9.0±0.3 |
| Energy at bulk onset (Electrical, kJ) | 8.5±0.3 | 7.3±0.4 | 4.9±0.2 |
| Energy at bulk onset (Thermal, kJ) | 8.6±0.6 | 8.0±0.3 | 6.3±0.2 |
| Time of maximum temperature (min) | 36.0±2.9 | 28.9±1.0 | 17.7±1.9 |
| Energy at maximum temp. (Mechanical, kJ) | 33.9±2.1 | 32.6±0.6 | 23.9±2.1 |
| Energy at maximum temp. (Electrical, kJ) | 22.4±1.4 | 19.4±0.4 | 12.9±1.1 |
| Energy at maximum temp. (Thermal, kJ) | 15.4±1.0 | 14.9±0.4 | 12.4±0.6 |
| Time of flat-line (min) | 42.0±3.2 | 28.9±1.0 | 17.7±1.9 |
| Energy at flat-line (Mechanical, kJ) | 38.4±2.0 | 32.6±0.6 | 23.9±2.1 |
| Energy at flat-line (Electrical, kJ) | 25.3±1.3 | 19.4±0.4 | 12.9±1.1 |
| Energy at flat-line (Thermal, kJ) | 16.5±1.1 | 14.9±0.4 | 12.4±0.6 |

Table 3-A2: Mixing statistics for the intensity comparison over single and triplicate measurements respectively. Glass microbeads 62 % v/v, DEHA 19 % v/v, HTPB 19 % v/v, 550 mbar pressure. Standard deviations shown.

| Intensity | 67 % | 75 % |
|---|---|---|
| Time of bulk onset (end of mix) (min) | 8.0 | 4.3±0.9 |
| Energy at bulk onset (Mechanical, kJ) | 8.1 | 5.6±1.2 |
| Energy at bulk onset (Electrical, kJ) | 4.1 | 2.6±0.6 |
| Energy at bulk onset (Thermal, kJ) | 6.0 | 4.6±0.9 |
| Time of maximum temperature (min) | 26.9 | 17.3±2.1 |
| Energy at maximum temperature (Mechanical, kJ) | 29.2 | 23.7±3.1 |
| Energy at maximum temperature (Electrical, kJ) | 19.7 | 14.7±2.0 |
| Energy at maximum temperature (Thermal, kJ) | 13.9 | 11.7±1.0 |
| Time of flat-line (min) | 33.7 | 17.3±2.1 |
| Energy at flat-line (Mechanical, kJ) | 36.2 | 23.7±3.1 |
| Energy at flat-line (Electrical, kJ) | 23.3 | 14.7±2.0 |
| Energy at flat-line (Thermal, kJ) | 15.6 | 11.7±1.0 |

Table 3-A3: The gradients and projected intercepts for the best fit lines of Figure 3-8, which plot mixer intensity (%) against acceleration (G) for LabRAMs ‘A’, ‘B’, and ‘C’.

| | LabRAM ‘A’ | LabRAM ‘B’ | LabRAM ‘C’ |
|---|---|---|---|
| Gradient | 0.6935 | 0.7617 | 0.9742 |
| Intercept | 2.112 | 2.557 | 2.985 |

# Paper 4 - The Effect of Vessel Material on the Efficiency of Resonant Acoustic Mixing for Polymer Bonded Explosives

Andrew J. Claydon, Guillaume Kister, Sally Gaulter, and Philip P. Gill

**Abstract:** The efficiency (time and energy required for mix completion) of Resonant Acoustic Mixing (RAM) applied to a Polymer Bonded Explosive (PBX) simulant is assessed for three different vessel materials. The materials chosen have low (poly(tetrafluoroethylene) - PTFE), medium (poly(methyl methacrylate) - PMMA), and high (titanium) surface free energies. An inert formulation based on glass microbeads (28.3 micron D50, 62% v/v in HTPB and plasticiser) is used for mixing. It is observed that mixing in the medium surface free energy vessel reduces mixing time by 17 % in comparison to the low surface free energy vessel. This is attributed to a higher work of adhesion between the formulation and vessel reducing wall slip in the medium surface free energy vessel. The high surface free energy vessel is found to perform similarly to the medium. This is attributed to complications arising from surface cleanliness reducing the apparent surface free energy.

**Keywords:** Resonant Acoustic Mixing, Polymer Bonded eXplosive, Surface Free Energy, Adhesion, LabRAM

## Introduction

Resonant Acoustic Mixing (RAM) is a novel mixing technique that has received significant attention[1] for use in the manufacture of cured Polymer Bonded eXplosives (PBXs). PBXs in their pre-cured state consist of a mixture of liquid prepolymer (typically hydroxyl-terminated polybutadiene - HTPB), isocyanate curative, plasticiser, and additives into which high explosive crystals are dispersed. The viscosity of the highly loaded (~87 % w/w[2]) suspension is such that it can be cast into a receptacle such as a bomb casing or warhead, where it cures to form an elastomeric composite. Thorough mixing is required to evenly disperse the components, ensuring the product has consistent properties throughout.[3] While conventional high shear mixing techniques (such as a planetary or z-blade mixers[3]) can be used to disperse the explosive filler, the use of RAM has a number of advantages such as shorter mixing times, reduced waste, and the ability to mix novel high viscosity formulations 'in-situ', where the final receptacle doubles as the mixing vessel.[4–6] These factors have previously been discussed by the author in more detail.[7]

RAM mixers consist of a spring-mounted vibrating plate to which a mixing vessel is attached. The vibrations are low amplitude (1.4 cm), and occur at the mechanical resonant frequency of the mass-spring system (typically around 60 Hz), at accelerations up to 100 G. The system is kept in resonance by the software that controls the driver motor.[4, 5] Efficient mixing of loaded suspensions requires churning, referred to as 'bulk mixing' when occurring at high mixer intensity,[8–10] where the material that is in contact with the vessel wall couples with it, ideally in a 'no-slip' condition. Conversely, the bulk of the material is accelerated by acoustic pressure waves (vibrations) from the oscillating plate. The resultant velocity gradient across the vessel induces the shear responsible for mixing.[8–10]

A literature review by the author[7] categorised the factors known or suspected to affect the effectiveness of churning into machine variables, vessel variables, and formulation variables, as listed in Table 4-1. By optimising these variables to minimise wall slip and maximise movement in the material, it is believed the velocity gradient (thus shear) can be maximised. It would follow that by maximising the shear, the time and energy required for homogeneity would be minimised, thus optimal mixing efficiency achieved. The aim of this work is to investigate the effects of a vessel variable on mixing efficiency, specifically wall material with regards to surface free energy. Materials with low (PTFE), medium (PMMA), and high (titanium) surface

free energies were chosen for the comparison.

Table 4-1: Machine variables, vessel variables, and formulation variables for Resonant Acoustic Mixing.

| Machine variables | Vessel variables | Formulation variables |
|---|---|---|
| Acceleration setting | Vacuum setting | Binder content |
| Intensity setting | Wall material | Plasticiser content |
| Mixer model | Wall surface finish | Additives |
| Mixer unit | Diameter | Solids loading |
| | Insulation | Particle shape |
| | Active heating | Filler type |
| | Active cooling | |

**Effect of vessel material**

A literature review by the author[7] concluded that the velocity gradient across the mixing vessel (thus shear) will increase if the inertial forces on the material are increased (e.g. with higher acceleration setting or reduced headspace pressure), the material becomes more compliant (easier to move, e.g. lower viscosity or surface tension), or wall slip is reduced at the interface (e.g. more viscous drag, higher tackiness, or greater adhesion). Wall slip of polymer bound suspensions in a general context can be categorised as either true slip, whereby slip occurs on the molecular level due to poor interaction between the binder and wall, or apparent slip, whereby there is a binder rich layer at the wall that lubricates bulk flow.[11–13] These have been previously reviewed by the author in the context of RAM.[7] In this work, true slip is of interest. It has previously been reported that when mixing in poly(tetrafluoroethylene) (PTFE, Teflon$^{TM}$) vessels, there is ineffective wall coupling (true slip) due to poor adhesion.[14] This was believed to be due to its low surface free energy (approximately[15] 20 mJ m$^{-2}$) causing the material to glide along the wall, and resulted in reduced efficiency and poor mix quality. Mixes performed in vessels made out of higher surface free energy materials such as stainless steel, titanium and aluminium, where passivated metals have surface free energies in the hundreds of mJ m$^{-2}$,[16] have not been reported to cause similar problems. Interestingly, neither have plastic vessels with only slightly higher surface free energies than PTFE, ranging from approximately[15] 30-50 mJ m$^{-2}$, such as polycarbonate (PC), polystyrene (PS), and poly(methyl methacrylate) (PMMA).

The way in which surface free energy would affect true wall slip is here explained in more detail. Chemical adhesion between a solid and liquid (e.g. mixing vessel

and binder) can be quantified by the work of adhesion (the energy required to separate the two phases) between them. For a fully characterised liquid and a fully characterised surface, the work of adhesion can be found using Equation 4-1.[17–19]

$$W_A = 2(\sqrt{\sigma^d_{SFT}\sigma^d_{SFE}} + \sqrt{\sigma^p_{SFT}\sigma^p_{SFE}}) \qquad \text{(Equation 4-1)}$$

where $W_A$ is the work of adhesion ( $mJ\,m^{-2}$), $\sigma_{SFT}$ is the surface tension of the liquid ( $mJ\,m^{-2}$), $\sigma_{SFE}$ is the surface free energy of the solid ( $mJ\,m^{-2}$), and the remaining terms are the dispersive and polar forces contributions thereof ( $mJ\,m^{-2}$). It would follow that increasing the work of adhesion (i.e. increasing the surface free energy of the surface or surface tension of the liquid) would reduce true slip, leading to improved mixing. However, the effects of cohesive forces within the liquid phase must be also be taken into account. That is to say material at the interface must prefer to stick to the wall (adhesion) rather than move with the bulk of the material (cohesion), which in the latter case would lead to increased true wall slip. In the case of the surface free energy comparison considered here, the surface tension of the binder components acts as a cohesive force and the work of adhesion between the binder components and vessel surface acts as an adhesive force. It is therefore postulated that a surface and binder combination which provides a high work of adhesion to surface tension ratio will reduce true wall slip, thus increase the velocity gradient and improve mixing efficiency. Higher ratios of this nature are reflected in lower contact angle between a droplet of the liquid in contact with the solid. This is shown in Equation 4-2.

$$\theta = cos^{-1}(\frac{W_A}{\sigma_{SFT}} - 1) \qquad \text{(Equation 4-2)}$$

where $\theta$ is expected the contact angle (degrees), $W_A$ is the work of adhesion ( $mJ\,m^{-2}$), and $\sigma_{SFT}$ is the surface tension of the liquid ( $mJ\,m^{-2}$). It is therefore apparent that increasing the surface free energy will increase the work of adhesion, thus, without modifying surface tension, the contact angle will decrease.

### Determining efficiency

Mixing efficiency can be deduced from measuring the energy transfer to the system up to the end of mix point. Previous work by the author[20, 21] carried out on an inert glass microbead formulation found that the mixer 'intensity' readout profile,[a] has a

[a] Where 'intensity' refers to the current supplied to the driver motor as a percentage up to 5 A

distinctive shape, and can be broken down into mixing (M), bulk motion (B), and flat-line (FL) stages. The homogeneity of the material has been found to be constant at the end of the mixing stage, with subsequent viscosity changes (thus intensity changes) in the bulk stage due to high intensity churning heating the material to its maximum of ∼75 ℃. At this point it is believed the viscous drag becomes too low to sustain a large velocity gradient across the vessel, and the profile has a sharp drop off to a lower intensity flat-line stage in which lower intensity churning occurs (despite the acceleration remaining constant). Two different mixing modes have previously been observed to happen at the same acceleration setting.[8] Easily recognisable features which mark the start and end point of the bulk motion stage can be used to compare the rate of mixing progression under different conditions without having to test material properties. Three methods have been used in the author's previous work[20, 21] to determine the energy supplied up to the end of mix point; a mechanical method, an electrical method, and a thermal method.

## Experiment

An inert simulant formulation (Table 4-2) consisting of glass microbeads (Glass Sphere s.r.o., Czech Republic) filler, hydroxyl-terminated polybutadiene (HTPB) binder (type Poly bd® R-45HTLO, Cray Valley, USA) and di(2-ethylhexyl) adipate (DEHA) plasticiser (≥ 97 %, Merck, UK) was used for mixing. Analysis of the glass microbeads as previously reported by the author[20] is given in 4-3.

Table 4-2: The glass bead formulation used for mixing.

| | Glass | DEHA | HTPB | Curative |
|---|---|---|---|---|
| Volume (%) | 62.00 | 19.00 | 19.00 | - |
| Actual mass (%) | 81.65 | 9.30 | 9.05 | - |
| RDX equivalent mass (%) | 76.48 | 11.91 | 11.60 | - |

Table 4-3: Density and particle size analysis of the glass beads.

| Density ( $g\,cm^{-3}$) | D10 (µm) | D50 (µm) | D90 (µm) |
|---|---|---|---|
| 2.4905±0.0002 | 12.7±2.3 | 28.3±1.7 | 45.4±1.5 |

Mixing vessels were milled from PTFE, PMMA, and Grade 5 titanium[b] blocks. An insulating plastic (polyoxymethylene) base plate was also used in the case of tita-

[b] 90 % titanium, 6 % aluminium, 4 % vanadium.

nium, in an attempt to normalise its cooling behaviour to that of the less thermally conductive plastic vessels. The vessels had a 48 mm diameter and a 47.5 mm height. The vessel lid was of polyether ether ketone (PEEK) construction and included vacuum application and monitoring ports, as well as a central conduit through which a rod thermocouple could be inserted into the vessel contents. A wire thermocouple was also attached to the vessel exterior with electrical tape. The lid was held in place with a clamshell clamp. Aftermarket equipment and software from Falcon Project Ltd. was used to monitor and control the mixer at constant acceleration setting.

### Characterisation of materials

The formulation heat capacity was taken as the values presented previously by the author.[20] The cooling behaviour was taken for each of the vessels once the machine was turned off, and analysed between 45 ℃ and 35 ℃ using Newton's Law of Cooling, as previously.[20]

Surface free energies were found by the sessile drop method, whereby the drop shape of probe liquids (deionised water, diiodomethane, and ethylene glycol - droplet volumes between 2 µL and 2.5 µL) in contact with polished samples of PMMA and PTFE were photographed from the side (DataPhysics OCA 20). Liquids that spread well have a low contact angle, and liquids that do not spread well have a high contact angle. Total spreading was expected in the case of titanium, thus the surface free energy was not initially characterised. However, a brief surface free energy characterisation was undertaken using water and diiodomethane contact angles. Each surface sample was first exposed to binder mixture (HTPB/DEHA coating) before being thoroughly washed twice using dish soap and water, and dried with paper towels, in the same cleaning procedure as the mixing vessels. Software[22] was then used to interpret (Young-Laplace method) the angle at which the drop was in contact with the surface. Since the polar and dispersive components of the surface tensions of the probe liquids are known from literature values, the polar and dispersive components of the surface free energy could be derived, where the full surface free energy was the summation of the two components. The relation of the contact angle of probe liquids to the polar and dispersive components of the surface free energy is given in its linear form in Equation 4-3.[17–19]

$$\frac{1}{2}(1+cos\theta)\frac{\sigma_{SFT}}{\sqrt{\sigma^d_{SFT}}} = \sqrt{\sigma^p_{SFE}}\sqrt{\frac{\sigma^p_{SFT}}{\sigma^d_{SFT}}} + \sqrt{\sigma^d_{SFE}} \qquad \text{(Equation 4-3)}$$

where $\theta$ is the contact angle (degrees), $\sigma_{SFT}$ is the total surface tension of the probe liquid ($\mathrm{mJ\,m^{-2}}$), $\sigma^d_{SFT}$ and $\sigma^p_{SFT}$ are the dispersive and polar components of the surface tension respectively ($\mathrm{mJ\,m^{-2}}$), $\sigma_{SFE}$ is the total surface free energy of the surface ($\mathrm{mJ\,m^{-2}}$), and $\sigma^d_{SFE}$ and $\sigma^p_{SFE}$ are the dispersive and polar components of the surface free energy respectively ($\mathrm{mJ\,m^{-2}}$).[c] By plotting the first term of Equation 4-3 ($\frac{1}{2}(1+cos\theta)\frac{\sigma_{SFT}}{\sqrt{\sigma^d_{SFT}}}$) against the third term ($\sqrt{\frac{\sigma^p_{SFT}}{\sigma^d_{SFT}}}$) for two or more probe liquids, the squares of the gradient and the intercept of the resulting line of best fit equate to the polar and dispersive components of the surface free energy respectively.

The pendant drop method was used to find the surface tensions of DEHA and a 50/50 v/v mixture of DEHA and HTPB, whereby a droplet of each liquid was suspended from a needle and its drop shape interpreted. The shape depends on the liquid's density with respect to its surroundings (i.e. gravity or buoyancy will attempt to elongate the drop shape) and the cohesive forces within the droplet (i.e. the intermolecular forces present will attempt to keep the droplet spherical). Pure HTPB was too viscous to be pushed through the needle available. The densities of the liquids were taken or derived from the supplier's literature values[23, 24] (specific gravities relative to water: DEHA - 0.925, HTPB - 0.901, thus DEHA/HTPB - 0.913). The full surface tensions were found through suspension in air, with the drop shape being analysed automatically by the software with the Young-Laplace interpretation. The largest possible drop sizes were used to maximise the accuracy of the measurements (DEHA - 3.86 µL, DEHA/HTPB - 4.31 µL). To find the polar and disperse components, droplet shapes in a water medium were found to derive the interfacial tension. Since the densities of the binder liquids were lower than that of water, the drops were suspended from an inverted needle. Again, the largest possible drop sizes were used (DEHA - 39.46 µL, DEHA/HTPB - 24.29 µL). The components of the surface tension were then found using Equation 4-4.[17–19]

$$\sigma_{IFT} = \sigma_{SFT_1} + \sigma_{SFT_2} - 2\left(\sqrt{\sigma^d_{SFT_1}\sigma^d_{SFT_2}} + \sqrt{\sigma^p_{SFT_1}\sigma^p_{SFT_2}}\right) \qquad \text{(Equation 4-4)}$$

where $\sigma_{IFT}$ is the interfacial tension of the two liquids ($\mathrm{mJ\,m^{-2}}$), $\sigma_{SFT_1}$ is the total surface tension of the liquid under investigation ($\mathrm{mJ\,m^{-2}}$), $\sigma_{SFT_2}$ is the total surface tension of the second liquid (water) ($\mathrm{mJ\,m^{-2}}$), $\sigma^d_{SFT_1}$ and $\sigma^p_{SFT_1}$ are the dispersive and polar components of the liquid under investigation respectively ($\mathrm{mJ\,m^{-2}}$), and $\sigma^d_{SFT_2}$ and $\sigma^p_{SFT_2}$ are the dispersive and polar components of the second liquid (wa-

[c] Conventionally, surface free energy is given in units of $\mathrm{mJ\,m^{-2}}$, and surface tension in units of $\mathrm{mN\,m^{-1}}$. Since the two are equivalent, only $\mathrm{mJ\,m^{-2}}$ is used in this work for simplicity.

ter) respectively ( $mJ\,m^{-2}$). Under normal circumstances, the second liquid would be selected as to not have a polar component, thus $\sigma^p_{SFT_2} = 0$ and $\sigma^d_{SFT_2} = \sigma_{SFT_2}$, meaning Equation 4-4 can be solved for $\sigma^d_{SFT_1}$ algebraically. $\sigma^p_{SFT_1}$ is then the difference between $\sigma^d_{SFT_1}$ and $\sigma_{SFT_1}$. However, this was not possible since DEHA is soluble in essentially every solvent but water, which has a very large polar component.[25] Therefore Equation 4-4 in this case was solved by substituting $\sigma^p_{SFT_1}$ as $\sigma_{SFT_1} - \sigma^d_{SFT_1}$, and finding $\sigma^d_{SFT_1}$ iteratively.

### Mixing procedure

The author has previously presented data from triplicate mixes performed in a PMMA vessel,[20] and the same mixing procedure is repeated for the PTFE and titanium vessels considered here. A volume of 65 mL of the glass bead formulation (added in the order - half of the filler, plasticiser, remaining filler, binder) was mixed at 50 G acceleration under 550 mbar pressure for 50 minutes. A LabRAM (LabRAM 'A' as characterised previously[20, 21]) was used. The pressure was reduced from ambient in 12 second intervals before the start of mixing. Three mixes (two in the case of titanium) were undertaken in each vessel. Since each of the mixing vessels had a different mass due to the different densities of the materials used, additional dead weights (washers) were added to all but the heaviest vessel in order to equalise the static masses (604 g in total) over the comparison.

## Results and discussion

### Characterisation of materials

Photographs of the observed drop shapes from the sessile drop experiments on PTFE and PMMA are given in Figure 4-1, where contact angles are given to the nearest integer. It was originally expected that full spreading would be achieved with all probe liquids on titanium due to the high reported literature values of metals and metal oxides. However, clear contact angles were seen, as shown in Figure 4-2. Pendant drop shapes are given in appendices (Figure 4-A1), along with the graphical form of Equation 4-3 as used to find the surface free energies (Figure 4-A2), and the iterative solution of Equation 4-4 used to find the surface tensions (Figure 4-A3). The surface tensions and surface free energies for each surface and liquid considered, along with their polar and dispersive components, are shown in Table 4-4. Also

shown are the surface tension components for HTPB as derived from PTFE contact angle data and total surface tension as reported by Ramirez and Kalman,[26] further analysed with Equation 4-3 and the PTFE literature data.

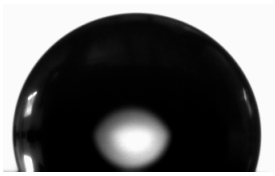

(a) PTFE/Water (108°)

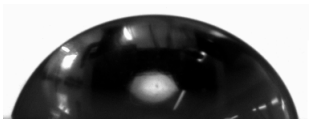

(b) PTFE/Diiodomethane (76°)

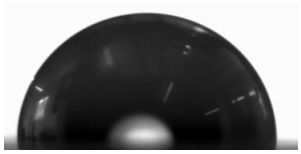

(c) PTFE/Ethylene glycol (93°)

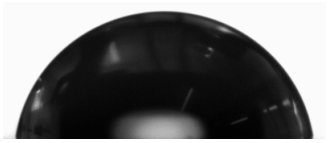

(d) PMMA/Water (82°)

(e) PMMA/Diiodomethane (50°)

(f) PMMA/Ethylene glycol (63°)

Figure 4-1: Photographs of sessile drop shapes seen for PTFE and PMMA.

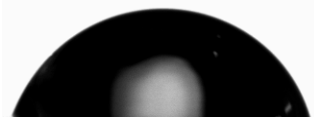

(a) Titanium/Water (73°)

(b) Titanium/Diiodomethane (49°)

Figure 4-2: Photographs of sessile drop shapes seen for titanium.

Table 4-4: The disperse and polar components of the surface free energies and surface tensions.

| Material | Data source | $\sigma^d$ ( mJ m$^{-2}$) | $\sigma^p$ ( mJ m$^{-2}$) | $\sigma$ ( mJ m$^{-2}$) |
|---|---|---|---|---|
| Water | Literature[25] | 26.00 | 46.80 | 72.80 |
| Diiodomethane | Literature[27] | 47.40 | 2.60 | 50.00 |
| Ethylene glycol | Literature[25] | 26.40 | 21.30 | 47.70 |
| PTFE | Literature[17] | 18.60 | 0.50 | 19.10 |
| | Experiment | 18.90 | 0.10 | 19.00 |
| PMMA | Literature[28] | 35.80 | 4.40 | 40.20 |
| | Experiment | 29.98 | 3.33 | 33.31 |
| Titanium Grade 5 | Experiment | 28.41 | 8.66 | 37.07 |
| DEHA | Experiment | 24.29 | 3.96 | 28.25 |
| DEHA/HTPB | Experiment | 20.60 | 9.12 | 29.72 |
| HTPB | Literature[26] | 18.13 | 22.47 | 40.60 |

Figure 4-1 shows that for all the probe liquids considered, the wettability of the PMMA is greater than that of the PTFE, as can be seen by the lower contact angle in each case. Table 4-4 shows that PTFE has a lower surface free energy than PMMA, both as a total and in the case of the polar and dispersive components. The values obtained for PTFE are in good agreement with the literature values, while the values for PMMA are slightly lower, possibly due to the surface not being quite as clean as for PTFE. One would expect the lower surface free energy PTFE to be more easily cleaned by the simple cleaning procedure performed in this work. This is not expected to impact the results however, since the same cleaning procedure was used for both the PMMA surface sample and mixing vessel. The surface free energy values for titanium are orders of magnitude lower than those expected of clean metal oxide surfaces, similar to those expected of plastics. The surface free energy of metals has previously been found to depend strongly on the surface preparation method, ranging from $40\,mJ\,m^{-2}$ (water cleaning treatment) to over $100\,mJ\,m^{-2}$ ($O_2$ plasma cleaning treatment) on stainless steel surfaces.[29]

An attempt was made to clean the titanium with hydrogen peroxide solution (30% w/w), in a similar way to Becker *et al.*[30] However, this method significantly discoloured the surface to a dark brown colour, and left a thick, uneven oxide crust that would render the vessel unsuitable for the mixing comparison. Whereas Becker *et al*[30] performed the treatment on pure titanium, the Grade 5 alloy used in this work was unsuitable for such a treatment, with the discolouration in keeping with the findings of Noguchi *et el.*[31] Even so, Becker *et al*[30] still reported clear water contact angles between 38° and 103° depending on prior contamination and the solvent cleaning treatment used. This suggests that even the most thorough solvent cleaning procedures are inadequate to expose the very high surface free energy metal oxide surfaces.

Table 4-4 shows that the total surface tension of DEHA is only slightly lower than that of DEHA/HTPB, though greater differences are seen between the polar and dispersive components, with the mixture having over twice the polar component of pure DEHA. This is likely due to the effects of the polar hydroxyl groups present in HTPB.

Using the data of Table 4-4 in conjunction with Equation 4-1 and Equation 4-2, Figure 4-3 was plotted to show spreading envelopes and work of adhesion isolines for DEHA/HTPB with solids of known surface free energy. The positioning of various vessel materials on the plot with regards to the isolines and spreading envelopes

describe the surface interactions they have with DEHA/HTPB in graphical form.[d] The surface free energy values found in this work for PTFE, PMMA, and titanium are plotted as points positioned as their total surface free energy against their polar component. In addition, literature values for a selection of common plastics are also plotted. In the case of PTFE, the plot shows that DEHA/HTPB falls within the 65-75 ° spreading envelope and the 40-50 mJ m$^{-2}$ isolines. In contrast, for PMMA the HTPB/DEHA mixture falls within the 0-5 ° spreading envelope and the 60-70 mJ m$^{-2}$ isolines. Therefore, by swapping PTFE for PMMA, the work of adhesion and spreading improves.

A higher $W_A/\sigma_{SFT}$ ratio is reflected by lower contact angle up to the point at which total spreading (0° contact angle) occurs at $W_A = 2\sigma_{SFT}$. Higher ratios are possible, however the spreading can not further improve. For DEHA/HTPB and PTFE the ratio is 1.39, while for DEHA/HTPB and PMMA the ratio is higher at 2.04. For titanium, the ratio is slightly higher again at 2.22. It was hypothesised that a higher $W_A/\sigma_{SFT}$ ratio (lower contact angle) would improve the efficiency of mixing, thus titanium and PMMA are expected to perform better than PTFE.

Lower contact angles may also be achievable by modifying the formulation with surface active additives, which would lower both the surface tension and work of adhesion. For example, commonly included in PBXs are processing aids (e.g. lecithin), bonding agents (e.g. Dantocol DHE), and anti-foaming agents (e.g. BYK-A 535), all of which may lower the interfacial tension. HTPB is also available in grades of differing molecular mass and hydroxyl content, which again may have different surface properties. This should be investigated in future work.

### Mixing Procedure

A comparison of intensity and temperature profiles for mixing in PTFE, PMMA, and titanium are given in Figure 4-4, with the full sets (in good agreement) being shown in appendices (Figure 4-A9 and Figure 4-A10). The horizontal dotted lines show the measured[20] intensity readout for an equivalent rigid body mass. The three mixing stages are the mixing stage (M), the bulk motion stage (B), and the flat-line stage (FL), where the two vertical dashed lines on each plot represent the beginning of the bulk and flat-line stages respectively. The time to the onset of bulk motion (taken to be the end of mix point[20]) and the energy (mechanical method) supplied up

[d] For reference, Figure 4-A4, Figure 4-A5, Figure 4-A6, Figure 4-A7, and Figure 4-A8 in appendices show similar isoline plots for PTFE, PMMA, and titanium surfaces. In these cases, the graphs are the 'reverse' of Figure 4-3, with various liquids instead shown as the plotted points.

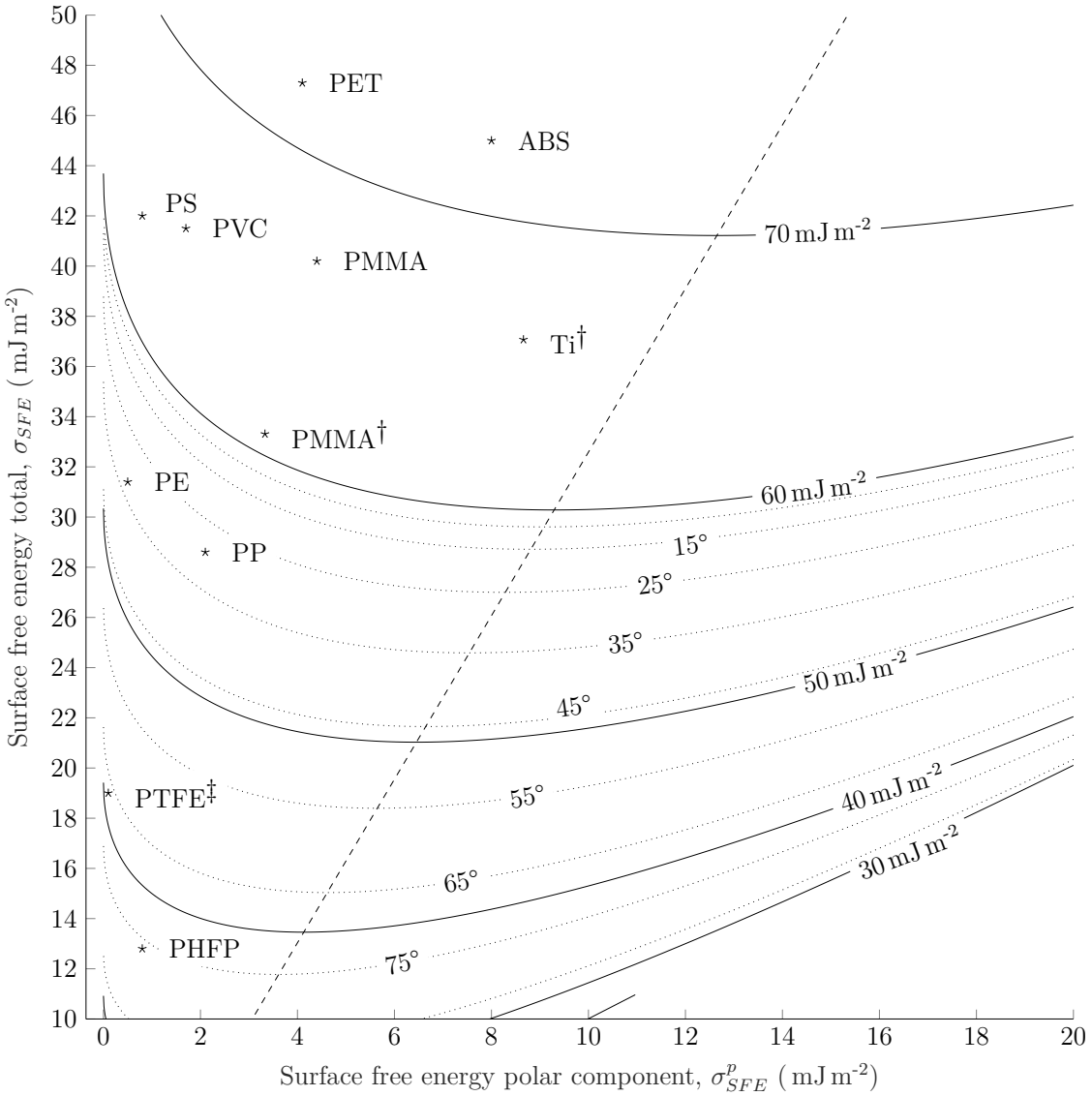


Figure 4-3: Work of adhesion and spreading envelope isoline plot for HTPB/DEHA.

†Denotes experimental values from this work. ‡Denotes experimental values which overlay literature values. The dashed line shows the ideal ratio of polar component to total surface free energy to get maximum work of adhesion for the minimum surface free energy. Materials and literature references: PHFP - poly(hexafluoropropylene),[28] PTFE - polytetrafluoroethylene,[17] PP - polypropylene,[32] PE - polyethylene,[33] PMMA - poly(methyl methacrylate),[28] PVC - polyvinyl chloride,[28] PS - polystyrene,[28] ABS - acrylonitrile butadiene styrene,[34] PET - polyethylene terephthalate,[17] Ti - titanium.

to that point are shown in Figure 4-5. The electrical and thermal methods gave the same trend (at the same order of magnitude) as the mechanical method, apart from the thermal method when applied to the titanium vessel, which underestimated in comparison. A similar figure showing the time and energy required for the flat-line onset, and the full data for the experiment are given in appendices (Figure 4-A11

and Table 4-A1). The average temperature (and standard deviation) over the eight mixes performed was 22±3 ℃.

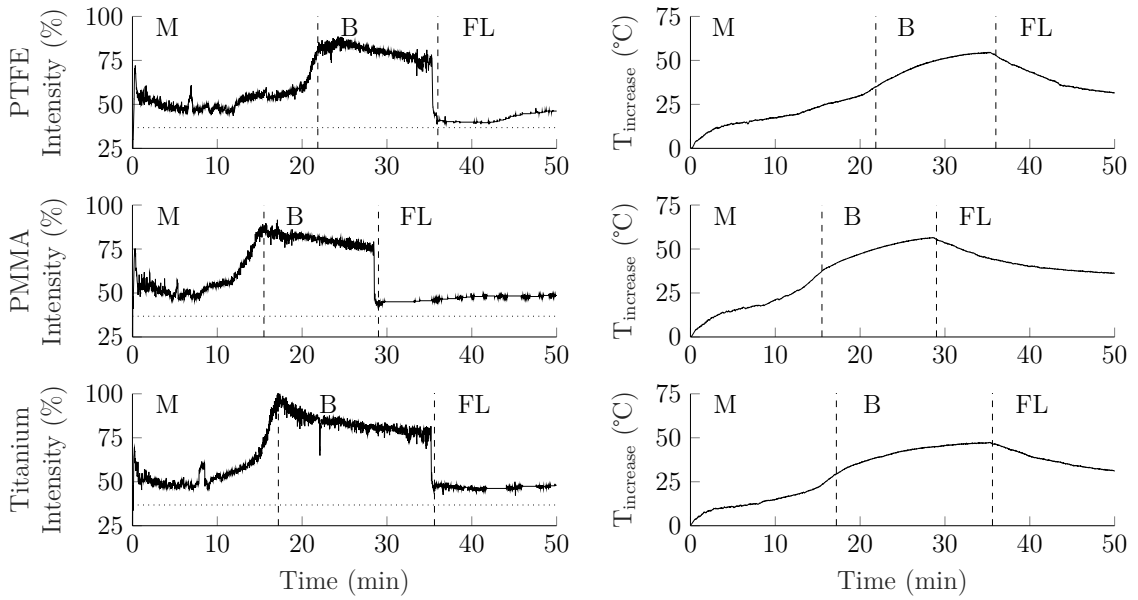


Figure 4-4: Comparison of intensity and temperature profiles for PTFE, PMMA, and titanium vessels. Glass microbeads 62 % v/v, DEHA 19 % v/v, HTPB 19 % v/v, 550 mbar pressure. Horizontal lines - equivalent RBM profiles, vertical lines - profile stage boundaries.

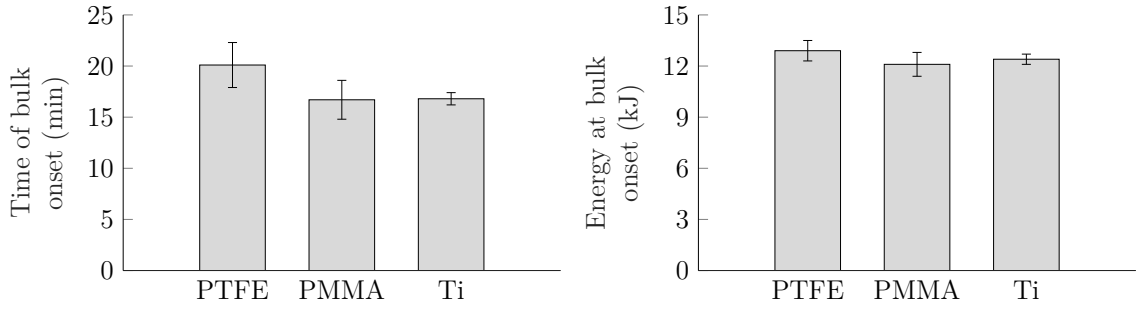


Figure 4-5: Bar graphs showing the average time (left) and average energy (mechanical method, right) required for mixing completion in PTFE, PMMA, and titanium vessels over triplicate, triplicate, and duplicate measurements respectively. Glass microbeads 62 % v/v, DEHA 19 % v/v, HTPB 19 % v/v, 50 G acceleration, 550 mbar pressure. Standard deviations shown.

Figure 4-4 shows there is good agreement in the general shape of the PTFE and PMMA profiles, though the bulk onset (end of mix point) for PTFE is shifted to longer time. Figure 4-5 shows that not only does the time required for mixing reduce (17 % less time required on average) for the higher surface free energy PMMA, but also the total energy required (6 % less energy required on average). This may

be the result of two effects, the primary effect being improved coupling creating more intense mixing, and the secondary effect being the more intense mixing more rapidly increasing the temperature, reducing the viscosity of the formulation. The lower viscosity then serves to further improve the efficiency since it requires less effort to move.

The example titanium vessel mixing profile shown in Figure 4-4 shows that the start of the bulk motion stage (end of mix point) occurs at a similar point to that of the PMMA vessel, while the flat-line occurs at a similar point to that of the PTFE vessel. The full set of profiles are given in appendices (Figure 4-A10), and show good agreement. While the similar surface free energies recorded between the PMMA and titanium vessels would explain the similarities in the time of bulk motion onset, the unexpectedly large length of the bulk motion stage is attributed to differences in the thermal properties between the polymeric (PTFE and PMMA) vessels and the metallic (titanium) vessel. Literature values of their thermal properties are given in Table 4-5.

Table 4-5: Thermal properties of PTFE, PMMA, and titanium (Grade 5).[35]

| | Volumetric Heat capacity, $S_p$ ( $J\,cm^{-3}\,K^{-1}$) | Thermal Conductivity, $\lambda$ ( $W\,m^{-1}\,K^{-1}$) | Thermal Diffusivity, $\alpha$ ( $mm^2\,s^{-1}$) | Thermal Effusivity, $e$ ( $W\,s^{0.5}\,m^{-2}\,K^{-1}$) |
|---|---|---|---|---|
| PTFE | 2.179 | 0.251 | 0.12 | 740 |
| PMMA | 1.728 | 0.209 | 0.12 | 601 |
| Ti | 2.327 | 7.113 | 3.06 | 4069 |

Volumetric heat capacity, $S_p$, describes the heat required for one unit volume of material to increase by one unit of temperature. Thermal conductivity, $\lambda$, describes the material's ability to conduct heat. Thermal diffusivity, $\alpha = \lambda/S_p$, describes thermal conductivity relative to the 'thermal bulk' - the rate of heat transfer from the hot to cold end. Thermal effusivity, $e = \sqrt{\lambda S_p}$, describes thermal responsiveness - the ability to exchange heat with the surroundings.

The results of the cooling rate analysis between the vessels are shown in Table 4-6, where the Newtonian cooling constants, $k$, are given. It can be seen that the cooling behaviour was consistent between the PTFE, PMMA and titanium vessels (when the titanium vessel is insulated with a plastic base plate).[e] Correspondingly, the thermal gradients between the interior and exterior vessel surfaces when cooling

[e] It should be noted that $k$ is not an intrinsic property of the material, rather a system specific parameter that will change depending on aspects such as the fill level, thermal properties of the mixture and mixing vessel, added insulation, and vacuum application.

were the same for all three vessels. The gradient is shown as the dashed line on Figure 4-6, normalised to ambient temperature. However, this thermal gradient is different to when the vessels are heating up, meaning the cooling constant, $k$, is not strictly valid for these cases, particularly titanium. In other words, the dashed line in Figure 4-6 (which is extrapolated from the cooling stage) is being used to describe the thermal gradients for the mixing and bulk stages.

Table 4-6: Cooling constants for each of the vessels when filled with 65 mL of the formulation.

| Vessel type | $k$ ($\text{min}^{-1}$) |
|---|---|
| Titanium Grade 5 (no insulation) | 0.05710 |
| Titanium Grade 5 (plastic base) | 0.04109 |
| PMMA | 0.04320 |
| PTFE | 0.04235 |

The author's previous work[20, 21] has shown the end point of the bulk motion stage (the flat-line) is determined by time it takes for the material's viscosity to lower to the value it has[20] at an absolute temperature of approximately 75 ℃ (note relative temperature is shown on the profile graphs). The increased time required for this to happen in the case of titanium is likely due to the titanium acting as a heat sink, slowing the rate of heating. When heating, the titanium vessel will more quickly heat up in response to the increase in temperature of the mixture (higher effusivity), and more quickly diffuse the heat to the exterior surface of the vessel (higher diffusivity). In other words, the rate at which heat is removed from each vessel is higher when the system is mixing (heating up), to when after the machine is switched off (cooling down), particularly in the case of titanium.

Figure 4-6 shows that the cooling gradient (dashed line) is a better approximation for the PMMA and PTFE vessels than for the titanium vessel, though the gradient is too shallow in all cases. This means that the cooling rate is being underestimated during the bulk motion stage for the all of the vessels, but for titanium in particular. Therefore despite being insulated, the titanium vessel will be losing more heat to the environment than the plastic vessels. This is probably why the thermal method to determine energy consumption (which relies on heat loss estimations) gave slightly lower values than expected. It is therefore apparent that normalisation of the Newtonian cooling constant is insufficient to match the thermal behaviours between metallic and polymeric vessels.

Knowing the effects of surface free energy will be important when considering 'in-situ' mixing of munitions. For example, industry has previously tested the use of

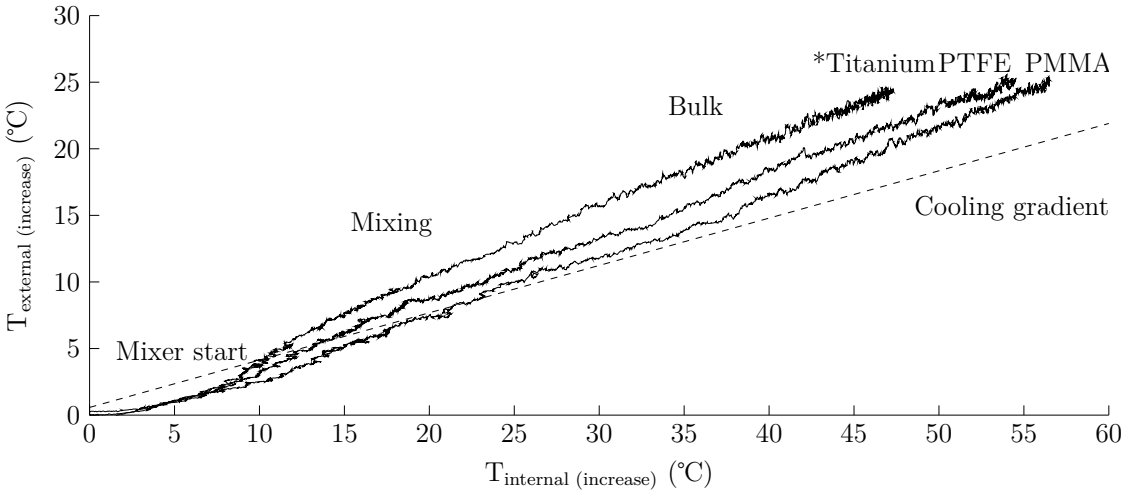


Figure 4-6: Comparison of internal and external vessel temperature for all vessels. *Plastic base plate insulated.

cast PBXs in artillery shells lined with a non-stick coating, to prevent damage to the PBX when it shrinks during curing. Damage would otherwise occur when the PBX pulls away from the wall. Rubber liners that bond to the PBX are also used, where the liner is flexible to the shrinkage. Mixing a PBX 'in-situ' with such non-stick coatings (which by design have a low surface free energy) may have different mixing characteristics (probably taking longer and requiring more energy input based on the findings of this work) to those mixed in a rubber liner. It may therefore be found that a rubber liner is preferable to a non-stick coating for the purposes of mixing munitions 'in-situ'.

## Conclusions

The aim of this work was to assess the effects of changing mixing vessel surface variables on mixing efficiency, with respect to surface free energy. Mixing in the higher surface free energy PMMA vessel was found to reduce mixing time and improve mixing efficiency in comparison to the lower surface free energy PTFE vessel. A greater work of adhesion between the material and vessel wall enhancing the no-slip coupling condition for PMMA is believed to be responsible. This supports the hypothesis that no-slip conditions are important for mixing efficiency. The inability of titanium to perform better than PMMA despite the nominally higher surface free energies of metals and metal oxides is attributed to surface contamination lowering the surface free energy to that characteristic of plastics, and significantly higher

thermal conductivity slowing the rate of internal temperature rise thus viscosity reduction.

## References

[1] M. Andrews, C. Collet, A. Wolff, and C. Hollands. ResonantAcosutic Mixing Processing and Safety. Munitions Safety Information Analysis Center, May 2019.

[2] J.P. Agrawal. *High Energy Materials - Propellants, Explosives and Pyrotechnics*. WILEY-VCH Verlag GmbH & Co. KGaA, Weinheim, 2010. pp. 108, 163-166, 173-174, 268.

[3] A.C. Hordijk and A.E.D.M. van der Heijden. Mixing. In *Energetic Materials; Particle Processing and Characterization*. Wiley-VCH Verlag GmbH, 2005.

[4] Inc. Resodyn Acoustic Mixers. Resonant Acoustic Mixing (Technical White Paper). ResoDyn Corp, Butte, MT, USA, 2009.

[5] Inc. Resodyn Acoustic Mixers. LabRAM Resonant Acoustic Mixer Manual. ResoDyn Corp, Butte, MT, USA, February 2012.

[6] M.D. McPherson. Propellant and explosives production method by use of resonant acoustic mix process. Patent WO 2009/091430 A1, July 2010.

[7] A.J. Claydon. *Resonant Acoustic Mixing of Polymer Bonded Explosives*. PhD thesis, Cranfield University, 2020. Paper 1.

[8] P.A. Lucon and J. Whaley. Liquids and Pastes. Resodyn Technical Interchange, Butte, Montana, USA, 2016.

[9] P.A. Lucon, G. Sperry, and J. Whaley. RAM Mixing of Liquids and Pastes. Resodyn Technical Interchange, Butte, Montana, USA, 2016.

[10] P.A. Lucon. Mixing with Vacuum Assist. Resodyn Technical Interchange, Butte, Montana, USA, 2016.

[11] H.A. Barnes. A review of the slip (wall depletion) of polymer solutions, emulsions and particle suspensions in viscometers: its cause, character, and cure. *J. Non-Newton Fluid*, 56:221–251, 1995.

[12] M. Cloitre and R.T. Bonnecaze. A review on wall slip in high solid dispersions. *Rheol Acta*, 56:283305, 2017.

[13] J-M. Piau, N. Kissi, and A. Mezghani. Slip flow of polybutadiene through fluorinated dies. *J. Non-Newton Fluid*, 59:11–30, 1995.

[14] E.R. Beckel, K.E. Lee, J.C. Marin, and A.H. Shah. Processing of Explosives at ARDEC Using the LabRAM. U.S. Army Armament Research, Development and Engineering Center, September 2016.

[15] M. Lewin, A. Mey-Marom, and R. Frank. Surface free energies of polymeric materials, additives and minerals. *Polym. Adv. Technol.*, 16:429–441, 2005.

[16] J.E. Castle. The Composition of Metal Surfaces After Atmospheric Exposure: An Historical Perspective. *J. Adhes.*, 84:368–388, 2008.

[17] D.K. Owens and R.C. Wendt. Estimation of the surface free energy of polymers. *J. App. Polym. Sci.*, 13:1741–1747, 1969.

[18] D. H. Kaelble. Dispersion-Polar Surface Tension Properties of Organic Solids. *J. Adhesion*, 2:66–81, 1970.

[19] W. Rabel. Einige Aspekte der Benetzungstheorie und ihre Anwendung auf die Untersuchung und Veränderung der Oberflächeneigenschaften von Polymeren. *Farbe und Lack*, 77:997–1005, 1971.

[20] A.J. Claydon. *Resonant Acoustic Mixing of Polymer Bonded Explosives*. PhD thesis, Cranfield University, 2020. Paper 2.

[21] A.J. Claydon. *Resonant Acoustic Mixing of Polymer Bonded Explosives*. PhD thesis, Cranfield University, 2020. Paper 3.

[22] DataPhysics Instruments GmbH. OCA Software. `https://www.dataphysics-instruments.com/products/oca/software/`. Accessed 17-08-2020.

[23] Sigma-Aldrich. Bis(2-ethylhexyl) adipate. `https://www.sigmaaldrich.com/catalog/product/aldrich/525197?lang=en&region=GB`. Accessed 17-08-2020.

[24] Cray Valley. Poly bd R45 HTLO. `http://www.crayvalley.com/docs/TDS/poly-bd-r-45htlo.pdf`. Accessed 17-08-2020.

[25] K.F. Gebhardt. Grundlagen der physikalischen Chemie von Grenzflächen und Methoden zur Bestimmung grenzflächenenergetischer GröSSen. FhG IGB Stuttgart, 1982.

[26] D. Ramirez and J. Kalman. Influence of HTPB Variants on the Wettability of Ammonium Perchlorate. AIAA SciTech Forum, Orlando, FL, USA, January 2020.

[27] H.J. Busscher, A.W.J. van Pelt, P. de Boer, H.P. de Jong, and J. Arends. The effect of surface roughening of polymers on measured contact angles of liquids. *Colloids Surf.*, 9:319–331, 1984.

[28] S. Wu. Calculation of interfacial tension in polymer systems. *J. Polym. Sci. C*, 34:19–30, 1971.

[29] M. Mantel and J.P. Wightman. Influence of the Surface Chemistry on the Wettability of Stainless Steel. *Surf. Interface Anal.*, 21:595–605, 1994.

[30] S. Becker, R. Merz, H. Hasse, and M. Kopnarski. Solvent cleaning and wettability of technical steel and titanium surfaces. *Adsorpt. Sci. Technol.*, 34:261–274, 2016.

[31] T. Noguchi, S. Takemoto, M. Hattori, M. Yoshinari, E. Kawada, and Y. Oda. Discoloration and dissolution of titanium and titanium alloys with immersion in peroxide- or fluoride-containing solutions. *Dent. Mater. J.*, 27:117–23, 2008.

[32] D.A. Berta. Formulating plastics for paint adhesion. In *Coatings of Polymers and Plastics*. Marcel Dekker, New York, NY, 2003.

[33] D. H. Kaelble and E. H. Cirlin. Dispersion and polar contributions to surface tension of poly(methylene oxide) and Na-treated polytetrafluoroethylene. *J. Polym. Sci. A-2*, 9:363–368, 1971.

[34] C.K. Schoff. Painting problems. In *Coatings of Polymers and Plastics*, page 227. Marcel Dekker, New York, NY, 2003.

[35] Thermtest Instruments Materials Properties Database. `https://thermtest.com/materials-database`. Accessed 01-04-2020.

# Appendices

(a) DEHA/Air ($\sigma_{SFT}$= 28.25 mJ m$^{-2}$)

(b) DEHA/HTPB/Air ($\sigma_{SFT}$= 29.72 mJ m$^{-2}$)

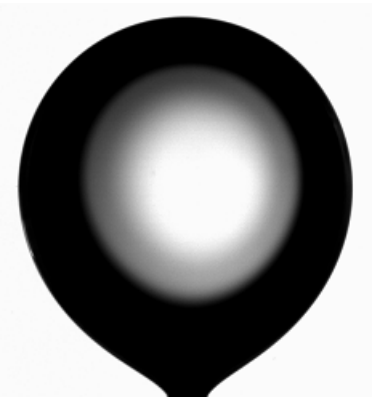

(c) DEHA/Water ($\sigma_{IFT}$= 23.57 mJ m$^{-2}$)

(d) DEHA/HTPB/Water ($\sigma_{IFT}$= 14.92 mJ m$^{-2}$)

Figure 4-A1: Photographs of pendant drop shapes for DEHA and DEHA/HTPB.

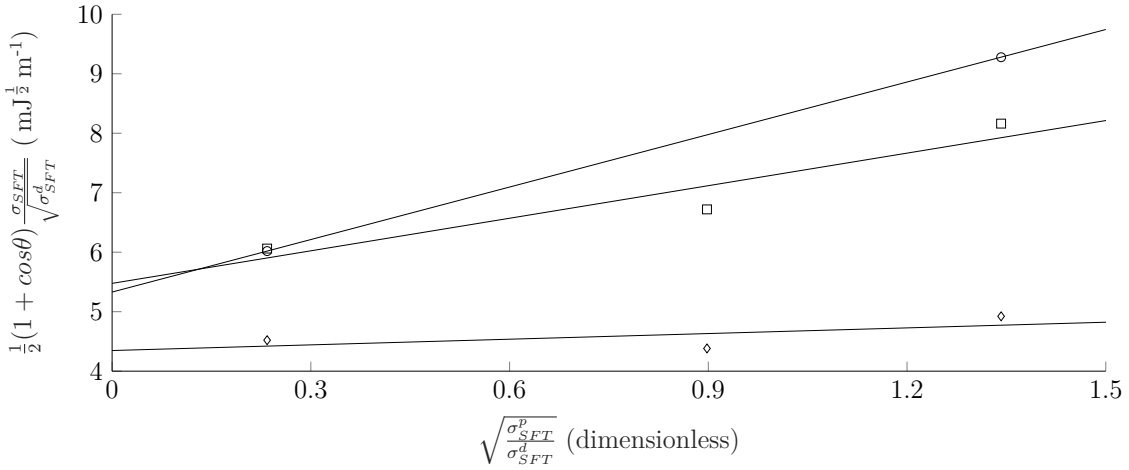


Figure 4-A2: The graphical form of Equation 4-3, from which the polar and disperse components of surface free energy of a subject solid are derived from the polar and disperse surface components of probe liquids and their contact angle on the subject solid. Probe liquids diiodomethane (left), ethylene glycol (middle), and water (right).

The diamonds, squares, and circles represent the probe liquids on PTFE, PMMA, and titanium respectively. The squares of gradients and intercepts correspond to the polar and dispersive components of the surface free energies respectively.

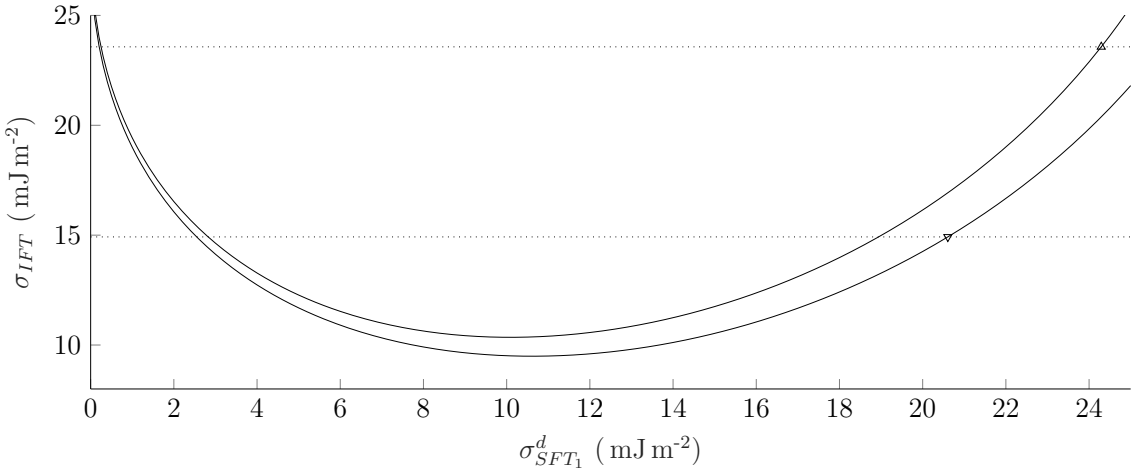


Figure 4-A3: The iterative solution of Equation 4-4, which relates the surface tensions, polar and disperse components, and interfacial tensions of a liquid under investigation (1) and probe liquid (2).

The triangle and inverted triangle represent the points of intersection where values of $\sigma^d_{SFT_1}$ satisfy Equation 4-4 for the measured values of $\sigma_{IFT}$ found for DEHA and DEHA/HTPB in water respectively. The points of intersection at lower $\sigma^d_{SFT_1}$ are artifacts of the method and are discounted.

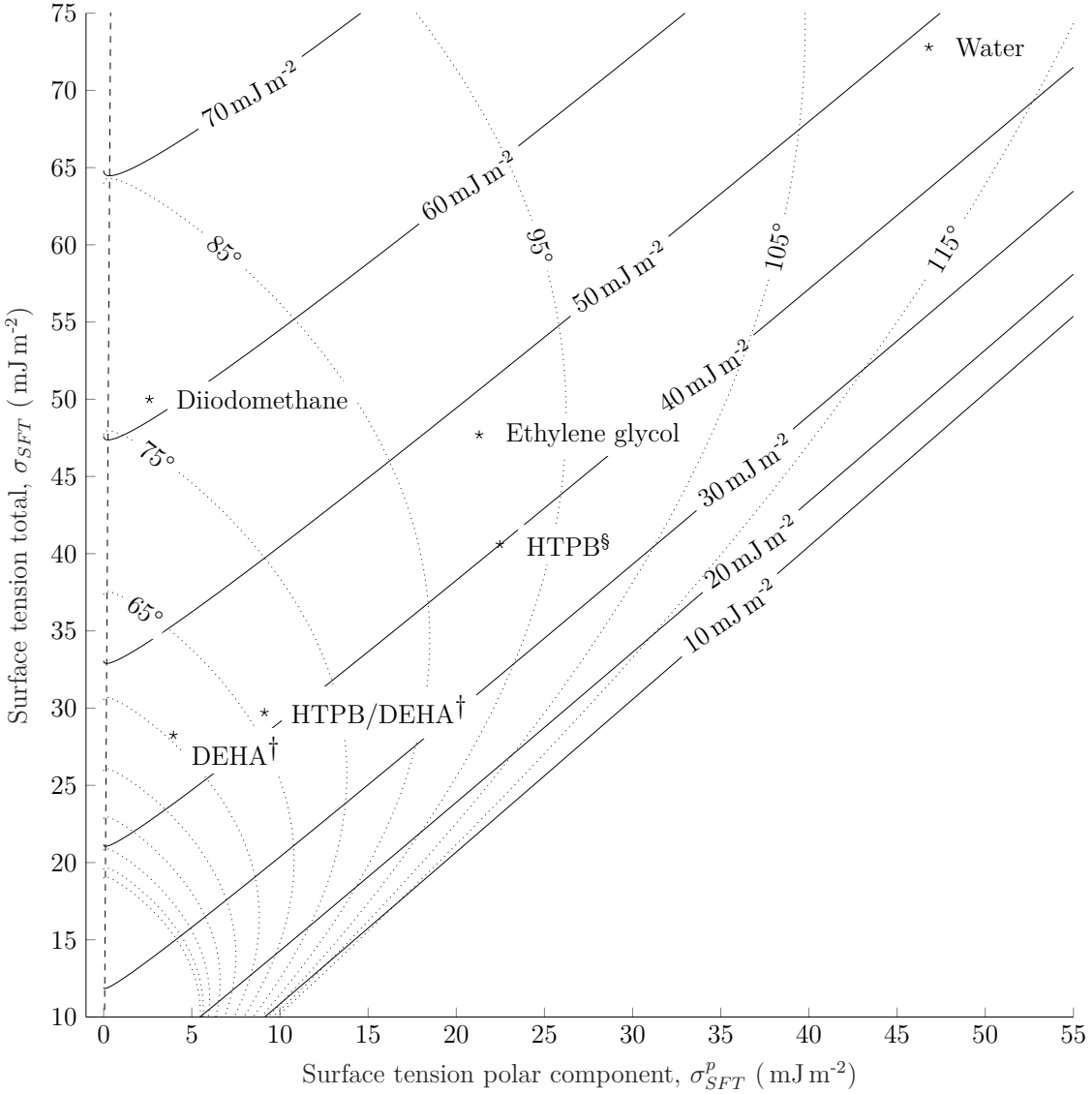


Figure 4-A4: Work of adhesion and spreading envelope isoline plot for PTFE.

†Denotes experimental values from this work. §Denotes values derived from Ramirez and Kalman.[26] The dashed line shows the ideal ratio of polar component to total surface tension to get maximum work of adhesion for the minimum surface tension.

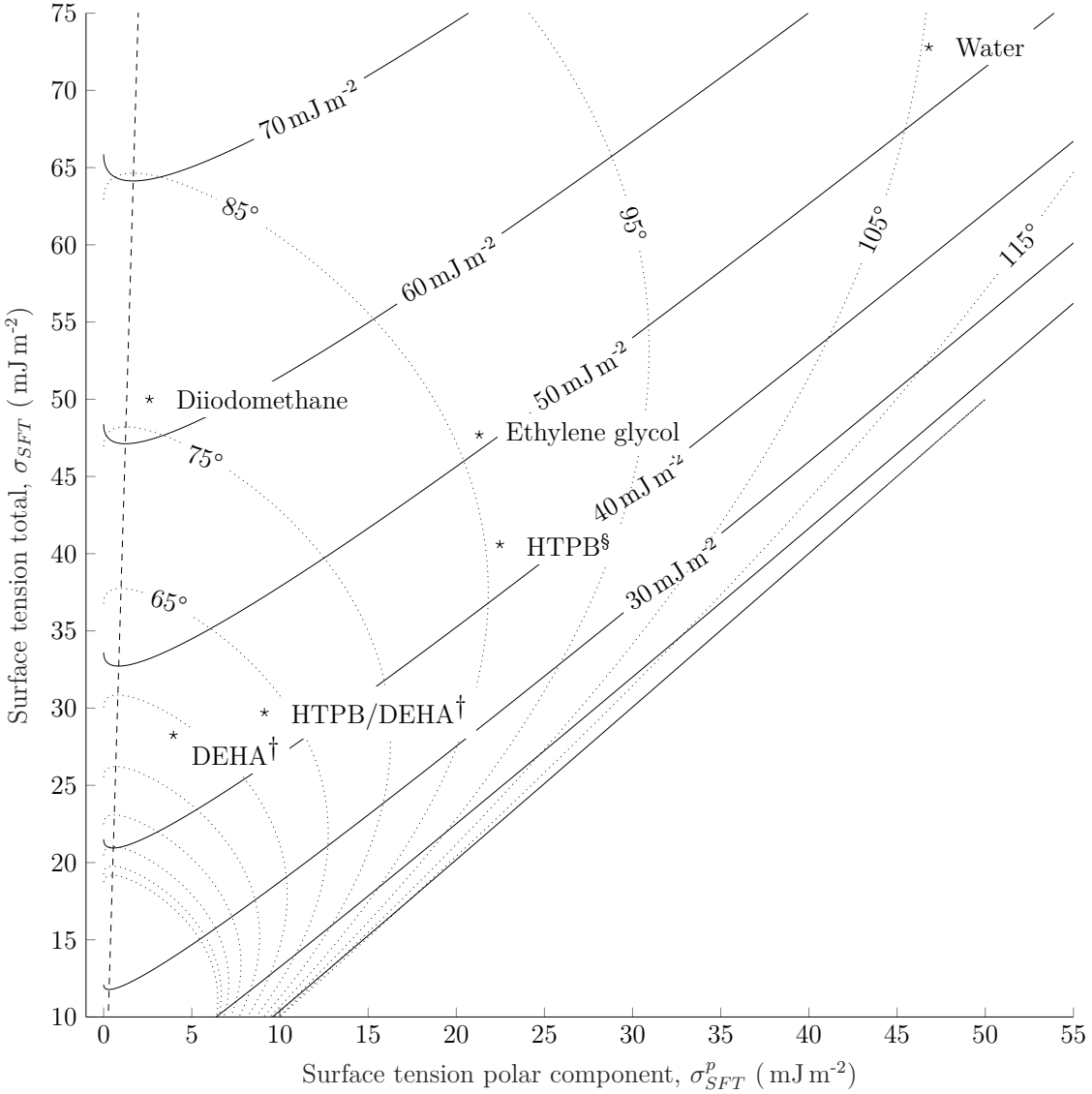


Figure 4-A5: Work of adhesion and spreading envelope isoline plot for PTFE (literature values).

†Denotes experimental values from this work. §Denotes values derived from Ramirez and Kalman.[26] The dashed line shows the ideal ratio of polar component to total surface tension to get maximum work of adhesion for the minimum surface tension.

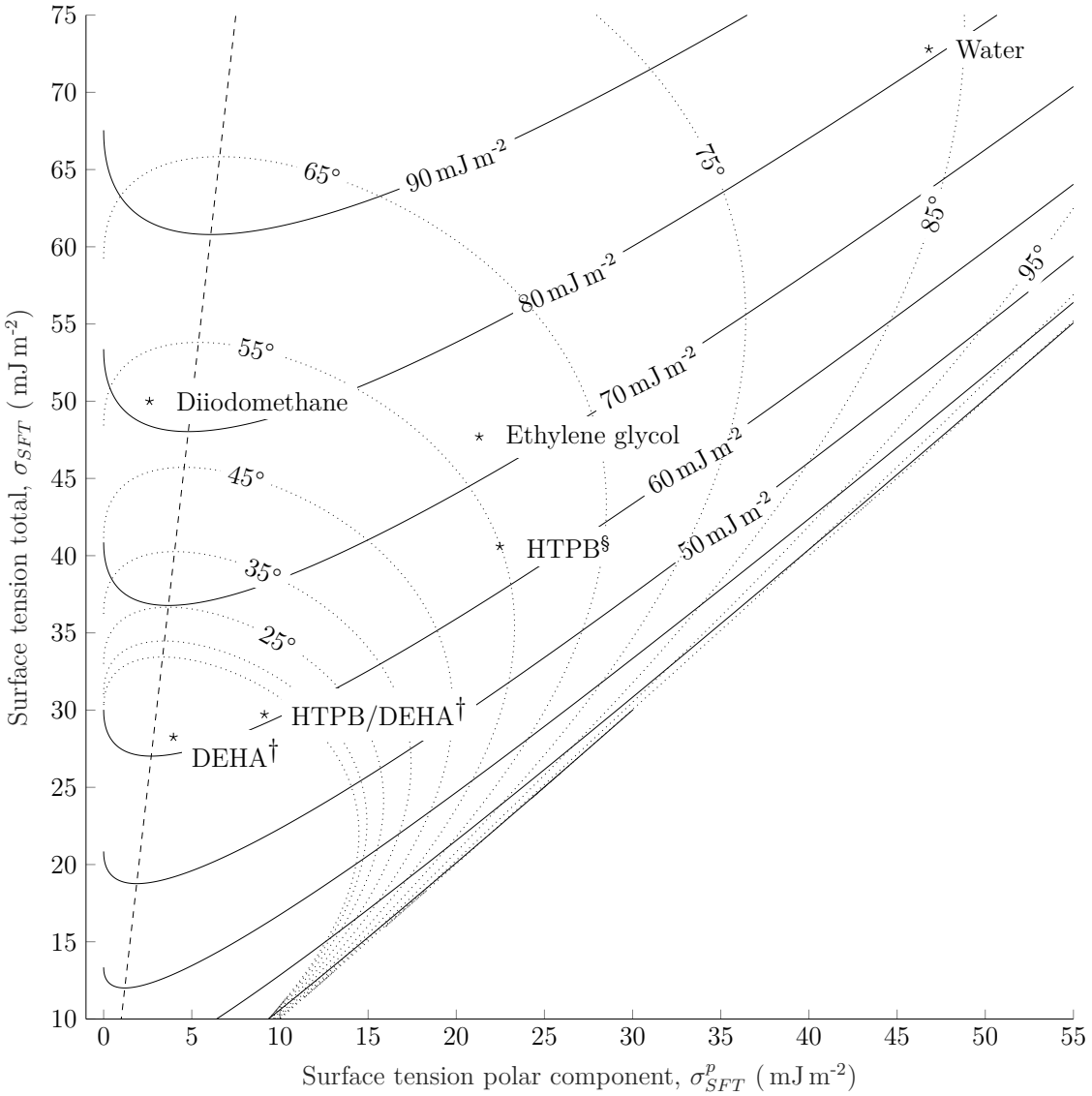


Figure 4-A6: Work of adhesion and spreading envelope isoline plot for PMMA.

†Denotes experimental values from this work. §Denotes values derived from Ramirez and Kalman.[26] The dashed line shows the ideal ratio of polar component to total surface tension to get maximum work of adhesion for the minimum surface tension.

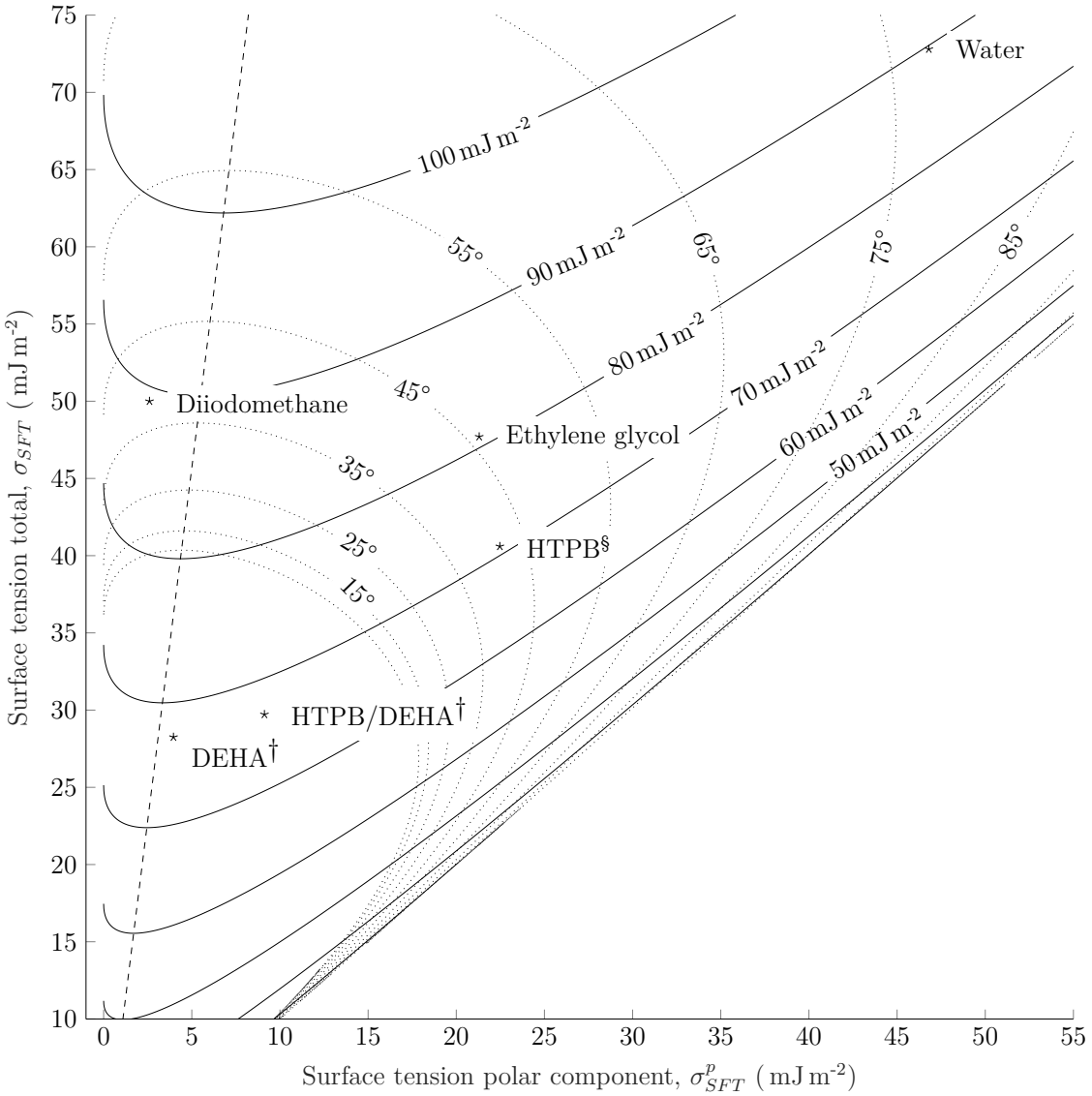


Figure 4-A7: Work of adhesion and spreading envelope isoline plot for PMMA (literature values).

†Denotes experimental values from this work. §Denotes values derived from Ramirez and Kalman.[26] The dashed line shows the ideal ratio of polar component to total surface tension to get maximum work of adhesion for the minimum surface tension.

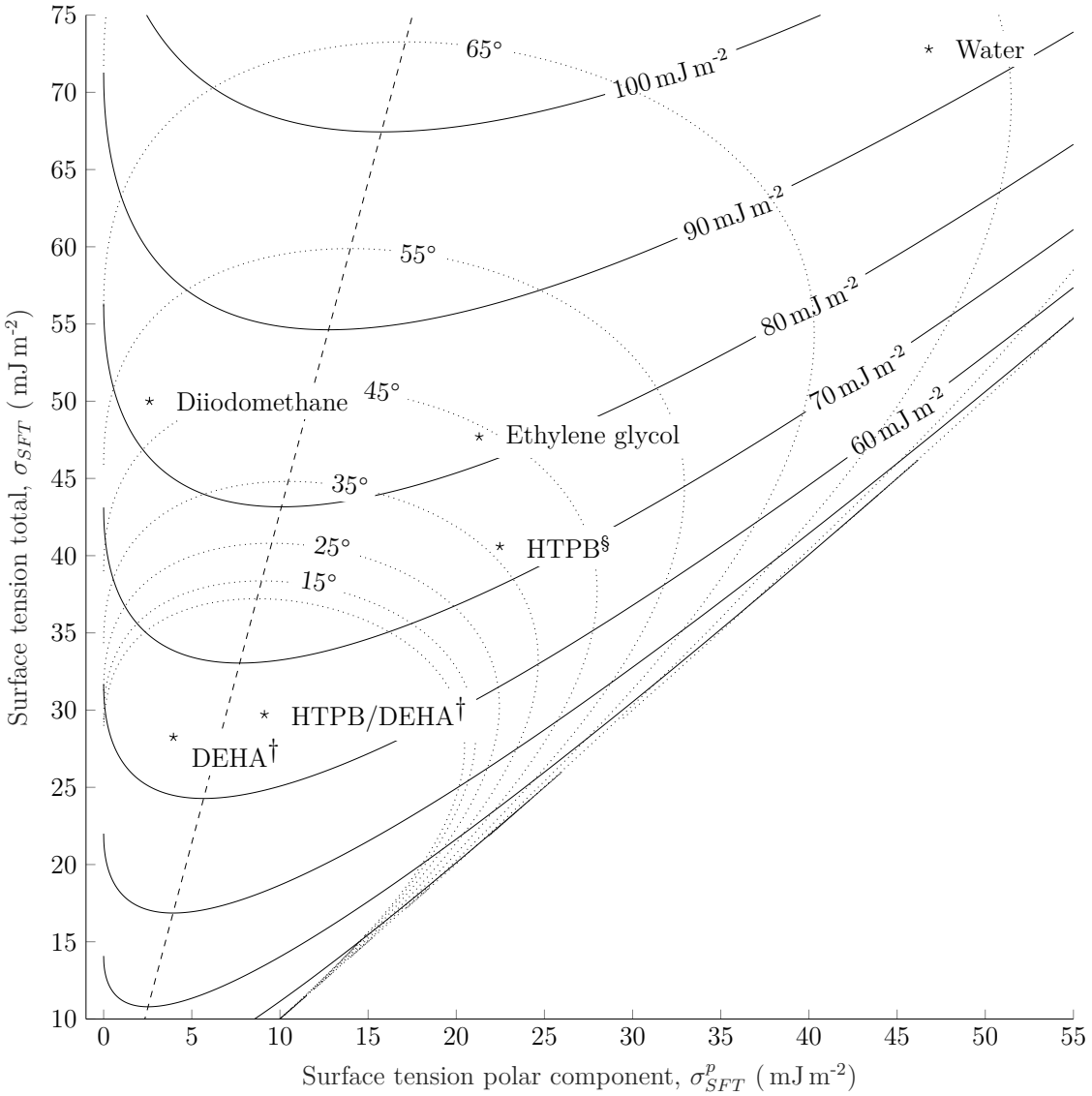


Figure 4-A8: Work of adhesion and spreading envelope isoline plot for titanium.

†Denotes experimental values from this work. §Denotes values derived from Ramirez and Kalman.[26] The dashed line shows the ideal ratio of polar component to total surface tension to get maximum work of adhesion for the minimum surface tension.

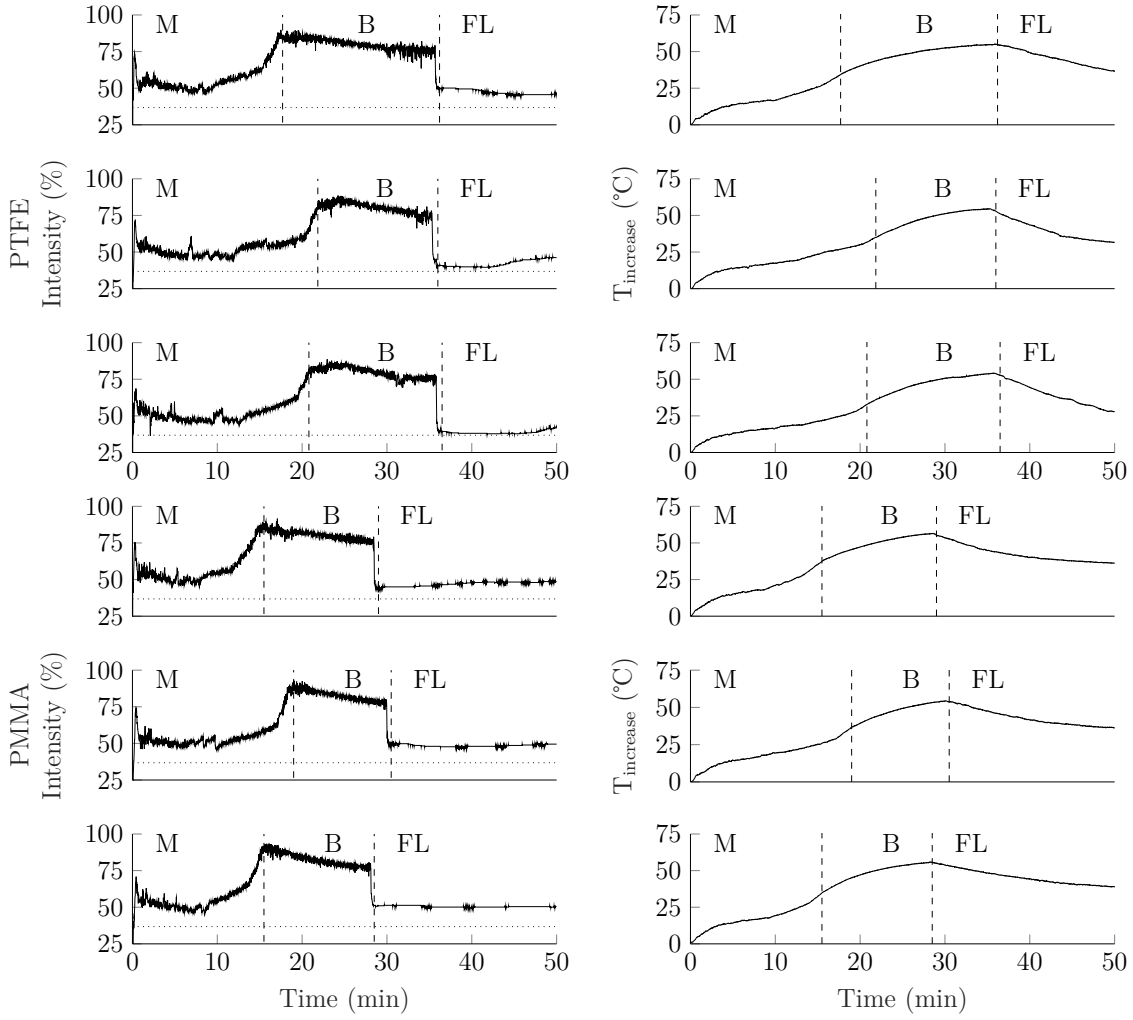


Figure 4-A9: Triplicate intensity and temperature profiles for PTFE and PMMA vessels. Glass microbeads 62 % v/v, DEHA 19 % v/v, HTPB 19 % v/v, 550 mbar pressure. Horizontal lines - equivalent RBM profiles, vertical lines - profile stage boundaries.

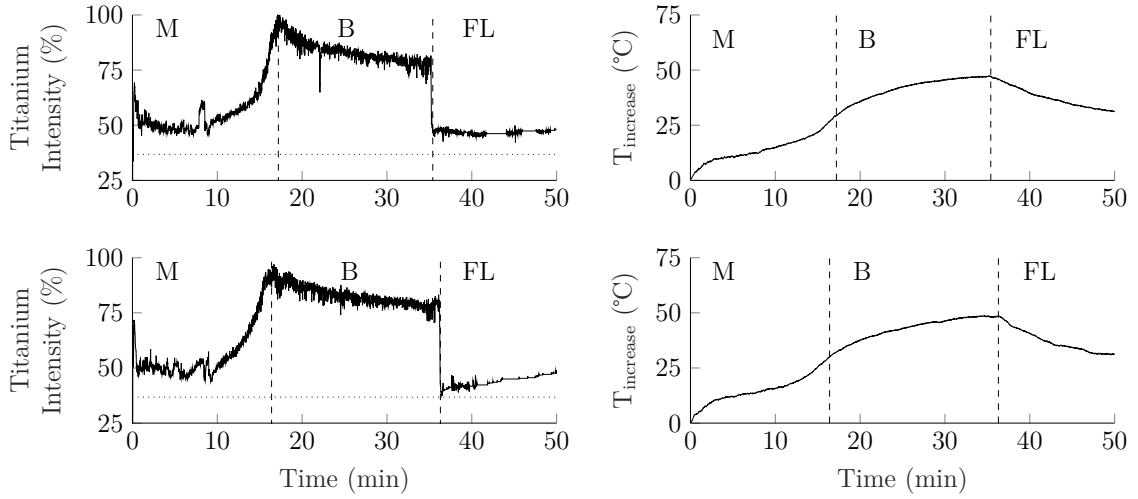


Figure 4-A10: Duplicate intensity and temperature profiles for the titanium vessel. Glass microbeads 62 % v/v, DEHA 19 % v/v, HTPB 19 % v/v, 550 mbar pressure. Horizontal lines - equivalent RBM profiles, vertical lines - profile stage boundaries.

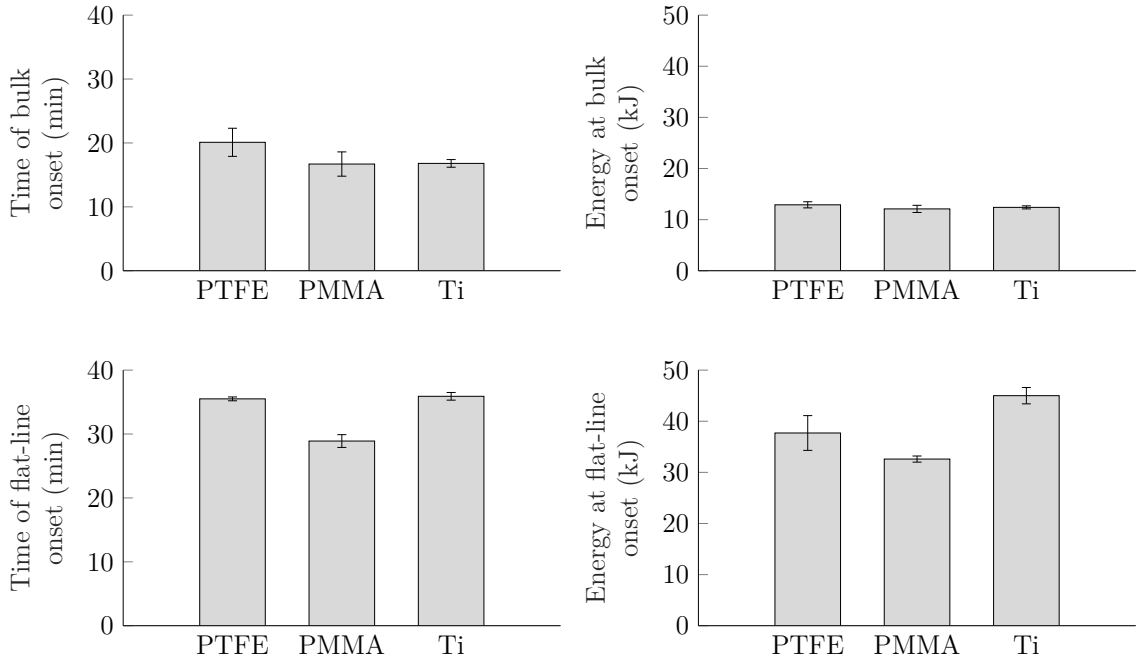


Figure 4-A11: Bar graphs showing the average time (left column) and average energy (mechanical method, right column) required for profile stages in PTFE, PMMA, and titanium vessels over triplicate, triplicate, and duplicate measurements respectively. Glass microbeads 62 % v/v, DEHA 19 % v/v, HTPB 19 % v/v, 50 G acceleration, 550 mbar pressure. Standard deviations shown.

Table 4-A1: Mixing statistics for the surface free energy comparison.

| Vessel material | PTFE | PMMA | Titanium |
|---|---|---|---|
| Time of bulk onset (end of mix) (min) | 20.1±2.2 | 16.7±1.9 | 16.8±0.6 |
| Energy at bulk onset (Mechanical, kJ) | 12.9±0.6 | 12.1±0.7 | 12.4±0.3 |
| Energy at bulk onset (Electrical, kJ) | 7.7±0.4 | 7.3±0.4 | 7.4±0.2 |
| Energy at bulk onset (Thermal, kJ) | 8.3±0.4 | 8.0±0.3 | 7.1±0.1 |
| Time of flat-line (min) | 35.5±0.3 | 28.9±1.0 | 35.9±0.6 |
| Energy at flat-line (Mechanical, kJ) | 37.7±3.4 | 32.6±0.6 | 45.0±1.6 |
| Energy at flat-line (Electrical, kJ) | 22.4±2.0 | 19.4±0.4 | 26.7±0.9 |
| Energy at flat-line (Thermal, kJ) | 16.5±0.4 | 14.9±0.4 | 15.1±0.6 |

# Paper 5 - The Effect of Vessel Finish on the Efficiency of Resonant Acoustic Mixing for Polymer Bonded Explosives

Andrew J. Claydon, Guillaume Kister, Sally Gaulter, and Philip P. Gill

**Abstract:** The effects of three vessel surface finishes (smooth, rough, and ribbed) are assessed with regards to the process efficiency of Resonant Acoustic Mixing (RAM) applied to a Polymer Bonded Explosive (PBX) simulant. 3D printing using acrylonitrile-butadiene styrene (ABS) plastic was used to construct the vessels, a technique that is found to be generally unsuitable due to porosity preventing effective vacuum application, and cracking under applied acceleration leading to leakage. An inert formulation (glass microbeads 28.3 micron D50, 62% v/v in HTPB and plasticiser) was used to facilitate mixing. Though no significant differences in process efficiency were observed, this may have been due to lack of vacuum application inhibiting the movement of the mixture.

**Keywords:** Resonant Acoustic Mixing, Polymer Bonded eXplosive, Surface Finish, LabRAM

## Introduction

Resonant Acoustic Mixing (RAM) is a novel mixing technique being increasingly employed[1] in the manufacture of Polymer Bonded Explosives (PBXs) - explosive crystals dispersed in a liquid pre-polymer which is then cured into an elastomeric composite. While RAM brings benefits such as reduced mixing times and the ability to mix high viscosity formulations 'in-situ' (factors previously reviewed by the author[2]), it has the drawback of being less well characterised than conventional techniques[3] such as planetary and 'z' blade mixing. RAM operates by vibrating the mixture (at accelerations of up to 100 G) at the mechanical resonance ( 60 Hz) of the mass-spring system to which the mixing vessel is attached. Energy transfer to loaded viscous suspensions (e.g. PBXs) is believed to rely on a velocity gradient across the mixture, perpendicular to the vessel wall. The gradient arises from the bulk of the material being accelerated by acoustic pressure waves (vibrations), while there is a coupling condition (ideally 'no-slip') at the wall. This movement is thought to create the shear responsible for mixing,[4–6] and is referred to as churning,[7] or bulk mixing[4–6] if occurring at high intensity. It would follow that by maximising the movement of the material or by minimising slip at the wall, the velocity gradient, thus shear, could be maximised. This would result in faster, more efficient mixing. The author has previously classified the factors known or suspected to affect movement and wall slip into the categories shown in Table 5-1.[2]

Table 5-1: Machine variables, vessel variables, and formulation variables for Resonant Acoustic Mixing.

| Machine variables | Vessel variables | Formulation variables |
|---|---|---|
| Acceleration setting | Vacuum setting | Binder content |
| Intensity setting | Wall material | Plasticiser content |
| Mixer model | Wall surface finish | Additives |
| Mixer unit | Diameter | Solids loading |
| | Insulation | Particle shape |
| | Active heating | Filler type |
| | Active cooling | |

The aim of this work is to investigate the effects of surface finish (a vessel variable) on mixing efficiency, a factor that has not previously been examined. This is achieved by comparing mixing behaviour in smooth, rough, and ribbed vessels.

### Effect of surface finish

Wall slip of filled polymer systems can occur in two forms, true slip and apparent slip.[8–10] True slip occurs on the molecular level due to a loss of adhesion between the binder and the shearing surface (vessel wall for RAM), while apparent slip occurs due to the formation of a binder rich layer in the vicinity of the wall that acts to 'lubricate' the bulk flow. The binder rich layer has a thickness on the order of the particle size, and is formed due to the filler being unable to penetrate the wall, locally diminishing the volume fraction. True slip and its mitigation when RAM mixing has previously been addressed by the author.[11] In this work, apparent slip is of interest.

Apparent slip can be mitigated by the use of shearing surfaces (i.e. vessel wall in the case of RAM) that have a textured (i.e. roughened) surface finish such that the asperities break through the lubricating layer and allow the surface to interact directly with the bulk of the material.[9] Surface finishing methods previously employed to roughen shearing surfaces in shear rheometry have included cross-hatching,[12, 13] sand blasting,[14–19] machining,[20, 21] and attaching particles[22–26] or sandpaper.[27–31] The result of the finishing method on the roughness can be quantified by measuring the roughness average ($R_a$) value - the arithmetic mean deviation of the surface profile from its centreline over a measured length.[32] It has previously been found[23] that apparent wall slip decreases as the particle size ($R$) to roughness average ($R_a$) ratio ($R/R_a$) is decreased until $R/Ra \cong 1$, at which point it becomes minimised.

### Determining efficiency

Mixing progression has previously[11, 33–35] been monitored by interpretation of the machine 'intensity' profile, where intensity refers to the percentage current being drawn by the motor up to 100 %. The author has found that when using a specific glass bead based formulation (Table 5-2) the profile can be broken down into easily recognisable stages that correspond to the rheological changes occurring in the mixture. These are the mixing stage, bulk motion stage, and a flat-line stage. In the mixing stage, most of the rheological changes due to 'degree of mixedness' occur, including wetting (where the solids and liquids are first introduced), incorporation (whereby the material becomes more fluidised), and churning (whereby material couples to the vessel wall and undergoes rolling and smearing). An intensity build up begins upon churning onset where an increasingly large velocity gradient made possible by the compliance of the material is responsible for drawing

more power from the mixer. At the end of the mixing stage, the degree of mixedness has been found to stop changing. During the bulk motion stage, high intensity churning occurs which heats the material, further lowering its viscosity. Eventually, the viscosity is believed to become so low such that the velocity gradient across the mixture becomes unstable, and there is a readjustment in the coupling condition to lower intensity churning, where temperature, mixer intensity, and viscosity tend towards an equilibrium in a flat-line stage. These stages can be used to monitor mixing progression, with end of the mixing stage taken to be the end of mix point. The amount of energy supplied to the mixture up until the end of mix point can be found using three methods (based on mechanical,[11, 33–36] electrical,[11, 34, 35] and thermal[11, 34, 35] monitoring) used previously.

## Experiment

An inert simulant formulation (Table 5-2) as used in previous work[11, 34, 35] was employed for mixing. Glass microbeads (Glass Sphere s.r.o., Czech Republic) were used as the filler, hydroxyl-terminated polybutadiene (HTPB) (type Poly bd® R-45HTLO, Cray Valley, USA) was used as the binder, and di(2-ethylhexyl) adipate (DEHA) was used as plasticiser ($\geq$ 97 %, Merck, UK). Glass bead density, and particle size distribution were taken as the values determined previously,[34] and are shown in Table 5-3

Table 5-2: The glass bead formulation used for mixing.

| | Glass | DEHA | HTPB | Curative |
|---|---|---|---|---|
| Volume (%) | 62.00 | 19.00 | 19.00 | - |
| Actual mass (%) | 81.65 | 9.30 | 9.05 | - |
| RDX equivalent mass (%) | 76.48 | 11.91 | 11.60 | - |

Table 5-3: Density and particle size analysis of the glass beads.

| Density ( $g\,cm^{-3}$) | D10 (µm) | D50 (µm) | D90 (µm) |
|---|---|---|---|
| 2.4905±0.0002 | 12.7±2.3 | 28.3±1.7 | 45.4±1.5 |

Fused deposition modelling (FDM) 3D printed (Dimension uPrint SE printer) acrylonitrile-butadiene styrene (ABS) vessels (48 mm diameter, 47.5 mm height) with three different surface finishes (ribbed, rough, and smooth) were manufactured for mixing. The ribbed finish was characteristic of the FDM technique, where the

horizontal bands of deposited plastic that comprised the vessel created the desired effect. A layer height of 254 µm was used. A rough finish was achieved by machining with a boring bar, and a smooth finish was achieved by machining followed by a chemical treatment with acetone solvent. The acetone partially dissolved the surface of the ABS, and then evaporated to leave a glossy finish. The vessel lid was of custom PEEK[a] construction, and was held on with a clamshell clamp. A central hole in the lid was such that a rod thermocouple could be placed into the mixture. The mixer was controlled with equipment and software from Falcon Project Ltd., which also recorded the temperature reading from the thermocouples and mixer intensity data.

### Characterisation of materials

The heat capacity of the formulation as required for the thermal method of energy determination was taken as the values presented previously by the author.[34] The cooling behaviour was assessed (Table 5-A1) for the vessels after the machine was turned off, and analysed between 45 ℃ and 35 ℃ using Newton's Law of Cooling, as previously.[34] Surface roughness of the vessels was quantified by stylus contact analysis (Taylor-Hobson Surtronic 2, 0.8 mm sampling length) along the vertical axis at three randomly selected points on the internal circumference. This was complimented with quantitative analysis using optical microscopy (20x magnification).

### Mixing procedure

Mixing occurred at 50 G acceleration for 50 minutes, on 65 mL of the glass bead formulation. Three mixing datasets were taken in each of the smooth, rough, and ribbed vessels. Ingredients were added in the order - half of the filler, plasticiser, remaining filler, binder. Vacuum was not applied since the porosity of the 3D printed vessels meant they were not airtight. A LabRAM (LabRAM 'B' as characterised previously[34]) was used in the experiment. The total mass of the filled equipment 604 g in total, normalised to that of previous work.[11, 34, 35]

[a] polyether ether ketone

## Results and discussion

### Characterisation of materials

The surface roughness analysis of the ABS mixing vessels is shown in Figure 5-1, where the $R_a$ values are given with their standard deviations over the three measurements taken in each case. As expected, the ribbed surface had the highest $R_a$, followed by the rough finish and smooth finish respectively. The optical micrographs were again as expected, with the ribbed finish showing regular banding at intervals of the layer height, the rough finish being irregular and porous, and the smooth finish being essentially featureless apart from a mild rippling effect likely left from uneven evaporation of the acetone.

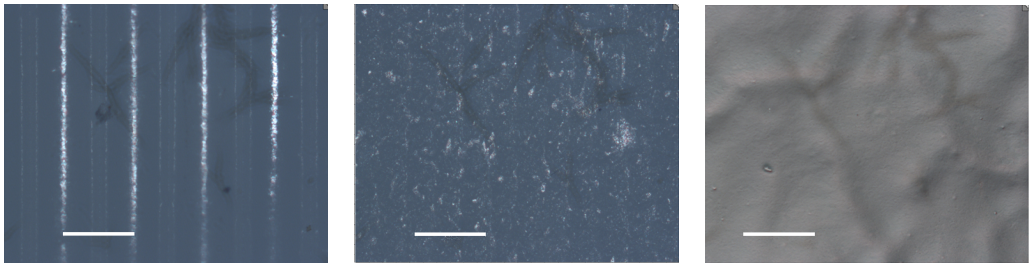

(a) Ribbed
$R_a$ = 115±5 µm

(b) Rough
$R_a$ = 15±3 µm

(c) Smooth
$R_a$ = 2±1 µm

Figure 5-1: Optical micrographs of the three surface finishes. The scale bar represents 254 µm, the layer height used for printing.

Table 5-4 shows the values for $R/Ra$ for each of the surface finishes, using $R$ values of the D10, D50 (median), and D90. Since apparent wall slip is expected to reduce as $R/Ra$ approaches unity,[23] Table 5-4 would suggest that wall slip would be best inhibited when using the rough surface.

Table 5-4: Ratios of particle radius ($R$) to mixing vessel surface roughness average ($R_a$).

| | Ribbed | Rough | Smooth |
|---|---|---|---|
| $R/R_a$ for D10 | 0.1±0.0 | 0.8±0.2 | 6.3±3.4 |
| **$R/R_a$ for D50 (median)** | **0.2±0.0** | **1.9±0.4** | **14.2±7.1** |
| $R/R_a$ for D90 | 0.4±0.0 | 3.0±0.6 | 22.7±11.4 |

A comparison of machine intensity and temperature profiles (and standard deviations) for mixing is given in Figure 5-2, where the horizontal dotted lines represent

the measured[34] intensity required to vibrate an equivalent rigid body mass (604 g). The profile shapes of these mixes do not have the same characteristics as those carried out previously,[11, 34, 35] where distinct mixing stages were seen. Most importantly, a high mixer intensity (90+ %) bulk mixing stage, whereby vigorous churning resultant of a large velocity gradient is believed to exist,[34] was not seen in any case. Instead, these profiles were generally confined to between 45 % and 50% intensity. A likely cause of this is the fact the mixes were not carried out under vacuum, which has been identified as an important factor for inducing bulk mixing,[2, 6] thus a requirement for efficiency.[6, 7, 37–39] This is because the presence of bubbles induced by the vacuum and reduced pressure in the head space make the material more compliant (easier to move) and reduces resistance to bulk flow (in essence increasing inertial forces). This allows the large velocity gradient across the mixture required for high intensity bulk mixing. Without vacuum, it is suspected churning only occurred with a much more shallow velocity gradient, thus much lower shear. Indeed, in all cases the material did appear to be fully mixed when inspected visually after the mixer was turned off.

Figure 5-3 shows the energy consumption for each surface finish after 10, 30, and 50 minutes of mixing, where the smooth vessel generally has the lowest energy uptake while the rough vessel has the highest energy uptake. Although this was as expected, the large error bars suggest the trend is not statistically significant in this case. Furthermore the trend is not replicated when the electrical and thermal methods for energy determination are used. These methods also have large errors. The full dataset is given in appendices (Table 5-A2). The reason no statistically significant differences were seen is unclear. However, it is possible that without a large amount of movement in the material, there was insufficient velocity at the vessel wall for apparent slip to be of significant consequence. It is therefore recommended the experiment be redesigned so vacuum can be applied, and repeated as part of future work to ascertain conclusive results.

Practically speaking, the use of roughened or ribbed interior mixing vessels would be of limited viability with regards to industrial batch mixing, mainly because they would be difficult to clean. A more suitable application would likely be with mixed 'in-situ' munitions, where there is no requirement for cleaning. The technique may also be beneficial to 'in-situ' munitions that are required to adhere to the case interior, where improved bonding has previously been reported with increased interfacial roughness.[40]

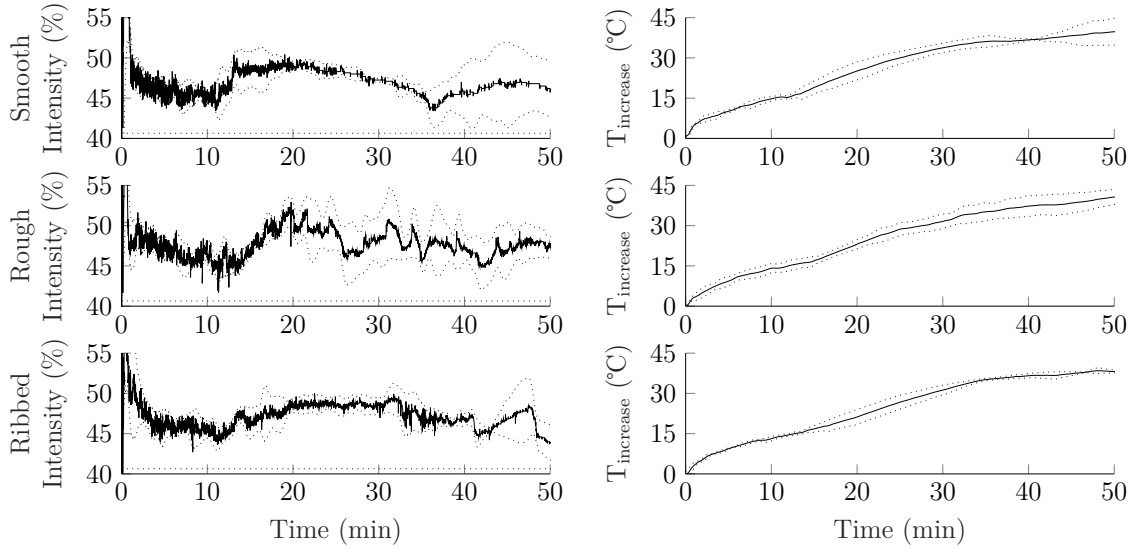


Figure 5-2: Average (of three) intensity and temperature profiles for smooth, rough, and ribbed vessel surfaces. Glass microbeads 62 % v/v, DEHA 19 % v/v, HTPB 19 % v/v, 1000 mbar pressure. Horizontal lines - equivalent RBM profiles. Standard deviations shown.

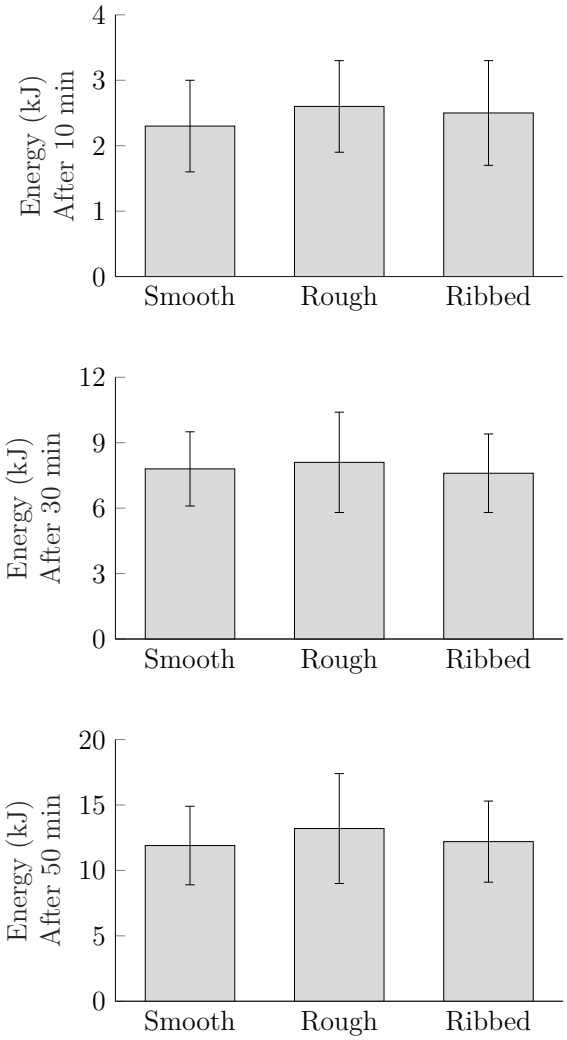


Figure 5-3: Bar graphs showing the average energy (mechanical method) uptake for mixing in smooth, rough, and ribbed ABS vessels up to 10, 30 and 50 minutes over triplicate measurements. Glass microbeads 62 % v/v, DEHA 19 % v/v, HTPB 19 % v/v, 50 G acceleration, 1000 mbar pressure. Standard deviations shown.

## Conclusions

The aim of this work was to assess the effects of changing surface variables on mixing efficiency, with respect to surface finish. Differing the surface finish was not found to affect mixing efficiency within the error of the experiment, however this was likely due to the absence of vacuum application inhibiting bulk flow. Plastic 3D printed vessels are concluded to be unsuitable for mixing, at least in the format presented here, due to their inability to hold vacuum. A surface profile comparison experiment undertaken with vacuum is recommended as future work.

## References

[1] M. Andrews, C. Collet, A. Wolff, and C. Hollands. ResonantAcosutic Mixing Processing and Safety. Munitions Safety Information Analysis Center, May 2019.

[2] A.J. Claydon. *Resonant Acoustic Mixing of Polymer Bonded Explosives*. PhD thesis, Cranfield University, 2020. Paper 1.

[3] A.C. Hordijk and A.E.D.M. van der Heijden. Mixing. In *Energetic Materials; Particle Processing and Characterization*. Wiley-VCH Verlag GmbH, 2005.

[4] P.A. Lucon, G. Sperry, and J. Whaley. RAM Mixing of Liquids and Pastes. Resodyn Technical Interchange, Butte, Montana, USA, 2016.

[5] P.A. Lucon and J. Whaley. Liquids and Pastes. Resodyn Technical Interchange, Butte, Montana, USA, 2016.

[6] P.A. Lucon. Mixing with Vacuum Assist. Resodyn Technical Interchange, Butte, Montana, USA, 2016.

[7] E.L. McCloy, P. Wilkinson, and P.P. Gill. Resonant Acoustic Mixing: Pushing The Boundaries. Master's thesis, Cranfield University, 2016.

[8] H.A. Barnes. A review of the slip (wall depletion) of polymer solutions, emulsions and particle suspensions in viscometers: its cause, character, and cure. *J. Non-Newton Fluid*, 56:221–251, 1995.

[9] M. Cloitre and R.T. Bonnecaze. A review on wall slip in high solid dispersions. *Rheol Acta*, 56:283305, 2017.

[10] J-M. Piau, N. Kissi, and A. Mezghani. Slip flow of polybutadiene through fluorinated dies. *J. Non-Newton Fluid*, 59:11–30, 1995.

[11] A.J. Claydon. *Resonant Acoustic Mixing of Polymer Bonded Explosives*. PhD thesis, Cranfield University, 2020. Paper 4.

[12] C. Nickerson and J. Kornfield. A novel "cleat" geometry for suppressing wall slip. *J. Rheol.*, 49:865874, 2005.

[13] V. Mansard, L. Bocquet, and A. Colin. Boundary conditions for soft glassy flows: slippage and surface fluidization. *Soft Matter*, 10:69846989, 2014.

[14] R. Buscall, J.I. McGowan, and A.J. Morton-Jones. The rheology of concentrated dispersions of weakly attracting colloidal particles with and without wall slip. *J. Rheol.*, 37:621641, 1993.

[15] T.G. Mason, J. Bibette, and D.A. Weitz. Yielding and flow of monodisperse emulsions. *J. Colloid Interface Sci.*, 79:439448, 1996.

[16] S.P. Meeker, R.T. Bonnecaze, and M. Cloitre. Slip and flow of soft particle pastes. *Phys. Rev. Lett.*, 92:198302, 2004.

[17] S.P. Meeker, R.T. Bonnecaze, and M. Cloitre. Slip and flow in pastes of soft particles: direct observation and rheology. *J. Rheol.*, 48:12951320, 2004.

[18] T. Gibaud, C. Barentin, and S. Manneville. Influence of boundary conditions on yielding in a soft glassy material. *Phys. Rev. Lett.*, 101:258302, 2008.

[19] P. Lettinga and S. Manneville. Competition between shear banding and wall slip in wormlike micelles. *Phys. Rev. Lett.*, 103:248302, 2009.

[20] A. Magnin and J.M. Piau. Cone-and-plate rheometry of yield stress fluids. Study of an aqueous gel. *J. Non-Newton Fluid*, 36:85108, 1990.

[21] S.A. Gulmus and U. Yilmazer. Effect of volume fraction and particle size on wall slip in flow of concentrated suspensions. *J. Appl. Polym. Sci.*, 98:439448, 2005.

[22] D.M. Kalyon, P. Yaras, B. Aral, and U. Yilmazer. Rheological behavior of a concentrated suspension: a solid rocket fuel stimulant. *J. Rheol.*, 37:3563, 1993.

[23] B.K. Aral and D.M. Kalyon. Effects of temperature and surface roughness on time-dependent development of wall slip in steady torsional flow of concentrated suspensions. *J. Rheol.*, 38:957972, 1994.

[24] S.V. Kao, L.E. Nielsen, and C.T. Hill. Rheology of concentrated suspensions of spheres I. Effect of the liquid-solid interface. *J. Colloid Interface Sci.*, 53:358366, 1975.

[25] S. Marze, D. Langevin, and A. Saint-Jalmes. Aqueous foam slip and shear regimes determined by rheometry and multiple light scattering. *J. Rheol.*, 52:10911111, 2008.

[26] R. Besseling, L. Isa, E.R. Weeks, and W.C.K. Poon. Quantitative imaging of colloidal flows. *Adv. Colloid Interf. Sci.*, 146:1–17, 2009.

[27] S.A. Khan, C.A. Schnepper, and R.C. Armstrong. Foam rheology: III. Measurement of shear flow properties. *J. Rheol.*, 32:6992, 1988.

[28] P. Coussot, Q.D. Nguyen, H.T. Huynh, and D. Bonn. Avalanche behavior in yield stress fluids. *Phys. Rev. Lett.*, 88:175501, 2002.

[29] J.M. Piau. Carbopol gels: elastoviscoplastic and slippery glasses made of individual swollen sponges: meso- and macroscopic properties, constitutive equations and scaling laws. *J. Non-Newton Fluid*, 144:1–29, 2007.

[30] T. Divoux, D. Tamarii, C. Barentin, S. Teitel, and S. Manneville. Yielding dynamics of a HerschelBulkley fluid: a critical-like fluidization behaviour. *Soft Matter*, 8:41514164, 2012.

[31] F. Ahonguio, L. Jossic, and A. Magnin. Influence of slip on the flow of a yield stress fluid around a flat plate. *AIChE J.*, 62:1356–1363, 2016.

[32] J.T. Black and R.A. Kohser. *Materials and Processes in Manufacturing, Tenth Edition*. John Wiley & Sons, Inc., 2008.

[33] A. Vandenberg and K. Wille. Evaluation of resonance acoustic mixing technology using ultra high performance concrete. *Constr. Build. Mater.*, 164:716–730, 2018.

[34] A.J. Claydon. *Resonant Acoustic Mixing of Polymer Bonded Explosives*. PhD thesis, Cranfield University, 2020. Paper 2.

[35] A.J. Claydon. *Resonant Acoustic Mixing of Polymer Bonded Explosives*. PhD thesis, Cranfield University, 2020. Paper 3.

[36] J.G. Osorio and F.J. Muzzio. Evaluation of resonant acoustic mixing performance. *Powder Technol.*, 278:46–56, 2015.

[37] T.G. Yew, P.P. Gill, and P. Wilkinson. Process Parameters for Resonant Acoustic Mixers (RAM). Master's thesis, Cranfield University, 2015.

[38] H. Howe, J. Warriner, A. Cook, S. Coguill, and L. Farrar. Apparatus and Method for Resonant Vibratory Mixing. Patent US 7188993 B1, March 2007.

[39] A.N. Patil and P.P. Gill. Resonant Acoustic Mixing  The Future of Propellant Manufacturing. Master's thesis, Cranfield University, 2018.

[40] D.E. Packham. Roughness and adhesion. In *Handbook of Adhesion, Second Edition*. John Wiley & Sons, Ltd., 2005.

# Appendices

Table 5-A1: Cooling constants for each of the vessels when filled with 65 mL of the formulation.

| Vessel type | $k$ ($min^{-1}$) |
|---|---|
| ABS (Smooth) | 0.02149 |
| ABS (Rough) | 0.02229 |
| ABS (Ribbed) | 0.02219 |

Table 5-A2: Mixing statistics for the surface finish comparison.

| | Time (min) | 10 | 30 | 50 |
|---|---|---|---|---|
| Smooth | Energy (Mechanical, kJ) | 2.3±0.7 | 7.8±1.7 | 11.9±3.0 |
| | Energy (Electrical, kJ) | 1.4±0.4 | 4.7±1.0 | 7.1±2.2 |
| | Energy (Thermal, kJ) | 2.7±0.1 | 7.5±0.4 | 10.7±1.8 |
| Rough | Energy (Mechanical, kJ) | 2.6±0.7 | 8.1±2.3 | 13.2±4.2 |
| | Energy (Electrical, kJ) | 1.5±0.4 | 4.9±1.4 | 7.9±2.5 |
| | Energy (Thermal, kJ) | 2.6±0.3 | 6.9±0.6 | 10.8±0.8 |
| Ribbed | Energy (Mechanical, kJ) | 2.5±0.8 | 7.6±1.8 | 12.2±3.1 |
| | Energy (Electrical, kJ) | 1.5±0.5 | 4.6±1.1 | 7.3±1.8 |
| | Energy (Thermal, kJ) | 2.4±0.1 | 6.8±0.4 | 10.2±0.3 |

# Paper 6 - The Effect of Mixing 'In-situ' on the Tensile Properties of Resonant Acoustic Mixed Polymer Bonded Explosives

Andrew J. Claydon, Guillaume Kister, Sally Gaulter, and Philip P. Gill

**Abstract:** A method for mixing samples of Polymer Bonded eXplosive (PBX) simulants 'in-situ' (whereby the final casing of the PBX doubles as the mixing vessel) is developed on the laboratory scale (155 mL), using Resonant Acoustic Mixing (RAM). Ammonium sulphate is used as an inert simulant for high explosives. Uniaxial tensile testing is used to compare differences between samples that are 'mixed and cast' and mixed 'in-situ', by determining the variation in elastic modulus and elongation at break. In this case, it is shown that the product outcome is statistically the same irrespective of the processing method used. However, solid settling occurred in all samples during curing, and is likely to have masked any differences in packing arrangement that may have been present between the two processing techniques. Also observed in the samples was a layering effect, whereby a lower modulus and higher elongation at break was apparent further down each sample, likely due to particle size segregation during solid settling. A repeat of the experiment using an optimised formulation that does not exhibit settling should be undertaken as future work, and incorporate a more diverse range of testing methods.

**Keywords:** Resonant Acoustic Mixing, Polymer Bonded eXplosive, In-situ mixing, Casting

## Introduction

Polymer Bonded eXplosives (PBXs) are explosive composites which comprise of a granular high explosive dispersed phase bound by a polymeric continuous phase. In the case of PBXs that are cast-cured, the binder is an elastomeric thermosetting polymer, commonly hydroxy-terminated polybutadiene (HTPB) pre-polymer crosslinked with an isocyanate such as isophorone diisocyanate (IPDI) to form a urethane. The manufacturing process of such PBXs first requires the components (explosive crystals, pre-polymer, curative, plasticiser and other additives) to be thoroughly mixed to form a homogeneous suspension, which can then be vacuum cast into a mould to cure. While mixing is conventionally performed in a high shear mixer, such as the commonly used z-blade and planetary mixers, there is now considerable interest[1] in the use of Resonant Acoustic Mixing (RAM) to perform this task. Consisting of a vibrating platform (∼60 Hz, up to 100 G acceleration) as opposed to mechanical blades to agitate the mixture, a major advantage of RAM is the possibility of mixing 'in-situ',[a] whereby the mixing vessel and intended receptacle are one and the same.[2] This brings many potential benefits to PBX manufacture, such as the possibility to formulate novel high viscosity PBXs that would otherwise be impractical to cast. 'In-situ' mixing also has advantages over conventional mixing when considering current-use castable formulations, mainly due to the elimination of cleaning requirement and associated explosive waste (constituting 12.5 % of batched mixed product on industrial scale[3]). This reduces both the hazard posed to workers and the environmental impact of explosive waste disposal by open burning.

Several differences may be apparent when comparing the properties of an 'in-situ' mixed PBX to those of a 'mixed and cast' PBX. For example, casting into a mould has the potential to fold air bubbles back into a degassed formulation. It is therefore possible that an RAM mixed PBX that is not pour cast after degassing will contain fewer air bubbles, particularly since mild stimulation from the mixer can assist in liberating entrapped gas.[4] It is also possible that the packing arrangement may become less dense, resultant of changes in particle orientation during the pouring process.[5] It has previously been reported that non-spherical particles align their longitudinal axis with the direction of flow when mould filling,[6] and explosive crystals are indeed well known to be anisometric to varying degrees.[7] Conversely, it is surmised that a denser packing arrangement will be achieved immediately after the

[a] Also referred to as mixing 'in-case'.

mixture is vibrated in the RAM process, in a similar manner to the way dry powders settle more closely together after vibration.[8] Packing arrangement (thus volume fraction to maximum volume fraction ratio) would be expected to influence the mechanical properties of the material, as approximated for highly loaded composites by Equation 6-1.[9–13]

$$E = E_0 \left(1 - \frac{\phi}{\phi_{max}}\right)^{-2} \qquad \text{(Equation 6-1)}$$

where $E$ is the elastic modulus ( MPa), $E_0$ is the elastic modulus of the continuous phase ( MPa), $\phi$ is the volume fraction of the solid (dimensionless), and $\phi_{max}$ is the maximum volume fraction for the particle shape and size distribution under consideration (dimensionless). By increasing $\phi$ to a value closer to $\phi_{max}$, it can be seen that the elastic modulus of the composite will increase.

The aim of this work is to compare the mechanical (tensile) properties of an inert PBX formulation that has been mixed 'in-situ' to those of the formulation 'mixed and cast'.

## Experiment

An ad hoc technique for lab-scale PBX sample production 'in-situ' was devised, and consisted of off-the-shelf polyethylene terephthalate (PET) jars (Figure 6-1) which could be placed into a slightly larger hermetically sealable polycarbonate (PC) vessel (Figure 6-2). This was then affixed to the vibrating plate of a LabRAM (LabRAM 'B' as characterised in previous work[14]). The internal diameter of the jars was 71 mm and the internal height was 73 mm. The internal dimensions of the PC vessel (with lid) closely matched the external dimensions of the PET jars, holding them securely in place without the need for clamping or adhesives. A rod thermocouple was inserted slightly off-centre through an air-tight portal in the lid, which also had vacuum and pressure sensor outlets. The lid was of custom design and PEEK[b] construction, and was secured to the PC vessel with a clamshell clamp (Figure 6-2). The enclosed system was such that vacuum could be applied to the mixture down to approximately 100 mbar. Since the jars were inexpensive and readily available, they could be treated as expendable.

Since only the mechanical properties of the composite were of interest, an inert

[b] Polyether ether ketone

Figure 6-1: PET jar

Figure 6-2: PC vessel

filler was used instead of live explosives. This meant the experiment could be carried out without the requirement for specialist facilities and safety considerations. In the author's previous work,[14–17] where the factors that affect mixing efficiency were studied, glass beads were chosen as the filler on account of their approximation of hard spheres, providing an idealised model suspension. However, glass beads would be unsuitable for this work since the effects of anisometric (i.e. non-spherical) particle alignment is one of the factors of interest. A milled crystalline filler was therefore chosen instead, with ammonium sulphate (AS, Merck, UK) selected on account of its density ($1.77\,\mathrm{g\,cm^{-3}}$) being close to that of RDX[c] high explosive ($1.82\,\mathrm{g\,cm^{-3}}$).

DEHA[d] plasticiser ($\geq$ 97 %, Merck, UK), HTPB binder (type Poly bd® R-45HTLO, Cray Valley, USA), and IPDI curative ($\geq$ 99 %, Merck, UK) formed the continuous phase. Raw materials were kept in a desiccator prior to use, and an isocyanate curing ratio of 1.05 was used to remove any remaining traces of water. The ammonium sulphate was milled and sieved to conform the nominal values of the 'Class 1' industry standard RDX granulation, as shown in Table 6-1. The filler was first weighed into the mixing vessels, followed by the plasticiser, isocyanate and binder. The formulation is given in Table 6-2, where at total of 155 mL was used for each mix.

[c] 1,3,5-trinitro-1,3,5-triazinane
[d] di(2-ethylhexyl) adipate, commonly known as DOA

Table 6-1: Specification for NATO standardised 'Class 1' particle size distribution for RDX.[18]

| Opening (µm) | % Through |
|---|---|
| 850 | 98 ± 02 |
| 300 | 90 ± 10 |
| 150 | 60 ± 30 |
| 75 | 25 ± 20 |

Table 6-2: The inert formulation used for the experiment.

| | AS | DEHA | HTPB | IPDI |
|---|---|---|---|---|
| Volume (%) | 66.00 | 17.00 | 15.70 | 1.30 |
| Actual mass (%) | 78.89 | 10.62 | 9.55 | 0.94 |
| RDX equivalent mass (%) | 79.35 | 10.39 | 9.34 | 0.92 |

The mixer was controlled at set 'intensity' setting, which refers to the percentage of electrical current supplied to the driver motor up to the maximum (5 A for the LabRAM mixer unit used). Set 'intensity' as opposed to set acceleration (as used in previous work[14–17]) was chosen here due to the mass of the filled equipment exceeding the stated capacity of the machine (500 g), coupled with the relatively large fill volume requiring a greater power draw than the smaller mixes performed previously. By avoiding fixed acceleration, the tendency for the machine to attempt to draw more power than was available to maintain a set acceleration as mixing progressed was eliminated. Mixing occurred at 90 % intensity for 13 minutes at 550 mbar pressure, during which the average achieved acceleration was approximately 55 G (varying between 80 G and 40 G), and bulk flow was observed. A 13 minute degassing stage followed at ∼100 mbar, initially at 30 % intensity for 7 minutes, then at 20 % and 10 % for 3 minutes each. Low accelerations were achieved during degassing ($< 10$ G), which gently stimulated the mixture (with air bubbles seen rising to the top) without bulk flow being observed.

Six identical mixes of the formulation were carried out, with three being left in their casings to become 'in-situ' samples and three being transferred into empty PET jars by vacuum casting. The casting equipment consisted of a desiccator modified with a glass funnel placed through a rubber bung in the lid. The funnel was heated by an external hot water tube wrapped around it and secured with tape, as shown in Figure 6-3. The stem of the funnel was 80 mm in length and 9 mm in diameter, approximately an order of magnitude greater than that of the largest particles. The

material was placed in the funnel after mixing, and sucked through into an empty container by reducing the pressure in the chamber (Figure 6-4). Casting occurred at a funnel temperature of 50 °C and a chamber pressure of 950 mbar pressure. All samples were then cured in an oven at 60 °C for a week in sealed desiccators, which were purged with nitrogen as an inert atmosphere.

The cured samples of material were sliced laterally using a bandsaw, with ~15 mm thick slabs taken from the uppermost and lowermost portions. CNC milling (Syil X3 CNC, spindle speed 1750 rpm) was then used to prepare tensile samples, with a 20 mm diameter 2 flute slot drill used for cutting. Material was first skimmed from both sides of each slab, smoothening the surfaces and reducing the thickness to the desired value (10 mm). The slabs were held in place with a vacuum chuck. Reduced size tensile specimens (Figure 6-5) based on the larger 'PERME C' geometry (Figure 6-6) were then milled from the slabs (Figure 6-7). The radius of the drill was chosen to match that of the curves in the samples. A lateral feed rate of 60 mm $min^{-1}$ was used, and the tool was lowered in steps of 0.5 mm, with an outline cut being made after each increment.

PC end tabs (30 mm by 30 mm, 10 mm thick) were then glued to the ends of the tensile specimens with structural epoxy (Araldite 2011), and attached with metal pins to a Zwick 1445 tensile testing machine (Figure 6-8, 10 kN capacity load cell). Elongation occurred at room temperature at a rate of 50 mm $min^{-1}$.

Figure 6-3: Heated funnel

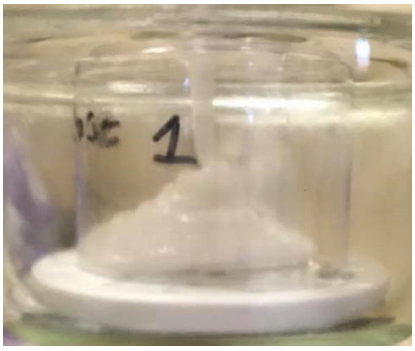


Figure 6-4: Casting

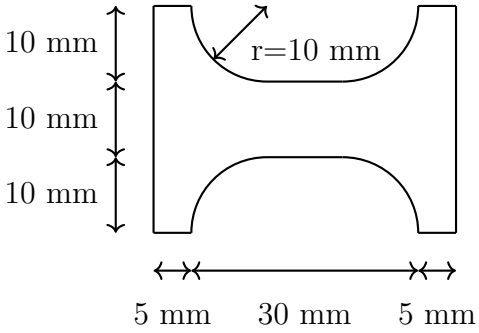


Figure 6-5: Geometry of the tensile specimens used, where the depth of the sample is 10 mm.

.

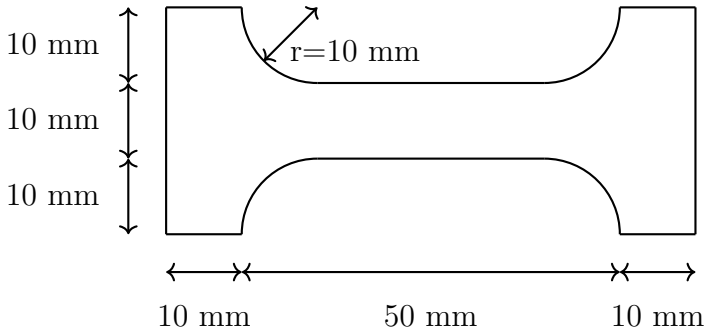


Figure 6-6: Geometry of a 'PERME C' tensile specimen, where the depth of the sample is 10 mm

.

Figure 6-7: CNC milling

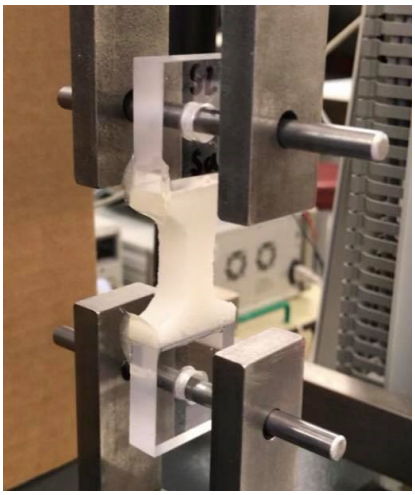

Figure 6-8: Tensile testing

## Results and discussion

The results are shown in Figure 6-9, where it can be seen that average values for the modulus and elongation at break over the three mixed 'in-situ' and three 'mixed and cast' samples show no statistical difference. This suggests that overall, the processing method had no measurable bearing on the average properties of the material.

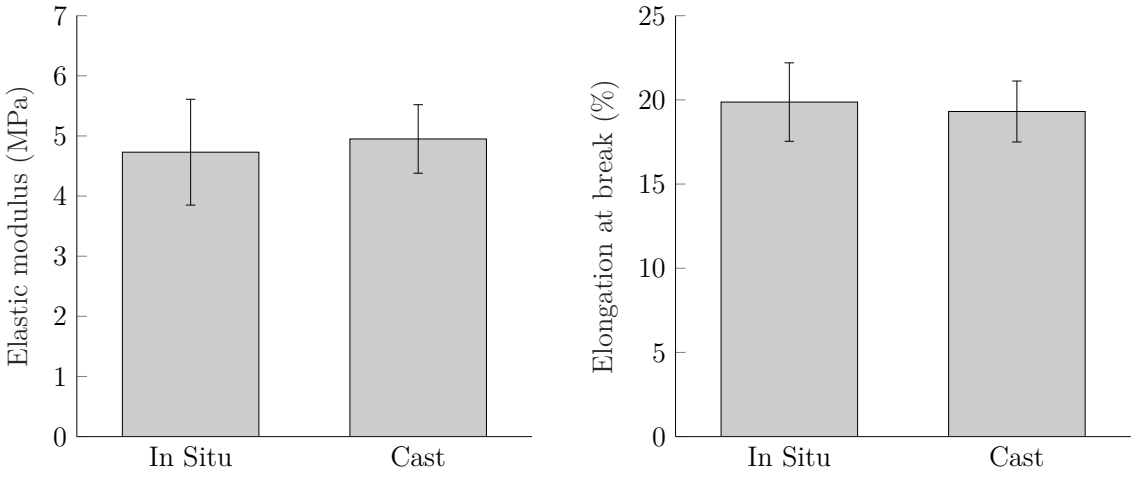


Figure 6-9: The modulus and elongation at break for samples mixed 'in-situ' and 'mixed and cast'. Each bar represents average values taken across six measurements (three samples per processing method, one upper and one lower specimen per sample). Standard deviations shown.

A possible reason for no differences being apparent may have been solid settling during curing. Settling was observed to have occurred, with a binder-only layer approximately 1 mm thick being present the top of each sample. These layers were discarded when slicing the material with the bandsaw. Since settling would considerably change the packing arrangements of the composites from their state immediately after processing ('in-situ' mixing or casting), it is likely that any subtle differences resultant of the processing techniques were lost. The full dataset is given in appendices (Table 6-A1).

Average values for the elastic modulus and elongation at break of specimens taken from each portion of the mixed 'in-situ' and 'mixed and cast' samples are shown in Figure 6-10. Interestingly, it can be seen that in all cases there was a reduction in modulus and increase in elongation at break the further down each sample the tensile specimens were taken from. These differences can also be seen in Figure 6-11, which shows a comparison of engineering tensile stress-stain curves

representative of specimens taken from the upper and lower portions of both mixed 'in-situ' and 'mixed and cast' samples. It is clear that the specimens from the lower portions have a more shallow gradient during their linear portion (lower modulus) and break at a greater strain. This would suggest that a structured layering effect is occurring between the upper-most and lower-most portions of the samples.

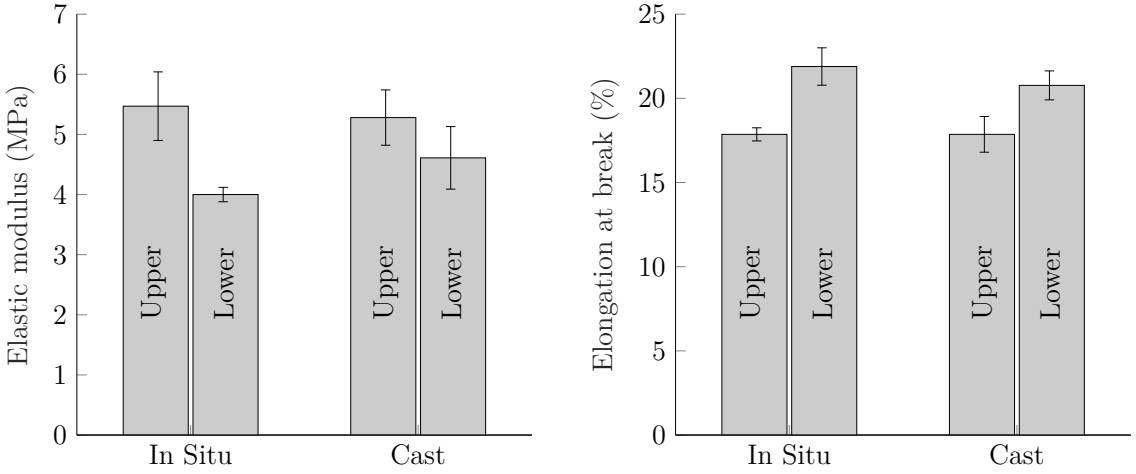


Figure 6-10: The modulus and elongation at break for samples mixed 'in-situ' and 'mixed and cast'. Each bar represents average values for the three upper or three lower specimens taken for each processing method respectively. Standard deviations shown.

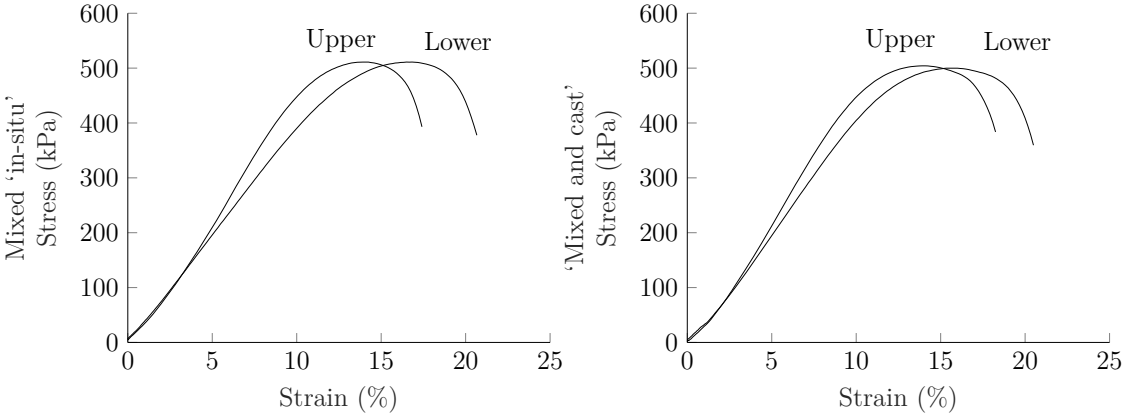


Figure 6-11: Comparison of stress-strain curves for specimens taken from the upper and lower portions of a PBX simulant that was mixed 'in-situ' (left) and 'mixed and cast' (right).

Of intrigue is the method by which the modulus would reduce and elongation at break would increase further down the samples. Higher packing density resultant of closer solid settling in the lower portion than the upper portion would be expected to have the opposite effect since there would be less binder to accommodate the

deformation. An initial explanation was that settling of the higher density plasticiser component towards the lower portions (specific gravities: DEHA - 0.925, HTPB - 0.901) would result in a lower cross-link density further down the samples, thus an increase the rubbery characteristic. However, this theory could quickly be eliminated since it is known that HTPB and DEHA are fully miscible.[19] A far more likely explanation is that particle size segregation accompanied the solid settling, with larger particles (which have greater weight) sinking lower down in the composite, stratifying particle size distribution. Snabre *et al*[20] showed that size segregation of this nature occurs even when the variation in particle size is small (i.e. quasi-monodisperse suspensions). Such variations in particle size distribution would be expected to affect the $\phi/\phi_{max}$ ratio, thus the elastic modulus, further down the samples.

Additional experiments such as density analysis and x-ray computed tomography (CT) scanning should be undertaken as future work to determine to what extent the packing arrangement and particle size distribution changes within individual samples and between the processing techniques, both when settling occurs and when the formulation is optimised. X-ray CT should particularly be employed in the latter case to determine to what extent entrapped air (bubbles) may be present between the two processing techniques.

## Conclusions

The aim of this work was to compare the mechanical properties of an inert PBX mixed when 'in-situ' to when 'mixed and cast'. No statistically significant differences in elastic modulus and elongation at break were observed overall, though any differences that may have been apparent were likely masked by solid settling during curing. Settling is also likely responsible for a layering effect occurring within the samples, whereby decreased modulus and increased elongation at break lower down the samples is apparent. The experiment should be repeated with an optimised formulation that does not settle during curing to address the original aim of the work, and should be complemented with density analysis and x-ray CT scanning.

## References

[1] M. Andrews, C. Collet, A. Wolff, and C. Hollands. ResonantAcosutic Mixing Processing and Safety. Munitions Safety Information Analysis Center, May 2019.

[2] M.D. McPherson. Propellant and explosives production method by use of resonant acoustic mix process. Patent WO 2009/091430 A1, July 2010.

[3] R.J. Davey, J.M. Wilgeroth, and A.O. Burn. Processing Studies of Energetic Materials using Resonant Acoustic Mixing Technology. BAE Systems Land UK, Glascoed, Monmouthshire, UK, 2019.

[4] D. Jubb. Private Communication, Falcon Project Ltd., July 2017.

[5] D. Fossey. Private Communication, Falcon Project Ltd., January 2018.

[6] F. Ramsteiner and R Theysohn. On the tensile behaviour of filled composites. *Composites*, 15:121–128, 1984.

[7] R.J. Hudson, M. Moniruzzaman, and P.P. Gill. Investigation of Crystal Morphology and Shock Sensitivity of Cyclotrimethylenetrinitramine Suspension by Rheology. *Propellants Explos. Pyrotech.*, 40:233–237, 2015.

[8] K.V.S. Sastry, H. Cooper, R. Hogg, T.L.P Jespen, F. Knoll, B.Parekh, R.K. Rajamani, T. Sorenson, I. Wechsler, C. McCleary, and D.B. Todd. Solid-solid operations and equipment. In *Perrys Chemical Engineers' Handbook, Seventh Edition*. McGraw-Hill Pub., 1997.

[9] J.W. Goodwin and R.W. Hughes. *Rheology for Chemists; An Introduction, Second Edition*. RSC Publishing, 2008.

[10] S.H. Maron and P.E. Pierce. Application of Ree-Eyring generalized flow theory to suspensions of spherical particles. *J. Colloid Sci.*, 11:80–95, 1956.

[11] T. Kitano, T. Kataoka, and T. Shirota. An empirical equation of the relative viscosity of polymer melts filled with various inorganic fillers. *Rheol Acta*, 20:207–209, 1981.

[12] D. Quemada. Rheology of concentrated disperse systems and minimum energy dissipation principle. *Rheol Acta*, 16:82–94, 1977.

[13] H.A. Barnes, J.F. Hutton, and K. Walters. *An Introduction to Rheology*. Elsevier Science Publishers, Amsterdam, 1989.

[14] A.J. Claydon. *Resonant Acoustic Mixing of Polymer Bonded Explosives*. PhD thesis, Cranfield University, 2020. Paper 2.

[15] A.J. Claydon. *Resonant Acoustic Mixing of Polymer Bonded Explosives*. PhD thesis, Cranfield University, 2020. Paper 3.

[16] A.J. Claydon. *Resonant Acoustic Mixing of Polymer Bonded Explosives.* PhD thesis, Cranfield University, 2020. Paper 4.

[17] A.J. Claydon. *Resonant Acoustic Mixing of Polymer Bonded Explosives.* PhD thesis, Cranfield University, 2020. Paper 5.

[18] NATO. Explosives, Specification for RDX (Hexogene). STANAG-4022.

[19] H. Abou-Rachid, L Louis-Simon, S. Ringuette, X. Lafleur-Lambert, M. Jaidann, and J. Brisson. On the Correlation between Miscibility and Solubility Properties of Energetic Plasticizers/Polymer Blends: Modeling and Simulation Studies. *Propellants Explos. Pyrotech.*, 33:301–310, 2008.

[20] P. Snabre, B. Pouligny, C. Metayer, and F. Nadal. Size segregation and particle velocity fluctuations in settling concentrated suspensions. *Rheol Acta*, 48:855870, 2009.

# Appendices

Table 6-A1: Full set of tensile properties for samples mixed 'in-situ' and 'mixed and cast'.

| Sample | Specimen | Modulus (MPa) | Elongation at break (%) |
|---|---|---|---|
| Mixed 'in-situ' | Upper | 5.02 | 18.00 |
| Sample 1 | Lower | 3.88 | 22.83 |
| Mixed 'in-situ' | Upper | 5.26 | 17.42 |
| Sample 2 | Lower | 4.01 | 20.66 |
| Mixed 'in-situ' | Upper | 6.12 | 18.16 |
| Sample 3 | Lower | 4.12 | 22.16 |
| 'Mixed and cast' | Upper | 4.81 | 18.66 |
| Sample 1 | Lower | 4.20 | 21.73 |
| 'Mixed and cast' | Upper | 5.73 | 16.66 |
| Sample 2 | Lower | 5.19 | 20.08 |
| 'Mixed and cast' | Upper | 5.29 | 18.25 |
| Sample 3 | Lower | 4.44 | 20.50 |

# Overall Perspective, Conclusions, and Future Work

The primary aim of the research was to better understand the factors affecting the efficiency (time and energy to mix) and product outcome of Resonant Acoustic Mixing for loaded polymers, with the core research question "how can RAM be optimised to maximise its benefits?". The following chapter will discuss the findings of the work in a wider perspective, present an industry guide of how to best implement RAM for next generation PBX ('PBneXt') manufacture, and state the overall conclusions and recommendations for future work.

## Summary of findings

Objective 1: To determine the current state of understanding with regards to the factors affecting PBX mixing efficiency with RAM, and identify the research gaps.

- Churning was identified from previous work[1–4] as the most effective movement mode for mixing of viscous suspensions.
- Reduced wall slip[5] and increased movement[1–4, 6] in the material are required for more effective churning.
- Variables relating to the machine, vessel, and formulation can be modified to improve the efficiency of churning (summarised in Table D-2).

Objective 2: To develop a robust methodology to assess RAM efficiency by determination of the end of mix time and the energy supplied up until that point.

- End of mix can be determined by the interpretation of mixer intensity profiles (Paper 2 - Efficiency Determination).
- Profile features can be resultant of rheology changes due to 'mixedness' and temperature changes (Paper 2 - Efficiency Determination).

- Different methods (based on mechanical, electrical, and thermal monitoring) to determine energy consumption generally give the same trend at the same order of magnitude (Paper 2 - Efficiency Determination).

Objective 3: To further the understanding of the effects mixing variables regarding the machine and mixing vessel have on RAM efficiency.

- There can be considerable variations/calibration errors between mixer models and units, resulting in considerable differences in inertial force thus mixing behaviour (Paper 3 - Machine Variables).
- Increasing acceleration by only 5 G (from 50 G to 55 G) can decrease mixing time by 43 % (Paper 3 - Machine Variables).
- Avoiding a low surface free energy vessel wall (PTFE[a]) can decrease mixing time by 17 % (Paper 4 - Vessel Material).
- The use of vessel surfaces with a roughness average akin to the particle size may improve mixing, though additional experiments are required to confirm this (Paper 5 - Surface Finish).
- Partial vacuum application is required for effective churning since it allows for the formation of a large velocity gradient across the mixture (Paper 5 - Surface Finish).

Objective 4: To investigate how product outcome may vary when a formulation is mixed 'in-situ' as opposed to 'mixed and cast'.

- Mixing 'in-situ' was not found to alter mechanical (tensile) properties within the error of the experiment undertaken (Paper 6 - Mixing 'In-situ').
- Solid settling can occur during curing, and is likely responsible for rearranging the packing arrangement such that differences between processing techniques are masked (Paper 6 - Mixing 'In-situ').
- Highly optimised formulations should be used to investigate differences in product outcome between processing techniques (Paper 6 - Mixing 'In-situ').

Objective 5: To discuss the expected impacts of the findings with regards to 'PB-neXt' implementation.

[a] poly(tetrafluoroethylene), Teflon$^{TM}$

- Mixing 'in-situ' is found to have the best potential for 'PBneXt' manufacture due to there being no restriction on viscosity, allowing for formulations with increased solid loading and reduced plasticiser content, thus improved performance, mechanical, safety, and ageing properties (Paper 1 - Literature Review).
- Rubber liners (higher surface free energy) are expected to be preferable to non-stick coatings (low surface free energy) for the purposes of mixing munitions 'in-situ' (Paper 4 - Vessel Material).
- Roughened surface vessels may be better suited to mixing 'in-situ' as opposed to batch mixing, as they may be difficult to clean (Paper 5 - Surface Finish).

## Overall perspective

### Linking the factors affecting efficiency

Throughout the work, machine variables (acceleration/intensity setting, mixer unit, mixer model) and vessel variables (vessel material and surface finish) were separately investigated with regards to mixing efficiency. Here, the findings are reconciled with each other, literature observations, and conjecture to provide a better understanding of how the parameters affect the movement mode of the material, thus the efficiency of mixing. Since the surface roughness comparison (Paper 5 - Surface Finish) gave a null result due to the experimental set-up, it is discussed here in a theoretical context.

The literature review found that the desired churning movement (responsible for shear generation) is based on the requirement for a velocity gradient to extend across the material, whereby material at the interface with the vessel wall has a lower velocity (ideally no-slip at the vessel wall), and material further towards the centre of the vessel has a higher velocity. It follows that by increasing movement or reducing wall slip, the velocity gradient (thus shear) will increase, and churning will become more intense. A summary of the conditions determined to be of importance are given in Table D-1, and the variables reported (or hypothesised) to determine the conditions summarised in Table D-2. A chart relating all the factors listed in Table D-1 and Table D-2 and their interdependence is given in Figure D-1, and is based on the observations made throughout this thesis, the observations reported in the literature, and conjecture.

Table D-1: The salient factors affecting the efficiency of churning.

| | Reduces wall-slip | Increases movement |
|---|---|---|
| Physical | | Higher acceleration<br>Higher density<br>-Greater inertial forces |
| | Higher viscosity formulation<br>-Greater interfacial drag<br>-Greater tackiness | Lower viscosity formulation<br>-Greater compliance |
| | Smaller diameter vessel<br>Optimised roughness average<br>-Greater interfacial drag | Larger diameter vessel<br>-Greater compliance |
| | | Vacuum application<br>-Greater inertial forces<br>-Greater compliance |
| Chemical | Lower surface tension<br>Higher surface free energy<br>-Greater spreadability | Lower surface tension<br>-Greater compliance |
| Other | | Mixer calibration<br>-Greater inertial forces |

Table D-2: Machine variables, vessel variables, and formulation variables for Resonant Acoustic Mixing.

| Machine variables | Vessel variables | Formulation variables |
|---|---|---|
| Acceleration setting | Vacuum setting | Binder content |
| Intensity setting | Wall material | Plasticiser content |
| Mixer model | Wall surface finish | Additives |
| Mixer unit | Diameter | Solids loading |
| | Insulation | Particle shape |
| | Active heating | Filler type |
| | Active cooling | |

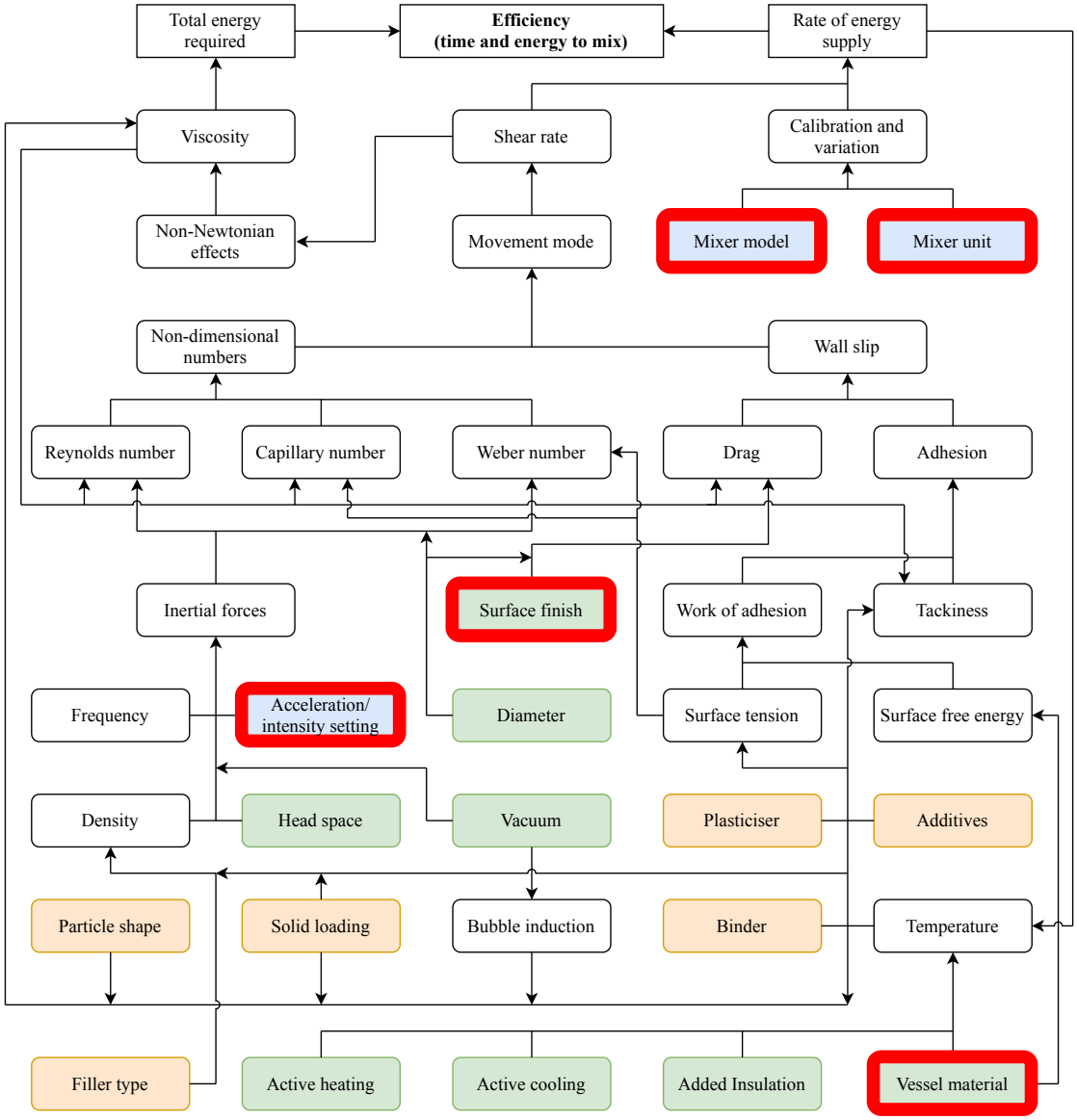


Figure D-1: Chart linking the factors believed to affect mixing efficiency, and their interdependence. Highlighted red are the factors investigated in this thesis. Coloured cells indicate: blue - machine variables, green - vessel variables, orange - formulation variables.

**Greater surface free energy** was expected[7] to reduce slip, since the spreadability of the binder on the vessel wall would be greater. This was supported by the thesis (Paper 4 - Vessel Material), where greater spreadability (brought about by using a vessel material with higher surface free energy) was correlated to improved mixing efficiency, in agreement with anecdotal reports from industry.[5] Spreadability can also be modified by changing the surface tension, which has a reliance on the contents of the formulation (i.e. surfactant additive addition). This should be further explored in future work. **Greater interfacial drag** was expected to reduce slip at the interface by slowing the formulation down at the wall. This was attempted to be achieved using roughened surfaces, which were expected[8, 9] to interact more directly with the bulk of the material (Paper 5 - Surface Finish, null result due to the experimental set-up). Drag may also be increased by reducing the vessel diameter[2] (higher surface area to volume ratio) and modifying the formulation, for example with higher viscosity binders.[10] **Greater tackiness** was also hypothesised (Paper 1 - Literature Review) to reduce wall slip, where tackiness is a viscoelastic property that determines contact adhesiveness and 'stickiness'.[11] Tack could be modified by changing the formulation, perhaps with the use of additives such as tackifying resins, and should be subject of future work.

**Greater inertial forces** were known to affect the amount of movement within the material, where higher Reynolds number (describing the relative importance of deforming inertial forces and resisting viscous forces) had been found to improve mixing.[6] By increasing the acceleration/intensity setting (thus inertial force), mixing time was found in this thesis to decrease (Paper 3 - Machine Variables). Application of vacuum (pressure reduction in the head space, see Paper 1 - Literature Review) was also found to result in high intensity churning (bulk motion), that was not apparent when vacuum was not used (Paper 5 - Surface Finish). Surprisingly, machine model and unit were also found to affect mixing. This was suspected to be due to variation and calibration errors providing a higher rate of energy supply to the material on some machines. **Greater compliance** was used to describe the effects of lower viscosity, lower surface tension, vacuum application (bubble induction, see Paper 1 - Literature Review), and larger diameter (lower surface area to volume ratio), where increasing compliance described making the material easier to move. With regards to non-dimensional numbers, greater compliance due to lower viscosity increases the Reynolds number, whereas greater compliance due to lower surface tension increases the Weber number (describing the relative importance of deforming inertial forces and resisting surface tension forces). Capillary number

describes the relative importance of Reynolds and Weber number, with it being calculated (Paper 1 - Literature Review) that Reynolds number is by far of greatest importance for PBX mixing due to the high viscosities and low surface tensions involved. However, Weber number may be of more importance when mixing low viscosity, high surface tension liquids/suspensions (i.e. water) where the movement mode is splashing, thus is included in Figure D-1 for completeness.

Perhaps the most important factor shown in Figure D-1 is movement mode, since it is this that determines the amount of shear (thus mixing) that occurs. Figure D-2 gives a graphical indication of how the movement mode of the material likely depends on the wall slip and movement of the material. For a material that is churning with an arbitrary intensity (say, the origin of Figure D-2), the velocity gradient will increase if wall slip is reduced[5] (Paper 4 - higher surface free energy, Paper 5 - optimised roughness average) and/or the material moves more vigorously (Paper 3 - higher acceleration/intensity setting, correctly calibrated machines), and the churning will become more intense. This is reflected in the non-dimensional numbers, with increased Reynolds number[6] being by far the most important for PBX mixing (see Paper 1 - Literature Review). However, if the material becomes too compliant or inertial forces become great enough (Reynolds number becomes too high), there will likely be a transition from laminar to turbulent flow and the movement mode will be splashing. This will probably happen regardless of whatever wall slip may be present. Reducing the amount of movement by reducing the compliance (i.e. making the material harder to deform, reducing Reynolds number[6]) will eventually result in quiescence (no motion) if wall slip is negligible, or decoupled movement (bouncing as a cohesive lump) if there is sufficient slip. Reducing the amount of movement by reducing inertial forces would eventually result in quiescence (no motion).

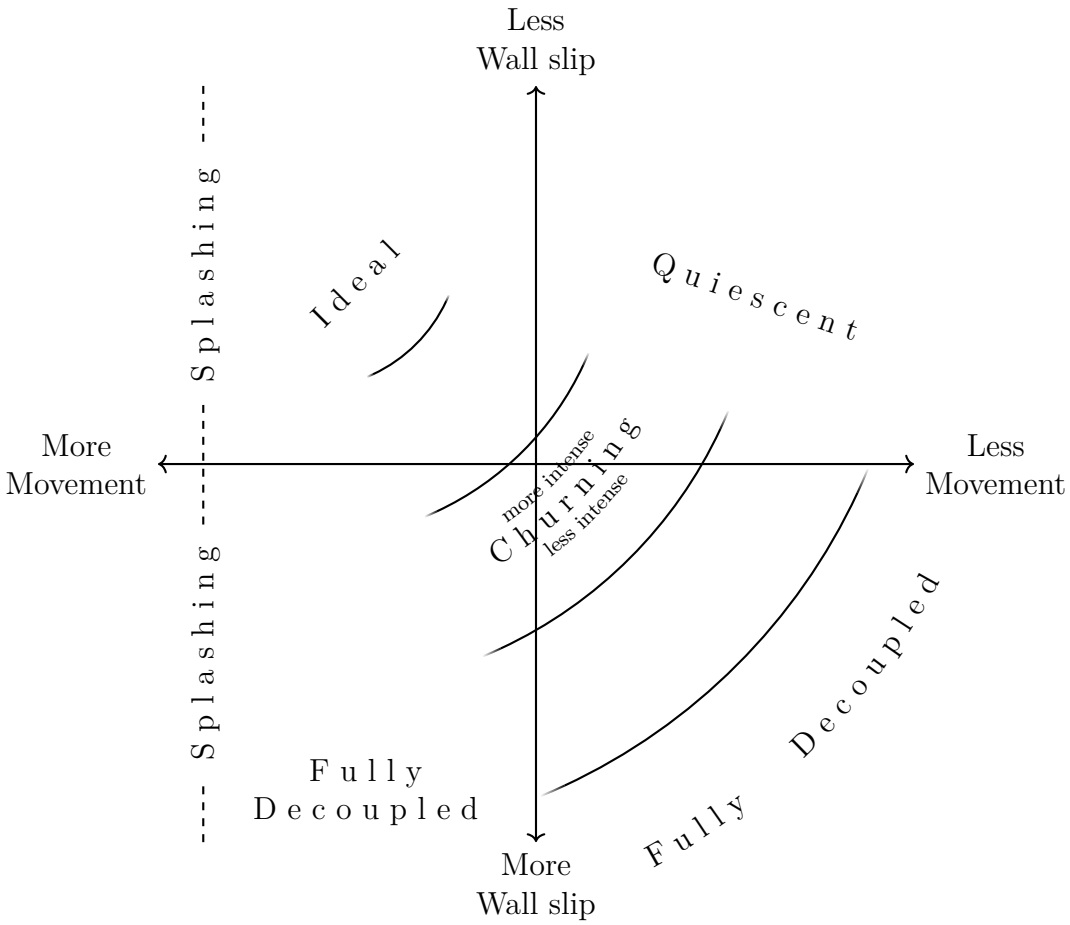


Figure D-2: Graphic of mixing mode dependence on wall slip and movement.

### End of mix determination

The movement mode, thus shear rate, present at any particular point in mixing evolution will determine the rate of energy supply. Energy supply rate is then reflected in the power draw of the machine, thus the mixer 'intensity' readout upon which the intensity profiles analysed throughout the thesis are based. The thesis has found that by interpreting intensity profiles, the changing shear rate, thus movement mode (decoupled, low intensity churning, high intensity churning - bulk motion), thus material properties (i.e. viscosity - related to 'mixedness' and temperature, see Paper 2 - Efficiency Determination) could be monitored. By correlating profile features to rheological data, the end of mix point could be determined.

### Energy determination

The total energy required for mixing completion (as interpreted from the intensity profiles) was found using three energy determination methods based on mechanical, electrical, and thermal monitoring (Paper 2 - Efficiency Determination). Generally, each method gave the same trend at the same order of magnitude when variables were changed, for example mixing at higher acceleration required less energy to reach mixing completion with all methods (Paper 3 - Machine Variables). However, the values the methods gave relative to each other (the accuracy of each method) was variable. Determined energies were observed in the order mechanical > electrical > thermal, mechanical > thermal > electrical, and thermal > mechanical > electrical, depending on the mixing stage and experimental set up (LabRAM used, vacuum application, vessel thermal properties). It is therefore advised that the methods be used with caution, and forewarned that they are of limited merit in determining absolute values.

### Mixing 'in-situ'

Mixing 'in-situ' was not found to result in any significant differences in tensile properties to when casting, likely due to solid settling during curing masking any subtle packing arrangement differences that may have been present. The experiment should be repeated with an optimised formulation that does not settle to provide conclusive results either way. In a theoretical context, differences in material properties between the processing methods may have both advantages and disadvantages. For example, while a higher packing density when mixing 'in-situ' may improve performance, current formulations may have to be re-optimised (i.e. some binder

removed) to account for the difference. Conversely, this would not be required if the product outcome was the same. Furthermore, the same product outcome would allow for flexibility in the processing method, whereby either method may be used to fill a munition depending on the practical requirements or preferences of the PBX manufacturer.

## Conclusions

The three major conclusions of the thesis that provide the most important contributions to knowledge are summarised below.

- **Characterisation of formulation-specific 'intensity' profiles in conjunction with rheological analysis provides an ideal non-intrusive way of monitoring mixing progression, thus end of mix point.** While interpretation of mixing data to determine mixing progression had previously been applied to concrete mixing,[12] it had not been extended to polymer bound suspensions. This thesis (Paper 2 - Efficiency Determination) has shown that when mixing with polymers, profile features can be resultant of both evolving 'mixedness' and evolving temperature. Care should therefore be taken to distinguish the end of mix point from further rheological changes brought about from energy dissipation in the material, or the effects of active heating or cooling. This will prevent mixer from being switched off too early (resulting in a PBX product with non-uniform properties), or continuing for unnecessarily long durations (resulting in reduced output rate and increased costs).

- **There can be considerable variation/calibration errors between mixer models and units, resulting in considerable differences in inertial force thus mixing behaviour when using different machines.** It had previously been assumed that mixing behaviour did not change between units of the same mixer or units of different models (when using the same size mixing vessel), since in all cases the principle behind mixer operation is the same (i.e. a vibrating platform that oscillates at 60 Hz at a defined acceleration). This thesis (Paper 3 - Machine Variables) has invalidated that assumption, where it was shown that mixing times can increase by 65 % when a different model is used (LabRAM II as opposed to LabRAM 'A') and 100 % when using different mixer units of the same model (LabRAM 'A' as opposed to LabRAM

'C'), despite the acceleration set-point being constant. PBX product outcome may therefore vary significantly between laboratories or manufacturing sites if the same mixing procedure (i.e. acceleration setting and duration) is used without first calibrating the machines and/or accounting for variation, since a higher or lower acceleration than intended may otherwise be applied.

- **Surface chemistry has a strong influence on mixing efficiency.** While anecdotal evidence[5] had suggested that low surface free energy vessel materials were unsuitable for mixing due to wall slip, the effects of surface chemistry had not been investigated in a controlled experiment. This thesis (Paper 4 - Vessel Material) found that mixing time could be decreased by 17 % by avoiding low surface free energy materials (PTFE[b]). The decrease was correlated to an increase in adhesive (work of adhesion) to cohesive (surface tension) forces ratio, thus a reduction in the contact angle between the vessel material and binder mixture. This particularly has implications for mixing munitions 'in-situ', where industry has previously tested the use of cast PBXs in artillery shells lined with a non-stick coating (to prevent damage to the PBX when it shrinks during curing). Mixing a PBX 'in-situ' with such non-stick coatings (which by design have a low surface free energy) may therefore not be effective. It may therefore be found that rubber liners (where the liner is flexible to the shrinkage) are preferable to non-stick coatings.

## Industrial guide

An ultimate aim of industry is the manufacture of next generation PBX ('PBneXt'), whereby formulation is optimised for final properties without the necessity to compromise for processability. Here, a short industry guide is presented on how to best optimise machine and vessel variables for this purpose, specifically with regards to mixed 'in-situ' munitions.

Machine variables:

- Ensure the mixer is correctly calibrated for acceleration before use, perhaps using a detachable accelerometer (Paper 3 - Machine Variables)
- When mixing, consider using low acceleration setting (∼30 G) initially (first few minutes), to avoid material being ejected into the vacuum lines.[4, 13, 14]

[b] poly(tetrafluoroethylene), Teflon$^{TM}$

- Use high acceleration setting (>50 G) subsequently (Paper 3 - Machine Variables), taking care to avoid switches in movement mode between churning[3] (the most effective movement mode for mixing[1–4]) and decoupled (an ineffective movement mode for mixing[3, 5]).

Vessel variables:

- Consider mixing under atmospheric pressure initially[14] or slowly reduce the pressure to that used for mixing before the machine is started (Paper 2 - Determining Efficiency), to avoid material being ejected into the vacuum lines.
- Mix under partial vacuum (∼550 mb) subsequently, to aid the movement of the material without immediately degassing it.
- Finish with a degassing stage under hard vacuum to remove entrapped air that would otherwise form voids during curing.
- Avoid the use of low surface free energy vessel interiors, such as fluoropolymers,[5] non-stick coatings, and varnishes to mitigate slip (Paper 4 - Vessel Material).
- Consider surface roughened vessel interiors, with a roughness average value akin to the particle size to mitigate slip (Paper 5 - Surface Finish).
- Consider using active heating (∼60 ℃) initially to aid the flow of material during wetting and incorporation.
- Active cooling may be required subsequently to prevent a reduction in viscosity such that there are undesirable changes in the movement mode (i.e. switch from high intensity to low intensity churning, Paper 2 - Determining Efficiency).

End of mix determination:

- Record the formulation and machine set-up specific mixer 'intensity' profile.
- Note that profile features may correlate to changes in rheology due to both 'mixedness' and temperature changes.
- Use rheological data collected on samples taken at various stages of the profile to correlate 'mixedness' to profile features.
- Determine the end of mix point to be the onset of profile features correlated to the desired 'mixedness', as determined from the rheological characterisation.

## Future work

### Further mixing experiments

The experiments as performed in the thesis should be extended to cover a wider range of scenarios, such as higher solids loadings, different fillers (i.e. explosives), larger scale mixers (e.g. OmniRAM), and more diverse ranges of variables. For example, the acceleration comparison was only taken over a tenth the available acceleration range in this work (the mid-range, 45 - 55 G), and should be extended to higher and lower extremes (i.e. 1 - 100 G). The surface finish comparison should be repeated under partial vacuum to ascertain conclusive results, and the comparison of material outcome between mixed 'in-situ' and 'mixed and cast' should be repeated with an optimised formulation that does not settle. Tests performed on the cured materials should also be extended to assess density and packing arrangement directly, and compare mechanical properties across different strain rates and temperatures.

### A new paradigm

Ideally needed is a new paradigm that links together all aspects (Table D-1, Table D-2, Figure D-2, Figure D-1, associated intensity profiles, and energy requirement) of the mixing process in a single model. Such a model would be an immense conceptual and computational undertaking, given the large number of variables and their interdependence. It would however bring huge benefits since by accounting for all aspects of the system, mixing behaviour and efficiency (time and energy to mix) could be predicted for any formulation.

### Round-robin

It is recommended that a round-robin comparison of RAM machines be undertaken across a range of units and models, perhaps using standardised supplementary accelerometers and rigid body masses of various weight as payloads, over a full sweep of acceleration settings. This would give a better idea of how much machines vary and how well they are calibrated, providing an indication as to how mixing and product outcome may vary across manufacturing sites. Using this method, the additional errors associated with testing cured PBX material manufactured on different machines to determine reproducibility are avoided, though such data would be complementary.

## References

[1] E.L. McCloy, P. Wilkinson, and P.P. Gill. Resonant Acoustic Mixing: Pushing The Boundaries. Master's thesis, Cranfield University, 2016.

[2] P.A. Lucon, G. Sperry, and J. Whaley. RAM Mixing of Liquids and Pastes. Resodyn Technical Interchange, Butte, Montana, USA, 2016.

[3] P.A. Lucon and J. Whaley. Liquids and Pastes. Resodyn Technical Interchange, Butte, Montana, USA, 2016.

[4] P.A. Lucon. Mixing with Vacuum Assist. Resodyn Technical Interchange, Butte, Montana, USA, 2016.

[5] E.R. Beckel, K.E. Lee, J.C. Marin, and A.H. Shah. Processing of Explosives at ARDEC Using the LabRAM. U.S. Army Armament Research, Development and Engineering Center, September 2016.

[6] S.L. Coguill and Z.R. Martineau. Vessel Geometry and Fluid Properties Influencing Mix Behavior of Resonant Acoustic Mixing. 38th International Pyrotechnics Seminar, Denver, CO, USA., 2012.

[7] J-M. Piau, N. Kissi, and A. Mezghani. Slip flow of polybutadiene through fluorinated dies. *J. Non-Newton Fluid*, 59:11–30, 1995.

[8] H.A. Barnes. A review of the slip (wall depletion) of polymer solutions, emulsions and particle suspensions in viscometers: its cause, character, and cure. *J. Non-Newton Fluid*, 56:221–251, 1995.

[9] M. Cloitre and R.T. Bonnecaze. A review on wall slip in high solid dispersions. *Rheol Acta*, 56:283305, 2017.

[10] A.N. Patil and P.P. Gill. Resonant Acoustic Mixing The Future of Propellant Manufacturing. Master's thesis, Cranfield University, 2018.

[11] D.W. Aubrey. Tack. In *Handbook of Adhesion, Second Edition*. John Wiley & Sons, Ltd., 2005.

[12] A. Vandenberg and K. Wille. Evaluation of resonance acoustic mixing technology using ultra high performance concrete. *Constr. Build. Mater.*, 164:716–730, 2018.

[13] T.G. Yew, P.P. Gill, and P. Wilkinson. Process Parameters for Resonant Acoustic Mixers (RAM). Master's thesis, Cranfield University, 2015.

[14] D. Jubb. Private Communication, Falcon Project Ltd., January 2018.

# Appendices

Further mixing experiments regarding formulation variables (particle shape and live explosive filler) were undertaken, though due to restrictions on laboratory access during the COVID-19 pandemic have insufficient data to be included in the main body of the thesis. The mixer intensity profile data that was collected is briefly reported on in Appendix 1 and Appendix 2. Appendix 3 describes the mixer intensity profile that was observed during the catastrophic failure of a mixing vessel. Appendix 4 describes a brief compatibility assessment of RDX and Araldite 2011 adhesive.

## Appendix 1 - Particle shape

Glass beads and crushed glass of similar particle size were used as inert simulants to approximate spherical and irregular shaped explosive fillers respectively. The experimental procedure used was generally the same as Papers 2-4 of this thesis. The glass beads (spherical) mixing intensity profile follows a similar shape to the profiles observed throughout the thesis, with a mixing (M), bulk motion (B), and flat-line (FL) stage clearly apparent. Up to approximately three minutes of mixing, the crushed glass mixing intensity profile is somewhat similar in shape to that of the glass beads profile. However, there is no subsequent build up in intensity to a bulk motion stage. The absence of this when using crushed glass would suggest that higher viscosity stemming from the angular particle shape is inhibiting a large velocity gradient and associated intensity build up. Instead, there is a far more subtle feature that would appear to mark the end of the mixing stage, whereby intensity increases slightly ($\sim$4 %) between 8 and 10 minutes. The profile then gently drops down into a what resembles a flat-line stage, but without ever undergoing high intensity bulk motion or a switch in coupling condition at the flat-line onset.

Table A-1: The glass bead and crushed glass formulation used for mixing.

| | Glass | DEHA | HTPB | Curative |
|---|---|---|---|---|
| Volume (%) | 62.00 | 19.00 | 19.00 | - |
| Actual mass (%) | 81.65 | 9.30 | 9.05 | - |
| RDX equivalent mass (%) | 76.48 | 11.91 | 11.60 | - |

Table A-2: Particle size analysis (Cilas 1190, dry mode) and tap density (500 taps) of glass microbeads and crushed glass.

| | D10 (µm) | D50 (µm) | D90 (µm) | Tap density |
|---|---|---|---|---|
| Glass beads | 13.9 | 28.7 | 45.5 | $\phi = 56.5$ |
| Crushed glass | 8.1 | 31.9 | 56.3 | $\phi = 47.2$ |

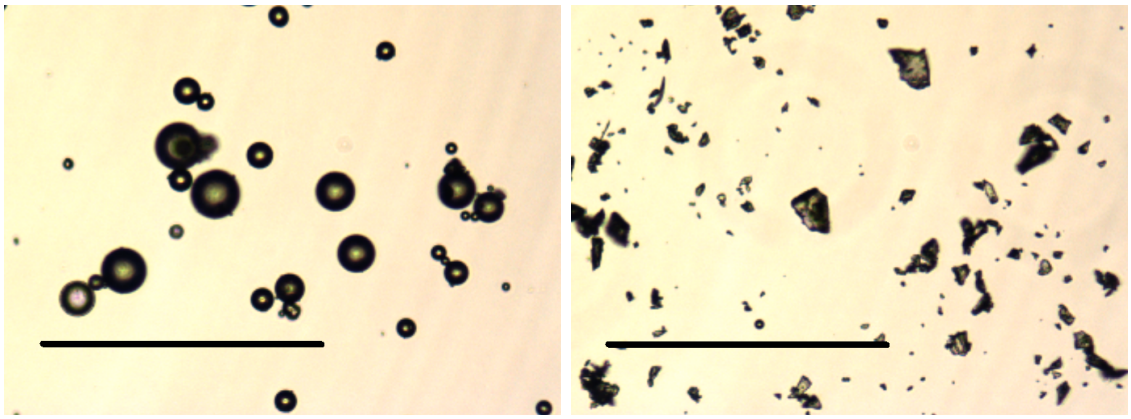

(a) Glass Beads (b) Crushed Glass

Figure A-1: Optical micrographs of glass beads and crushed glass. The scale bar represents 250 µm. The spherical nature of the glass beads is in stark contrast to the angular and irregular shaped crushed glass particles.

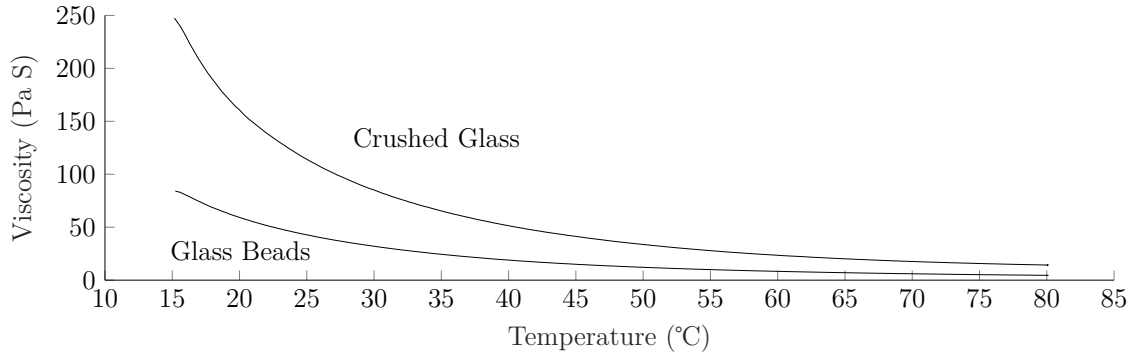


Figure A-2: Glass bead and crushed glass formulation viscosity comparison over triplicate measurements. TA Instruments HR-1, 25 mm diameter parallel plates, 500 µm gap height, 2.5 $s^{-1}$ shear rate, 2 ℃ per minute heating rate. The crushed glass formulation has a viscosity on average 2.8±0.1 times greater than the glass beads formulation across all temperatures.

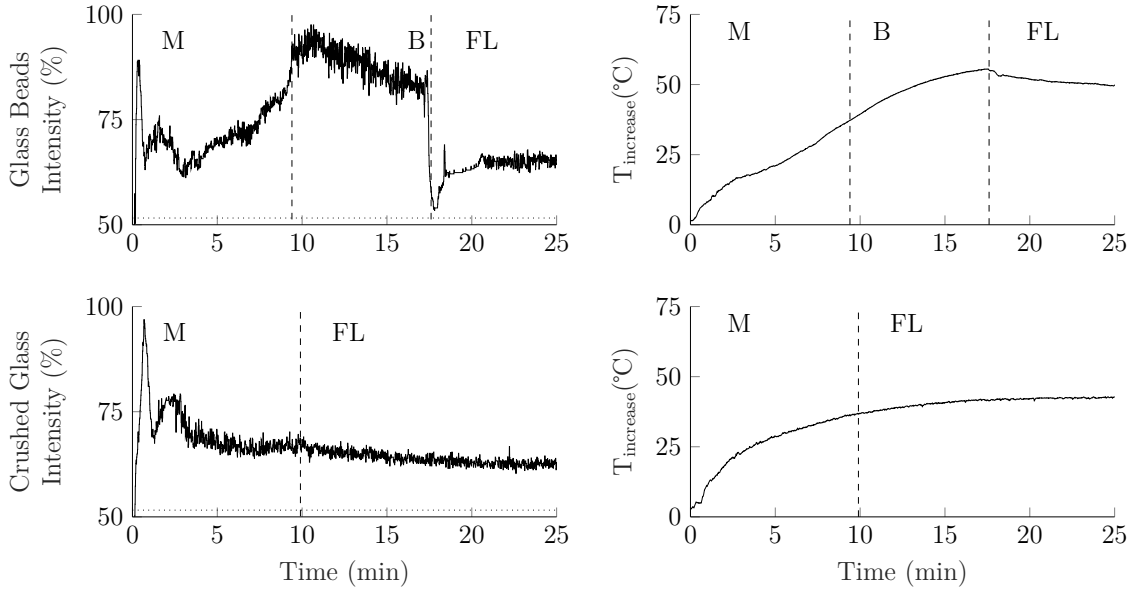


Figure A-3: Comparison of intensity and temperature profiles for glass bead and crushed glass formulations. Glass 62 % v/v, DEHA 19 % v/v, HTPB 19 % v/v, 550 mbar pressure, 50 G acceleration, LabRAM 'C', 48 mm diameter 47.5 mm height polyether ether ketone (PEEK) vessel.

## Appendix 2 - Live explosives

Remotely operated mixing with live explosives was undertaken. The formulation used is shown in Table A-3. RDX Type II (Chemring Nobel, Norway) conforming to the 'Class 1' particle size distribution (Table A-4) was used. The desired amount was sampled from 5 kg (wetted) stock by coning and quartering, and oven dried.

Duplicate intensity and temperature increase profiles are shown in Figure A-5 and are in good agreement with each other. What may resemble a mixing stage is apparent up the intensity peak at approximately seven minutes, followed by a gentle reduction in intensity to form a flat-line stage. While these profile features were not correlated to rheological properties, their presence reinforces the argument that each formulation will have its own unique profile with which to monitor mixing progression. This also demonstrates the ability of RAM to mix live explosives.

Table A-3: RDX formulation used for live mixing.

| | RDX | DEHA | HTPB | Curative |
|---|---|---|---|---|
| Volume (%) | 54.00 | 23.00 | 23.00 | - |
| Mass (%) | 70.06 | 15.17 | 14.77 | - |

Table A-4: Specification for NATO standardised 'Class 1' RDX particle size distribution,[1] and the particle size distribution of the Type II RDX product under investigation.

| Opening (µm) | Nominal % Through | Actual % Through |
|---|---|---|
| 850 | 98 ± 02 | 100 |
| 300 | 90 ± 10 | 100 |
| 150 | 60 ± 30 | 51 |
| 75 | 25 ± 20 | 10 |

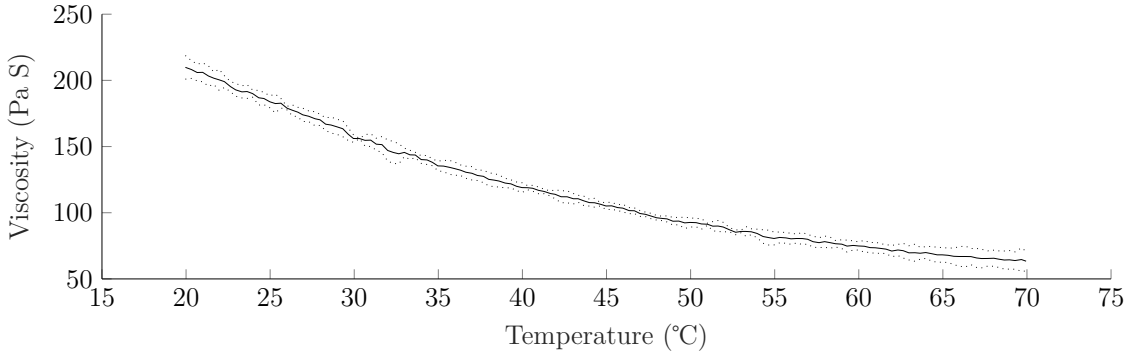


Figure A-4: RDX formulation viscosity comparison over duplicate measurements, taken after 35 minutes of mixing. Standard deviations shown. TA Instruments HR-1, 25 mm diameter parallel plates, 2500 µm gap height, 0.1 $s^{-1}$ shear rate, 2 ℃ per minute heating rate.

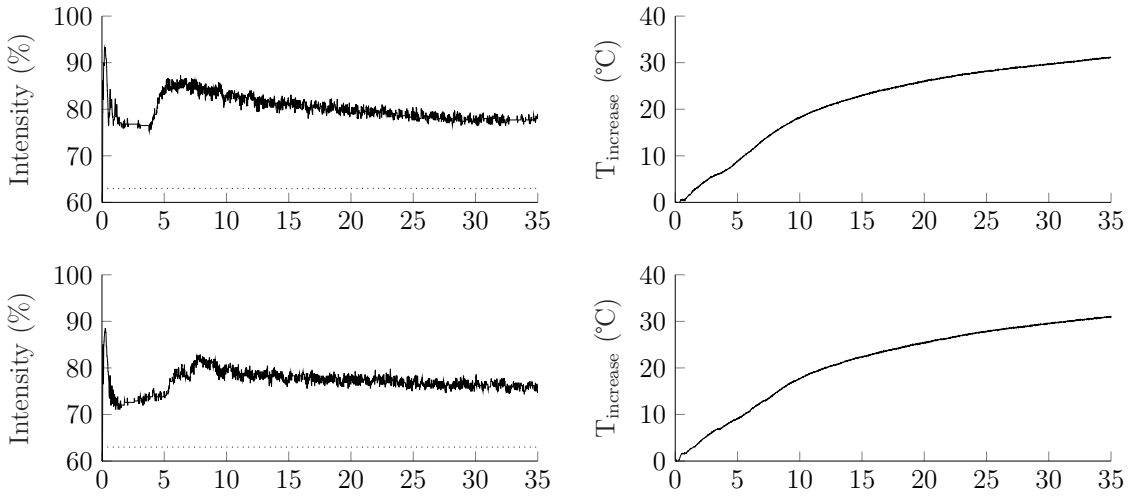


Figure A-5: Duplicate intensity and temperature profiles for RDX mixing. RDX 54 % v/v, DEHA 23 % v/v, HTPB 23 % v/v, 550 mbar pressure, 60 G acceleration, LabRAM 'C', 48 mm diameter 47.5 mm height poly(tetrafluoroethylene) (PTFE) vessel.

## Appendix 3 - Vessel failure

The apparatus for 'in-situ' mixing as described in Part 6 - Processing Variables was being used to conduct further mixing. To recap, the set-up consisted of off-the-shelf polyethylene terephthalate (PET) jars which were securely placed into a slightly larger hermetically sealable polycarbonate (PC) vessel (77 mm external diameter, 76 mm external height). A 'base clamping' mechanism was being use to hold the PC vessel to the vibrating plate of the mixer. In this instance, the jars were filled with a formulation containing 175 g of filler and 63 g of binder. The total mass attached to the clamp was 299 g, and an acceleration of 30 G was being used.

After mixing for 11 minutes, the vessel catastrophically failed at the base, as shown in Figure A-6 and Figure A-7. Although ejected from the plate, the body of the mixing vessel and its contents were held in the vicinity of RAM by the thermocouple and vacuum line attachments, and the vessel contents contained by the PET jar. The intensity profile is shown in Figure A-8.

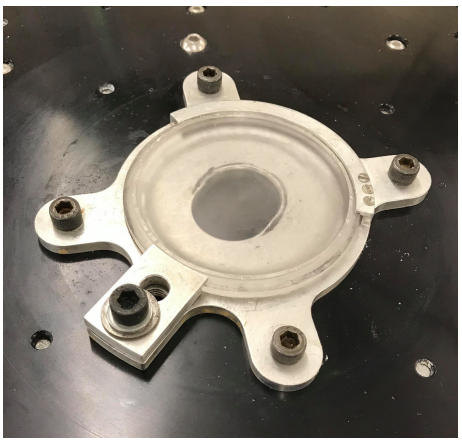

Figure A-6: Detached vessel base

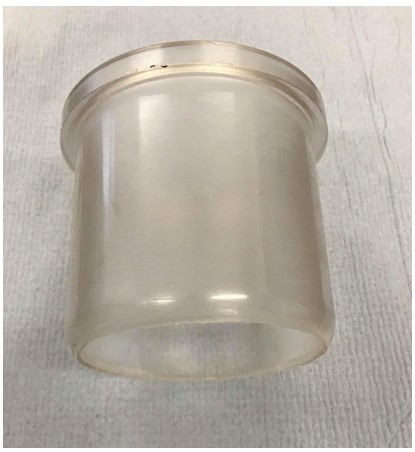

Figure A-7: Detached vessel body

Up to approximately 10.5 minutes of mixing, the profile shows no irregularities. Beyond this point, the mixer begins to rapidly draw an increasing amount of power, reflected in the runaway increase in the mixing intensity to 100 % and inability to maintain the set acceleration. This was likely due to energy expenditure in fatiguing the base of the vessel. This weakening stage took place over approximately 40 seconds. After 11 minutes of mixing, the body of the vessel fully detached from the base. At this point, energy was no longer being drawn by the mixing or fatiguing processes. This is reflected in the instantaneous drop in the intensity and rise in acceleration, as the machine attempted to rebalance power output to the new

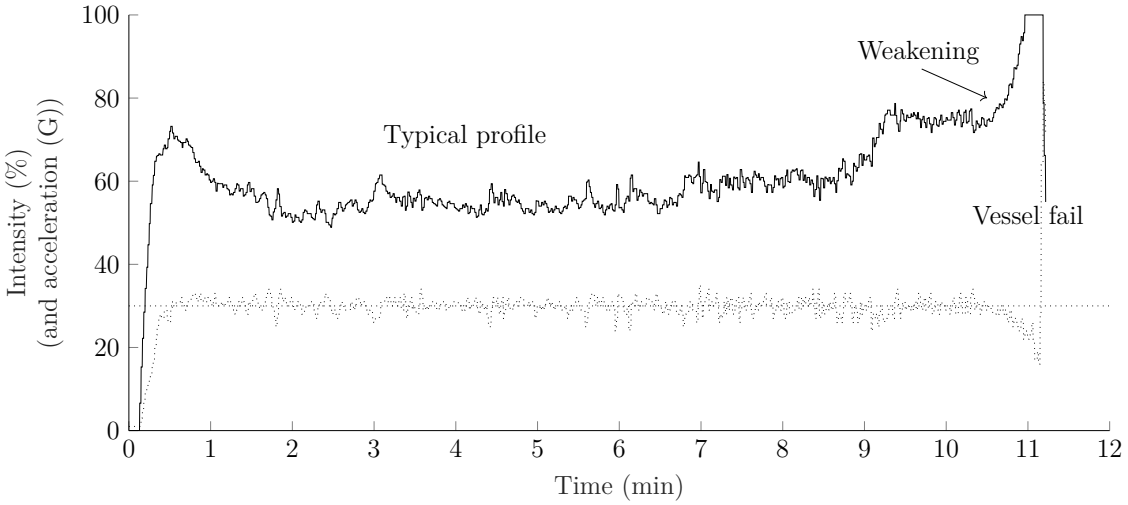


Figure A-8: Intensity profile for the polycarbonate vessel failure at 30 G acceleration, LabRAM 'C'. The dotted lines show the acceleration set point and achieved acceleration.

resonance condition after the loss of the mixing vessel. The machine was stopped manually within 1.8 seconds of the vessel detaching from its base. A crack in the vessel base had been repaired with cyanoacrylate glue and epoxy resin prior to routine usage (over 20 mixes) before the failure. It is recommended that all components be monitored for signs of fatigue or cracking, and should be discarded once such signs are observed. Ideally, weak points in component design should be avoided, and components should be of single or limited repeat usage where possible. While plastic mixing vessels are not typically used for industry scale-up, the observation that mechanical failure can be predicted in the seconds prior to total breakage is significant. Forewarning of failure (resultant of metal fatigue for example) could be of critical importance in an industry scenario, where the mixer could be switched off prior to breakage. Steps should therefore be taken to characterise the 'usual' intensity readout profile for any particular mixing sequence, and monitor the intensity profile in real-time during production to watch for significant deviations that could indicate failure is imminent.

## Appendix 4 - Araldite 2011 compatibility with RDX

Compatibility testing of Araldite 2011 (the epoxy used to bond the polycarbonate end tabs to the tensile experiments in Paper 6 - Mixing 'In-situ') with RDX was undertaken for if the experiment were to be repeated using live explosive filler.

250 µg of RDX and a roughly equal amount of fresh epoxy were hand-mixed with a spatula, and observed after 10 minutes and one day. The mixed epoxy (clear yellow in colour) did not undergo a colour change when in contact with RDX, giving a preliminary indication that the two are chemically compatible.

## References

[1] NATO. Explosives, Specification for RDX (Hexogene). STANAG-4022.

## Colophon

This thesis was created by the author with the TEX typesetting language using the LATEX $2_\varepsilon$ and BIBTEX macro packages, and edited in the TEXmaker environment. The TEX distribution used was MiKTEX, and the engine used to generate the final document was LuaLATEX. The typeface used is Computer Modern, with a body text size of 12pt. Most figures were created in vector graphic format using PGF/Ti*k*Z output exported from the MATLAB® curve fitting toolbox, using the MATLAB**2**Ti*k*Z package.